# Resistance mechanisms to mTOR inhibition in renal cancer

*Submission for the degree of Doctor of Philosophy (DPhil)*
*Department of Oncology*

Dr Philip L. Earwaker
Jesus College, University of Oxford

Trinity Term 2015

# Contents

## List of Figures

# List of Tables

## List of Abbreviations

| | |
|---|---|
| Abl | Abelson murine leukaemia viral oncogene homolog 1 |
| ADAM | Disintegrin and metalloproteinase |
| ADP | Adenosine diphosphate |
| AKT | 'AK' thymoma (also known as protein kinase B or PKB) |
| AMPK | 5' AMP-activated protein kinase |
| ANOVA | Analysis of variance |
| atg13 | Autophagy related gene 13 |
| ATM | Ataxia telangiectasia mutated |
| ATP(ase) | Adenosine tri-phosphate (hydrolase) |
| BCA | Bicinchoninic acid |
| BHD | Birt-Hogg-Huber |
| BLAST | Basic local alignment search tool |
| BRAF | Murine sarcoma viral (v-RAF) oncogene homolog B (rapidly accelerated fibrosarcoma) |
| BSA | Bovine serum albumin |
| CaMKII | Calcium calmodulin dependent protein kinase II |
| CCRCC | Clear cell renal cell carcinoma |
| Cdc2 | Cyclin dependent kinase 2 |
| CI | Confidence interval |
| CML | Chronic myeloid leukaemia |
| Crk | CT10 regulator of kinase |
| CSF-1R | Receptor for macrophage colony-stimulating factor |
| CTG | CellTiter-Glo |
| CV | Coefficient of variation (ratio of mean to standard deviation) |
| DBZ | Dibenzazepine (gamma secretase inhibitor ) |

| | |
|---|---|
| DEPTOR | DEP domain containing mTOR interacting protein |
| DLL | Delta like |
| DMEM | Dulbecco's modified eagle's medium |
| DMSO | Dimethyl sulfoxide |
| (c)DNA | (complementary) Deoxyribonucleic acid |
| DR5 | Death receptor 5 |
| 4E-BP1 | eIF4E binding-protein 1 |
| EDTA | Ethylenediaminetetraacetic acid |
| EGFR | Epidermal growth factor receptor |
| eIf4A/B/E/F/G | Eukaryotic initiation of translation factor |
| EMT | Epithelial mesenchymal transition |
| ERK | Extracellular signal-regulated kinase |
| FCS | Foetal calf serum |
| FGFR | Fibroblast growth factor receptor |
| FIP200 | Focal adhesion kinase family-interacting protein of 200 kDa |
| FKBP12 | FK506-binding protein |
| FLT3 | FMS-like tyrosine kinase-3 |
| FoxO1/3a | Forkhead box O1/3a |
| GDP | Guanosine diphosphate |
| $GI_{50}$ | The concentration of drug required to inhibit viability to 50% of untreated cells |
| GIST | Gastrointestinal stromal tumour |
| Grb2/10 | Growth factor receptor-bound protein 2/10 |
| GTP(ase) | Guanosine triphosphate (hydrolase) |
| HAT | Histone acetyltransferases |
| HDAC(i) | Histone deacetylase (inhibitor) |
| HER2 | Human epidermal growth factor receptor 2 |

| | |
|---|---|
| HES1 | Hairy and enhancer of split 1 |
| HEY1 | Hairy/enhancer of split related with YRPW motif |
| HCl | Hydrochloric acid |
| HGF | Hepatocyte growth factor |
| HIF | Hypoxia inducible factor |
| HSL | Hormone sensitive lipase |
| $IC_{50}$ | The concentration of drug required to inhibit activity of an enzyme to 50% of untreated control |
| IFN α | Interferon α |
| IGF-1(R) | Insulin like growth factor 1 (receptor) |
| IP3 | Inositol triphosphate |
| IR | Insulin receptor |
| IRS-1 | Insulin receptor substrate 1 |
| KIT | Stem cell factor receptor |
| LDH | Lactate dehydrogenase |
| LIMK1 | Stem cell factor receptor |
| LKB1 | Liver kinase B1 |
| LRRK2 | Leucine-rich repeat kinase 2 |
| mA | Milliamperes |
| MAPK | Mitogen activated protein kinase |
| MAPKAPK2 | Mitogen activated protein kinase activated protein kinase 2 |
| MEF | Mouse embryonic fibroblast |
| MEK | Mitogen-activated protein kinase kinase |
| MET | MNNG-hos transforming gene (hepatocyte growth factor receptor) |
| mLST8 | Mammalian lethal with sec-13 protein 8 |
| mSin1 | Mammalian stress-activated kinase-interacting protein 1 |

| | |
|---|---|
| mTOR(C1/2) | Mammalian target of rapamycin (complex 1/2) |
| MYC | Avian myelocytomatosis viral oncogene homolg |
| NCBI | National Centre for Biotechnology Information |
| NICD | Notch intracellular domain |
| NFκB | Nuclear factor kappa-light-chain-enhancer of activated B cells |
| NSCLC | Non small cell lung cancer |
| PAGE | Polyacrylamide gel electrophoresis |
| PBS | Phosphate buffered saline |
| PCDC4 | Programmed cell death protein 4 |
| PDGFR | Platelet derived growth factor receptor |
| PDK1 | Phosphoinositide-dependent kinase-1 |
| PI3K (*PIK3CA*) | Phosphoinositide 3-kinase (gene of) |
| PIP2 | Phosphatidylinositol 4,5-biphosphate |
| PP2A | Protein phosphatase 2A |
| PPM1G | Metal-dependent protein phosphatase 1G |
| PRAS40 | Proline-rich AKT substrate 40 kDa |
| PROTOR | Protein observed with rictor 1 and 2 |
| PTEN | Phosphatase and tensin homolog |
| qRT- PCR | Quantitative real time polymerase chain reaction |
| Raf | Rapidly accelerated fibrosarcoma |
| Rag | Ras related GTP binding protein |
| RAPTOR | Regulatory associated protein of mammalian target of rapamycin |
| Ras | Rat sarcoma |
| RasGRF1 | Ras guanine release factor 1 |
| Rb | Retinoblastoma |
| RCC | Renal cell carcinoma |

| | |
|---|---|
| RCC4S | RCC4 cells grown in solvent control medium |
| RCC4B20(-S) | BEZ235 resistant RCC4 cells grown in 20 nM BEZ235 (returned to solvent control medium and resensitised to BEZ235) |
| REDD1 | Regulated in development and DNA damage responses 1 |
| RET | Glial cell-derived neurotrophic factor receptor (rearranged during transfection) |
| Rheb | Ras homology enriched in brain |
| RICTOR | Rapamycin-insensitive companion of mTOR |
| RIPA | Radio-immunoprecipitation assay |
| (si)(m)RNA | (small interfering) (messenger) Ribonucleic acid |
| S6(K) | Ribosomal protein S6 (kinase) |
| SDS | Sodium dodecyl sulphate |
| SEM | Standard error of the mean |
| $SF_{50}$ | Concentration of a drug required to inhibit survival to 50% of untreated cells |
| SGK1 | Serum - and glucocorticoid – induced protein kinase 1 |
| SH2 | Src homology 2 domain |
| Shc | Src homology 2 domain containing |
| sos | Son of sevenless |
| SREBP1/2 | Sterol regulatory element-binding protein 1/2 |
| STAT | Signal transducer and activator of transcription |
| TBS-T | Tris buffered saline, 0.1% TWEEN20 |
| TGF | Transforming growth factor |
| TSC1/2 | Tuberous sclerosis complex 1/2 |
| ULK1 | Unc-51 like kinase |
| VEGF(R) | Vascular endothelial growth factor (receptor) |
| VHL | von Hippel Lindau |

## Acknowledgements

I have learned and been taught much during my DPhil for which I will forever be grateful. I am of course indebted to Val for taking me on for a fellowship and providing a supportive and challenging environment in which to work. I would like also to thank my second supervisor Andy for his insightful comments on my research throughout my time working in the lab. You both gave me more support than I felt I deserved and will have my thanks for that forever.

To the members of the IGF lab, with special mention to Kunal, Meenali and Roger, I write these words in the knowledge that you will understand their true meaning and feel the heartfelt thanks contained within. I hope I was the support for you to lean on that you were for me. A DPhil cannot be accomplished on your own. It requires comradeship through the lows, empathy through the hysteria, and a healthy dose of self-deprecating perspective to keep you grounded. But above all I learned from your example – hard work, dedication and efficiency.

From the post docs in the lab I have learned that there are vanishingly few problems in science that cannot be surmounted. You each had your own unique style to bring to bear on whatever problem I came to you with.

Tamara, you were a great sounding board for scientific reasoning. The clarity of your thought and force of your convictions was at times quite literally like a galvanising thunderbolt through all the background noise. Gao Shan, you had a finely honed technique for everything. It set us straight, and was always accompanied by the timeless words “you can do”.

I have many members of the neighbouring labs to thank including Lonnie Swift for help with the histone modification work and for being my unofficial thesis committee, Stephan Feller for help with Abl and CrkII, Kenji Hashimoto for help with Met, Ulrike, Sofia, Helen and Ji Liang from Prof Harris lab for help with numerous reagents, but particularly the Notch pathway, and of course Professor Adrian Harris for providing funding.

I would like to acknowledge the help received from the microarray service at the Cancer Research UK Paterson Institute in Manchester, and Steve Taylor, Head of the Computational Biology Group at the Weatherall Institute of Molecular Medicine.

## Personal Thanks

It is with the love and support of my family that I have made it through this DPhil. My parents quietly brought me up with without any boundaries to ambition and I hope that through my achievements I have made them proud.

My wife Victoria has provided unending support for me during my DPhil. She has provided the love and security to give me the strength to complete this work.

## Abstract

**Introduction:** Advanced clear cell renal cell cancer (CCRCC) is incurable, but molecularly targeted treatments have improved the prognosis. One such molecular target is the mammalian target of rapamycin (mTOR) and two rapalogues (everolimus and temsirolimus) have been licensed for the treatment of advanced CCRCC, but resistance to treatment is a significant problem. Novel mTOR kinase inhibitors show more complete blockade of mTOR downstream targets, and greater *in vitro* anti proliferative activity, although resistance remains a problem.

**Hypotheses:** 1) CCRCC cell lines, resistant to mTOR kinase inhibition could be generated *in vitro* through continuous culture in drug, and 2) mediators of resistance could be identified through screening cells at the mRNA and protein/phosphoprotein level, or by examining the signalling in resistant cells to identify the re-activation of key mTOR targets.

**Methods:** Resistant cells were created by continuous culture in the PI3K-mTOR kinase inhibitor BEZ235. Resistance was assessed by CellTiter-Glo viability assays and clonogenic assays. mRNA microarray and antibody arrays were conducted. Intra-cellular signalling was assessed by western blotting. The functional relevance of identified markers of resistance were assessed with small molecule inhibitors and siRNA protein depletion.

**Results:** BEZ235 resistant cells were created and had a 14 fold higher growth inhibitory 50 ($GI_{50}$) concentration compared to sensitive cells (99 nM vs. 7 nM).

Array screening of the cells identified markers, but not mediators of resistance (MET, Abl, MEK/ERK and the Notch pathway).

In BEZ235 resistant cells, the downstream mTOR target 4E-BP1 was re-phosphorylated, despite evidence of on-going blockade of another mTOR target, S6. Recovery of 4E-BP1 phosphorylation was associated with increased protein expression of the mTOR binding partner RAPTOR, and could be reduced by depletion of RAPTOR, or by the addition of rapamycin. Both of these interventions partially reversed BEZ235 resistance.

**Conclusions:** RAPTOR protein up-regulation, represents a novel mechanism of resistance to mTOR kinase inhibition and can be partially overcome by rapamycin. The combination of BEZ235 and rapamycin warrants further investigation to evaluate its potential to overcome resistance to mTOR kinase inhibition in RCC.

# 1 Introduction

## 1.1 Renal cancer

Renal cell cancer (RCC) is an abnormal and uncontrolled growth of cells that arises within the kidney, but that has the potential to invade local structures and spread to distant parts of the body. It shares the characteristics of cancer that were first published by Hanahan and Weinberg in 2000, and updated in 2011 (Hanahan and Weinberg 2000, Hanahan and Weinberg 2011). The original six hallmarks of cancer as they called them were "self-sufficiency in growth signals, "insensitivity to anti-growth signals", "tissue invasion and metastasis", "limitless replicative potential", "sustained angiogenesis", and "evading apoptosis". In 2011 two emerging hallmarks were added, "deregulating cellular energetics" and "avoiding immune destruction", as well as two enabling characteristics, "genome instability and mutation", and "tumour promoting inflammation".

As will be detailed in the following sections, renal cancer is a significant public health problem, but is not a single entity. Rather, this is a heterogenous group of cancers that all arise from the kidney, but do not share all of the same characteristics (Linehan et al. 2013). As will be shown, renal cancer is sometimes curable, and in recent years much more treatable than in the recent past, but metastatic disease remains fatal and resistance to treatment is a major problem.

### 1.1.1 Epidemiology of renal cancer

The latest statistics on renal cancer within the UK come from 2011 and showed 10,144 new diagnoses per annum (http://www.cancerresearchuk.org/health-professional/cancer-statistics/statistics-by-cancer-type/kidney-cancer). There is a male preponderance of renal cancer with an incidence of 20.1 cases per 100,000 men compared to 12.1 cases per 100,000 women. This made renal cancer the 8$^{th}$ most common cancer overall (7$^{th}$ most common cancer in men, and 10$^{th}$ most common in women) (ONS 2014). The risk of developing renal cancer increases with age, and 75% of cases are diagnosed in individuals over the age of 65. The incidence of renal cancer is also increasing with time over the last 40 years (Ljungberg et al. 2011).

The prevalence of renal cancer reveals some keys facts about its prognosis. Despite an annual incidence of approximately 10,000, the one year prevalence is 5080 (in 2006), while five year prevalence is 17,237, and the 10 year prevalence is 26,503 ((NCIN) 2010). The relatively lower prevalence with time indicates that there is a short life expectancy associated with renal cancer. In 2011, there were 4,189 deaths from renal cancer in the UK (61% in men) making renal cancer the 12$^{th}$ most common cause of cancer death in the UK accounting for 3% of all cancer deaths (http://www.ons.gov.uk/ons/rel/vsob1/mortality-statistics--deaths-registered-in-england-and-wales--series-dr-/2013/index.html).

While metastatic disease remains incurable, there have been significant improvements in survival from renal cancer in the last 40 years. One year survival rates have risen from 45% to 71%, 5 year survival rates from 28% to

54%, and 10 year survival rates from 25% to 44%. In many cancers, 5 year survival is often equated with cure, but in renal cancer, survival continues to decline beyond five years. Renal cancer is known for its late recurrences after prolonged disease free intervals, and also the rate of progression varies greatly between individuals such that 5 year survival with metastatic disease also occurs (Jonasch et al. 2014).

There are several risk factors for renal cancer, both environmental and genetic. The risk of developing renal cancer is associated with cigarette smoking (Mellemgaard et al. 1994), hypertension (Shapiro et al. 1999b) and obesity (Shapiro et al. 1999a), as well as workplace exposure to chemicals such as the solvent trichloroethylene (Brauch et al. 1999). Renal failure is also associated with increased risk of renal cancer (Doublet et al. 1997). A family history of renal cancer confers a 2.5 fold risk of developing renal cancer and there are also several familial cancer syndromes that predispose to renal cancer (Ljungberg et al. 2011). Inactivating mutations of the tumour suppressor von Hippel Lindau (*VHL*) gene cause von Hippel Lindau disease which is characterised by renal and pancreatic cysts and clear cell renal carcinomas, as well as haemangioblastomas of the retina and central nervous system, phaeochromocystomas, neuroendocrine tumours, endolymphatic sac tumours, and broad ligament cystadenomas (Latif et al. 1993). Activating mutations of the MNNG-Hos Transforming gene (*MET*) oncogene cause hereditary type I papillary renal carcinomas (Schmidt et al. 1997). Hereditary leiomyomatosis and type II papillary renal cell carcinoma is predisposed to by mutations of the gene encoding the tumour suppressor fumarate hydratase, a component of the Krebs cycle (Tomlinson et al. 2002). The Birt-Hogg-Huber (BHD) syndrome is caused by mutations in the *BHD* gene and is associated with benign hamartomas of the hair follicle, pulmonary cysts, increased risk of spontaneous pneumothorax, and chromophobe renal cancer (Nickerson et al. 2002).

### 1.1.2 Subtypes and molecular biology of renal cancer

Renal tumours most commonly arise from the renal cortex, and cells of the proximal tubules are thought to be the cells of origin (Cairns 2010). Sporadic renal tumours tend to be unilateral, and there is no difference in incidence between left and right-sided tumours. Tumours can be cystic or solid, and are often highly vascular, with frequent areas of necrosis and haemorrhage.

The majority, 75-80%, of renal cancers are clear cell renal cell carcinomas (CCRCC), and are characterised by loss of functional VHL in 70-80% of cases either through mutation, or through epigenetic mechanisms (Gnarra et al. 1994, Herman et al. 1994). Histologically CCRCC has vacuolated cytoplasm high in cholesterol and lipids, which gives a clear staining cytoplasm, and gives rise to the name “clear cell” renal cell carcinoma.

*VHL* is a tumour suppressor gene that gives rise to the eponymous syndrome if mutated in the germ line, but also accounts for the vast majority of sporadic CCRCC. The *VHL* gene product, VHL is a 30 kDa protein that forms the substrate recognition subunit of the E3 ubiquitin ligase complex. It recognises hypoxia inducible factors (HIF) for polyubiquitination and degradation by the proteasome (Maxwell et al. 1999, Ohh et al. 2000). In normoxia, HIFs are hydroxylated on conserved proline residues by prolyl hydroxylases, which allows HIFs to be recognised by VHL and targeted for destruction. In hypoxia, HIF's accumulate, and HIF1α or HIF2α dimerise with HIF1β and act as a transcription factor in the nucleus (Wang et al. 1995). HIFs upregulate a range of genes to adapt cells for survival in hypoxia. These genes include vascular endothelial growth factor (VEGF), platelet derived growth factor receptor β (PGDFRβ), erythropoietin, glucose transporter 1, transforming growth factor (TGF) and epidermal growth factor receptor (EGFR) (Sung et al. 2007, Biswas et al. 2012).

The second most common type of renal cancer is papillary renal cell carcinoma, which makes up approximately 15% of all cases. It has been subdivided into type I and type II based on morphological features. Both types are characterised by the presence of papillae, but type I has small cells with pale cytoplasm, whereas type II cancers have large cell with eosinophilic staining (Delahunt and Eble 1997). Type II papillary cancers are often more aggressive, with a worse prognosis (Delahunt and Eble 1997, Antonelli et al. 2010). Papillary renal cancers do not have mutations in *VHL,* but are associated with mutations in specific oncogenes*.* Familial type I cases are associated with activating mutations of *MET*, as described above. *MET* mutations are also found in 13% of sporadic cases of type I papillary RCC (Schmidt et al. 1999). Familial cases of type II papillary renal cancer harbour mutations in the fumarate hydratase gene, but it is not known whether mutations of this gene are found in sporadic cases (Jonasch et al. 2014)

The third commonest type of renal cancer is chromophobe renal cancer, characterised by large polygonal cells with pale reticular cytoplasm (Yamazaki et al. 2003). Rare forms of renal cancer include renal medullary cancer, renal collecting duct carcinoma, mucinous tubular and spindle-cell carcinoma, translocation carcinoma and post-neuroblastoma carcinoma (Srigley and Delahunt 2009). All forms of renal cancer can present with areas of sarcomatoid change where the cells have dedifferentiated, and this feature is associated with a worse prognosis (Cangiano et al. 1999).

### 1.1.3 Intratumor heterogeneity in renal cancer

In addition to the recognised heterogeneity between types of renal cancer as described above, it has become increasingly recognised that significant intratumoral heterogeneity exists in CCRCC. Exome sequencing from multiple sites of the primary renal tumour and multiple metastases from individual patient's tumours have revealed that 63-69% of identified mutations are not found in all sampled areas (Gerlinger et al. 2012). Phylogenetic analysis revealed a branching pattern of somatic mutations. Aberrations of VHL have been found ubiquitously, but up to 75% of other driver aberrations have been found to be clonal (Gerlinger et al. 2014). These findings have implications for personalised medicine based on the analysis of single biopsies, which may well not be indicative of the true sensitivity of the cancer being treated. There are also implications for the preclinical study of CCRCC using established cell lines, which are clonal expansions of single cells and therefore do not model this heterogeneity.

### 1.1.4 Treatment of early stage renal cancer

The treatment of choice for early stage renal cancer is surgical resection. Traditional surgery is open radical nephrectomy, where the entire kidney is removed together with Gerota's fascia and the ipsilateral adrenal gland. Open surgery is now largely replaced by laparoscopic surgery (Ogan et al. 2003). Smaller renal tumours, generally less than 4 cm in diameter, may be removed by partial nephrectomy. This so called "nephron sparing" surgery is particularly useful in cases of bilateral renal cancer, cancers in solitary kidneys, or in patients with impaired renal function (Gill et al. 2003, Yap et al. 2014).

In selected patients and tumours, a less invasive form of treatment with radiofrequency ablation has been performed, and early data on the technique suggests that outcomes may be comparable to that of partial nephrectomy. Factors suggesting suitability for radiofrequency ablation include small tumours, and comorbidity that increases the risks of surgery (Chang et al. 2014).

If curative intent surgery is performed in cases where the renal tumour is confined to the kidney (not invading into major vessels, or the collecting system, or extending into perinephric tissues) with no signs of lymph node involvement, then cure rates are 80% or greater. This falls to 60% if any of the above features are present (Jonasch et al. 2014).

There is as yet, no standard adjuvant therapy that reduces the chance of recurrence, or increases the chance of survival post surgery for renal cancer. Trials with immunotherapy have been published, where no benefit from interferon α or interleukin 2 was seen (Clark et al. 2003, Messing et al. 2003).

Trials of newer targeted agents including sorefenib, the VEGF receptor (VEGFR) and murine sarcoma viral (v-RAF) oncogene homolog B (BRAF) inhibitor are on going (Janowitz et al. 2013).

### 1.1.5 Treatment of metastatic renal cancer

The prognosis of metastatic renal cancer varies, but risk factors for poor prognosis have been defined in the Memorial Sloane Kettering Cancer Centre Score. Five independent adverse features were identified and defined three groups of patients with differing prognosis ranging from 30 months to 4.8 months median survival (0 adverse features, 1 or 2 adverse features, and 3 or more adverse features). The factors identified were Karnofsky performance status less than 80, less than 1 year between diagnosis and first systemic treatment, hypercalcaemia, anaemia and lactate dehydrogenase (LDH) greater than 1.5 times the upper limit of normal (Motzer et al. 2002).

Metastatic renal cancer is not amenable to curative surgical resection. The majority of treatment options are systemic therapies, although as yet none of these offer the prospect of cure. Traditional chemotherapeutics are ineffective in renal cancer (Yagoda et al. 1995), but an understanding of the molecular biology of renal cancer has led to the development of targeted therapies. These targeted therapies will be discussed in detail below, but there is also a role for a variety of local therapies.

#### 1.1.5.1 Local therapies for metastatic renal cancer

Nephrectomies are performed in a subset of patients with metastatic disease. Historical reports suggest that this can induce a low rate of spontaneous regression of metastases of approximately 1% (Janiszewska et al. 2013). The role of cytoreductive nephrectomy in influencing survival outcomes in the current era of targeted therapies is unclear, but some reports suggest survival benefit, particularly in patients with prognosis greater than 12 months, and fewer than 4 poor prognostic markers (Abern et al. 2014, Heng et al. 2014). Cytoreductive nephrectomy also has a role in symptom control (Mickisch et al. 2001).

Spontaneous regressions of renal cancer have also been observed, for example a response rate of 6% was noted in the placebo control arm of one study, but these responses are generally not durable (Gleave et al. 1998). This phenomenon suggests an immunological mechanism of tumour regression, and another such effect has also been reported in renal cancer. The abscopal effect has been reported in renal cancer, where radiation to one tumour site causes regression in metastases distant to the irradiated area (Wersall et al. 2006). Renal cancers are generally considered to be radio-resistant, and the use of radiotherapy in renal cancer has generally been confined to palliative situations such as whole brain radiotherapy for brain metastases, or irradiation of painful bone metastases (Ljungberg et al. 2010).

Surgery also has a role in the treatment of recurrent disease post nephrectomy, particularly in patients where there is a prolonged disease free interval (greater than 12 months) post nephrectomy, and where recurrence is solitary. Removal of isolated metastases is reported to achieve 5 year survival of 55%, and there may even be a role for multiple resections of metachronous metastases, e.g. in very indolent disease (Kavolius et al. 1998, Alt et al. 2011). As well as solitary recurrence, and long disease free interval, other important prognostic factors suggesting suitability for metastectomy are young age, good performance status, and feasibility of complete resection of metastasis. For patients in whom surgery is not possible, it is sometimes now possible to radiofrequency ablate metastases, including at multiple sites, with results comparable to surgical removal in some case series (Soga et al. 2009).

#### 1.1.5.2 Multi-targeted tyrosine kinase inhibitors

The first advancements in the treatment of metastatic renal cancer were made from the observation that tumours are highly vascular, and that the main genetic driver of CCRCC is loss of function of VHL, which leads to constitutive HIF signalling, promoting angiogenesis (Maxwell et al. 1999). Targeting angiogenesis therefore became a rational approach to the treatment of renal cancer. The main driver of angiogenesis is VEGF, and the VEGF receptors. This axis has been targeted by two classes of drugs. The first targets VEGF with monoclonal antibodies, and the second targets receptor activity with small molecule tyrosine kinase inhibitors (Jonasch et al. 2014).

Bevacizumab is a recombinant humanised VEGF monoclonal antibody which at high dose was shown to prolong progression free survival in comparison to low dose bevacizumab or placebo in patients with metastatic renal cancer, but did not alter overall survival in a phase II trial (Yang et al. 2003). When combined with interferon α in a large phase III study, bevacizumab resulted in a significant prolongation of progression free survival (10.2 vs. 5.4 months on inferferon alone) (Escudier et al. 2007b). However, there was no difference in overall survival, although these data may have been confounded by the use of subsequent lines of therapy (Escudier et al. 2010). The use of bevacizumab in renal cancer therefore remains unclear, and largely due to the availability of alternative treatments, is used very little in the UK.

During the same period of time during which bevacizumab was being tested, the multikinase inhibitor sorefenib was being developed. Sorafenib is a multikinase inhibitor of VEGFR, PDGFR and Raf kinases, originally developed to inhibit B-Raf (Wilhelm et al. 2004). Post immunotherapy in metastatic renal cancer, sorafenib prolonged progression free survival (5.5 vs. 2.8 months on placebo) with a 10% response rate, but no increase in overall survival (Escudier et al. 2007a, Escudier et al. 2009a). A phase II trial of sorafenib versus interferon α showed comparable progression free survival, but more responses in the sorafenib group and the addition of interferon α to sorafenib gave no additional benefit (Escudier et al. 2009b, Jonasch et al. 2010, Procopio et al. 2013).

After failure of other VEGF/VEGFR targeted agents, sorafenib, has an 8-10% response rate (Di Lorenzo et al. 2009, Di Lorenzo et al. 2010, Garcia et al. 2010, Kontovinis et al. 2012). Second or third line sorafenib therefore was used in several phase III studies as a comparator arm for new agents. For example, sorafenib compared with axitinib, a new generation VEGFR tyrosine kinase inhibitor, as second line treatment in CCRCC, showing response rates of a 9% for sorafenib, and 19% for axitinib, which was associated with prolonged progression free survival of 6.7 months vs. 4.7 months, although no prolongation of overall survival (Rini et al. 2011, Motzer et al. 2013a). In the third line setting, sorafenib was compared to fibroblast growth factor receptor (FGFR) inhibitor dovitinib. Both drugs showed very modest benefit, with progression free survival of 3.6 months, response rates of 4% and overall survival of 11 months (Motzer et al. 2014).

In summary, the precise role for sorafenib remains unclear, and it has largely been surpassed by other multikinase and mTOR inhibitors as will be discussed below.

Sunitinib is a small molecule multikinase inhibitor that inhibits VEGFR, PGDFR, stem cell factor receptor (KIT), glial cell-derived neurotrophic factor receptor (Rearranged during Transfection; RET), FMS-like tyrosine kinase-3 (FLT3) and the receptor for macrophage colony-stimulating factor (CSF-1R) (Christensen 2007). Sunitinib has become established as a standard first line treatment of renal cancer. In untreated patients, sunitinib achieved progression free survival of 11 months, in comparison to 5 months for interferon α, accompanied by a higher objective response rate (31% vs. 6%) and improved quality of life (Motzer et al. 2007). Updated trial data increased the response rates to 47% and 12% respectively, and despite 33% of the interferon α group receiving sunitinib, and 32% receiving an alternative anti VEGFR therapy, overall survival was still statistically longer in the sunitinib group at 26.4 months vs. 21.8 months (Motzer et al. 2009). Sunitinib has not been compared directly to sorafenib in a clinical trial, but was adopted as first line treatment based on apparently better progression free survival, overall survival and response rates.

A direct competitor to sunitinib is the drug pazopanib, which targets many of the same tyrosine kinases. In comparison to placebo, pazopanib prolonged progression free survival in the untreated, or interferon α treated metastatic setting. Progression free survival was 9.2 months with a 30% objective response rate (Sternberg et al. 2010). Updated results for overall survival were comfounded, once again by extensive cross-over from placebo to active drug. Consequently, the increased overall survival of 22.9 vs 20.5 months, did not reach statistical significance (Sternberg et al. 2013).

Although both pazopanib and sunitinib appeared to have comparable efficacy, the side effects differ. Most obviously, pazopanib is given continuously, while sunitinib is given in six week cycles, of four weeks on treatment, followed by a two week break, which allows for recovery from side effects. Initial comparisons suggested that sunitinib caused more mucositis and fatigue, whereas pazopanib caused more diarrhoea (Powles et al. 2012).

In a randomised phase III trial, comparing pazopanib and sunitinib the outcome suggested non-inferiority of pazopanib in median progression free survival (8.4 months versus 9.5 months for sunitinib), overall response rate (31 % vs. 25% for sunitinib) and median overall survival (28.4 months vs. 29.3 months for sunitinib) (Motzer et al. 2013b). Sunitinib was noted to cause fatigue, hand and foot syndrome, and thrombocytopaenia more frequently, whereas pazopanib caused deranged liver transaminases more frequently (Motzer et al. 2013b). Both drugs are frequently used as first line treatments in renal cancer in the UK. Pazopanib has become increasingly accepted as first line treatment on the basis of non-inferiority data and better tolerance/quality of life data.

Axitinib is a new generation multi-targeted VEGFR inhibitor that has gained acceptance as second line treatment and tivozanib, is a VEGFR-1, -2 and -3 inhibitor that showed improved progression free survival compared to sorafenib in the first line treatment of metastatic renal cancer (Motzer et al. 2013c)

The rationale for the use of agents targeting angiogenesis in renal cancer comes from the knowledge that loss of VHL function causes up-regulation of these pathways. As described above, this is the case in the majority of CCRCCs, which in turn make up the majority of renal cancers (Gnarra et al. 1994, Herman et al. 1994). There is however a significant proportion of renal cancers that are not VHL/HIF driven. Many trials of sunitinib and sorafenib selected for patients with CCRCC, but reports suggest that these drugs are also active in papillary and chromophobe renal cell cancer (Choueiri et al. 2008).

#### 1.1.5.3 Inhibitors of the mammalian target of rapamycin

The second major class of drug used to treat renal cancer clinically is the mammalian target of rapamycin (mTOR) inhibitors. These drugs block the translation of proteins involved in cell proliferation and angiogenesis (Laplante and Sabatini 2012). It was through the discovery of the parent molecule rapamycin that mTOR was discovered (Vezina et al. 1975, Heitman et al. 1991). In order to understand the mechanism of action of these drugs, it is necessary to understand the mTOR pathway.

## 1.2 The mammalian target of rapamycin (mTOR) pathway

mTOR is the protein target of the macrolide rapamycin (also known as sirolimus) that is produced by the bacteria *Streptomyces hygroscopicus*, and first discovered on Easter Island (Vezina et al. 1975). mTOR was identified and characterised through this interaction, initially in yeast as the target of rapamycin, and then in mammals as the mammalian target of rapamycin (mTOR) (Heitman et al. 1991, Brown et al. 1994). mTOR is a serine threonine kinase that exists in two distinct protein complexes, mTOR complex 1 (mTORC1) and mTOR complex 2 (mTORC2), defined by its binding partners. Each complex has different functions, and is controlled by different mechanisms (Laplante and Sabatini 2012). mTORC1 regulates the balance in the cell between anabolic and catabolic processes, integrating signals from growth factors, nutrients, oxygen and energy levels. When conditions are favourable, mTORC1 is activated and stimulates protein synthesis, lipid synthesis, energy metabolism, growth and proliferation (Dowling et al. 2010). Simultaneously, mTORC1 activation inhibits autophagy, which is the main catabolic process by which organelles are recycled either because they are damaged, or because the cell requires amino acids during times of poor nutrient availability (Hosokawa et al. 2009). mTORC2 lies upstream in the signalling cascade from mTORC1, receiving input from growth factors, and as well as activating mTORC1, has roles in cytoskeletal organisation, cell survival and metabolism (Jacinto et al. 2004, Sarbassov et al. 2004, Sarbassov et al. 2005). The main components, activators and downstream effects of the mTOR pathway are illustrated in Figure 1-1.

### 1.2.1 mTOR complex 1 structure

mTORC1 is composed of 6 components, four of which are common to mTORC2: mTOR, mammalian lethal with sec-13 protein 8 (mLST8), DEP domain containing mTOR interacting protein (DEPTOR), and the tti1/Tel2 complex (Kim et al. 2003, Peterson et al. 2009, Kaizuka et al. 2010). The proteins that are unique to mTORC1 are regulatory associated protein of mammalian target of rapamycin (RAPTOR), and proline-rich AKT substrate 40 kDa (PRAS40) (Hara et al. 2002, Kim et al. 2002, Sancak et al. 2007). mTOR is the kinase of the complex, DEPTOR and PRAS40 are both inhibitors of mTOR, tti1/Tel2 are scaffold proteins, mLST8 is of unknown function, and RAPTOR is a scaffold protein and binds mTORC1 substrates (Foster et al. 2010b).

### 1.2.2 mTOR complex 2 structure

Instead of RAPTOR and PRAS40, the mTORC2 complex contains rapamycin-insensitive companion of mTOR (RICTOR), mammalian stress-activated kinase-interacting protein 1 (mSin1) and protein observed with rictor 1 and 2 (protor1/2) as unique binding partners. These three proteins are scaffolding proteins and mediate substrate binding and specificity (Jacinto et al. 2004, Sarbassov et al. 2004).

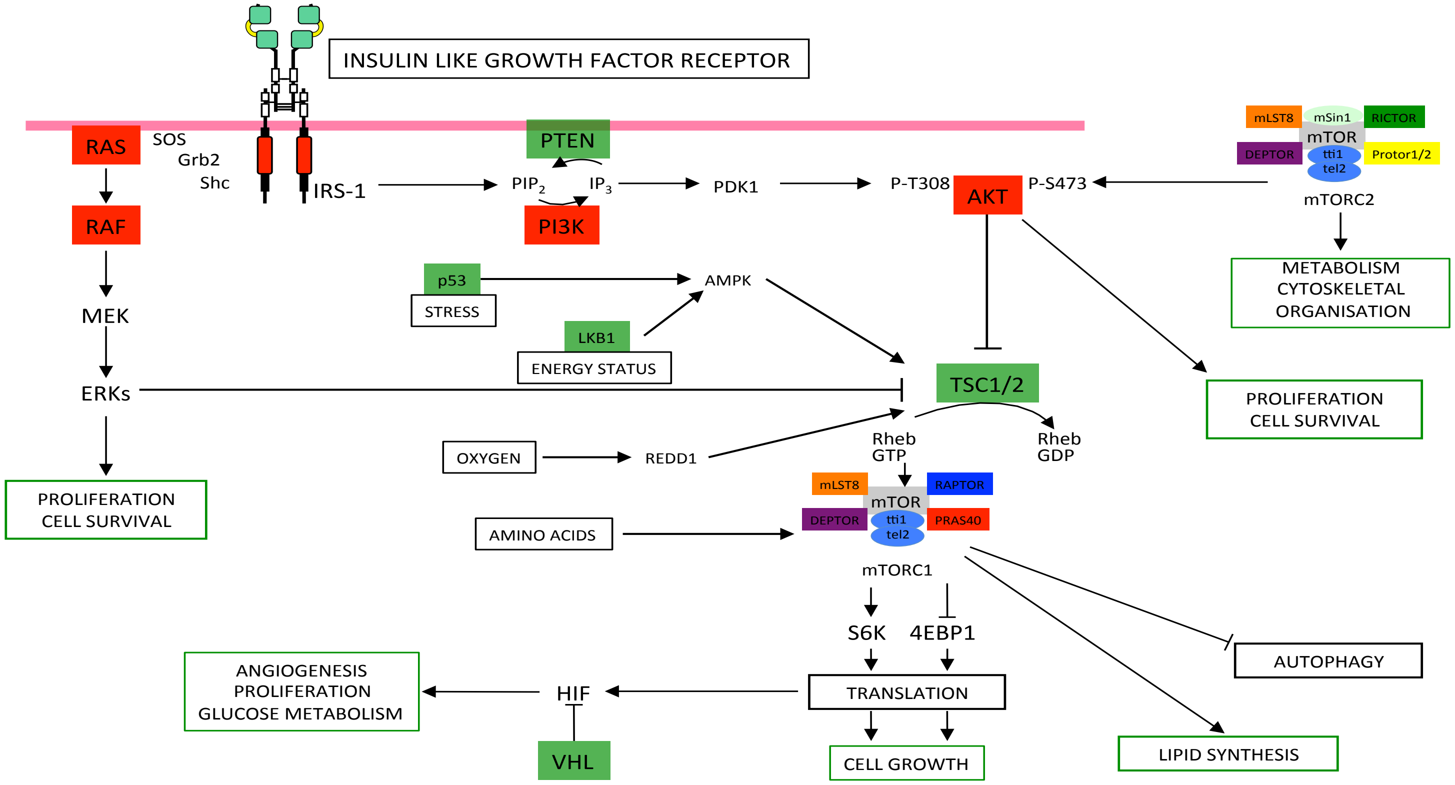


**Figure 1-1 The mTOR pathway**

The structure of mTORC1 and mTORC2 are illustrated in a simplified mTOR signalling network. Boxes with black borders mark regulators of mTOR activity. Boxes with green borders mark oncogenic actions of mTOR. Solid red and green boxes mark oncogenes and tumour suppressors respectively. 4E-BP1 (eukaryotic translation initiation factor 4E binding protein 1) AMPK (5' AMP-activated protein kinase) AKT (protein kinase b) ERK (extracellular signal-regulated kinase) Grb2 (growth factor receptor-bound protein 2) HIF (hypoxia inducible factor) IP3 (inositol triphosphate) IRS-1 (insulin receptor substrate 1) LKB1 (liver kinase B1) MEK (mitogen-activated protein kinase kinase) PDK1 (phosphoinositide-dependent kinase-1) PI3K (phosphoinositide 3-kinase) PIP2 (phosphatidylinositol 4,5-biphosphate) PTEN (phosphatase and tensin homolog) RAF (rapidly accelerated fibrosarcoma) RAS (rat sarcoma) REDD1 (regulated in development and DNA damage responses 1) Rheb (ras homology enriched in brain) S6K (ribosomal protein S6 kinase) Shc (Src homology 2 domain containing) SOS (son of sevenless) TSC1/2 (tuberous sclerosis complex 1/2) VHL (von Hippel-Lindau)

## 1.2.3 Activation of mTORC1

Many of the signals and environmental cues that activate mTOR converge on tuberous sclerosis 1 and 2 (TSC1/2), also known as hamartin and tuberin. TSC1/2 is a guanine triphosphate hydrolase (GTPase) activating protein that facilitates Ras homology enriched in brain (Rheb) GTPase activity, and hydrolysis from Rheb-guanine triphosphate (GTP) to Rheb-guanine diphosphate (GDP). When Rheb is bound to GTP it binds and strongly activates mTORC1 kinase activity. Therefore, when TSC1/2 is active, mTOR is inactivated (Inoki et al. 2003a).

Tuberous sclerosis complex is an autosomal dominant inherited disorder in which mutations in either *TSC1* or *TSC2* are found. Inactivation of TSC1/TSC2 leads to constitutive mTOR activation, and the disease is characterised by multiple harmartomas (benign tumours) in numerous organs including the kidney and brain (Crino et al. 2006). The following sections will consider the different pathways through which the TSC1/2 – Rheb – mTOR interaction is altered, and alternative mechanisms by which mTORC1 activity is controlled.

#### 1.2.3.1 Growth factors

By binding to receptor tyrosine kinases, growth factors can activate mTOR by two pathways. One of the most well characterised activators of mTOR is the insulin and insulin like growth factor 1 (IGF-1) pathway. Receptor activation leads to downstream signalling along the phosphoinositide 3-kinase (PI3K) – protein kinase b (AKT) pathway and the rat sarcoma (Ras) – rapidly accelerated fibrosarcoma (Raf) – mitogen-activated protein kinase kinase (MEK) –

extracellular signal-regulated kinase (ERK) pathways (described in more detail in section 1.3). ERK and AKT both phosphorylate and inactivate TSC1/2, thereby activating mTORC1 (Inoki et al. 2002, Manning et al. 2002). AKT has also been shown to phosphorylate PRAS40 causing it to dissociate from mTORC1, releasing mTORC inhibition (Sancak et al. 2007).

#### 1.2.3.2 Amino acids

Amino acids, especially leucine, arginine and tryptophan, are essential for full activation of mTORC1, but the mechanism for this has only relatively recently been uncovered and shown to be dependent on the Ras related GTP binding protein (Rag) GTPases (Sancak et al. 2008, Wang et al. 2015). There are four Rag GTPases, A – D, which form heterodimers. Amino acids stimulate Rag A/B, through a vacuolar adenosine triphosphate hyrdrolase (ATPase), to interact with RAPTOR, and recruit mTORC1 to the lysosomal surface where it docks with a protein called Ragulator, which is required for mTORC1 activation (Sancak et al. 2010, Zoncu et al. 2011).

#### 1.2.3.3 Cellular stresses

The energy status of the cell is sensed as the adenosine diphosphate:adenosine triphosphate (ADP:ATP) ratio by liver kinase B1 (LKB1). When ATP levels fall, LKB1 activates AMP-activated protein kinase (AMPK), which has two actions. The first is to phosphorylate and activate TSC2 (Inoki et al. 2003b). The second is to reduce mTOR activity through phosphorylating RAPTOR and reducing mTOR activity (Gwinn et al. 2008).

One of the HIF target genes that is induced by hypoxia is regulated in development and DNA damage response 1 (REDD1). REDD1 is a TSC2 activator, and consequently an inhibitor of mTOR in hypoxia (Brugarolas et al. 2004). mTOR can also be inhibited by DNA damage, which inhibits mTORC1 via a variety of p53 dependent mechanisms including increased phosphatase and tensin homolog (PTEN) expression which dephosphorylates PI3K and down-regulates mTORC1 activity, increased TSC2 expression and activation of AMPK (Feng et al. 2005, Budanov and Karin 2008).

### 1.2.4 Activation of mTORC2

Little is known of the precise mechanisms that activate mTORC2. This mTOR complex is not sensitive to the nutrient inputs that control mTORC1, but is activated by growth factors such as insulin and IGF-1, possibly in a PI3K dependent manner (Jacinto et al. 2006). There is possibly also a role for TSC1/2, where inactivating mutations supresses growth factor stimulated phospho AKT in a Rheb/mTORC1 independent manner (Huang et al. 2008).

### 1.2.5 Actions of mTORC1

#### 1.2.5.1 Translation

The best characterised action of mTORC1 is to promote protein synthesis. It does this through the phosphorylation of two downstream targets, the eukaryotic initiation factor 4E binding protein 1 (4E-BP1) and S6 kinase (S6K) (Figure 1-1).

When 4E-BP1 is unphosphorylated, it binds eukaryotic initiation of translation factor 4E (eIF4E), sequestering it and preventing it from joining the eIF4F complex (Pause et al. 1994, Beretta et al. 1996). The eIF4F complex is the initiator of cap dependent translation, and initiation of translation is the rate determining step and therefore the key determinant of protein synthesis (Gross et al. 2003). 4E-BP1 is phosphorylated by mTORC1 at multiple sites including threonines 36, 45 and 69, and serine 64. mTOR itself is the kinase of at least threonine 36 and 45 phosphorylations and causes 4E-BP1 to dissociate from eIF4E (Heesom and Denton 1999, Livingstone and Bidinosti 2012) (Figure 1-2).

S6K promotes translation, and its target S6 is often used as a measure of mTOR activity (Boulay et al. 2004). The first S6K target to be identified was the ribosomal S6 protein (S6). S6 forms part of the 40S ribosomal subunit and has been shown to interact with messenger RNA (mRNA) and transfer RNA (tRNA). Phosphorylation of S6 has been associated with increased cell size and translation of mRNA with 5' terminal oligopyrimidine tracts (TOP) (Ruvinsky and Meyuhas 2006). S6K also phosphorylates and targets programmed cell death protein 4 (PCDC4) for degradation. PCDC4 is an inhibitor of the RNA helicase eIF4A, which unwinds complex structures in the 5' untranslated region of mRNA (Dorrello et al. 2006). In addition to this indirect release of eIF4A activity, SK6 also phosphorylates eIF4B, which activates eIF4A (Raught et al. 2004) (Figure 1-2). mTOR also promotes translation by causing an increase in ribosome biogenesis, including synthesis of ribosomal RNA and transfer RNA (tRNA)(Kantidakis et al. 2010).

Protein synthesis is required to increase cell size, and cell proliferation. Work in 4E-BP1 knockout cells suggests that the 4E-BP1 – eIF4E pathway regulates cell proliferation, but that the S6K pathway regulates cell size (Dowling et al. 2010).

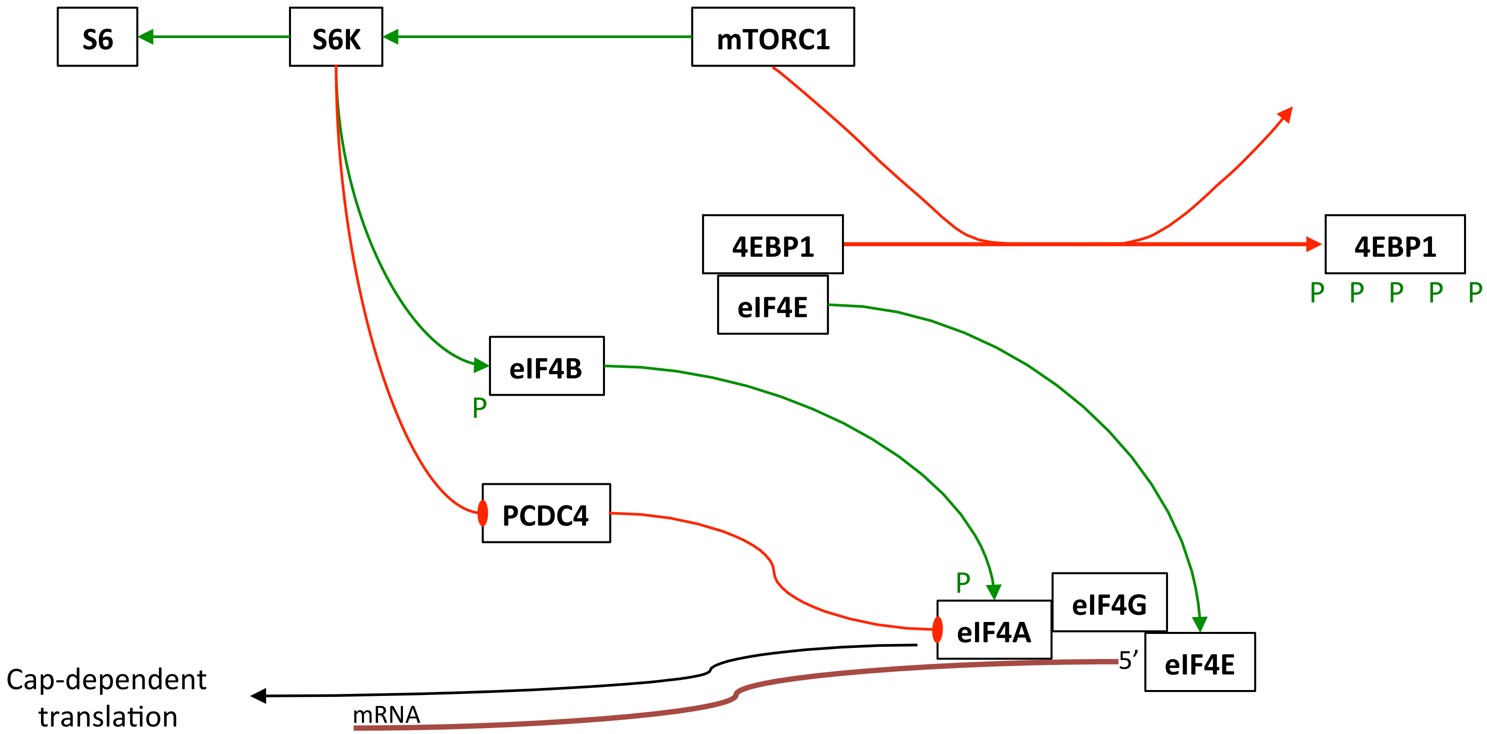


**Figure 1-2 Translation initiation**

When activated, mTORC1 promotes cap-dependent translation through the release of eIF4E from 4E-BP1 and activation of the RNA helicase eIF4A. EIF4A, eIF4E and eIF4G together make up the eIF4F complex. eIF (eukaryotic initiation of translation factor) PCDC4 (programmed cell death protein 4)

#### 1.2.5.2 Metabolism

mTOR affects metabolism in two ways to facilitate protein synthesis, cell growth and division. The first is through the translation of HIF1α, which increases glycolytic flux (Hudson et al. 2002, Duvel et al. 2010). The second effect is on lipid biogenesis, through sterol regulatory element-binding protein 1/2 (SREBP1/2) transcription factors (Duvel et al. 2010).

#### 1.2.5.3 Autophagy

In addition to activating anabolic processes, mTORC1 also phosphorylates and inactivates the kinase complex required to initiate autophagy. This complex consists of three proteins, unc-51 like kinase (ULK1), mammalian autophagy related gene 13 (atg13) and focal adhesion kinase family-interacting protein of 200 kDa (FIP200). RAPTOR binds to ULK1, and both ULK1 and atg13 are phosphorylated by mTOR. When mTORC1 is inactivated, RAPTOR releases ULK1 (Hosokawa et al. 2009). The role of autophagy in cancer appears to be complex, and may contribute to the ability of cancer cells to survive during periods of starvation, or during drug treatments, which suggests a role in tumourogenesis, but there is also evidence that autophagy works in a tumour suppressor role (Chen and Debnath 2010).

### 1.2.6 Actions of mTORC2

mTORC2 was discovered to be the kinase responsible for the phosphorylation of AKT on S473 (Sarbassov et al. 2005). AKT is also phosphorylated on threonine 308 by phosphoinositol dependent kinase 1 (PDK1) in response to ligand stimulation of receptor tyrosine kinases and PI3K activation. S473 phosphorylation of AKT by mTORC2 facilitates phosphorylation on threonine 308 and full activation of AKT (Scheid et al. 2002). As well as activating AKT, mTORC2 regulates other members of the AGC family including protein kinase C-α (PKC-α) and serum - and glucocorticoid – induced protein kinase 1 (SGK1) (Garcia-Martinez and Alessi 2008, Ikenoue et al. 2008). mTORC2 influences the cytoskeleton to promote cell spreading *in vitro* through activating PKC-α, paxillin and Rho GTPases (Jacinto et al. 2004, Sarbassov et al. 2004).

Through activating AKT and SGK1, mTORC1 controls the activity of the transcription factor forkhead box O1/3a (FoxO1/3a). AKT and SGK1 phosphorylate FoxO1/3a and promote its nuclear export and inactivation (Brunet et al. 1999a, Schachter et al. 2012). FoxO1/3a is a transcription factor that promotes expression of pro apoptotic proteins such as Bim, and downregulates antiapoptotic proteins (Dansen and Burgering 2008). AKT also has a known role in activating mTORC1, through phosphorylation of TSC2 and PRAS40, as discussed earlier, but this role may not be mediated by mTORC2, given that RICTOR null mouse models show defective pAKT signalling to FoxO1/3a, but not to TSC2 (Guertin et al. 2006).

## 1.2.7 Inhibitors of mTOR

### 1.2.7.1 Allosteric mTOR inhibitors

The first inhibitor of mTOR to be identified was rapamycin, and as explained above, it was actually through rapamycin that mTOR was identified and characterised. Rapamycin was originally developed as a macrolide antibiotic, but immunosuppressive effects limited its use. It subsequently found a role in transplant medicine as an anti-rejection immunosuppresive. Its use however is complicated by poor bioavailability, which is altered by fat content in meals, and has necessitated monitoring of drug levels to optimise dosing in individual patients (Murakami et al. 2014).

Subsequently, several rapalogues were manufactured based upon rapamycin, but with improved bioavailability. The two most clinically advanced of these are everolimus and temsirolimus. Everolimus is an oral medication, and temsirolimus is an intravenous preparation. Temsirolimus is a pro drug that is converted to sirolimus, with both compounds detectable in the blood of treated patients.

All the rapalogues share a common mechanism of action, and also share common side effects. Rapalogues are allosteric inhibitors of mTOR, and the precise mechanism of their action is not completely understood (Guertin and Sabatini 2009). What is known is that rapamycin binds to the intracellular FK506-binding protein (FKBP12) (Brown et al. 1994, Sabatini et al. 1994) and that FKBP12 – rapamycin then interacts with mTOR at a site distant to the kinase domain. Although the mechanism by which this causes inhibition of mTOR is not established, it has been noted that binding causes the dissociation of RAPTOR from the mTORC1 complex (Kim et al. 2002, Yip et al. 2010).

Rapalogues show specificity for binding and inhibiting mTORC1, and indeed, mTORC2 was initially characterised as rapamycin insensitive. This insensitivity is not however complete, and prolonged rapamycin treatment in myeloma, prostate cancer, hepatic cancer, glioblastoma, melanoma, leukaemia and lymphoma cell lines has been shown to inhibit mTORC2 activity, possibly through binding to free mTOR and preventing the formation of the mTORC2 complex (Sarbassov et al. 2006).

There are some notable class side-effects of rapalogues. All can cause immunosuppression, and the consequent risk of infection, and additionally all rapalogues have metabolic effects, resulting in hyperglycaemia and hypercholesterolaemia in a subset of patients. In phase III trials, the use of temsirolimus and everolimus was associated with an approximately 10% incidence of pneumonitis, which could range from an asymptomatic radiological finding, to a treatment limiting symptomatic condition characterised by cough and dyspnoea, requiring cessation of rapalogue and treatment with corticosteroids (Hudes et al. 2007, Motzer et al. 2008). Retrospective reviews of treated patents suggest that the incidence of pneumonitis may in fact be higher (Dabydeen et al. 2012).

The efficacy of the rapalogues has been tested in a number of clinical trials over the last 7-8 years. Temsirolimus is licenced for the first line treatment of advanced renal cancer with poor prognostic features, following a phase III clinical trial in which temsirolimus was compared to interferon α, or the combination of interferon α and temsirolimus. Temsirolimus as single agent prolonged overall survival from 7.3 months with interferon α to 10.9 months, and progression free survival increased from 1.9 months to 3.8 months. Objective response rates were modest, with 8.4% of patients experiencing a response to temsirolimus. The combination treatment did not improve efficacy (Hudes et al. 2007). This trial recruited patients with clear cell and non-clear cell renal carcinomas, and subgroup analysis indicated that temsirolimus was active in both groups (Dutcher et al. 2009).

Second line temsirolimus was compared to sorafenib after progression on sunitinib, and although progression free time was the same, the overall survival with sorafenib was longer than with temsirolimus (16.6 months vs. 12.3 months) and although the causes for this are unclear, it is possible once again that overall survival was confounded by subsequent treatments, and data on these was not systematically recorded in the trial. The overall response rate with both drugs was 8% (Hutson et al. 2014).

The second licenced mTOR inhibitor is everolimus, which is used as second line treatment after failure of sunitinib or sorafenib. In this setting, everolimus prolonged median progression free survival from 1.9 months for placebo, to 4 months. Response rates were lower than seen for first line temsirolimus, at 4%, but disease stabilisation (stable disease for greater than 56 days) was seen in 63% (Motzer et al. 2008). Updated results increased the median progression free survival with everolimus to 5.5 months, but overall survival, at 14.8 months was not greater than placebo. As with many other recent trials in renal cancer, the overall survival data are likely confounded by crossover from placebo to active drug, and in this trial, 80% of the placebo group received everolimus (Motzer et al. 2010). Similarly to temsirolimus, there is evidence that everolimus is active against renal cancer histologies of both clear cell and non-clear cell type (Koh et al. 2013).

In addition to its use in renal cancer, everolimus is also used in combination with the aromatase inhibitor exemestane in hormone receptor positive advanced breast cancer (Baselga et al. 2012). In pancreatic neuroendocrine tumours everolimus has shown efficacy as a single agent, and in combination with octreotide (Pavel et al. 2011, Yao et al. 2011). In subependymal giant cell astrocytomas, which are found in 20% of children with tuberous sclerosis complex, everolimus has been shown to reduce the bulk of these brain tumours and decrease seizure frequency (Krueger et al. 2010)

Despite the fact that some case series report evidence of activity of VEGFR targeted therapy including sunitinib, pazopanib and sorafenib in non clear cell renal cell carcinoma, the response rates may be quite low in comparison to clear cell renal cell carcinoma (Tannir et al. 2012, Bellmunt and Dutcher 2013). In light of the uncertainty of the benefit derived from anti-VEGFR therapies in non clear cell renal cell carcinoma, trials are underway comparing mTOR inhibition to VEGFR inhibition in the first line setting in this group.

#### 1.2.7.2 Kinase inhibitors of mTOR

The latest generation of mTOR inhibitors target the kinase domain of mTOR in an ATP dependent manner, and consequently inhibit both mTORC1 and mTORC2 with comparable potency. The first two mTOR kinase inhibitors to be developed were Torin and PP242 (Feldman et al. 2009, Thoreen et al. 2009). Both showed the expected activity against mTORC1 and mTORC2, but also revealed more incomplete inhibition of mTORC1, particularly showing greater and more prolonged inhibition of phosphorylation of 4E-BP1. Other mTORC kinase inhibitors have followed including AZD2014 and AZD8055 (Chresta et al. 2010). A second class of mTORC kinase inhibitors that also inhibit the closely related

PI3K have also been developed, including BEZ235 (Maira et al. 2008) and PI-103 (Knight et al. 2006).

These drugs have entered early phase clinical development. Preliminary results indicate that AZD2014 was tolerable, and inhibited mTORC1 and mTORC2 *in vivo* in mixed solid tumours (Banerji et al. 2012). This drug is currently undergoing further clinical testing, including in renal cancer. An earlier compound AZD8055 was also tested in a phase I trial, but is not being actively pursued in further clinical trials (Naing et al. 2012a).

BEZ235 has completed early phase clinical trials and despite problems with bioavailability and formulations, the drug has entered further clinical trials, and results of additional trials, including in renal cancer, are awaited (Burris et al. 2010, Peyton et al. 2012). Other PI3K/mTORC kinase inhibitors including SAR245409 (Papadopoulos et al. 2014), GSK2126458 (Munster et al. 2011), PF-04691502 (Britten et al. 2014), GDC-0980 (Wagner et al. 2009), and BGT226 (Markman et al. 2012) have been tested in phase I clinical trials.

Although there are now numerous targeted therapies for the treatment of renal cell carcinoma, beyond first line treatment, response rates are low, and time to progression remains relatively short. Primary and acquired resistance to these drugs is a real clinical problem, and will be discussed in more detail below. Understanding of these problems may lead to identification of biomarkers upon which to select patients for particular treatments, or to suggest combination treatments to overcome resistance.

### 1.2.8 Predictors of sensitivity and resistance to mTORC1 inhibition

It is a growing theme throughout the clinical practise of oncology that treatments should be targeted towards appropriate groups of patients. This practice is well established in terms of using physical criteria (cancer staging) to select local therapies such as surgery, and is increasingly being applied through use of biomarkers to guide systemic treatments. Some such biomarkers are selected because their presence predicts response to treatment, e.g. the use of anti oestrogens and human epidermal growth factor receptor 2 (HER2) antibodies in breast cancer based upon expression of oestrogen receptor and overexpression of HER2 receptor respectively (Andre et al. 2014). Mutations have also been identified as positive predictive factors, for example in the treatment of non-small-cell lung cancer with inhibitors of EGFR, where activating *EGFR* mutation predicts for response (Lynch et al. 2004). Mutations can also be negative predictive factors, such as the influence of activating *KRAS* mutations as predictors of resistance to EGFR antibody cetuximab in the treatment of colorectal cancer (Sorich et al. 2014).

There has been interest in identifying similar markers that could guide use of mTOR inhibitors, but without the same level of success. At present there are no validated biomarkers of response or resistance, although several pathways have shown limited promise. The use of mTOR inhibitors in renal cancer was trialled in part because recognition that mTOR promotes the translation of HIF, which is an important oncogenic protein in VHL deficient renal cancer (Maxwell et al. 1999, Biswas et al. 2012). Therefore absence of functional VHL was thought to be a good candidate for predicting response to treatment, and some preclinical data supported the hypothesis (Thomas et al. 2006). However, results from the phase III clinical trials of temsirolimus and everolimus were not supportive of VHL as a potential biomarker. The general response rate was low despite the majority of CCRCC lacking functional VHL due to mutations or epigenic gene silencing (Gnarra et al. 1994, Herman et al. 1994). Moreover, responses were seen in non-clear cell renal cancer, which does not harbour *VHL* mutation (Hudes et al. 2007, Motzer et al. 2008, Dutcher et al. 2009, Koh et al. 2013). Other markers that have been considered are activators of the mTOR pathway, including *PTEN* and *PIK3CA*, which are commonly mutated in cancers (see Figure 1-1)(Li et al. 1997, Steck et al. 1997, Samuels et al. 2004, Chalhoub and Baker 2009). Inactivation of PTEN, or activation of PI3K both cause AKT activation, and downstream mTORC1 activation. There is some evidence that PTEN null mouse embryonic fibroblasts (MEFs) and human cancer cell lines are more sensitive to mTOR inhibition (Neshat et al. 2001). There is also evidence that cell lines harbouring activating mutations in *PIK3CA* are more sensitive to mTOR inhibition, and those with KRAS mutation are more resistant, while cell lines harbouring mutations in both genes have an intermediate sensitivity (Ducker et al. 2013).

As well as searching for pre-treatment biomarkers of response or resistance, there has also been interest in the implications for sensitivity of the signalling response of the cell to treatment with mTOR inhibition. Particular attention has focused on a feedback circuit that potentiates signalling via the insulin like growth factor 1 receptor (IGF-1R). When mTOR is active, S6K phosphorylates insulin receptor substrate 1 (IRS1) on serine 612, which leads to IRS-1 dissociating from the IGF-1R and being degraded, limiting signalling from the

IGF-1R to PI3K and AKT. However, when mTORC1 is inactivated by rapamycin this feedback loop is inactivated, signalling via the IGF-1R to AKT is potentiated, and AKT is activated (O'Reilly et al. 2006, Wan et al. 2007). This pathway is summarised in Figure 1-3.

Previous work in our group showed that this feedback loop is also active in CCRCC cell lines, and that treatment with rapamycin causes an increase in pAKT. Further work showed that small interfering RNA (siRNA)-induced depletion of the IGF-1R abrogated this signalling, and sensitised renal cancer cell lines to treatment with rapamycin (Yuen et al. 2009).

Other groups have shown similar feedback activation acting via the PDGFR (Zhang et al. 2007, Ho et al. 2012). Alternative feedback loops may also activate the mitogen activated protein kinase (MAPK) pathway resulting in increased phosphorylation of ERK (Carracedo et al. 2008). There is considerable interest in these pathways as potential mediators of clinical resistance to mTOR inhibition.

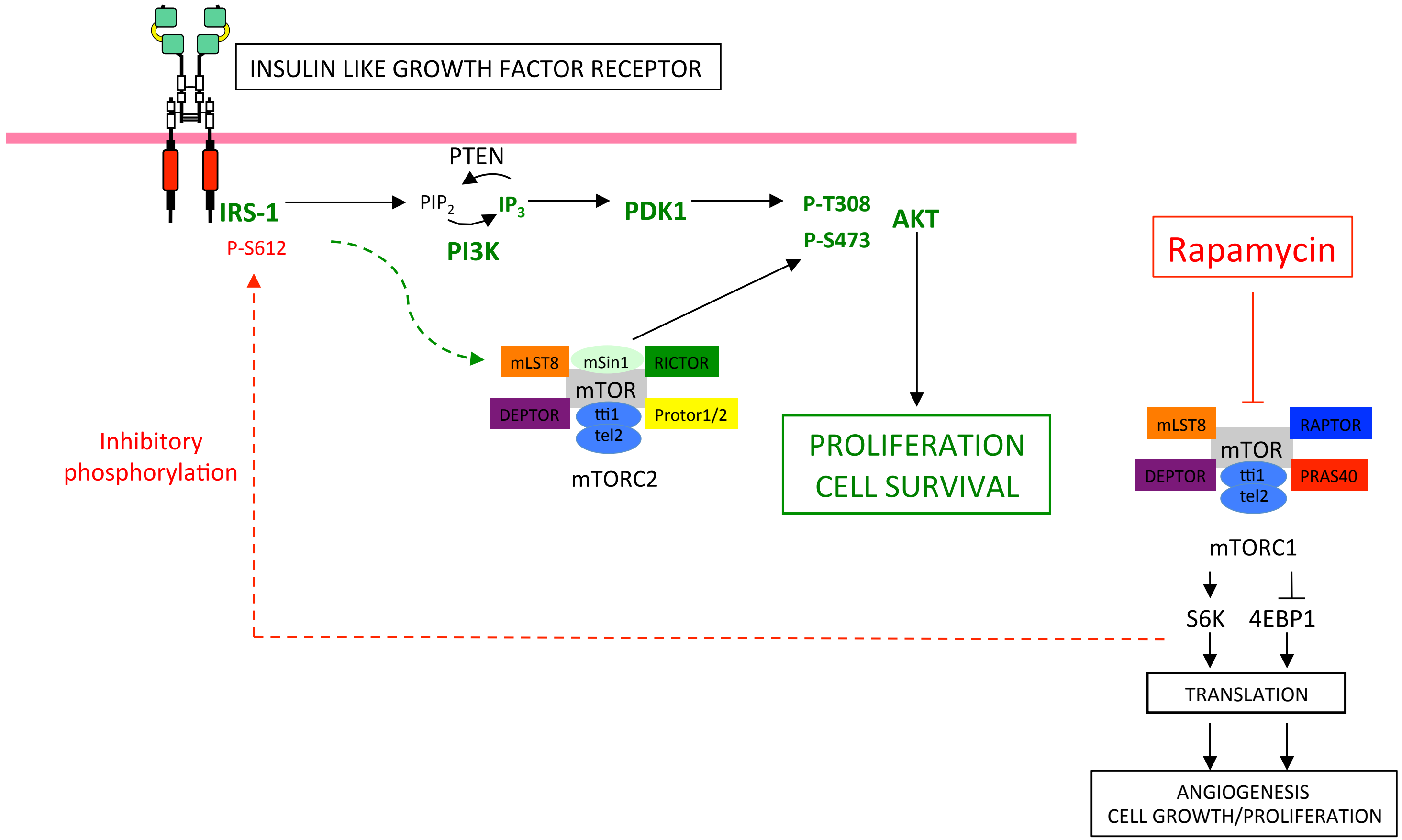


**Figure 1-3 Inhibition of mTORC1 by rapamycin potentiates signalling via the IGF-1R to AKT**

S6K phosphorylates IRS-1 on S612, which leads to dissociation from IGF-1R and degradation, thereby abrogating IGF-1R signalling. When mTORC1 is inhibited by rapamycin, S6K activity decreases and the inhibitory feedback onto IRS-1 is relieved. This allows potentiation of IGF-1R signalling. Dashed green arrow indicates activation of mTORC2 via an unknown mechanism of action.

## 1.3 The insulin like growth factor 1 receptor

The IGF-1R is a receptor tyrosine kinase that is ubiquitously expressed in normal tissues (Moschos and Mantzoros 2002). The IGF-1R axis consists of the ligands IGF-1, and IGF-2, the IGF binding proteins (1-6), the IGF-1R and hybrid receptors formed with the insulin receptor (IR). The highest affinity ligand for the IGF-1R is IGF-1, which has 5 fold greater affinity than IGF-2, and one thousand fold greater affinity than insulin. IGF-1 is produced and secreted by the liver in response to growth hormone, and locally in tissues where it exerts paracrine and autocrine effects (Cohick and Clemmons 1993, De Meyts et al. 1994).

### 1.3.1 Structure of the IGF-1R

The IGF-1R is a heterotetrameric receptor comprising of 2 extracellular α subunits, and 2 transmembrane β subunits linked by disulphide bonds. $\alpha$ and β subunits are cleaved from a single proreceptor (Chitnis et al. 2008). The IGF-1R and IR share 70% homology, which is greater in the kinase domain at 84% (Ullrich et al. 1986). The IGF-1R can form hybrid receptors with two isoforms of the insulin receptor. IRB, which contains exon 11, forms hybrid receptors that behave similarly to the IGF-1R and are responsive to IGF-1. The IRA is the foetal isoform, that lacks exon 11, and which behaves more like IGF-1R, being activated by IGF-2 to induce proliferation and cell survival. IRA also forms hybrids with IGF-1R, and these are responsive to IGF-1, IGF-2 or insulin and elicit proliferative and migratory effects (Belfiore et al. 2009).

### 1.3.2 Activation of the IGF-1R

Upon ligand binding, the IGF-1R undergoes conformational change, and autophosphorylates tyrosines 1131, 1135 and 1136, all of which lie within the kinase domain, activating the IGF-1R tyrosine kinase. The IGF-1R also autophosphorylates other residues which act as docking sites for scaffolding proteins (Adams et al. 2000). The recruitment and tyrosine phosphorylation of IRS-1 allows for recruitment of the p85 subunit of PI3K via its src homology 2 (SH2) domain (Engelman et al. 2006a). The p110 catalytic subunit of PI3K then catalyses the conversion of phosphatidylinositol 4,5-biphosphate ($PIP_2$) into phosphatidylinositol 3,4,5-triphasphate ($PIP_3$) at the plasma membrane. $PIP_3$ recruits AKT to the plasma membrane, where it is phosphorylated at threonine 308 by PDK1 (Courtney et al. 2010).

Recruitment of other scaffold proteins allows activation of a second major signalling pathway. Src homology and collagen domain protein (Shc) is recruited tp activated IGF-1R, leading to recruitment of by growth factor receptor bound protein 2 (GRB2) and son of sevenless (SOS) which is a guanine nucleotide exchange factor. SOS activates Ras proteins, leading to activation of the MAPK pathway (illustrated in Figure 1-1) (Katz et al. 2007).

### 1.3.3 Functions of the IGF-1R

Through activating the PI3K – AKT – mTOR and RAS - RAF – ERK pathways, the IGF-1R has effects on cell growth, proliferation and survival. It also exerts effects on motility, invasion and angiogenesis, by inducing the expression of matrix-metalloproteinases and the pro-angiogenic HIF and consequently VEGF (Fukuda et al. 2002, Zhang et al. 2003).

The IGF-1R axis has been associated with malignancy in numerous ways. Increased circulating IGF-1 levels are associated with increased risk of developing malignancy (Hankinson et al. 1998, Pollak et al. 2004). Conversely, congenital IGF-1 deficiency in Laron Syndrome confers a reduced risk of malignancy (Guevara-Aguirre et al. 2011, Steuerman et al. 2011). The IGF-1R appears to be important for anchorage independent growth, and is absolutely required for cellular transformation (Sell et al. 1993, Sell et al. 1994).

### 1.3.4 The IGF-1R in renal cancer

The IGF-1R is frequently overexpressed in cancer, including renal cancer where it confers a worse prognosis and is associated with higher grade tumours (Ahmad et al. 2004a, Parker et al. 2004). Previous work in our group showed that IGF-1R mRNA is upregulated in VHL deficient CCRCC, but not VHL proficient papillary renal carcinoma. This was shown to be due to the ability of VHL to sequester the Sp1 transcription factor, preventing activation of the IGF-1R promoter (Yuen et al. 2007). Our group further showed that the cellular location of the IGF-1R is of prognostic importance in renal cancer: IGF-1R can translocate to the nucleus of renal cancers, and is associated with worse prognosis (Aleksic et al. 2010).

### 1.3.5 Inhibitors of the IGF-1R

There are three main classes of clinical IGF-1R inhibitor: monoclonal IGF-1R antibodies, which tend to be specific for the IGF-1R, antibodies against the ligands, and small molecule inhibitors, which also inhibit the IR, because of the homology in the kinase domains (Ullrich et al. 1986, King et al. 2014). Although responses to single agent IGF-1R inhibition have been seen in rare tumours including Ewings sarcoma, (Olmos et al. 2010), there have not been dramatic response in other solid tumours (Haluska et al. 2007). Clinical development therefore focused on use of IGF-1R inhibitors in combination with standard therapies or other targeted agents. One such example was the addition of the monoclonal antibody figutumumab to carboplatin and paclitaxel in non-small cell lung cancer. Despite encouraging data from a phase II trial, results from a large phase III trial were not positive (Langer et al. 2014). This trial, and others with similar designs were for the treatment of unselected patients, and there are, as yet, no biomarkers indicating likely response to IGF-1R treatment.

IGF-1R tyrosine kinase inhibitors such as OSI-906 (Mulvihill et al. 2009) offer potential advantages over monoclonal antibodies. They are orally administered, which is preferred by patients, and they have a shorter half-life, which allows flexibility in timing of dosing in combinations with chemotherapeutics. Small molecule inhibitors may be able to penetrate the blood brain barrier in a manner that monoclonal antibodies cannot (Pan et al. 2007). In the IGF-1R field in particular, small molecule inhibitors may have one other advantage. By inhibiting the anti-apoptotic insulin receptor variant IRA as well as the IGF-1R, they may be more effective as the IRA may play a role in compensating for IGF-

1R inhibition (Ulanet et al. 2010, Buck and Mulvihill 2011). The disadvantage of this dual IGF-1R/IR inhibition is that blockade of the IRB causes hyperglycaemia as dose limiting toxicity (Macaulay et al. 2011, Puzanov et al. 2015).

## 1.4 The aims of this project

The principal objective of this project was to understand the mechanisms by which cancers are resistant to the effects of mTOR inhibition, specifically in the context of clear cell renal cell cancer.

### 1.4.1 Hypotheses:

1. Activation of the IGF-1R – PI3K – AKT pathway in clear cell renal cell cancer contributes to resistance to mTOR inhibition.
    a. Inhibition of this pathway with small molecule inhibitors of the IGF-1R can sensitise to rapalogue inhibition of mTOR.
    b. Mutant *VHL* status, which upregulates IGF-1R, is a biomarker for activation of this resistance pathway and sensitisation by IGF-1R inhibition.

    **Aims:**

    Test small molecule inhibitors of the IGF-1R – PI3K – AKT pathway, developed for clinical use, in CCRCC *in vitro* and to test the ability of such inhibitors to sensitise CCRCC cells to rapamycin.
    Use isogenic *VHL* mutant pairs of cell lines with stably transfected wild type *VHL*, or empty vector to test the role of *VHL* mutation status in affecting the ability of IGF-1R inhibitors to sensitise to mTOR inhibition.
2. CCRCC cells resistant to mTOR kinase inhibition can be created *in vitro* by continuous culture in an mTOR kinase inhibitor.
    a. mTOR kinase resistant CCRCC cells will have altered signalling pathways characterised by altered gene expression, protein

expression, or posttranslational modification (phosphorylation) that mediate resistance.

**Aims:**

To create mTOR kinase resistant CCRCC cells by continuous culture in drug by two methods; firstly by slow incremental increase in the concentration of drug as cells adapt to its presence, secondly by introducing the drug at high concentration and culturing surviving cells.

To screen mTOR kinase resistant CCRCC cells at the protein and phosphoprotein level to detect altered signalling networks.

To screen mTOR kinase resistant CCRCC cells at the gene transcription (mRNA) level by micro array.

To validate the hits from the screens by alternative techniques and to test the functional relevance of the altered pathways by the use of small molecule inhibitors and protein depletion with siRNA.

3. The properties of the mTOR kinase resistant CCRCC cells will reveal insight into the mechanism of resistance
    a. mTOR kinase resistant CCRCC cells may show reactivation of key mTOR targets, i.e. resistance occurs through reactivation of the inhibited mTOR pathway.
    b. The stability of the mTOR kinase resistance phenotype on withdrawal of the inhibitor from continuous culture will give insight into the mechanism through which resistance to drug was gained, i.e. reversible inhibition may indicate an epigenetic mechanism, stability of the phenotype may indicate gene mutation.

**Aims:**

To test the mTOR kinase resistant CCRCC cells to alternative inhibitors of the mTOR pathway.

To examine the downstream signalling from mTORC1 and mTORC2 and investigate the mechanism of any reactivated signalling.

To establish the stability of mTOR kinase resistance phenotype during prolonged withdrawal of drug from continuous culture. If loss of resistance is detected, to investigate the contribution of epigenetic modifications to mTOR kinase inhibition through the use of clinical inhibitors of histone deacetylases.

# 2 Methods

## 2.1 Cell culture

### 2.1.1 General techniques

Cell culture was performed in sterile tissue culture hoods. Cells were maintained in tissue culture grade flasks dishes or plates (Falcon or Nunc) in humidified incubators with 10% $CO_2$ and 90% air. Cells were negative for mycoplasma when tested with the MycoAlert detection kit (Lonza, UK).

#### 2.1.1.1 Recovery of cryopreserved cells

To unbank cells from cryostorage, a vented cap tissue culture flask was prepared and warmed to 37$^{O}$C with 50 ml of complete medium. A cryovial was retrieved from the liquid nitrogen store and kept on dry ice until ready to be thawed. Thawing was performed in a 37$^{O}$C water bath with regular mixing to ensure rapid thawing. As soon as the cells were fully thawed they were transferred into the pre-warmed tissue culture flask. The following day medium was exchanged for 25 ml of fresh complete medium. Cells were passaged three times as described below before use.

#### 2.1.1.2 Subculture

Cells were cultured in the growth media specified in Table 2-1 supplied by Invitrogen Gibco, supplemented with 10% foetal calf serum (FCS PAA Laboratories) and 100 units/ml penicillin and 0.1 mg/ml streptomycin. For routine passaging of cells, disaggregation was performed with 3 mM EDTA in phosphate buffered saline (PBS) for 5 minutes at 37$^{O}$C followed by gentle tapping of the flask sides. The EDTA was diluted with an equal volume of complete medium before transfer to a centrifuge tube for pelleting of cells by centrifugation at 1200 rpm for 5 minutes. Cells were resuspended in complete medium for reseeding into tissue culture flasks. Routine weekly passage was conducted by a 1:30 split for 786-0EV, 786-0VHL, RCC4EV and RCC4VHL cell lines, and 1:5 for UMRC2VA and UMRC2VHL cells.

#### 2.1.1.3 Cryopreservation and cell banking

To cryopreserve and bank cells, disaggregation and cell pelleting was performed as above followed by resuspension in 1 ml of ice cold freezing medium (10% DMSO, 50% FCS and 40% Dulbecco's Modified Eagle Medium (DMEM)) and aliquoting into round bottom cryovials (Corning, Fisher Scientific, UK). Vials were frozen down to -80$^{O}$C at 1$^{O}$C/min in an isopropanolol-bath freezing container. After 24 hours vials were transferred to liquid nitrogen.

### 2.1.2 Cell lines

The cell lines used in this project are listed in Table 2-1. Three isogenic pairs of human CCRCC cell lines were used. The parental cell lines all lack functional pVHL due to mutations in the *VHL* gene as described in Table 2-2. Functional wild type pVHL had been re-expressed by stable transfection. The 786-0 cells had been stably transfected with empty vector (pRc) or wild type pVHL (pRc HA.VHL (1–213)) containing an $NH_2$-terminal HA epitope tag, to generate sublines 786-0EV, 786-0VHL (Iliopoulos et al. 1995). RCC4 (Maxwell et al. 1999) and UMRC2 (Zatyka et al. 2002) were transfected with empty vector or pcDNA3-VHL and stable integrants were selected using G418 to create RCC4EV, RCC4VHL and UMRC2VA, UMRC2VHL. The 786-0 and RCC4 isogenic pairs were obtained from Cancer Research UK Laboratories, Clare Hall, Hertfordshire, UK. The UMRC2 isogenic pair was gifted by Dr D Mole, Wellcome Trust Centre for Human Genetics, University of Oxford. All cell lines were maintained in complete media as described above with the addition of G418 0.5 mg/ml (Invitrogen). Cell lines were not formally authenticated by short tandem repeat profiling during this project.

| Cell Line | Origin | Medium | Culture Conditions |
|---|---|---|---|
| 786-0EV | Human CCRCC | DMEM | 10% $CO_2$ |
| 786-0VHL | Human CCRCC | DMEM | 10% $CO_2$ |
| RCC4EV | Human CCRCC | DMEM | 10% $CO_2$ |
| RCC4VHL | Human CCRCC | DMEM | 10% $CO_2$ |
| UMRC2VA | Human CCRCC | DMEM | 5% $CO_2$ |
| UMRC2VHL | Human CCRCC | DMEM | 5% $CO_2$ |

**Table 2-1 Cell lines used in this project. EV (transfected with empty vector), VA (transfected with vector alone) VHL (transfected with wild type VHL)**

| Cell Line | Mutation | Consequence | Reference |
|---|---|---|---|
| 786-0 | 1 nt deletion 523 | Codon 104 Frameshift | (Gnarra et al. 1994, Zatyka et al. 2002) |
| RCC4 | C407G | Ser65Trp | (Gnarra et al. 1994) |
| UMRC2 | G458C | Arg82Pro | (Zatyka et al. 2002) |

**Table 2-2 VHL status of cell lines used in this project**

### 2.1.3 Treatment with small molecule inhibitors

The small molecule inhibitors used in this project are listed in Table 2-3. Rapamycin was purchased as 5 mM solution in DMSO (Calbiochem) and was aliquoted into single use aliquots before being stored at -20$^{O}$C and protected from light. All other inhibitors were supplied as powders and were dissolved in the required volume of DMSO to achieve the stock concentration as listed in Table 2-3 before aliquoting into single use aliquots and storing at -20$^{O}$C or -80$^{O}$C.

For individual experiments OSI-906 was first diluted in DMSO before being further diluted in pre-warmed complete medium containing 5% DMSO to produce a 10X stock solution of OSI-906. All other drugs were diluted to the required concentration directly into complete medium. Control cells in each experiment were treated with complete medium containing an equal concentration of DMSO to that of drug treated cells.

| Drug | Source | Stock Concentration | Molecular Target | Notes |
|---|---|---|---|---|
| Rapamycin | Calbiochem | 5 mM (DMSO) | mTORC1 | Allosteric inhibitor. Specific to mTORC1, but prolonged exposure inhibits mTORC2 in some models. |
| OSI-906 | OSI Pharmaceuticals | 10 mM (DMSO) | IGF-1R | Kinase inhibitor of IGF-1r with $IC_{50}$ 0.035 μM. Inhibits IR at $IC_{50}$ 0.075 μM. |
| AZ12253801 | AstraZeneca | 10 mM (DMSO) | IGF-1R | Kinase inhibitor. Also inhibits IR. Off target effects against aurora kinase above 300 nM. |
| BKM120 | Selleckchem | 20 mM (DMSO) | PI3K | ATP competitive inhibitor, also inhibits PI3K with known activating mutations. See Table 3-3 |
| BEZ235 | Selleckchem | 10 mM (DMSO) | mTORC1, mTORC2 | APT competitive inhibitor of mTOR, also active against PI3K. For IC50's see Table 3-3. Also inhibits DNAPK and ATM. |
| AZD2014 | Selleckchem | 10 mM (DMSO) | mTORC1, mTORC2 | ATP competitive inhibitor, specific for mTOR, $IC_{50}$ 0.028 μM. $IC_{50}$ PI3Kα 3.8 μM, PI3Kβ > 30 μM, PI3Kγ >30 μM, PI3Kδ >29 μM. |
| AZD5363 | Selleckchem | 10 mM (DMSO) | AKT | ATP competitive inhibitor. Equipotent against AKT isoforms. Also active *in vitro* against PKA, P70S6K and 14 AGC family members. |
| Panobinostat | Selleckchem | 10 mM (DMSO) | HDAC | Hydroxamic acid based compound. Activity against class I, II and IV HDACs. $IC_{50}$ <13.2 nM for all HDACs except HDAC4, 7 and 8 ($IC_{50}$ 203 – 531 nM). |
| INC280 | Selleckchem | 10 mM (DMSO) | MET | Small molecule kinase inhibitor. Specific for MET. |
| AZD6244 | Selleckchem | 10 mM (DMSO) | MEK1 | Non ATP competitive. Specific for MEK. |
| Imatinib | Selleckchem | 10 mM (MDSO) | ABL kinase | ATP competitive inhibitor. Specific for ABL. Not active against related kinase SRC. |

**Table 2-3 Small molecule inhibitors used in this project**

OSI-906 and AZ12253801 were obtained under Material Transfer Agreement (MTA) from their respective pharma companies. All other agents were purchased commercially.

### 2.1.4 Creation of BEZ235 resistant cells

RCC4 and 786-0 cells resistant to BEZ235 were generated as part of this project, and a detailed description of this method can be found in results chapter 2. In brief cells were continuously cultured in BEZ235 and serially tested for development of resistance as defined by $GI_{50}$ (see section 2.2.2 CellTiter-Glo cell viability assay for details of methods of testing for $GI_{50}$). Two approaches were used to create BEZ235 resistant RCC cells. The first method was to treat cells with a high concentration of BEZ235 (100 nM) and culture the surviving cells, as used by Sharma (Sharma et al. 2010). This method proved successful in creating BEZ235 resistant 786-0 cells, but was not tolerated by RCC4 cells. The second method was to initiate treatment with low concentrations of BEZ235 (10 nM) and slowly increase the concentration of serial passages, as in (Ricci et al. 2002, Engelman et al. 2006b). This method was successful in producing RCC4 cells that were resistant to BEZ235 20 nM.

### 2.1.5 Treatment with IGF-1 ligand

Stimulation of cells with IGF-1 was used to test the ability of IGF-1R inhibitors to inhibit IGF-1 induced phosphorylation of the IGF-1R and downstream signalling pathways. Human long $R^3$ IGF-1 (Sigma-Aldrich) was dissolved in 10 mM HCl, aliquoted and stored at -80$^{\circ}$C. In order to stimulate with IGF-1, adherent cells were washed with PBS and then incubated with serum free medium for 24 hours. Cells were treated with 10 nM IGF-1 in serum free medium for 10 minutes before harvesting as described below (2.3.1). Control cells were treated with an equivalent volume of 10 mM HCl.

### 2.1.6 Gene silencing by RNA interference

Cells were reverse transfected with siRNA using DharmaFECT transfection reagent (Dharmacon, USA). Stock siRNA (20 μM ) was diluted in serum and antibiotic free medium to a concentration of 100 nM. DharmaFECT transfection reagent was diluted 1:400 into the 100 nM siRNA solution. The siRNA/DharmaFECT solution was added to an appropriate dish/96-well plate and cells were seeded into this in an equal volume of serum and antibiotic free medium. Following 6 hours incubation, the transfection reagent mixture was removed, and replaced with complete medium. Control cells were transfected with non-silencing control siRNA (Qiagen) to control for the non-specific effects of siRNA transfection.

| Name | Target | Source | Catalogue Number | DharmaFECT Transfection Reagent |
|---|---|---|---|---|
| All Stars negative control | Human non-silencing control | Qiagen | 1027281 | 1 |
| HS_MET_10 | Human MET | Qiagen | S102654897 | 1 |
| SASI_HS01_00048380 | Human RAPTOR | Sigma-Aldrich | NM_020761 | 1 |

**Table 2-4 siRNA used in this project**

## 2.2 Cellular assays

### 2.2.1 Clonogenic survival/growth assay

Cells were disaggregated as described above (2.1.1.2) and cells were counted using trypan blue dye (Sigma) and a haemocytometer. All cells were seeded at 3000 cells per 10 cm dish in triplicate, except BEZ235 resistant cells, which were seeded at 6000 cells per 10 cm dish. The following day, cells were treated with drug or solvent control dissolved in complete medium, and incubated for 6-8 days at 37$^o$C and 10% $CO_2$. Colonies were defined as being ready for fixation when control treated colonies were at least 50 cells in number, and were fixed and stained with 0.1% Coomassie Blue, 7% acetic acid and 50% methanol for 20-

30 minutes. After washing and drying, colonies were counted on a Colcount automated colony counter (Oxford Optronix). Results were expressed as a percentage of survival in solvent treated control dishes. Unless otherwise stated in the figure legend, data presented are from taken from three independent experiments, and graphed using GraphPad Prism v6. Curves were fitted and used to extrapolate the concentration of drug required to inhibit survival to 50% of untreated cells (defined as the $SF_{50}$).

### 2.2.2 CellTiter-Glo cell viability assay

Cells were disaggregated and counted as described above and seeded at 1000 cells per well of an opaque side-wall, clear bottomed 96 well plate (Grenier Bio-one) in triplicate. The following day cells were treated with drug or solvent and incubated for 72 hours at $37^{O}C$ and 10% $CO_2$. Cell viability was measured using CellTiter-Glo (CTG) Luminescent assay reagent (Promega) mixed in a 1:1 ratio with medium in wells, and after 30 minutes incubation in the dark on a rocker at room temperature, luminescence was read on a luminometer (Fluorstar Optima, BMG Labtech). CTG reagent lyses cells, and contains luciferin and recombinant luciferase, which in the presence of ATP and oxygen produces oxyluciferin in an electrically excited state, which emits light. Viability was expressed as a percentage of solvent treated controls. Unless otherwise stated, data presented are from three independent experiments, and graphed using GraphPad Prism v6. Curves were fitted and used to extrapolate the concentration of drug required to inhibit viability to 50% of untreated cells (defined as the $GI_{50}$). The extrapolated plateau of the curve of best fit was taken as the population of cells resistant to the drug treatment and was used as additional marker of efficacy of drug treatments, particularly if the $GI_{50}$ was not reached.

## 2.3 Protein analysis

### 2.3.1 Collection and lysis of adherent cells

Monolayer cells were washed twice with ice-cold PBS before being collected by scraping in PBS. Cells were pelleted by centrifugation at 14,000 rpm at 4$^{O}$C followed by aspiration of the supernatant. Cell pellets could be stored at -20$^{O}$C following snap freezing in dry ice with 100% ethanol. Cell pellets were lysed in IGF-1R lysis buffer (50 mM HEPES, 100 mM sodium chloride, 10 mM EDTA, 4 mM sodium pyrophosphate, 2 mM sodium orthovanadate, 10 mM sodium fluoride and 1% Triton X-100) or radio-immunoprecipitation assay (RIPA) Lysis buffer (20 mM Tris pH7.5, 1 mM EDTA, 100 mM sodium chloride, 1% Triton X-100, 0.5% sodium deoxycholate, 0.1% sodium dodecyl sulphate (SDS)) for 30 minutes on ice. Both lysis buffers were supplemented with EDTA-free protease cocktail inhibitor cocktail, 1.5 mM Pefabloc (Roche) and phosphatase inhibitor complex II (Sigma P5725) and complex III (Sigma P0044).

### 2.3.2 Protein quantification

Protein concentration was calculated against bovine serum albumin (BSA) standards (0.1-2 ml/ml) using Pierce Bicinchoninic Acid (BCA) assay and analysed on a plate reader at 562nm (μQuant Universal Microplate Spectrophotometer, NorthStar Scientific). This assay quantifies protein content through the peptide bond reduction of $Cu^{2+}$ to $Cu^{+}$, which BCA collates to produce a purple coloured product. Equal amounts of protein were denatured with 3X Laemmli Buffer (70 mM Tris pH 6.8, 5% (v/v) β-mercaptoethanol, 40% (v/v) glycerol, 3% (w/v) SDS, 0.05% (w/v) Bromophenol Blue) at $95^{0}$C for 5 minutes.

### 2.3.3 Direct lysis and collection of adherent cells

For experiments using drug treatments of 6 hours or less and only comparing treatments within one cell line, an alternative method of collecting and lysing cells was used. Equal numbers of cells were seeded into dishes and 24 hours later drug treatments applied. Cells were washed twice with chilled PBS and lysed in the dish with 3X Laemmli Buffer, sonicated for 10 seconds and then denatured by heating to $95^{0}$C for five minutes. In order for this method to produce samples containing equal concentrations of protein, two assumptions are made; firstly that the same number of cells are present and being lysed in each dish, and secondly that each cell contains the same amount of protein. In order for these assumptions to hold true, this method of lysis was only used for comparisons of drug treatments within the same cell line, and secondly for treatments of six hours or less, which were not expected to significantly alter cell number through anti-proliferative or cytotoxic effects. Equal volumes of each sample were analysed by SDS-PAGE as described below.

### 2.3.4 SDS polyacrylamide gel electrophoresis (SDS-PAGE)

Proteins were separated according to their electrophoretic mobility by SDS polyacrylamide gel electrophoresis (PAGE) on 5%, 7.5%, 10% or 12% polyacrylamide gels. Proteins were electrophoresed at 125 volts in a gel running tank (Bio-Rad) with running buffer (192 mM glycine, 25 mM Tris-Cl, 0.1% SDS) for approximately 90 minutes. Proteins were transferred onto Hybond ECL nitrocellulose membrane (Amersham) in semi-dry transfer buffer (48 mM Tris, 49 mM glycine, 20% methanol, 0.039% SDS, final pH 9.2) using a semi-dry transfer apparatus (Hoefer SemiPhor Transfer Unit, TE 77 PWR, Amersham Biosciences) at a constant current of 40 mA per membrane for 3 hours, or 150 mA per membrane for 1 hour. Alternatively when intending to probe for cleaved Notch, proteins were transferred to PVDF membranes (IMMOBILON-P, Millipore) in transfer buffer (NuPAGE Life Technologies) in a wet transfer tank (Hoeffer standard transfer tank with cooling apparatus, TE62) at 20 V for 15 hours. To reduce nonspecific binding of primary antibodies, membranes were blocked for 1 hour using 5% non fat dry milk (Sigma-Aldrich) or 5% BSA (Sigma) in tris-buffered saline (TBS) with 0.1% Tween 20 (TBST) on a shaking platform. Primary antibodies were made up as indicated in Table 2-5 and were incubated with the membrane overnight at 4°C on a shaking platform. Membranes were washed for ten minutes in TBST three times before incubation with the indicated (see Table 2-5) HRP conjugated secondary goat anti-rabbit or goat anti-mouse antibodies (Dako or Cell Signaling) at room temperature for one hour on a rocking platform. A further three washes in TBST were performed, for ten minutes each. Proteins were detected using enhanced chemiluminescence (ECL+ or ECL Prime, Amersham) and membranes were either exposed to radiographic film (Super RX Fugifilm) or visualised on a gel-doc chemiluminescence imaging machine (Fusion FX, Vilber Lourmat). Radiographs were scanned and imported into Adobe Photoshop (Abobe). Densitometry quantification was performed in ImageJ (NIH, USA) and normalized to a loading control protein, typically β-actin or β-tubulin.

| Antibody | Source | Primary Dilution | Secondary Antibody | Predicted Molecular Weight (kDa) |
|---|---|---|---|---|
| 4E-BP1 | Cell Signaling (#9644) | 1:1000 | Rabbit 1:10000 | 15-20 |
| c-ABL | Cell Signaling (#2862) | 1:1000 | Rabbit 1:10000 | 135 |
| Acetyl-Histone H3 | Merk Millipore (#06-599) | 1:1000 | Rabbit 1:10000 | 17 |
| β-Actin | Abcam (ab8224) | 1:10000 | Mouse 1:10000 | 42 |
| AKT | Cell Signaling (#9272) | 1:1000 | Rabbit 1:10000 | 60 |
| CaMKII | Cell Signaling (3362) | 1:1000 | Rabbit 1:10000 | 60, 50 |
| CRK II | Cell Signaling (#3492) | 1:1000 | Rabbit 1:10000 | 42 |
| Cyclin D1 | Cell Signaling (#2922) | 1:500 | Rabbit 1:10000 | 36 |
| EGFR | Cell Signaling (#2232) | 1:1000 | Rabbit 1:10000 | 175 |
| eIF4E | Cell Signaling (#2067) | 1:1000 | Rabbit 1:10000 | 25 |
| HES1 | Anti-Hes1 was a gift from Dr. Tatsuo Sudo, Toray Industries, Kamakura, Japan (Aleksic and Feller 2008) | 1:1000 | Rabbit 1:10000 | 30 |
| HIF1α | BD Transduction Laboratories (#610959) | 1:500 | Mouse 1:10000 | 120 |
| HIF2α | Novus Biologicals ( NB100-122) | 1:500 | Rabbit 1:10000 | 118 |
| HSL | Cell Signaling (#4107) | 1:500 | Rabbit 1:10000 | 81, 83 |
| IGF-1 R β | Cell Signaling (#3027) | 1:1000 | Rabbit 1:10000 | 95 |
| IGF-1 R β | Thermo Scientific(PA5-17530) | 1:1000 | Rabbit 1:10000 | 95 |
| IR β | Cell Signaling (#3025) | 1:1000 | Rabbit 1:10000 | 95 |
| Jagged 1 | Cell Signaling (#2620) | 1:1000 | Rabbit 1:10000 | 180 |
| LIMK 1 | Cell Signaling (#3842) | 1:1000 | Rabbit 1:10000 | 70 |
| LIMK 2 | Cell Signaling (#3845) | 1:1000 | Rabbit 1:10000 | 70 |
| MAPKAPK-2 | Cell Signaling (#3042) | 1:1000 | Rabbit 1:10000 | 47, 49 |
| MEK 1/2 | Cell Signaling (#4694) | 1:1000 | Mouse 1:10000 | 45 |
| MET | Cell Signaling (#8198) | 1:1000 | Rabbit 1:10000 | 140, 170 |
| Notch1 (Cleaved) (Val1744) | Cell Signaling (#4147) | 1:1000 | Rabbit 1:10000 | 110 |
| P44/42 MAPK (Erk1/2) | Cell Signaling (#4695) | 1:1000 | Rabbit 1:10000 | 42, 44 |
| PARP | Cell Signaling (#9542) | 1:1000 | Rabbit 1:10000 | 86, 116 |

| Antibody | Source | Primary Dilution | Secondary Antibody | Predicted Molecular Weight (kDa) |
|---|---|---|---|---|
| Phospho-4E-BP1 (Thr37/46) | Cell Signaling (#2855) | 1:1000 | Rabbit 1:10000 | 15-20 |
| Phospho-AKT (Ser473) | Cell Signaling (#4051) | 1:1000 | Mouse 1:10000 | 60 |
| Phospho-AKT (Thr308) | Cell Signaling (#9275) | 1:500 | Rabbit 1:5000 | 60 |
| Phospho-CRKII (Tyr221) | Cell Signaling (#3491) | 1:1000 | Rabbit 1:10000 | 42 |
| Phospho Cyclin D1 (Thr286) | Cell Signaling (#3300) | 1:500 | Rabbit 1:10000 | 36 |
| Phospho-IGF-1R β (Tyr1135/6 / IR β Tyr1150/1) | Cell Signaling (#3024) | 1:500 | Rabbit 1:2000 | 95 |
| Phospho-MEK1 (Ser221) | Cell Signaling (#2388) | 1:1000 | Rabbit 1:10000 | 45 |
| Phospho-MET (Tyr1234/1235) | Cell Signaling (#3077) | 1:500 | Rabbit 1:2000 | 145 |
| Phospho-Met (Tyr1356) | Abnova (#PAB0536) | 1:500 | Rabbit 1:2000 | 145 |
| Phospho-MET (Tyr1356) | Abgent (#AP3168a) | 1:500 | Rabbit 1:2000 | 145 |
| Phospho-p44/42 MAPK (Erk1/2) (Thr202/Tyr204) | Cell Signaling (#4377) | 1:1000 | Rabbit 1:10000 | 42, 44 |
| Phospho-PRAS40 (Thr246) | Cell Signaling (#2640) | 1:1000 | Rabbit 1:10000 | 40 |
| Phospho-S6 Ribosomal Protein (Ser235/236) | Cell Signaling (#2211) | 1:2000 | Rabbit 1:10000 | 32 |
| PP2A C | Cell Signaling (#2259) | 1:1000 | Rabbit 1:10000 | 36, 38 |
| PPM1G | Bethyl Laboratories (#A300-880A) | 1:1000 | Rabbit 1:10000 | 70 |
| PRAS40 | Cell Signaling (#2610) | 1:1000 | Rabbit 1:10000 | 40 |
| PTEN | Cell Signaling (#9559) | 1:1000 | Rabbit 1:10000 | 54 |
| Raptor | Cell Signaling (#2280) | 1:500 | Rabbit 1:2000 | 150 |
| RAS-GRF1 | Cell Signaling (#3322) | 1:500 | Rabbit 1:2000 | 155 |
| S6 | Cell Signaling (#2217) | 1:1000 | Rabbit 1:10000 | 32 |
| β-Tubulin | Sigma-Aldrich (#T4026) | 1:5000 | Mouse 1:10000 | 55 |

**Table 2-5 Antibodies used for western blotting in this project**

### 2.3.5 Immunoprecipitation

Monolayer cells were washed twice with ice cold PBS before being collected by scraping in ice-cold PBS. Cells were pelleted by centrifugation then lysed in RIPA buffer for 30 minutes on ice as described in section 2.3.1. Typically 0.5-1mg of protein was precleared with 10µg of control Rabbit IgG and 30µl of 50% slurry of agarose-conjugated protein A or protein G beads (Sigma), for one hour at $4^0$C on a rotating wheel. Protein beads were prepared by weighing lypophilized beads and swelling in ten times the volume of ice cold PBS for 30 minutes on ice. Beads were washed three times in ice cold PBS before re-suspending to the original volume with PBS. Lysates were centrifuged at 3000 rpm for 2 minutes and then pre-cleared lysates were transferred to a new screw cap eppendorf tube for incubation with primary antibody (2µg per 1mg of lysate) overnight at $4^0$C on a rotating wheel. Immunoprecipitates were collected with 30µl of 50% slurry of agarose-conjugated protein A or protein G beads, for one hour at $4^0$C on a rotating wheel. The beads with collected immunoprecipitates were washed three times in ice cold RIPA lysis buffer for 5 minutes on a rotating wheel at $4^0$C. After the final wash samples were denatured for 5 minutes in 3X Laemmli Buffer, and analysed by SDS PAGE and western blotting.

## 2.4 Antibody array

A commercial antibody array service, the Phospho Explorer Array, was purchased from Full Moon Biosystems (www.fullmoonbiosystems.com). This approach uses proprietary antibodies that are printed onto glass micro-array slides.

### 2.4.1 Collection of cell samples

Monolayer cells growing in 10 cm dishes were washed twice in ice-cold PBS on ice, followed by collection by scraping in 1 ml ice cold PBS. Cells were pelleted by centrifugation and the supernatant removed. Cell pellets were snap frozen in ethanol/dry ice and stored at -20$^{O}$C. Samples were couriered on dry ice to Full Moon Biosystems, 754 North Pastoria Avenue, Sunnyvale, CA 94085, USA, who performed the following steps to complete the antibody array.

### 2.4.2 Protein extraction

Cell pellets were lysed by the addition of lysis beads with extraction buffer (containing phosphatase inhibitors), vortexing for 30 seconds and incubation for 10 minutes on ice. Vortexing and incubating was repeated at 10 minute intervals for a total of 60 minutes. Lysates were next centrifuged at 10,000 g for 20 minutes and the supernatant transferred to a fresh tube. Spin columns were used to exchange the buffer in the supernatant to labeling buffer and then protein concentration was measured.

### 2.4.3 Biotin labeling of protein extracts

Labeling buffer was added to the protein sample to bring the total volume to 75 μL and 3 μL of Biotin/Dimethylformamide (DMF) was added (10 μg/μL Biotin). The sample was mixed, incubated at room temperature for 2 hours with constant mixing, and then 35 μL of stopping reagent was added and incubated for 30 minutes with mixing to terminate the reaction.

### 2.4.4 Coupling

The antibody array included 1318 antibodies directed against phospho-proteins, with corresponding antibodies to the non-phosphorylated epitopes of the same proteins (full list available online at www.fullmoonbiosystems.com). Each antibody was spotted onto the slide in duplicate. The antibody arrays were blocked using blocking buffer for 40 minutes at room temperature on a rocking platform to reduce non-specific binding of proteins, and then washed in milli-Q grade water. In a coupling chamber 95 μg of labelled protein in 6 mL coupling solution was incubated with the antibody array on an orbital shaker for 2 hours at room temperature. Antibody array slides were then washed three times with washing buffer and finally rinsed with de-ionised water.

### 2.4.5 Detection of antibody-bound proteins

Antibody-bound biotinylated proteins were detected with streptavidin. To 60 ml of detection buffer, 30 μL of Cy3-streptavidin was added and incubated with the antibody array slides for 45 minutes at room temperature in the dark. The slides were then washed three times in washing buffer, rinsed in de-ionised water and dried with compressed nitrogen. The slides were scanned on an Axon Genepix Array Scanner.

### 2.4.6 Data analysis

For each spot on the array the median signal intensity was recorded, and then the median signals of replicate spots were averaged (the *average signal intensity of replicate spots*), and coefficient of variation for each set of replicates calculated. Data were normalised to the median of replicate averages (the *median signal intensity*).

*Normalized data = Average signal intensity of replicate spots / median signal intensity*

Normalised data were used to calculate the fold change between samples.

*Fold change = Treated normalised data / Control normalised data*

A "true signal" on the antibody array was defined as an average signal intensity of replicate spots at least 3 times the level of background signal.

## 2.5 RNA analysis

### 2.5.1 General techniques for working with RNA

All work surfaces and equipment were cleaned prior to any work with RNA using RNaseZAP (Ambion). Filter tips were used for pipetting (Axygen), RNase and DNase free tubes (Axygen) and nuclease free water (Ambion) were used throughout.

### 2.5.2 RNA extraction from cultured cells

An RNeasy micro kit (Qiagen, UK) was used to extract RNA according to the manufacturers protocol, including the optional on column DNase treatment step. Approximately $10^6$-$10^7$ monolayer cells were cultured in a 10cm dish. Cells were washed in ice cold PBS and then lysed in 600 µL of buffer RLT containing β-mercaptoethanol, and the resulting lysate was homogenised by passing through a blunt 20-gauge needle five times. An equal volume of 70% ethanol was added, and mixed by pipetting. The resulting mixture was added to a silica membrane RNeasy spin column and centrifuged at 13,000 for 15 seconds. Silica bound RNA was washed with 350 µL of Buffer RW1 by centrifugation at 13,000 rpm for 15 seconds. Next an on-column DNA digestion step was performed with DNase (RNase-free DNase set, Qiagen, UK), using 80 µL of DNase incubation mix (10 µL DNase 1 stock solution and 70 µL buffer RDD), which was added to the spin column. After incubating for 15 minutes at room temperature, 350 µL buffer RW1 was added and the column centrifuged at 13,000 rpm for 15 seconds. Next, the column was washed twice with buffer RPE before RNA was eluted in 40 µL of RNase-free water by centrifugation at 13,000 rpm for 1 minute.

RNA concentration was determined by spectrophotometry (Nanodrop Technologies, Wilmington, DE, USA) supported with NanoDrop version 3.5.2 software. Purity of the RNA was assessed by the ratio of absorbance at 260 nm versus 280 nm (ratio of 2.0 for pure RNA). RNA was stored at -80$^{O}$C.

### 2.5.3 Gene expression microarray analysis

Monolayer RCC4 control cells (BEZ235 sensitive) were grown in 10 cm dishes and treated with 20 nM BEZ235 or solvent control for one hour. Cells were collected and RNA extracted as described above (section 2.5.2). RCC4 BEZ235 resistant cells were grown in 10 cm dishes in media containing 20 nM BEZ235 (their standard growing conditions). The medium was exchanged for fresh medium containing 20 nM BEZ235 and one hour later cells were collected and RNA extracted as described above. Triplicate independent samples were collected for each condition. Microarray analysis was performed at the Cancer Research UK Manchester Institute Microarray Service (Cancer Research UK Manchester Institute, University of Manchester, UK) using the Affymetrix GeneChip Human Exon 1.0 ST Array platform. To perform the analysis, 500 ng of total RNA at a minimum of 100 ng/µL was provided. RNA integrity was confirmed on an Aligent Bioanalyzer (Agilent Technologies UK Limited, Cheshire, UK) at the Cancer Research UK Manchester Institute. cDNA was synthetised from RNA and then amplified, fragmented and biotin labelled. Labelled cDNA was allowed to hybridize with gene probes on the affymetrix GeneChip Human Exon 1.0 ST array, which contains multiple probes for each gene. The slide was then stained and scanned before data were uploaded onto the online database MIAME VICE. Data analysis was performed by Stephen Taylor (Head of Computational Biology Research Group, Weatherall Institute of Molecular Medicine, University of Oxford, Oxford, UK) to generate a list of transcripts showing altered expression in BEZ235 resistant cells compared to BEZ235 sensitive cells, and BEZ235 sensitive cells acutely treated with BEZ235. Transcripts were filtered by p value <0.05 and arranged in order of log fold of change. Results were uploaded to Metacore (http://thomsonreuters.com/metacore/) for pathway analysis.

### 2.5.4 Reverse transcription

cDNA was synthesised by reverse transcription using the SuperScript III First-Strand Synthesis System for RT-PCR (Invitrogen, Life Technologies) according to the manufacturers protocol. Up to 5 µg of RNA was added to 1 µl of 10 ng/µL random hexamers and 1 µL 10 mM dNTP mix, and the final volume made up to 10 µL with nuclease free water. The reaction mix was heated to $65^{0}$C for 5 minutes then placed on ice for at least 1 minute. To this, 10 μL of cDNA synthesis mix was added (2 μL 10X RT buffer, 4 μL 25 mM $MgCl_2$, 2 μL 0.1 mM DTT, 1 μL 40 U/μL RNase OUT and 1 μL 200U/μL SuperScript III RT). Samples were placed in a Peltier Thermal Cycler (MJ Research, Waltham, MA, USA) and incubated at 25$^{O}$C for 10 minutes, then 50$^{O}$C for 50 minutes. The reaction was terminated by heating to 85$^{O}$C for 5 minutes, then cooling to 4$^{O}$C. Samples of cDNA were stored at -20$^{O}$C until analysis by qRT-PCR.

## 2.5.5 Quantitative real time PCR (qRT-PCR)

### 2.5.5.1 Primer design

NCBI mRNA reference sequence accession numbers (RefSeq) were entered into the National Centre for Biotechnology Information (NCBI) Primer BLAST (Basic local alignment search tool) program, which automatically generated the primer sequences (http://www.ncbi.nlm.nih.gov/tools/primer-blast/). Parameters for primer design were set for a melting temperature of 60$^{O}$C, amplicon length less than 400 bases and spanning at least one exon-exon boundary. The HEY1 primer pair was a gift from Dr Helen Sheldon (Department of Oncology, Weatherall Institute of Molecular Medicine, University of Oxford, Oxford, UK). The primers were synthesised by Invitrogen (Life Technologies Ltd., UK) and sequences are listed in Table 2-6.

| Target Gene | RefSeq | Forward Primer 5'-3' | Reverse Primer 3'-5' |
|---|---|---|---|
| HEY1 | NM_001040708 | CGAGCTGGACGAGCCCAT | GGAACCTAGAGCCGAACTCA |
| HES1 | NM_005524 | CAGCCAGTGTCAACACGACA | GTGCGCACCTCGGTATTAAC |
| JAG1 | NM_000214 | CCAGTGTCAGAATGACGCCT | ACTCTTGCACTTCCCGTGAG |
| FN1 | NM_002026 | ACCATACCCGCCGAATGT | GTGTAGGGGTCAAAGCACGA |
| Actin | NM_001101 | CCCAGCACAATGAAGATCAA | CGATCCACACGGAGTACTTG |

**Table 2-6 Primers used for qRT-PCR**

#### 2.5.5.2 qRT-PCR

All quantitative real time polymerase chain reactions (qRT-PCR) reactions were performed in triplicate for each primer pair in each condition tested using the Rotor Gene qPCR System (Corbett Research, Sydney, Australia). The SensiMix SYBR kit (Bioline Ltd., UK) was used as per the manufacturers instructions. SensiMix SYBR was provided as a 2X mastermix containing all the components required for real-time PCR (SYBR Green I dye, dNTPs and stabilisers). Primers were added to a working concentration of 0.5 µM with 20 ng cDNA, and nuclease free water to make up to final volume of 25 µl per reaction. Conditions for the PCR reaction were 95$^{O}$C for 15 minutes to activate the DNA polymerase, followed by 40 cycles of 15 seconds at 95$^{O}$C and 30 seconds at 60$^{O}$C.

## 2.6 Apoptosis assay

Cells were disaggregated and counted as described above (2.1.1.2 and 2.2.1) and seeded at 5000 cells per well of an opaque side-wall, clear bottomed 96 well plate (Grenier Bio-one) in triplicate. The following day cells were treated with drug or solvent and incubated for 24 or 48 hours at 37$^{O}$C and 10% $CO_2$. Apoptosis was measured using Caspase-Glo 3/7 assay reagent (Promega) mixed in a 1:1 ratio with medium in wells, and after 60 minutes incubation in the dark on a rocker at room temperature, luminescence was read on a luminometer (Fluorstar Optima, BMG Labtech). Caspase-Glo reagent contains a substrate for caspase 3/7 containing a DEVD sequence, Ultra-Glo recombinant luciferase (a proprietary thermostable luciferase) and buffers optimised for cell lysis, caspase activity and luciferase activity. When the substrate is cleaved by active caspase 3/7 released from lysed cells, aminoluciferin, a luciferase substrate, is released and following reaction with luciferase, light is emitted. Luminescence is proportional to the amount of activated caspase 3/7 in the treated cells. Apoptosis was expressed as a percentage of solvent treated controls.

## 2.7 Statistical analysis

Data were analysed and graphed using Excel (Microsoft, USA) and Prism v6 (GraphPad, USA). Graphs were plotted to show mean and standard error of the mean (SEM). Student's t-test was used to compare two groups of data, one-way analysis of variance (ANOVA) to compare more than two groups of data or Friedman's test for non-normally distributed data, and two way ANOVA to compare sets of data. Where non-linear regression was used to calculate $GI_{50}$ and $SF_{50}$ values, 95% confidence intervals were given. Statistical significance was defined as 95% ($p<0.05$).

# 3 Results 1: Testing the functional relevance of mTOR inhibitor induced, IGF-1R mediated, AKT activation in CCRCC

## 3.1 Introduction

Previous work suggested the concept that the IGF-1R is important in renal cancer biology. The IGF-1R is frequently overexpressed in renal cancer where it confers a poor prognosis (Parker et al. 2004) and is associated with higher grade tumours (Ahmad et al. 2004b). Our group has previously shown that CCRCC shows increased IGF-1R mRNA expression compared to adjacent normal kidney, and furthermore that the mechanism of the difference is that VHL sequesters the transcription factor SP1 thereby reducing IGF-1R transcription (Yuen et al. 2007). More recently we have shown that the IGF-1R translocates to the nucleus in human tumours including renal cancer, where intense or widespread nuclear IGF-1R was associated with a worse prognosis (Aleksic et al. 2010).

The IGF-1R has been implicated in resistance to inhibition of the mTOR pathway in a number of studies. In prostate and breast cancer cell lines, inhibition of mTORC1 with rapamycin results in an increase in IRS-1 expression and phosphorylation of S473-AKT, and small molecule or antibody inhibitors of IGF-1R or PI3K abrogate this signalling, and sensitise to mTOR inhibition (O'Reilly et al. 2006). Our group has previously shown that in renal cancer, inhibition of mTOR with rapamycin relieves phosphorylation of IRS-1 at S612, which potentiates signalling via the IGF-1R to increase pAKT S473. Knockdown of the IGF-1R *in vitro* and *in vivo* abrogates pAKT S473 activation and sensitises CCRCC cells to rapamycin (Yuen et al. 2009).

The initial aim of this project was to establish whether the sensitisation to rapamycin induced by IGF-1R knockdown in CCRCC could be replicated with small molecule IGF-1R inhibitors. A secondary aim was to assess whether *VHL* mutation status, and levels of IGF-1R expression altered the sensitivity to inhibition of mTOR or IGF-1R, alone or in combination.

## 3.2 Results

### 3.2.1 The HIF status and IGF-1R expression of cell lines used in this project

This project used the isogenic pairs of cell lines described in section 2.1.2. The parental cell lines all harbour mutant, non functional *VHL* and have been stably transfected with empty vector (EV, or vector alone - VA). The corresponding paired cell lines had all been transfected with wild type, functional *VHL* (VHL)(Iliopoulos et al. 1995, Maxwell et al. 1999, Zatyka et al. 2002). In normoxia, in the absence of functional VHL, HIF1/2α is not ubiquitinated and targeted for degradation and was therefore detectable by western blotting in 786-0EV, RCC4EV and UMRC2EV cells (Figure 3-1). As previously reported, 786-0 cells do not express HIF1α (Yuen et al. 2007) whereas RCC4 and UMRC2 cells do. All three cell lines express HIF2α. The stably transfected cell lines 786-0VHL, RCC4VHL and UMRC2VHL all showed decreased levels of HIF2α in normoxia, consistent with the presence of functional VHL. It has previously been shown that the replacement of functional VHL reduced the expression of IGF-1R in 786-0 and RCC4 cells (Yuen et al. 2007). The reduction in IGF-1R was seen in 786-0VHL and UMRC2 cells, but not in RCC4VHL cells. The expression of IGF-1R in RCC4EV and RCC4VHL cells was checked 5 times during the course of this project, and no clear pattern was evident, with findings of increased IGF-1R expression in RCC4VHL (n=2), no change (n=2), or reduction in IGF-1R in RCC4VHL cells (n=1) as shown in Figure 3-12. The cause of this variation is currently unclear; consistent differences in HIF2α expression suggested that the EV and VHL sublines had not been mixed.

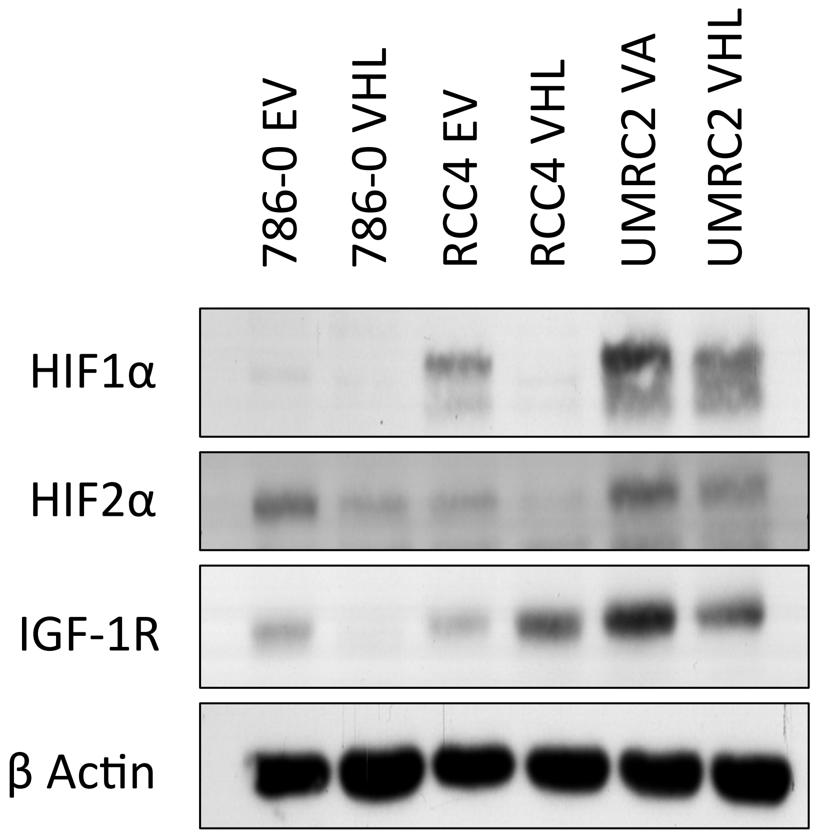


**Figure 3-1 HIF status and expression of IGF-1R in cell lines used in this project**

Cells growing in normoxia were lysed in Laemmli buffer and western blotted for HIF1α and HIF2α to assess the expression of HIF1/2α isoforms in the isogenic paired cell lines 786-0EV and VHL, RCC4 EV and VHL, and UMRC2 VA and VHL. Membranes were also probed for levels of IGF-1R, and β-Actin as loading control. Similar results seen in 5 independent experiments.

### 3.2.2 The effects of rapamycin on renal cancer cell lines

Initial experiments tested the response of renal cancer cell lines to acute treatment with rapamycin. A six hour time point was chosen for this assessment based on the data previously published by our group showing feedback increase in pAKT S473 at this timepoint (Yuen et al. 2009). In all tested cell lines 100 nM rapamycin inhibited the action of mTORC1 as assessed by reduction in the phosphorylation of S6 (Figure 3-2) and this effect did not vary between *VHL* mutant and *VHL* wild type cell lines. The RCC4EV and RCC4VHL cell pair showed increase in phosphorylation of AKT at S473 and at T308 (pAKT S473 and pAKT T308), and this effect was more marked in the RCC4VHL cell line. The 786-0 cells showed higher levels of AKT phosphorylation, consistent with mutant *PTEN* status (http://cancer.sanger.ac.uk/cell_lines/mutation/overview?id=5164), and the 786-0EV cells did not show a clear change in pAKT S473 or pAKT T308 on treatment with rapamycin. In contrast, the 786-0VHL cells showed a decrease in pAKT S473 and pAKT T308. The UMRC2 cell pair showed no changes in pAKT S473 or pAKT T308. No cell line showed evidence of rapamycin-induced activation through the RAS-RAF-MEK-ERK pathway as evidenced by unchanging phosphorylation of ERK (pERK).

The response of 786-0EV cells seen in this experiment, and two other similar experiments did not match data previously published by our group (Yuen et al. 2009), where an increase in pAKT S473 was clearly evident after 6 hours of treatment with rapamycin. In an effort to resolve this discrepancy, the effects of rapamycin upon 786-0EV cells was assessed in further detail.

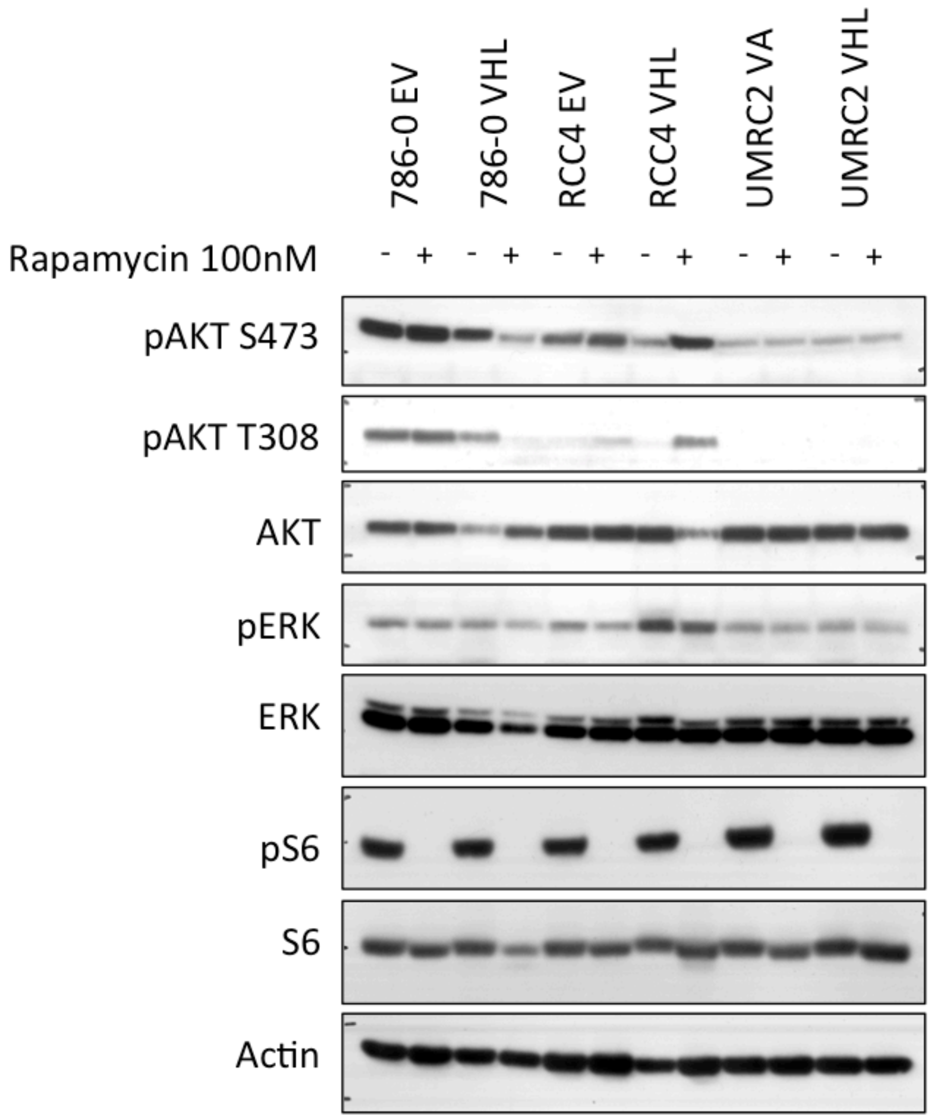


**Figure 3-2 The response of the CCRCC cell line panel to acute treatment with rapamycin**

Monolayer cells were treated with 100 nM rapamycin, 6 hours later cells were collected and lysates analysed by SDS-PAGE and immunoblotting. Reduction in phosphorylation of S6 (pS6) indicates mTORC1 blockade in all cell lines. RCC4EV and RCC4VHL showed an increase in pAKT at both T308 and S473 phosphorylation sites. Similar results seen in one other experiment.

### 3.2.3 The effects of rapamycin on 786-0EV cells

The time-course of the effects of rapamycin on 786-0EV cells was assessed. Two experiments were conducted, firstly with time points up to 24 hours (Figure 3-3 A), and secondly with time-points from 1 – 7 days (Figure 3-3 B). The activity of rapamycin to inhibit mTORC1 was assessed by S6 phosphorylation, and this revealed that mTORC1 inhibition was evident after 1 hour and was maintained up to and including 7 days of treatment. Quantification of western blots from three independent experiments revealed that feedback activation of AKT at S473 increased to approximately 150% of basal levels at 3 hours (Figure 3-3 C), which was a similar magnitude of increase to that seen previously by our group at 6 hours (Yuen et al. 2009). AKT phosphorylation at T308 peaked after 9 hours of treatment (Figure 3-3 D). At time-points beyond 24 hours, the levels of pAKT S473 and pAKT T308 fell below baseline levels (Figure 3-3 B). This biphasic effect with initial increase in pAKT followed by a fall below baseline is consistent with published data on long-term mTOR inhibition with rapamycin. Rapamycin interacts with FKBP12 and then is able to bind to and inhibit mTORC1 in an allosteric manner. Rapamycin-FKBP12 is not able to bind mTORC2, which is defined by the binding partner RICTOR (Jacinto et al. 2004, Sarbassov et al. 2004). Sarbassov and colleagues however showed that during prolonged treatment, rapamycin is able to prevent the formation of mTORC2 and that this results in a decrease in pAKT S473 and pAKT T308 (Sarbassov et al. 2006).

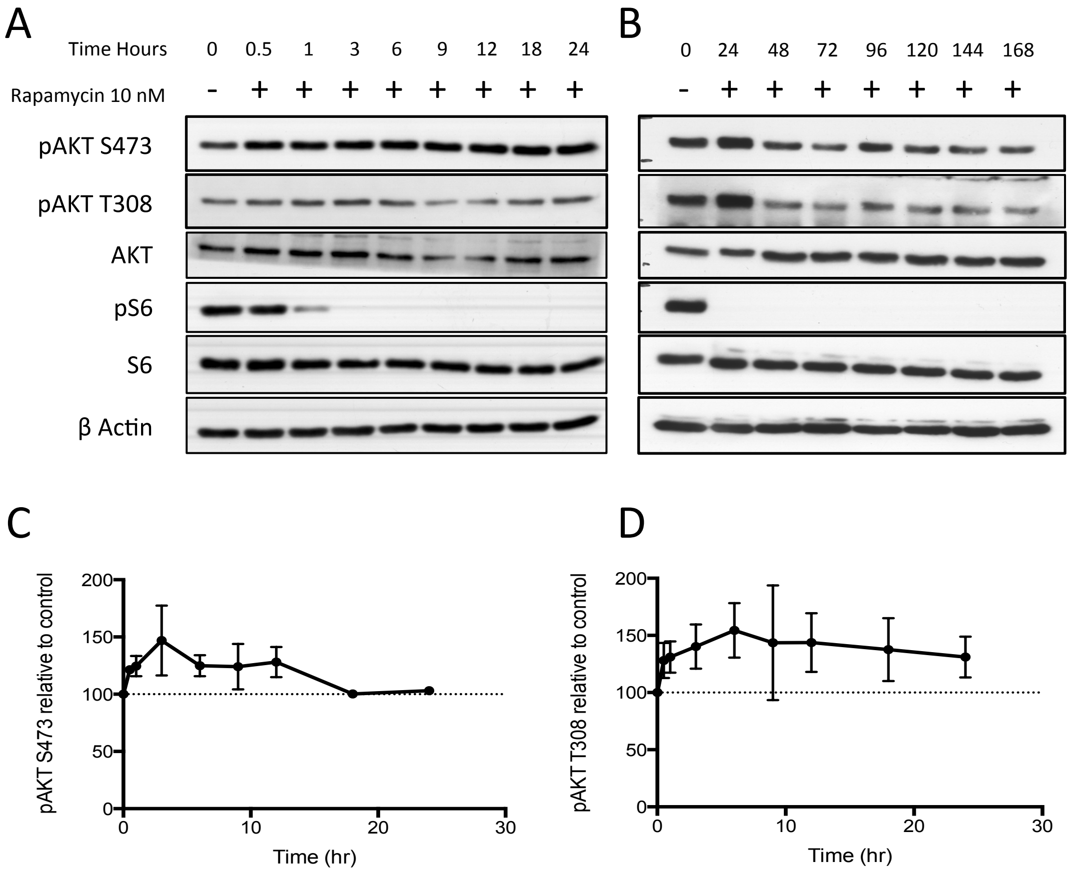


**Figure 3-3 Time-course of effects of rapamycin on 786-0EV cells**

A) and B) Representative western blots of 786-0EV cells treated with 10 nM rapamycin for the indicated times between 0 and 24, and 0 and 168 hours respectively. C) pAKT S473: total AKT ratio. The bands from three independent western blots as in A) were quantified using ImageJ and the ratio of pAKT S473:total AKT was expressed relative to untreated control cells. D) pAKT T308:total AKT. The bands from three independent western blots as in A) were quantified using ImageJ and the ratio of pAKT T308:total AKT was expressed relative to untreated control cells.

### 3.2.4 The anti-proliferative effects of rapamycin

The anti-proliferative effects of rapamycin were assessed by CellTiter-glo (CTG) cell viability assay. Rapamycin induced concentration dependent inhibition of cell viability at sub nM levels, with a plateau at and above 1 nM in all cell lines, at or near 50% of maximum viability in solvent treated controls. Comparison between 786-0EV and 786-0VHL, and also between RCC4EV and RCC4VHL cells showed no difference in effects ($p>0.05$ by two way ANOVA) (Figure 3-4 A and B). The comparison between UMRC2VA and UMRC2VHL cells (Figure 3-4 C) showed a statistically significant difference by two way ANOVA ($p<0.0001$) but the $GI_{50}$ was not reached in either cell line ($GI_{50}>300$ nM). Although the difference in anti-proliferative effect of rapamycin on the UMRC2 cell pair reached statistical significance, it was felt that the difference was unlikely to be biologically important and that neither cell line could be considered to be sensitive to rapamycin.

Clonogenic survival assays were used to assay the effects of rapamycin on cell survival and this revealed that the VHL mutant 786-0EV cells were statistically significantly more sensitive than the 786-0VHL cells ($p<0.001$ by two way ANOVA) (Figure 3-4 D). Bonferroni's multiple comparisons test however revealed that no individual concentration of rapamycin showed a statistically significant difference between 786-0EV and 786-0VHL. Furthermore, the $SF_{50}$ of 786-0EV was 0.4 nM (95% confidence interval 0.3 – 0.5 nM) and of 786-0VHL 0.8 nM (95% confidence interval 0.5 – 1.2 nM). The fold change in $SF_{50}$ was therefore small (2), and the absolute difference in $SF_{50}$ was very small (0.4 nM), so it is unlikely that this represents a significant biological difference.

Clonogenic survival/growth assays were also performed in UMRC2VA and UMRC2VHL cells, but both cell lines grew poorly in clonogenic format and produced data with relatively poor reproducibility as evidenced by wide error bars (Figure 3-4 E). Statistical significance was reached by two way ANOVA ($p<0.0105$) and Bonferroni's multiple comparisons test revealed statistically significant differences at 0.1 and 0.3 nM rapamycin. The $SF_{50}$ for UMRC2VA was 1.1 nM (95 % confidence intervals 0.6 – 2.1 nM) and for UMRC2VHL 0.12 nM (95% confidence intervals 0.11 – 0.14 nM). Once again, the absolute difference in $SF_{50}$ was very small, which questions the biological significance. Furthermore, the direction of the effect was the opposite from that seen in cell viability assays, and was also the opposite from that seen in the 786-0EV and VHL cell line pair. It was therefore felt that this was unlikely to be of biological importance, and due to the technical difficulties with the assay in this cell pair, further experiments were not carried out to improve the quality of the data.

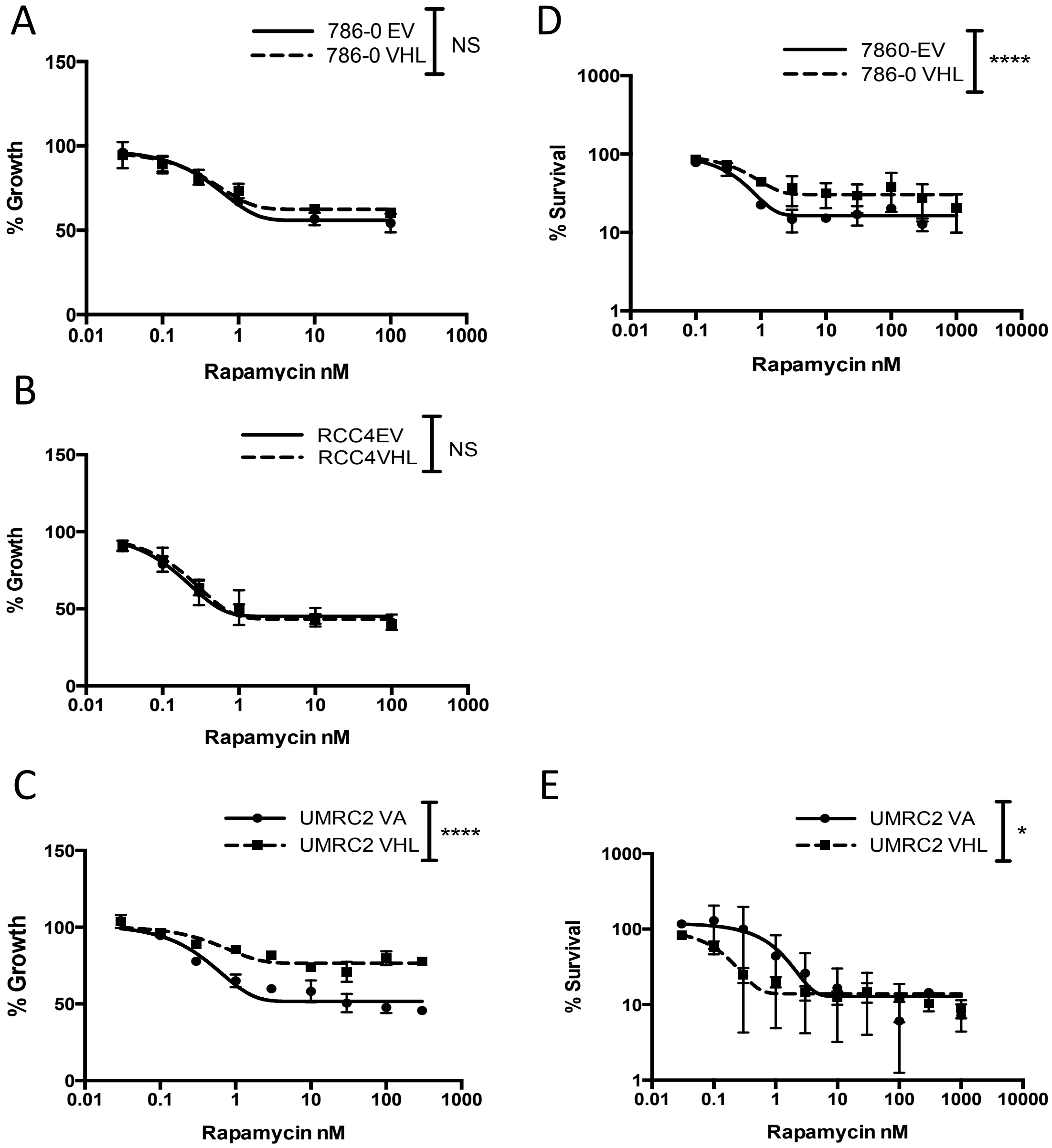


**Figure 3-4 VHL status has no major effect on the sensitivity of CCRCC cell lines to rapamycin**

CTG cell viability assay of A) 786-0 EV and 786-0 VHL, B) RCC4 EV and RCC4 VHL and C) UMRC2 VA and UMRC2 VHL. Mean and SEM of three independent experiments plotted for 786-0 and RCC4 cell pairs, and two independent experiments plotted for the UMRC2 cell pair. NS, $p>0.05$ by 2 way ANOVA, **** $p<0.0001$ by two way ANOVA. Clonogenic survival/growth assay of D) 786-0 EV and 786-0 VHL cells (Mean and SEM of three independent experiments for 786-0EV and of two assays for 786-0 VHL cells), and E) UMRC2 VA and UMRC2 VHL cells (Mean and SEM of two independent experiments). **** $p<0.0001$ by 2 way ANOVA. * $p=0.0105$ by two way ANOVA.

### 3.2.5 The effects of the IGF-1R Inhibitor OSI-906 on renal cancer

OSI-906 is a small molecule tyrosine kinase inhibitor of the IGF-1R (Mulvihill et al. 2009). It is relatively specific for the IGF-1R with an $IC_{50}$ (concentration to inhibit activity by 50%) of 0.035 µM. The kinase domain of the IGF-1R shares great homology with the IR (Buck et al. 2010) and the $IC_{50}$ for this is 0.075 µM. Other kinases have $IC_{50}$ values greater than 10 µM (Mulvihill et al. 2009). OSI-906 is in early clinical trials and plasma concentrations in the µM range are achievable (Carden et al. 2010, Evans et al. 2010, Macaulay et al. 2011).

The ability of OSI-906 to inhibit the autophosphorylation of the IGF-1R and downstream signalling pathways was assessed in 786-0EV cells by western blotting (Figure 3-5). Monolayer 786-0EV cells were serum deprived overnight, and treated with OSI-906 for 1 hour, with stimulation with 10 nM IGF-1 ligand for the final 10 minutes. This revealed that OSI-906 inhibited the autophosphorylation of the IGF-1R in a concentration dependent manner, with no detectable pIGF-1R above 100 nM OSI-906. pAKT S473 was also inhibited in a concentration dependent manner, but the concentration of OSI-906 required to inhibit pAKT S473 was higher, with 1 µM OSI-906 required to cause maximal inhibition.

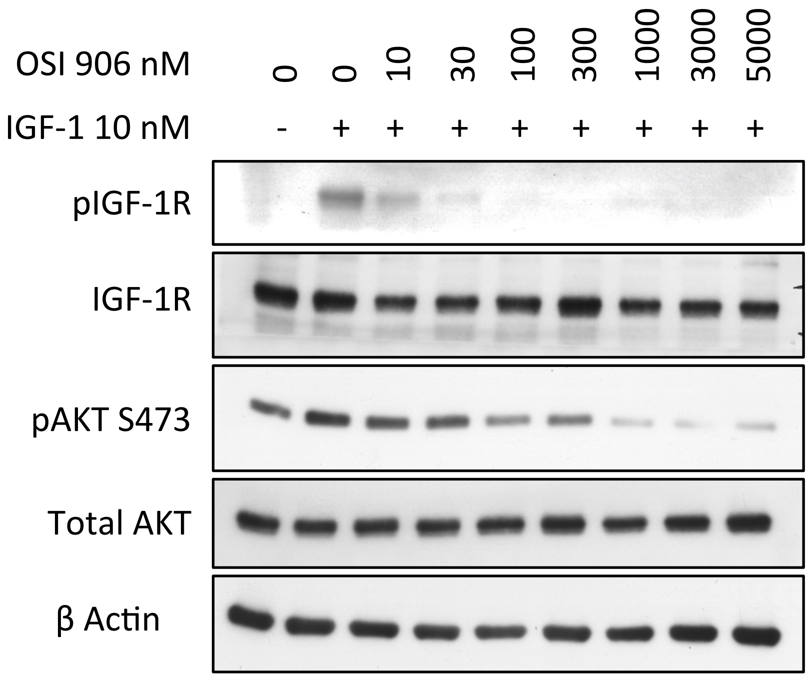


**Figure 3-5 OSI-906 inhibits IGF-1R signalling**

Monolayer 786-0EV cells were serum deprived for 24 hours and then treated with the indicated concentration of OSI-906 or solvent control (0.6% DMSO) for 1 hour in serum depleted conditions. For the last 10 minutes of this time cells were stimulated with 10 nM IGF-1 or solvent control (HCl). Cells were lysed directly in Laemmli buffer, and analysed by SDS-PAGE. Similar results seen in 3 independent experiments.

### 3.2.6 The anti-proliferative effects of OSI-906 in renal cancer cell lines

The effect of OSI-906 on cell viability was assessed by CTG assay, and cell line pairs were compared. OSI-906 inhibited the viability of 786-0 and RCC4 cells, but not UMRC2 (Figure 3-6). There was no significant difference observed between 786-0EV and VHL, RCC4EV and VHL, or UMRC2VA and UMRC2VHL (Figure 3-6 A, B and C respectively). $GI_{50}$ values and fold changes between VHL mutant and wild type cells are shown in Table 3-1.

Clonogenic cell survival/growth assays were performed in 786-0 EV and VHL cells (Figure 3-6 D) and in UMRC2VA and UMRC2VHL (Figure 3-6 E). OSI-906 inhibited 786-0 cell survival in a concentration dependent manner at concentrations greater than 1 μM, but did not inhibit the survival of UMRC2 cells, which showed the same pattern of effect as seen in CTG cell viability assays. Statistical significance by two way ANOVA was reached in the 786-0 cell pair, but Bonferroni multiple comparisons testing showed that at no individual concentration was statistical significance reached. $SF_{50}$ concentrations for 786-0EV were 6.5 μM and for 786-0VHL 10.2 μM giving a 1.6 fold change, which is of doubtful biological significance as the magnitude of change is small, and the $SF_{50}$ concentrations are higher than plasma concentrations that are achievable in humans (≈1 μM) (Evans et al. 2010). In the UMRC2 cell pair statistical significance by two way ANOVA was also reached, but in neither cell line did OSI-906 inhibit cell survival.

In summary, at concentrations of OSI-906 that inhibited autophosphorylation of the IGF-1R, no effect was seen on proliferation or cell survival in any of the tested RCC cell lines. VHL status, and levels of expressed IGF-1R did not alter sensitivity to OSI-906. Taken together, these data do not provide a rationale for pursuing single agent IGF-1R inhibition as a treatment strategy for renal cancer.

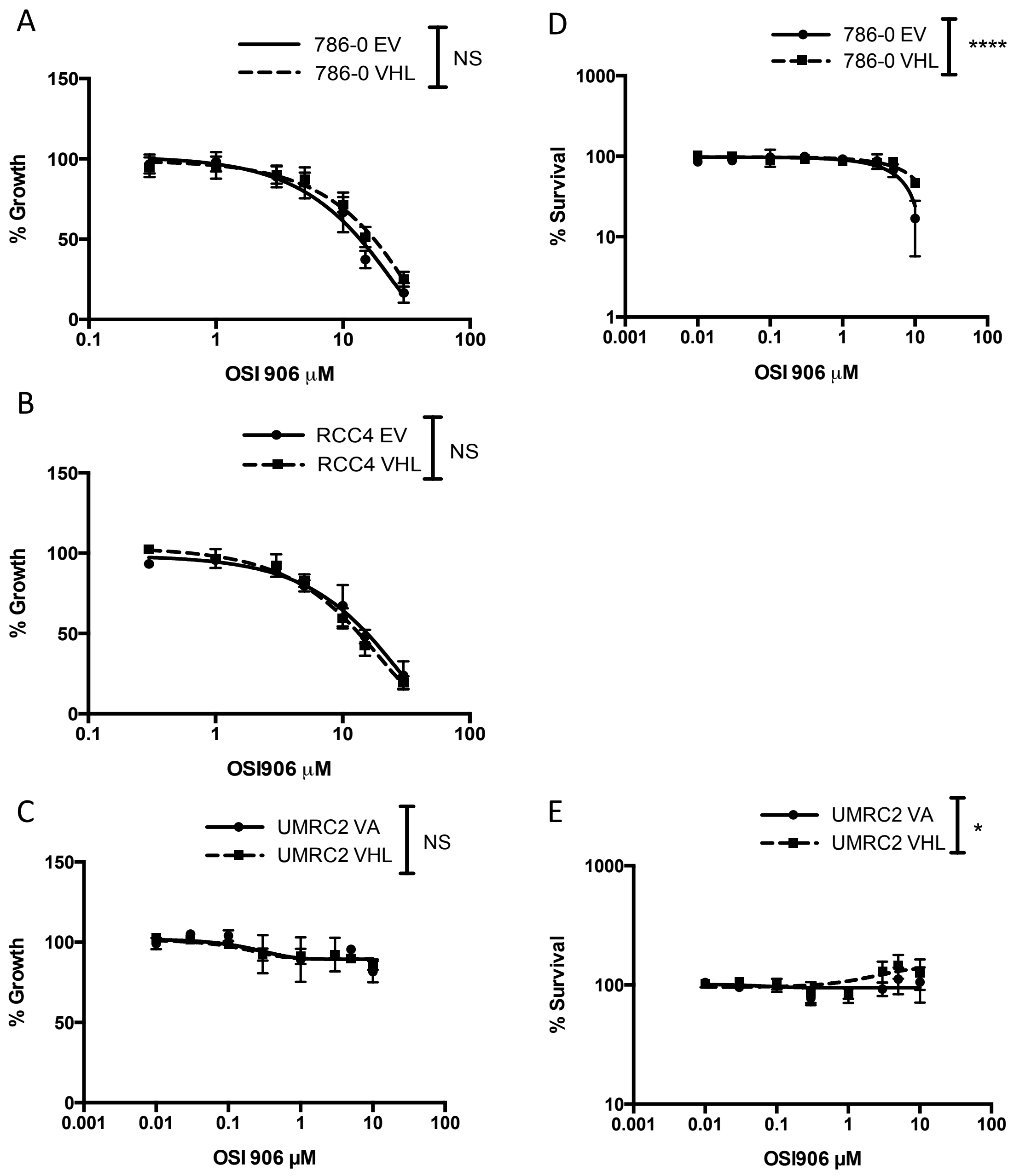


**Figure 3-6 Effects of OSI-906 on proliferation and cell survival in CCRCC cells**

CTG cell viability assay of A) 786-0 EV and 786-0 VHL, B) RCC4 EV and RCC4 VHL and C) UMRC2 VA and UMRC2 VHL. Mean and SEM of three independent experiments plotted for 786-0 and RCC4 cell pairs, and two independent experiments plotted for the UMRC2 cell pair. NS, $p>0.05$ by 2 way ANOVA. Clonogenic survival/growth assay of D) 786-0 EV and 786-0 VHL cells (Mean and SEM of three independent experiments for 786-0EV and of one assay for 786-0 VHL cells), and E) UMRC2 VA and UMRC2 VHL cells (Mean and SEM of two independent experiments). **** $p<0.0001$ by 2 way ANOVA. * $p=0.0107$.

| Cell Line | $GI_{50}$ µM (95% Confidence Intervals) | Fold Change VHL/EV (95% Confidence Intervals) |
|---|---|---|
| 786-0 EV | 14 (11.6 – 15.8) | 1.3 (0.99 – 1.7) |
| 786-0 VHL | 18 (15.7 – 19.4) | |
| RCC4 EV | 16 (13.7 – 17.6) | 0.86 (0.69 – 1.09) |
| RCC4 VHL | 13 (12.1 – 14.9) | |
| UMRC2 VA | >10 | NA |
| UMRC2 VHL | >10 | |

**Table 3-1 GI50 values for OSI-906 in CCRCC cell lines**

GI50 values calculated by nonlinear regression from results of the CTG cell viability assays in Figure 3-6. For the 786-0 and RCC4 cell line pairs there were minor differences in sensitivity to OSI-906 between EV and VHL sublines. Fold changes represent the ratio of $GI_{50}$ values for VHL/EV sublines (95% confidence intervals).

### 3.2.7 The effects of combined mTOR and IGF-1R inhibition with OSI-906

Even though renal cancer cells did not prove to be sensitive to single agent IGF-1R inhibition, it still could have been possible that IGF-1R inhibition would sensitise to rapamycin, where activation of AKT has been observed, and in light of the effects of IGF-1R gene silencing (Yuen et al. 2009). Therefore, cell viability assays were performed comparing effects of rapamycin alone or with OSI-906 in RCC4EV and RCC4VHL cell lines (Figure 3-7A and B). Drug treatments were applied simultaneously, and a concentration of 3 µM OSI-906 was chosen for this experiment given that signalling experiments (Figure 3-5) suggested that low micro molar concentrations of OSI-906 were required to inhibit AKT phosphorylation, and phase I clinical trials suggest that these concentrations are clinically achievable at dosing regimens chosen for further clinical evaluation (Evans et al. 2010). With this experimental design in RCC4EV and RCC4VHL cells OSI-906 made only a very minor difference to the response to rapamycin (Figure 3-7) with only small differences in terms of $GI_{50}$, or resistant population (marked X in Figure 3-7A) as illustrated in Table 3-2. Therefore, despite reaching statistical significance by two way ANOVA, there did not appear to be a biologically significant difference in the response to rapamycin alone, or with 3 μM OSI-906.

In order to test whether OSI-906 was blocking feedback activation of AKT in response to mTORC1 blockade, RCC4EV cells were treated with rapamycin at 0, 0.1, 0.3 or 1 nM with solvent, or with 3 μM OSI-906. Treatments were applied for 6 hours in complete media (Figure 3-7 C). It can be seen that single agent rapamycin completely inhibited the mTORC1 target pS6 even at the lowest concentration used, but only partially inhibited the phosphorylation of another mTORC1 target, 4E-BP1. Feedback increase in phosphorylation of AKT S473 was detected from 0.1 nM and higher concentrations of rapamycin, but increase in pAKT T308 was not clearly seen. In cells treated with rapamycin and OSI-906, the feedback activation of AKT at S473 was completely blocked, and there were no changes in pS6 and p4E-BP1 downstream of mTORC1. This experiment confirmed that the feedback activation of AKT was blocked by IGF-1R inhibition, but this did not sensitise significantly to rapamycin.

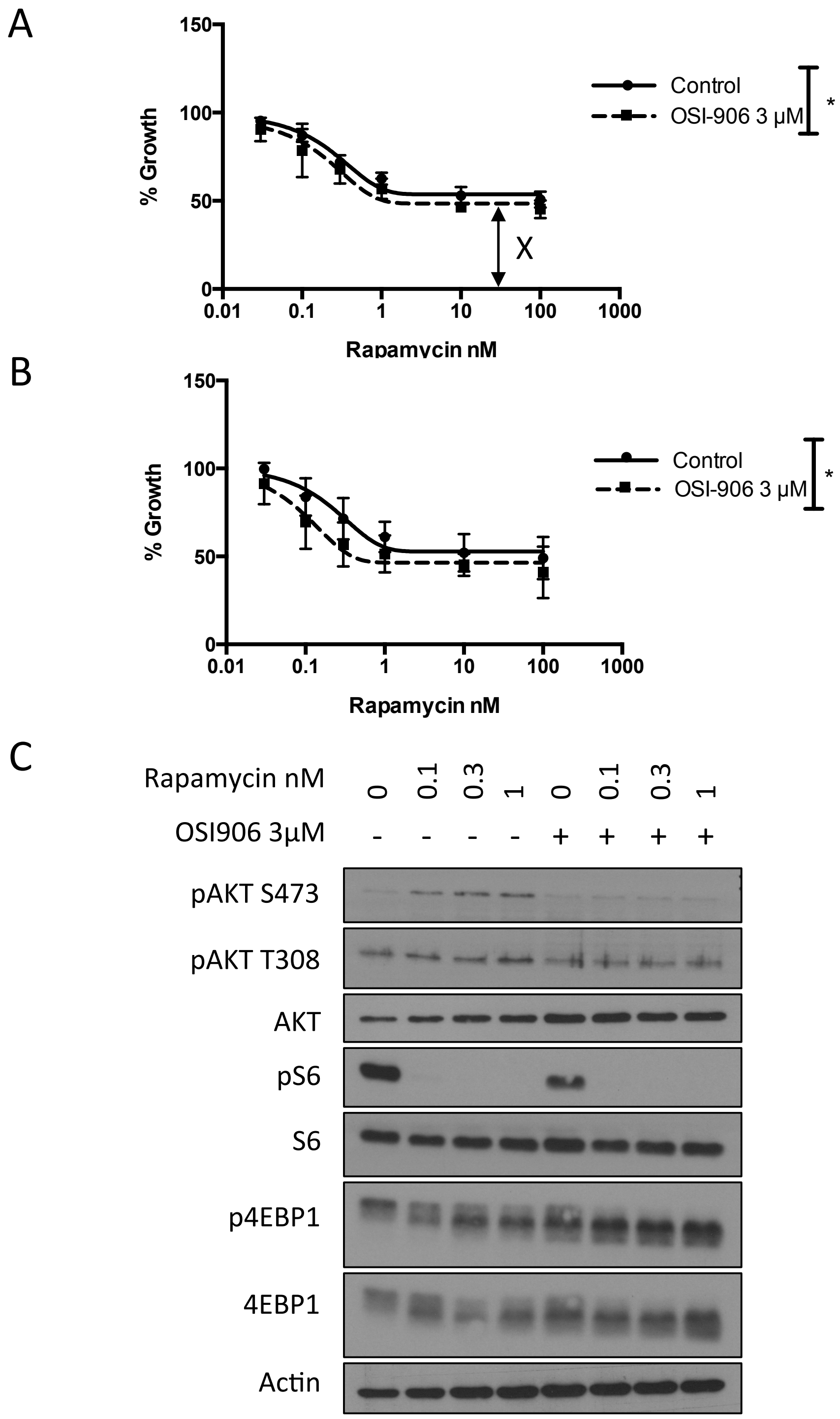


**Figure 3-7 The addition of OSI-906 does not sensitise RCC4 cells to rapamycin**

Cell viability assay of A) RCC4 EV and B) RCC4 VHL cells treated with rapamycin and solvent, or rapamycin and 3 μM OSI-906. Graph shows the mean and SEM of three independent experiments. "X" shows the population of cells resistant to treatment with rapamycin or rapamycin and OSI-906. The value of this resistant population was taken as the non-linear regression plateau best-fit value in GraphPad PRISM. * $p<0.05$ by 2 way ANOVA. Response curves were statistically significantly different by two way ANOVA ($p<0.05$), but no individual concentrations showed statistically significant differences by Bonferroni multiple comparisons testing. C) RCC4 EV cells were treated with rapamycin and OSI-906, or solvent control, simultaneously. After 6 hours cells were collected, and lysates analysed by SDS PAGE. Similar results seen in 2 independent experiments.

The combination of rapamycin and OSI-906 was also tested in 786-0EV and 786-0VHL cell lines. The addition of 3 μM OSI-906 did not induce any differences in response to rapamycin (Figure 3-8 A and B). Preliminary data in UMRC2VA (Figure 3-6 C) and UMRC2VHL (Figure 3-8 D) showed response curves that were statistically significantly different, but the change in sensitivity was unlikely to be biologically significant, as the cells were still considered resistant to rapamycin because $GI_{50}$ concentrations were not reached and the resistant populations of cells were not reduced (see Table 3-2).

Clonogenic survival/growth assays were performed in 786-0EV and 786-0VHL to test the combination of rapamycin and OSI-906 (Figure 3-8 E and F). In 786-0EV cells, OSI-906 did not induce sensitisation to rapamycin, while in 786-0VHL cells, preliminary data suggested a very minor change in response that was statistically significant by two way ANOVA. However, the addition of OSI-906 to rapamycin did not alter the $SF_{50}$, which was 0.7 nM either with, or without OSI-906.

There was no difference between VHL mutant cell lines, or their VHL wild type isogenic pairs in the response to rapamycin alone, or with OSI-906.

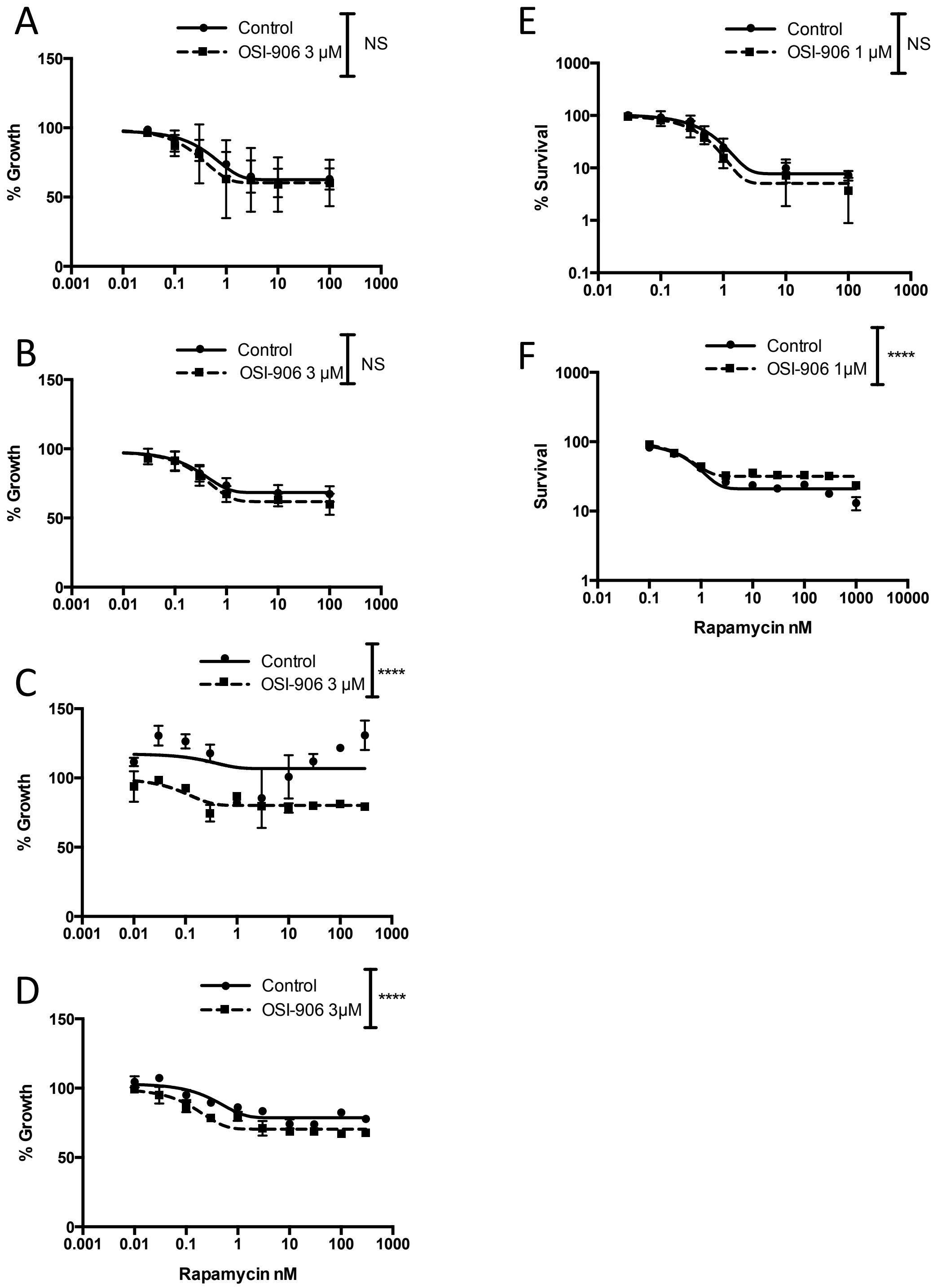


**Figure 3-8 The addition of OSI-906 does not sensitise CCRCC cells lines to rapamycin**

Cell viability assay of A) 786-0 EV, B) 786-0 VHL, C) UMRC2VA and D) UMRC2VHL cells treated with rapamycin and solvent, or rapamycin and 3 μM OSI-906. Graph shows the mean and SEM of three independent experiments (786-0EV and 786-0VHL) and mean and SEM of one experiment (UMRC2VA and UMRC2VHL). Clonogenic assay of E) 786-0EV and F) 786-0VHL cells treated with rapamycin and solvent, or rapamycin and 1 μM OSI-906. Graph E shows mean and SEM of three independent experiments, graph F shows mean and SEM of one experiment. NS, $p>0.05$, ****, $p<0.0001$ by two way ANOVA.

| Cell Line | $GI_{50}$ nM (95% CI) | | Fold change (95% CI) | % Resistant Population (95% CI) | | Fold change (95% CI) |
|---|---|---|---|---|---|---|
| | Rapamycin | Rapamycin + OSI-906 | | Rapamycin | Rapamycin + OSI-906 | |
| **RCC4 EV** | >100 | 1 (0.6 – >100) | NA | 54 (50 – 57) | 48 (42 – 54) | 0.89 (0.75 – 1.08) |
| **RCC4 VHL** | >100 | 0.4 (0.2 – >100) | NA | 53 (46 – 60) | 46 (39 – 54) | 0.87 (0.65 – 1.17) |
| **786-0 EV** | >100 | >100 | NA | 63 (58 – 67) | 60 (51 – 70) | 0.96 (0.76 – 1.21) |
| **786-0 VHL** | >100 | >100 | NA | 68 (64 – 73) | 62 (58 – 66) | 0.91 (0.79 – 1.03) |
| **UMRC2 VA** | >300 | >300 | NA | 107 (93 – 116) | 80 (78 – 83) | 0.75 (0.67 – 0.89) |
| **UMRC2 VHL** | >300 | >300 | NA | 79 (76 – 81) | 70 (68 – 73) | 0.89 (0.84 – 0.96) |

**Table 3-2 Summary of effects of rapamycin alone or with OSI-906 on growth of CCRCC cells**

Table shows the $GI_{50}$ (nM) and the population of CCRCC cell lines resistant to rapamycin in solvent control or with 3 µM OSI-906 expressed as a percentage of untreated control. The resistant population was taken as the non-linear regression plateau best-fit value in GraphPad PRISM.

There was no significant difference observed in $GI_{50}$ of rapamycin with the addition of OSI-906. There was no significant difference between EV and VHL cell pairs in the response to rapamycin alone or with OSI-906. Comparison of fold change in resistant population with OSI-906 between EV and VHL pairs of cell lines showed overlapping 95% confidence intervals in all three pairs indicating no difference in effects of OSI-906 between cells with wild type and mutant, non functional VHL.

### 3.2.8 The effects of AZ12253801

Before rejecting the hypothesis that IGF-1R inhibition can sensitise CCRCC cell lines to rapamycin, an alternative inhibitor of the IGF-1R was tested. AZ12253801 (AZ3801) is a novel tyrosine kinase inhibitor of the IGF-1R developed by Astra Zeneca (Aleksic et al. 2010, Chitnis et al. 2013). Initially, the anti-proliferative effects of single agent AZ3801 were tested in RCC4EV and RCC4VHL cell lines (Figure 3-9 A) and in 786-0EV and 786-0VHL (Figure 3-9 B). There was a statistically significant trend by two way ANOVA in both cell line pairs, for the VHL wild type cells to be more sensitive, although the differences were very minor. Higher concentrations of AZ3801 were not used to fully explore the potential differences in proliferative response to single agent treatment because Astra Zeneca reported finding off target effects on aurora kinase at higher concentrations (personal communication to Dr V. Macaulay). This effect has been observed by our group in flow cytometry, immunofluorescence and cell proliferation assays by the presence of giant polyploid cells. There were no such cells visible at any concentration of AZ3801 used in the proliferation assays performed in this project, suggesting that significant inhibition of aurora kinase was unlikely.

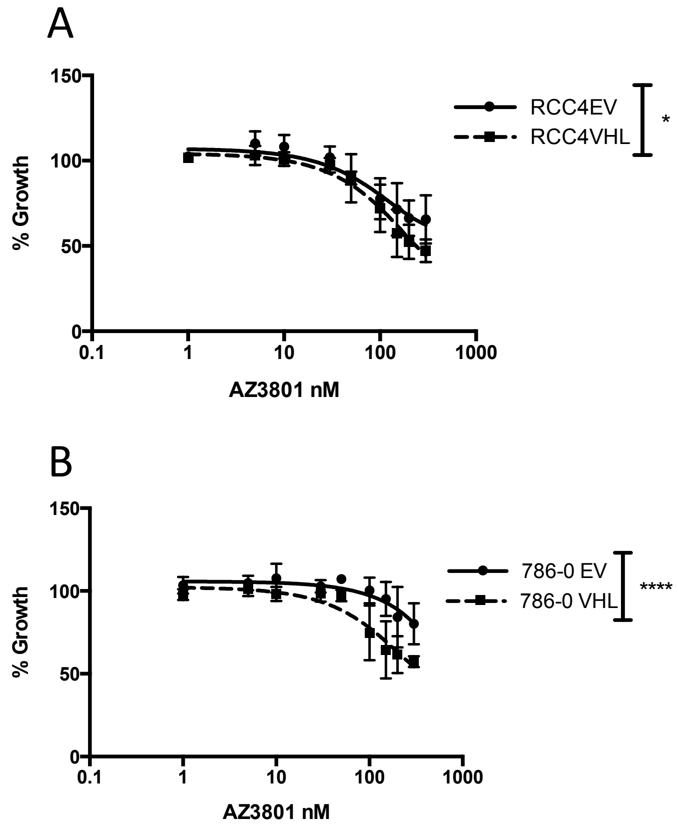


**Figure 3-9 Anti-proliferative effects of AZ3801 in RCC4 and 786-0 CCRCC cell lines**

CTG cell viability assays of A) RCC4 EV and RCC4 VHL and B) 786-0 EV and 786-0 VHL CCRCC cell lines. Graphs show mean and SEM of three independent experiments. * $p=0.0105$, ****$p<0.0001$ by two way ANOVA.

In order to test the combination of AZ3801 with rapamycin, the concentration of 50 nM AZ3801 was used based upon previous work in our group in prostate cancer and melanoma cell lines showing consistent inhibition of pIGF-1R at this concentration (Chitnis et al. 2013). This combination was tested in cell viability assays in both the RCC4 cell line pair (Figure 3-10 A and B) and in the 786-0 cell line pair (Figure 3-10 C and D). None of the tested cell lines showed a change in response to rapamycin as judged by $GI_{50}$ value, or in the rapamycin resistant population.

Since two IGF-1R inhibitors failed to sensitise to rapamycin it was accepted that the hypothesis that chemical IGF-1R inhibition could sensitise to rapamycin was incorrect. This was in contrast to previous published data from our group that showed depletion of the IGF-1R with siRNA was able to sensitise to rapamycin (Yuen et al. 2009), so thought was given to why the chemical inhibitors may be ineffective. Data obtained so far indicated that rapamycin was active in CCRCC cell lines in culture for at least 7 days (Figure 3-3 B), and that the IGF-1R inhibitor OSI-906 was able to block AKT activation for at least 6 hours in the presence of rapamycin. The duration of cell viability assays was 72 hours, and of clonogenic survival/growth assays 7 days. The effects of OSI-906 over this time-course were unknown, and were explored in more detail, aiming to identify possible reasons for the discrepancy with the previous data (Yuen et al. 2009).

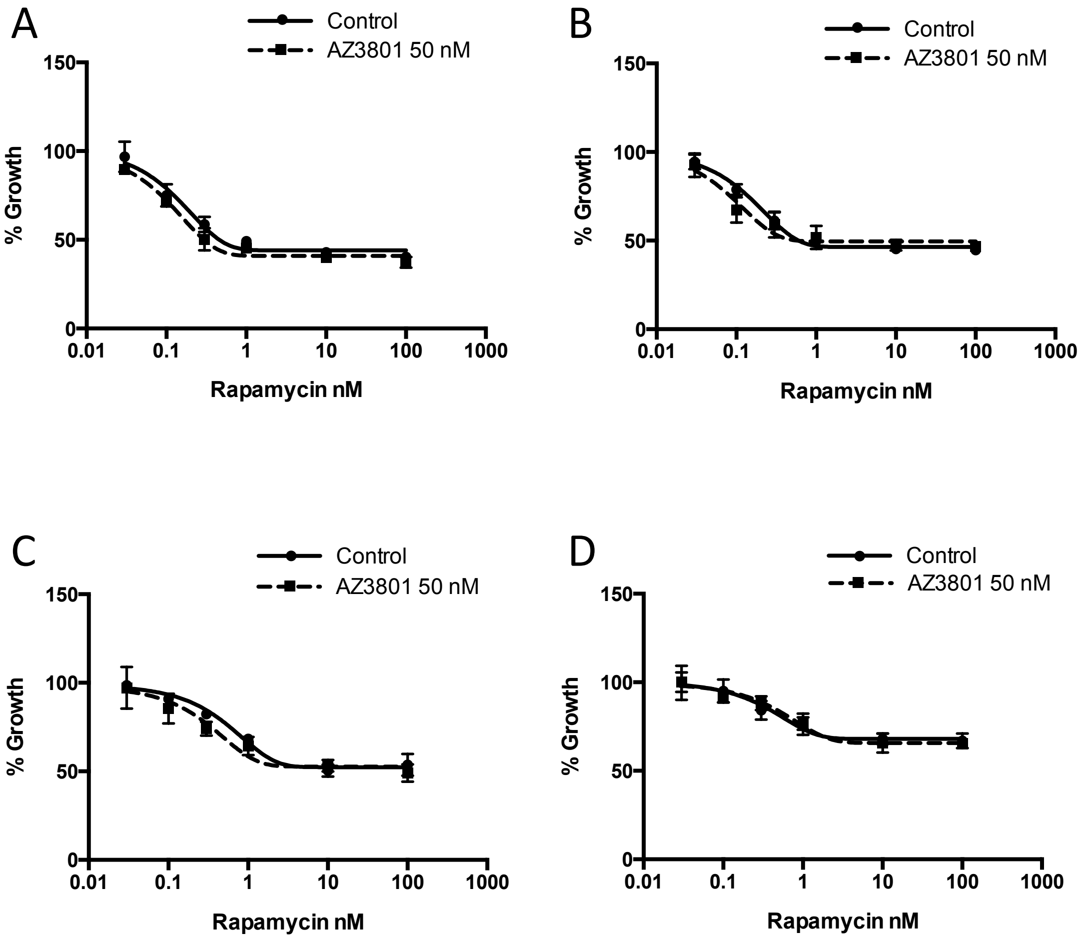


**Figure 3-10 The addition of AZ3801 does not sensitise CCRCC cells to rapamycin**

CTG cell viability assays of A) RCC4 EV, B) RCC4 VHL, C) 786-0 EV and D) 786-0 VHL cells treated with rapamycin and solvent, or rapamycin and 50 nM AZ3801. Graphs show mean and SEM of one assay.

### 3.2.9 Signalling response to prolonged IGF-1R blockade

The stability of OSI-906 in culture and the duration of its inhibition of the IGF-1R was established in 786-0EV cells. In order to readily detect pIGF-1R by western blot, it was necessary to serum deprive cells, followed by stimulation with IGF-1 ligand. If cells were treated with prolonged OSI-906 in complete medium, and then serum deprived, the addition of fresh OSI-906 would be required in the serum-deprived media, and information on the stability of OSI-906 in culture would be lost, although information on prolonged IGF-1R inhibition would be retained. It was therefore decided to treat 786-0EV cells with OSI-906 during prolonged serum deprivation, and stimulate by the addition of 10 nM IGF-1 for the final ten minutes of treatment. This experiment would therefore show the duration of action of a single application of OSI-906, and closely mimic the conditions of a cell viability, or clonogenic survival/growth assay. Under these conditions, it was clear that OSI-906 was able to inhibit IGF-1 stimulated autophosphorylation of the IGF-1R for up to, and including 96 hours (Figure 3-11). Downstream of the IGF-1R however, OSI-906 was able to inhibit pAKT S473 and T308 at 1 hour, but by six hours of treatment, AKT phosphorylation recovered to levels in the untreated control. This reactivation of AKT could in part explain the failure of OSI-906 to sensitise to rapamycin. It is possible that OSI-906 blocked the rapamycin induced feedback release of inhibition of AKT activation via the IGF-1R at early time-points (Figure 3-7 C), but that AKT became reactivated at later times allowing on-going proliferation and protection from apoptosis.

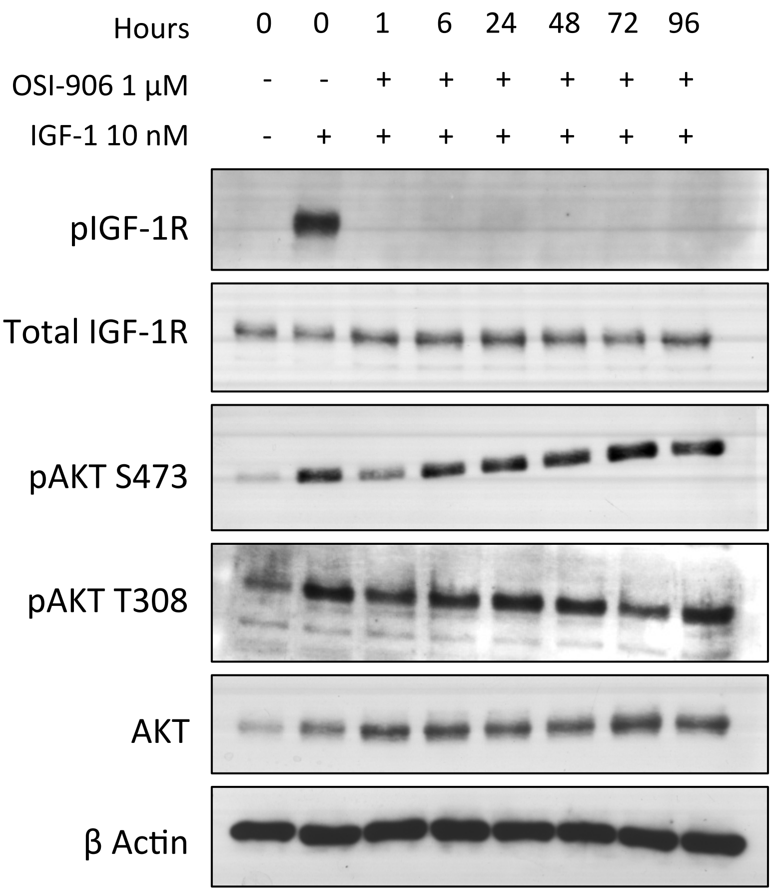


**Figure 3-11 Reactivation of AKT despite on-going IGF-1R blockade in OSI-906 treated cells**

Monolayer 786-0 EV cells were serum deprived for 24 hours and then treated with 1μM OSI-906, or solvent control in serum free medium for the indicated time, and in the last ten minutes with 10 nM IGF-1 ligand, or solvent control. Cell lysates were analysed by SDS-PAGE. Representative western blot shown. Similar results were seen in a second set of independently prepared cell lysates. Similar results seen in 2 independent experiments.

### 3.2.10 Possible pathways leading to AKT re-activation

There are a number of potential explanations for the reactivation of AKT during prolonged treatment with OSI-906. There are numerous reports of cross-talk between receptor tyrosine kinases, including activation of the IR in response to IGF-1R blockade (Buck et al. 2010) and that the IR is implicated in intrinsic and acquired resistance to IGF1-R inhibition (Ulanet et al. 2010). Although OSI-906 is active against the IR due to the homology in their kinase domains, it shows a two-fold selectivity for the IGF-1R over the IR. It is possible therefore that despite maintaining blockade of the IGF-1R, some activity remains, or recovers sooner in the IR. Two pieces of evidence point against this hypothesis: firstly, the antibody used to detect pIGF-1R (Cell Signaling #3024) also detects pIR, and secondly, 786-0EV cells do not express detectable levels of IR (Figure 3-12).

There are well characterised reports of cross talk between the IGF-1R and the EGFR whereby small molecule inhibition of one receptor causes feedback activation of the other (Buck et al. 2008, Desbois-Mouthon et al. 2009). These data could suggest an approach to screen for activated receptor tyrosine kinases in response to OSI-906, with a view to combining multiple drugs against these targets, e.g. combining rapamycin with OSI-906 and the EGFR inhibitor erlotinib if increases in activity of the EGFR were seen. There are in fact reports of synergy between rapamycin and the EGFR inhibitor gefitinib in pancreatic neuroendocrine tumour models where the two drugs combined decreased pAKT levels (Chiu et al. 2010). Rapamycin and erlotinib have been shown to work synergistically in non-small cell lung, pancreatic, colon and breast cancer, through inhibition of AKT activation (Buck et al. 2006). Rapamycin and gefitinib have also been combined in renal cancer *in vitro* with synergistic effects on growth, though not through inhibition of AKT activation (Gemmill et al. 2005).

Two factors suggested an alternative approach to assess whether the AKT re-activation was causative of rapamycin resistance and lack of effect of IGF-1R inhibition. The first factor was the likely redundancy in the feedback loops activating tyrosine kinase receptors, such that targeting individual receptors with specific drugs can be quickly bypassed by the cell, with resulting reactivation of AKT. The inhibition of AKT has been shown to cause feedback activation of IGF-1R, IR and HER3 in a variety of cancers (Chandarlapaty et al. 2011, Tao et al. 2014). In this case, targeting IGF-1R and one other receptor tyrosine kinase may prove ineffective if a third, fourth, or multiple receptors become activated. The second factor was the possibility of redundancy in the relief of inhibitory feedback when mTORC1 is inhibited by rapamycin. As well as IGF-1R – IRS1 signalling, AKT activation following mTORC1 inhibition has also been linked specifically to the PDGFR (O'Reilly et al. 2006, Zhang et al. 2007, Yuen et al. 2009, Ho et al. 2012). In addition to feedback onto IRS-1, mTORC1 also feeds back onto the adaptor protein growth factor receptor-bound protein 10 (Grb 10), which is a direct phosphorylation target of mTOR kinase (Hsu et al. 2011). On inhibition of mTOR, Grb 10 stability is decreased and AKT is activated. Grb 10 is best characterised as negative regulator of IGF-1R and IR signalling, but has also been shown to bind to other receptors including c-KIT, EGFR, Eph family, growth hormone receptor (GHR), FGFR, PDGFβR, Ret and VEGFR, although the physiological role of these interactions is not clear (Holt and Siddle 2005).

Given the predicted large redundancy in feedback signalling, the alternative approach taken here was to target the pathway of AKT activation downstream of receptor tyrosine kinases, at a point common to all pathways. In the first instance this intervention was made at the level of PI3K, and then also with direct inhibitors of AKT action.

For this part of the project, only the 786-0 and RCC4 pairs of cell lines were used. The UMRC2 pair was not used because of difficulty growing them in clonogenic and viability assays. The UMRC2VA cells in particular were very slow growing and it proved difficult to obtain reproducible data.

In 786-0 and RCC4 cells, baseline signalling along the IGF-1R – PI3K – AKT – mTOR pathway was assessed by western blotting (Figure 3-12). 786-0EV and VHL cells have a c.445C>T nonsense mutation (http://cancer.sanger.ac.uk/cell_lines/mutation/overview?id=5164) in *PTEN*, which results in no detectable PTEN expression. Consequently they showed high basal levels of phosphorylation of AKT, and the AKT target PRAS40. RCC4 cells are PTEN wild type, but showed higher basal phosphorylation of ERK1/2.

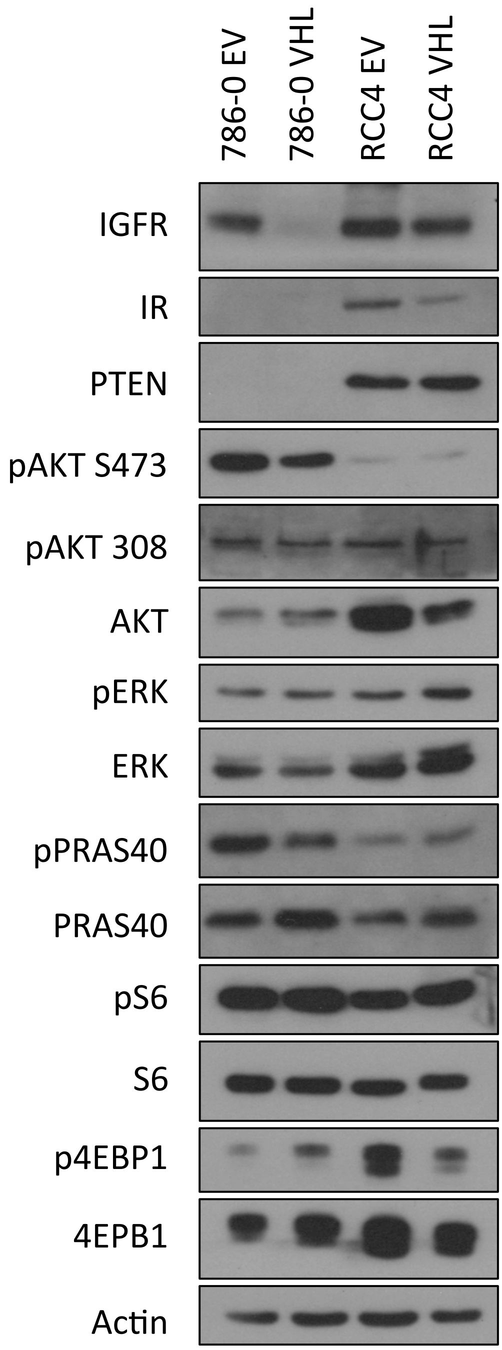


**Figure 3-12 Characterisation of IGF-1R - AKT - mTOR pathway in 786-0 and RCC4 cell lines**

Western blot of whole cell lysates from the indicated cell lines prepared from cells growing in full medium with 10% FCS, showing basal expression and phosphorylation of the major proteins of the IGF-1R – AKT – mTOR signalling pathway. Similar results were seen in two sets of independently prepared lysates.

### 3.2.11 The effects of PI3K inhibitors in CCRCC cell lines

Two novel PI3K inhibitors with different specificities, both created by Novartis, were used to more directly test the hypothesis that AKT activation was contributing to resistance to rapamycin. BKM120 is a pan class one PI3K inhibitor, which is in early clinical phase trial development (Bendell et al. 2012, Maira et al. 2012). BEZ235 is a dual PI3K and mTORC kinase inhibitor, which is also in early phase clinical testing (Maira et al. 2008, Arkenau et al. 2012). The published $IC_{50}$ values for these two drugs against PI3K and mTORC kinases are listed in Table 3-3. BEZ235 has also been shown to inhibit two kinases that are involved in the response to double-strand DNA breaks, DNA dependent protein kinase (DNAPK) and ataxia telangiectasia mutated (ATM) (Mukherjee et al. 2012). These properties of BEZ235 were not examined in this work.

| **Enzyme** | | **$IC_{50}$ nM** | |
|---|---|---|---|
| | | **BKM120** | **BEZ235** |
| **Class I PI3K** | p110α | 52 | 4 |
| | p110α-H1047R | 58 | 4.6 |
| | p110α-E545K | 99 | 5.7 |
| | p110β | 166 | 75 |
| | p110δ | 116 | 7 |
| | p110γ | 262 | 5 |
| **Class IV PI3K** | mTOR | 2866 | 6.5 |

**Table 3-3 Published IC50 concentrations of BKM120 and BEZ235**

IC50 concentrations from the original reports of BKM120 and BEZ235 (Maira et al. 2008, Maira et al. 2012).

In the first instance, the two compounds were tested for their ability to inhibit PI3K, mTORC1 and mTORC2 *in vitro* in renal cancer cells (Figure 3-1). BEZ235 inhibited PI3K with evidence of decrease in pAKT T308 seen at 50 nM BEZ235, and complete inhibition at 1000 nM. A similar pattern was observed in its ability to inhibit mTORC2 as evidenced by a decrease in pAKT S473 detectable at 10 nM, with complete inhibition by 500 nM BEZ235. BEZ235 was able to inhibit mTORC1, as evidenced by complete inhibition of S6 phosphorylation at 10 nM BEZ235.

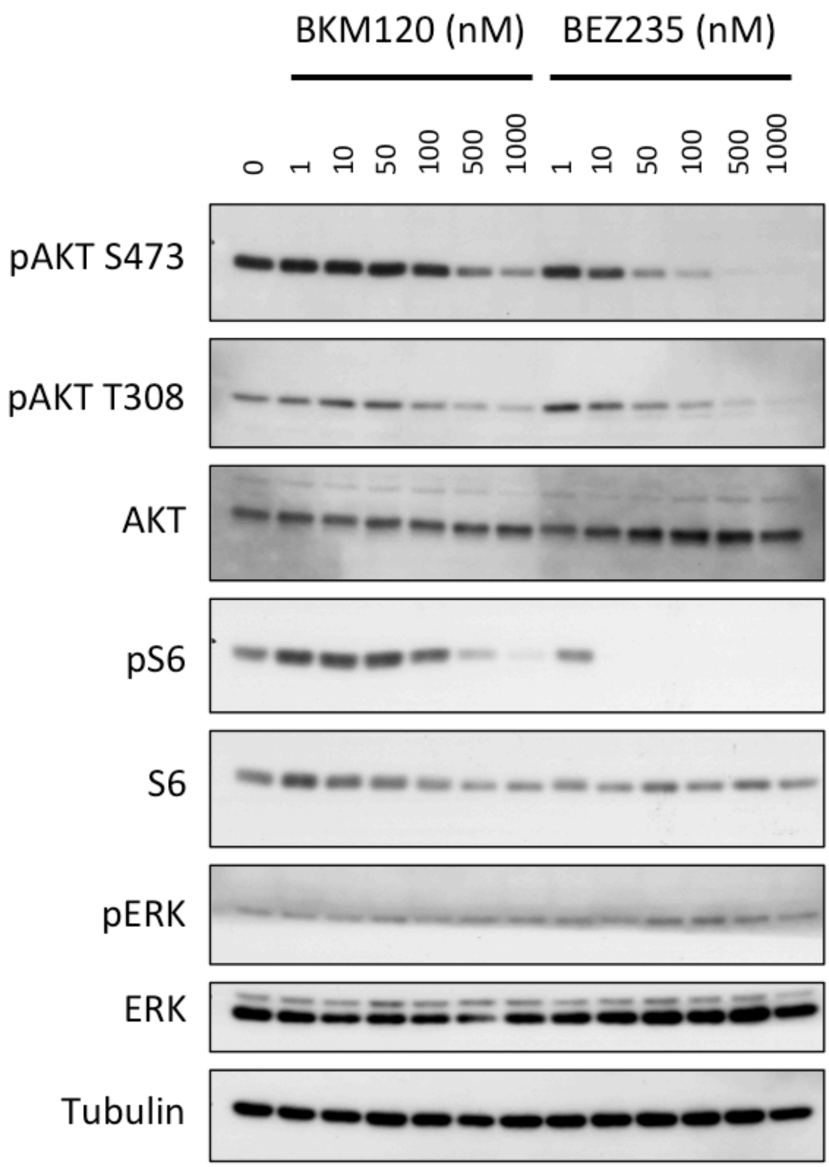


**Figure 3-13 BKM120 and BEZ235 inhibit the phosphorylation of AKT**

Monolayer 786-0 EV cells were treated with solvent, BKM120 or BEZ235 at the indicated concentration for 1 hour. Cell lysates were analysed by SDS PAGE. Similar results were seen in another set of independently prepared cell lysates.

In contrast to BEZ235, BKM120 only inhibited PI3K at higher concentrations. Decreases in pAKT T308 were seen from 100 nM, but even at 1000 nM, PI3K was not completely inhibited and pAKT T308 was still detectable. BKM120 also exhibited activity against mTORC1 and mTORC2 at 500 nM and above, as seen in decreasing levels of pS6 and pAKT S473 respectively (Figure 3-13).

Next, the effects of single agent BKM120 on cell viability were assessed in RCC4 and 786-0 cells, in both *VHL* mutant and *VHL* wild type sublines (Figure 3-14 A and B). BKM120 caused concentration dependent inhibition of cell viability in all four cell lines. In the RCC4 cell pair, the RCC4VHL subline was slightly more sensitive, with a statistically significant difference in the response as assessed by two-way ANOVA (Figure 3-14 A), but no individual concentration reached statistical significance by Bonferroni's multiple comparisons test, the fold change in $GI_{50}$ was relatively modest and the 95% confidence interval for this fold change crossed 1 (Figure 3-14 C). It was therefore felt that this difference was unlikely to be of biological significance. The 786-0 cell pair showed no statistical significance in their response to BKM120. It was noted that 786-0 cells are PTEN null, and had a higher $GI_{50}$ compared to RCC4 cells, which are *PTEN* wild type (Figure 3-12).

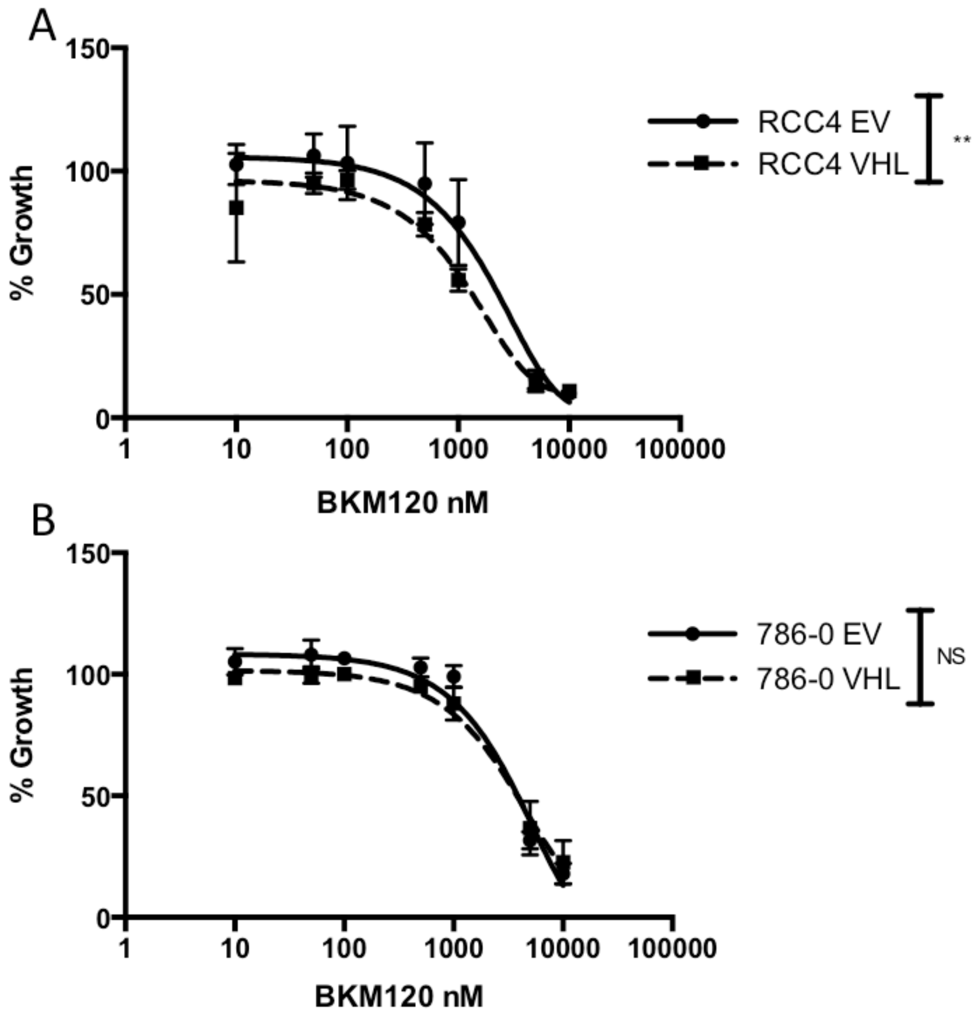


C

| Cell Line | GI50 (nM) (95% CI) | Fold Change (95% CI) |
|---|---|---|
| RCC4 EV | 2300 (1700 – 3200) | 0.57 (0.31 – 1.06) |
| RCC4 VHL | 1300 (1000 – 1800) | |
| 786-0 EV | 3900 (3100 – 4700) | 0.97 (0.64 – 1.48) |
| 786-0 VHL | 3800 (3000 – 4600) | |

**Figure 3-14 BKM120 inhibits the proliferation of CCRCC cells**

CTG proliferation assay of A) RCC4 EV and RCC4 VHL, and B) 786-0 EV and 786-0 VHL cells. Graphs show mean and SEM of three independent experiments. ** p=0.0073, NS p>0.05. C) Table of $GI_{50}$ values and fold change in $GI_{50}$ values (EV:VHL). RCC4VHL cells appeared more sensitive to BKM120 than RCC4EV by two-way ANOVA (** p=0.0073) with lower $GI_{50}$ value, but the changes were relatively minor, and the 95% confidence intervals of the fold change crossed 1. There was no difference in the sensitivity of 786-0EV and 786-0VHL cells.

### 3.2.12 The effects of combining the PI3K inhibitor BKM120 with rapamycin

The combination of BKM120 and rapamycin was tested to see whether inhibiting PI3K could block the rapamycin induced feedback increase in pAKT, irrespective of which cell surface receptor was activated to cause that increase. For these experiments a concentration of 500 nM BKM120 was chosen. At this concentration, clear changes in pAKT T308 and pAKT S473 had been observed, with only a small inhibition in pS6 (Figure 3-13). Cell viability assays were performed in RCC4EV, RVV4VHL, 786-0EV and 786-0VHL cells (Figure 3-15 A, B, C and D respectively). No difference was seen in the response of RCC4EV cell with the addition of BKM120, and although a statistically significant difference by two-way ANOVA was detected in RCC4VHL cells, the resistant population did not change significantly. Without BKM120, the resistant population was 52% (95% CI 47 – 57) and with BKM120 it was 47% (95% CI 42 – 52). The pattern was the same for the 786-0EV and VHL pair of cell lines, with no statistical difference detected in 786-0EV cells, and a statistically significant difference in 786-0VHL cells by two-way ANOVA, but without a significant change in the resistant population (58% without BKM120, and 57% with BKM120).

Analysis of the effects of the combination of 500 nM BKM120 with rapamycin on signalling along the AKT – mTOR pathway revealed that BKM120 completely inhibited the rapamycin induced increase in pAKT T308 and pAKT S473 (Figure 3-15 E). The combination had only a small effect on signalling downstream of mTORC1 as seen by small reductions in pS6 and p4E-BP1.

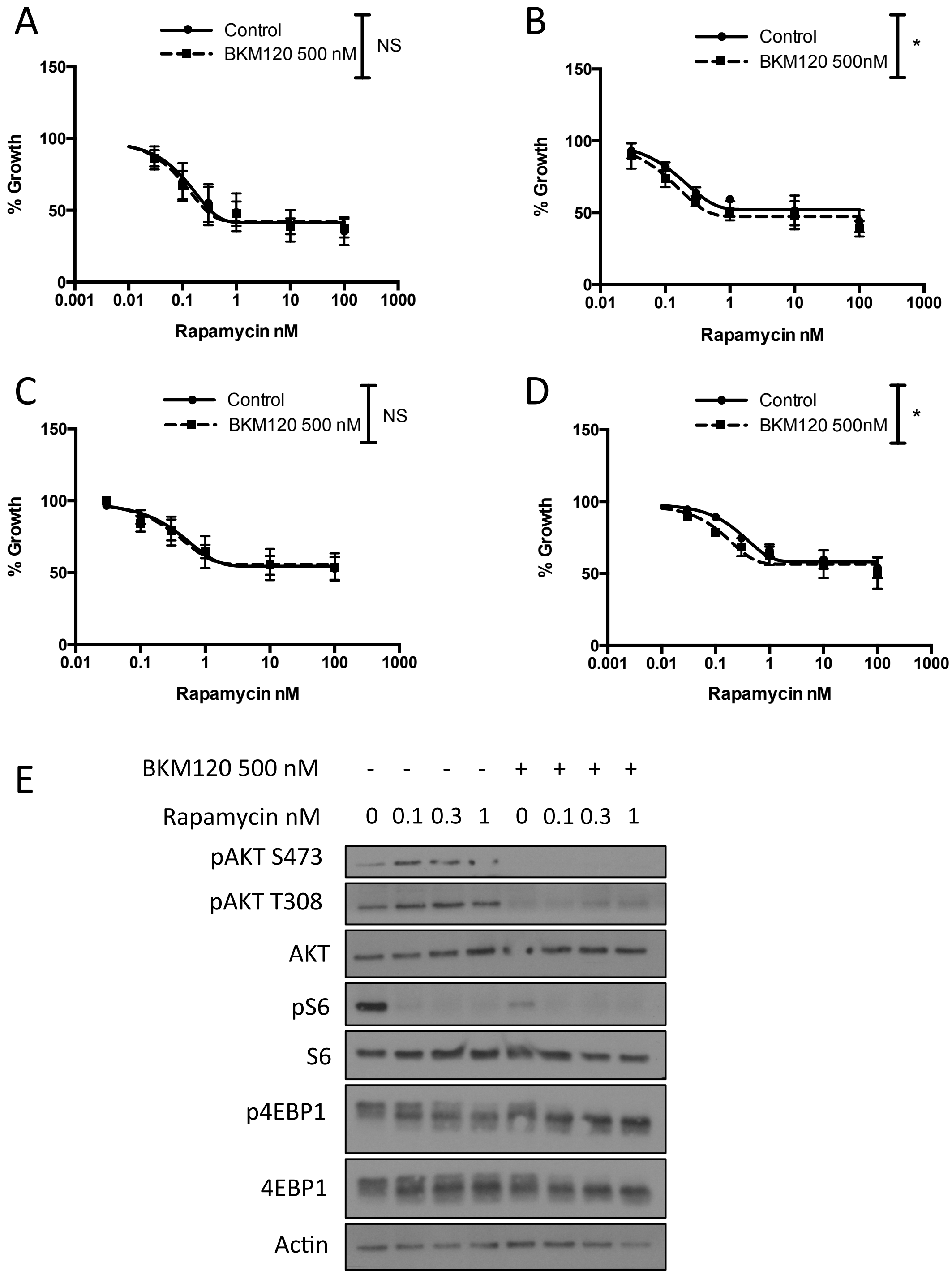


**Figure 3-15 The addition of the PI3K inhibitor BKM120 does not sensitise CCRCC cells to rapamycin**

CTG proliferation assay of A) RCC4 EV, B) RCC4 VHL, C) 786-0 EV and D) 786-0 VHL cells treated with rapamycin and solvent, or rapamycin and BKM120 500 nM. Graphs show mean and SEM of three independent experiments. NS p>0.05, *p<0.05. E) Monolayer RCC4 EV cells were treated simultaneously with the indicated concentration of rapamycin and solvent, or rapamycin and 500 nM BKM120 for 6 hours. Cell lysates were analysed by SDS PAGE. Similar results were seen in another independent experiment.

In addition to blocking PI3K to block the activation of AKT, a direct AKT inhibitor was tested in combination with rapamycin. AZD5363 is a novel AKT inhibitor made by AstraZeneca that is in early phase clinical trials (Davies et al. 2012). The use of this drug allowed another approach to test whether AKT activation was a key resistance mechanism to mTOR inhibition, regardless of which feedback loop was activated to result in increased pAKT. Cell viability assays were performed on RCC4EV and 786-0EV (Figure 3-16 A and B). As in experiments with BKM120, AZD5363 caused no significant effect on the response to rapamycin, as determined by $GI_{50}$ values or resistant population.

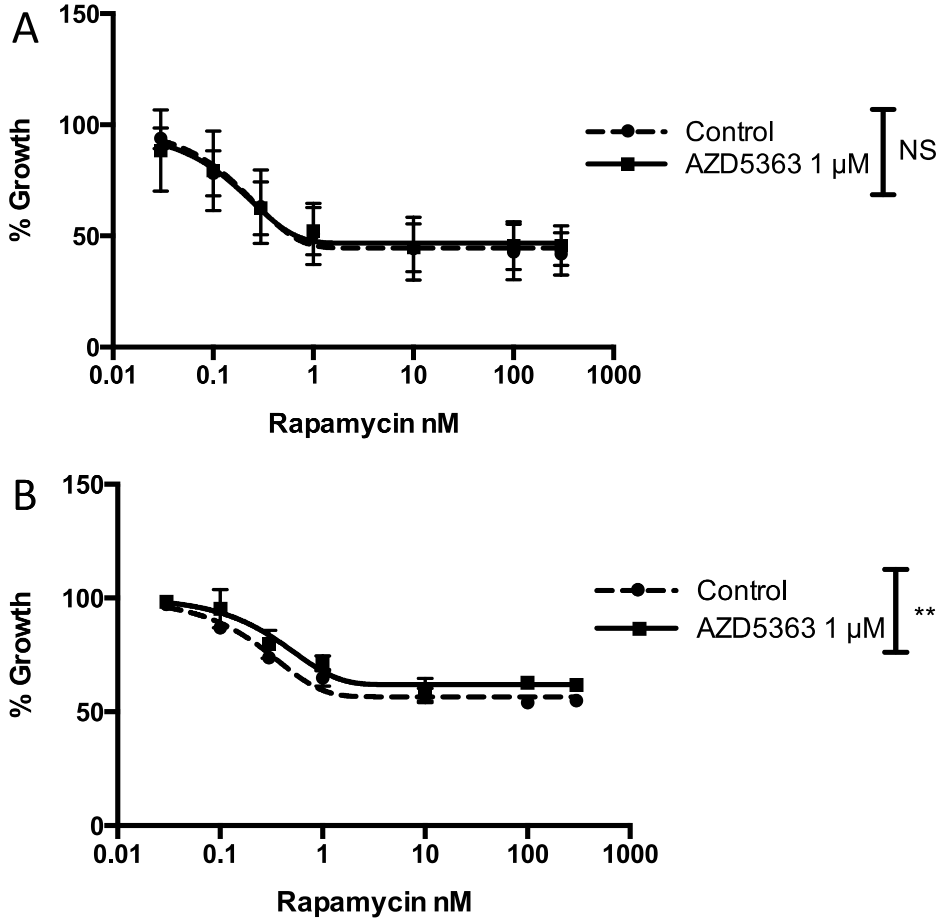


**Figure 3-16 The addition of the AKT inhibitor AZD5363 does not sensitise to rapamycin**

CTG cell viability assays of A) RCC4EV and B) 786-0EV cells treated with rapamycin and solvent, or rapamycin and 1 μM AZD5363. Graphs show mean and SEM of two independent experiments. NS $p>0.05$, ** p0.0015 by two way ANOVA.

### 3.2.13 The relative effects of BEZ235 and rapamycin

The drug BEZ235 inhibits PI3K, and so it was thought that it could be capable of inhibiting rapamycin-induced AKT activation. Additionally it directly inhibits mTOR kinase in an ATP dependent manner (Maira et al. 2008), which is in contrast to rapamycin, which inhibits mTOR in an allosteric manner through its interaction with FKBP12. As explained earlier this gives rapamycin specificity for inhibiting mTORC1. BEZ235, as a direct mTORC kinase inhibitor inhibits both mTORC1 and mTORC2. Therefore, with a single compound, mTORC1 is inhibited, as well as the two kinases that phosphorylate AKT at T308 (PI3K) and at S473 (mTORC2). In theory, this should produce a greater effect on viability and cell survival if AKT activation is implicated in resistance to mTORC1 inhibition.

The first experiment was to compare BEZ235 to rapamycin to examine the effects on AKT – mTOR signalling. In RCC4EV cells, rapamycin caused a dose dependent increase in pAKT S473 (Figure 3-17) as seen previously, while BEZ235 inhibited AKT phosphorylation at concentrations of 10 nM or greater. Both compounds blocked mTORC1 signalling to S6, though with differing potency. Rapamycin caused complete inhibition at the lowest concentration tested of 0.1 nM. BEZ235 caused only a partial inhibition at the lowest concentration tested (1 nM) and 10 nM was required for complete inhibition. Although both compounds caused a complete inhibition of S6 phosphorylation, they had differing effects on the alternative downstream target of mTORC1, 4E-BP1. Rapamycin caused only a small degree of inhibition, whereas BEZ235 caused a clear dose-dependent decrease in p4E-BP1.

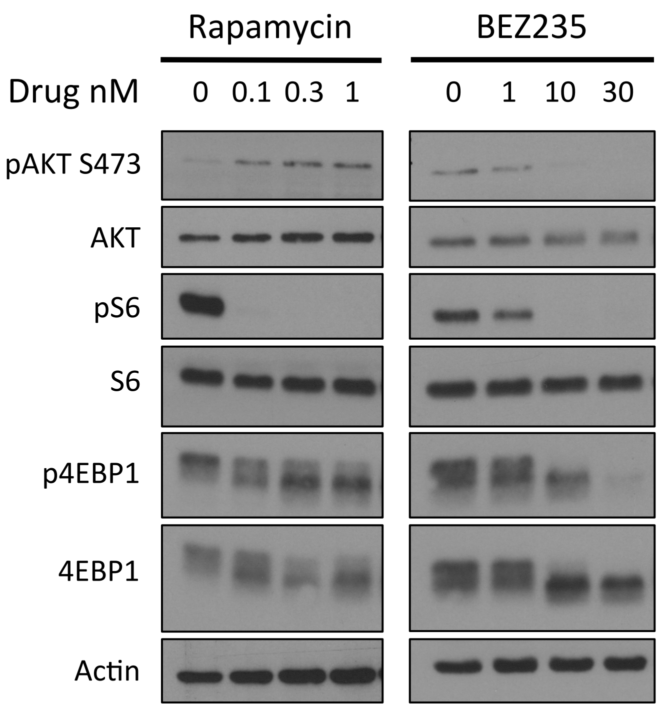


**Figure 3-17 The effects of rapamycin and BEZ235 on mTOR signalling in RCC4EV cells**

Monolayer RCC4 EV cells were treated with the indicated concentration of solvent, rapamycin or BEZ235 for 6 hours. Cell lysates were analysed by SDS-PAGE. Similar results seen in 3 independent experiments.

Cell viability assays were conducted in RCC4 cells to compare effects of rapamycin and BEZ235 (Figure 3-18 A and B). As predicted from its molecular action, and observed changes in signalling, BEZ235 caused greater inhibition of viability as evidenced by a smaller resistant population in the BEZ235 treated cells. The same pattern was seen in 786-0EV and 786-0VHL cells (Figure 3-18 C and D). In slight contrast, but in keeping with the potency of target inhibition seen in Figure 3-17, the $GI_{50}$ for BEZ235 was greater than for rapamycin in RCC4EV and VHL cells (Figure 3-18 E). The picture for 786-0EV and 786-0VHL cells was similar in that higher concentrations of BEZ235 were required to begin to inhibit viability, but BEZ235 achieved a smaller residual resistant population than did rapamycin. The $GI_{50}$ values and resistant populations are summarised in Figure 3-18 E.

It was interesting to note that the decrease in p4E-BP1 observed in Figure 3-17 correlated well with the ability of rapamycin and BEZ235 to inhibit viability, while the levels of pAKT S473 and pS6 did not. This is in keeping with results seen by other groups and with other mTORC kinase inhibitors: 4E-BP1 has been called a rapamycin insensitive target of mTORC1 and has been uncovered largely as a result of the development of this class of drugs, the first two of which were Torin1 (Thoreen et al. 2009) and PP242 (Feldman et al. 2009). Similar results showing that inhibition of 4E-BP1 phosphorylation correlates with inhibition of proliferation have been reported for BEZ235 both in renal cancer, and other cancers including breast cancer, and glioblastoma (Serra et al. 2008, Breuleux et al. 2009, Cho et al. 2010, Nyfeler et al. 2012).

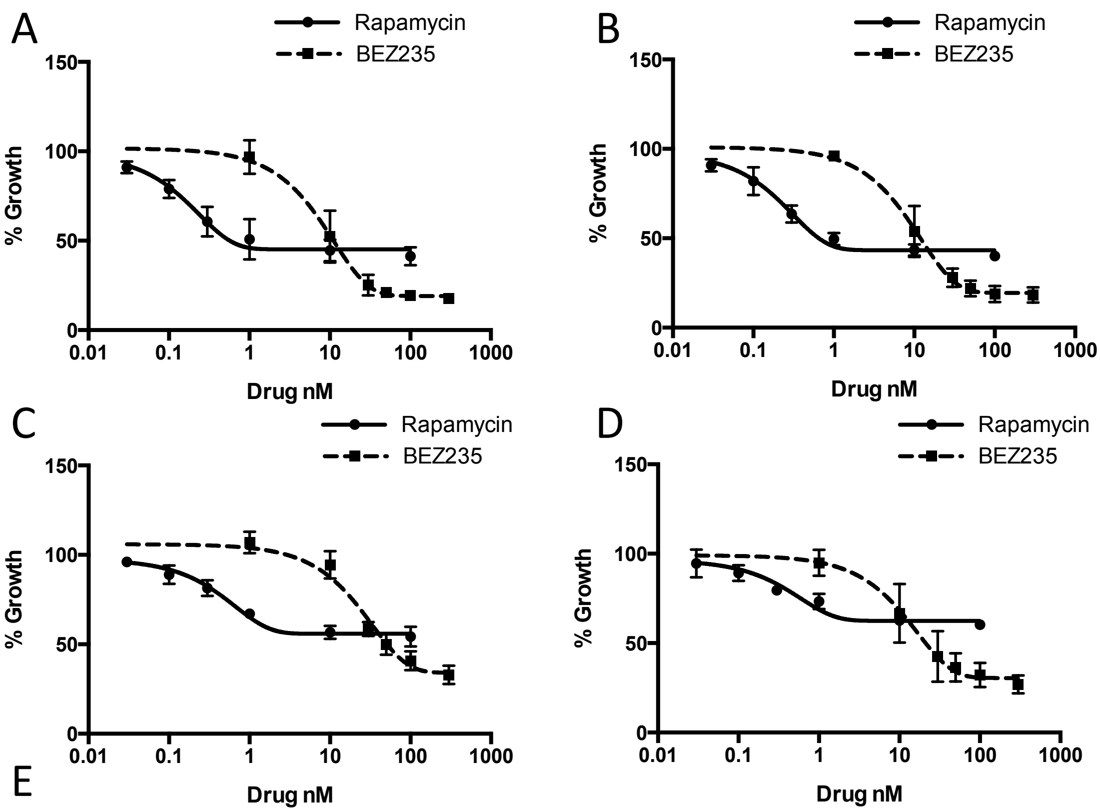


E

| Cell Line | Rapamycin GI$_{50}$ nM (95% CI) | Rapamycin Resistant Population % (95% CI) | BEZ235 GI$_{50}$ nM (95% CI) | BEZ235 Fold Change (95% CI) | BEZ235 Resistant Population % (95% CI) | BEZ235 Fold Change (95% CI) |
|---|---|---|---|---|---|---|
| RCC4EV | 0.6 (0.4 – 1.0) | 45 (41 – 50) | 11 (9 – 14) | 1.1 (0.71 – 1.7) | 19 (15 – 23) | 1.0 (0.65 – 1.60) |
| RCC4VHL | 0.7 (0.5 – 0.8) | 43 (40 – 47) | 12 (10 – 15) | | 19 (15 – 24) | |
| 786-0EV | > 100 | 56 (53 – 59) | 51 (41 – 63) | 0.41 (0.24 – 0.71) | 34 (27 – 41) | 0.88 (0.59 – 1.37) |
| 786-0VHL | >100 | 62 (59 – 66) | 21 (15 – 29) | | 30 (24 – 37) | |

**Figure 3-18 Relative effects of BEZ235 and rapamycin on viability of RCC cells**

CTG viability assay of A) RCC4 EV, B) RCC4 VHL, C) 786-0 EV and D) 786-0 VHL cells treated with rapamycin or BEZ235. Graphs show mean and SEM of three independent experiments. E) Table of GI$_{50}$ values (nM) and resistant populations of cells (%) and fold change (EV:VHL) for BEZ235.

Clonogenic survival/growth assays in RCC4EV and 786-0EV cells (Figure 3-19 A and B) replicated the effects seen in cell viability assays. $SF_{50}$ concentrations for BEZ235 were higher than for rapamycin in both cell lines (Figure 3-19 C). However, BEZ235 was able to produce more complete inhibition of cell survival in both RCC4EV and 786-0EV cells at the highest concentrations of BEZ235 as compared to 10% cell survival with the highest concentrations of rapamycin.

The effects of BEZ235 causing a greater total inhibition of phosphorylation of 4E-BP1 in renal cancer cell lines in comparison to rapamycin and also in causing a greater inhibition in viability has also been shown by Cho and colleagues (Cho et al. 2010). This group also went on to show that BEZ235 in comparison to rapamycin, caused nuclear localization of p27, and decreased expression of HIF2α and cyclin D.

A

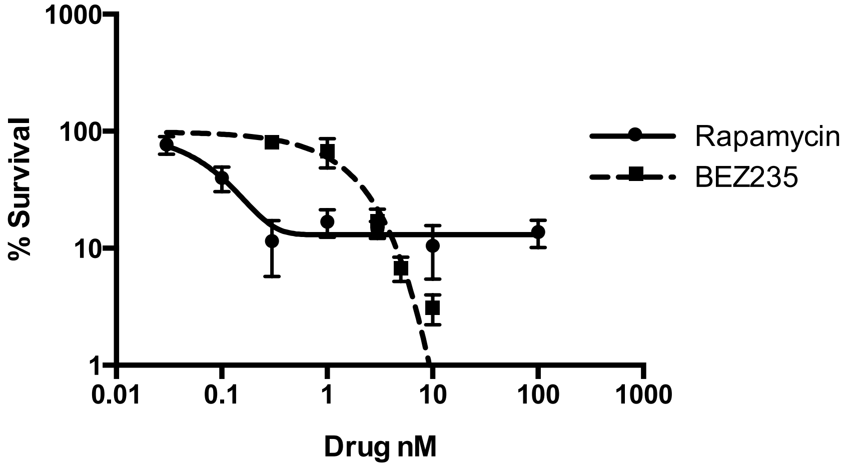


B

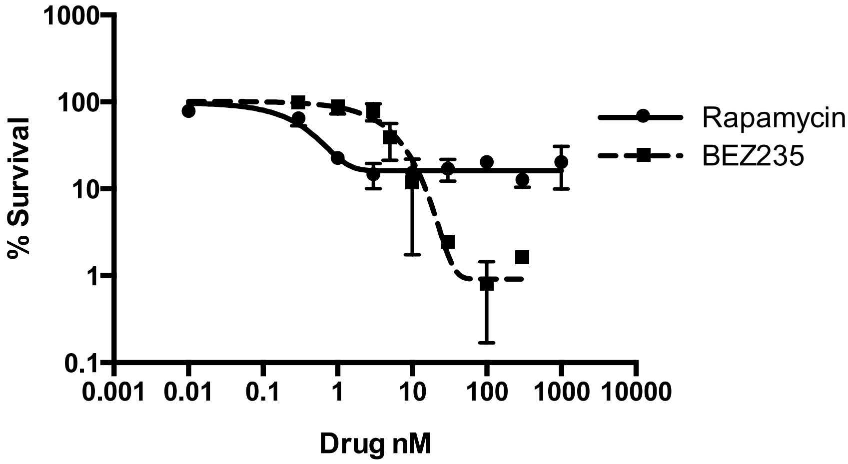


C

| Cell Line | Rapamycin $SF_{50}$ nM | BEZ235 $SF_{50}$ nM |
|---|---|---|
| RCC4 EV | 0.1 | 1.3 |
| 786-0 EV | 0.4 | 4.5 |

**Figure 3-19 Relative effects of BEZ235 and rapamycin on survival of RCC cells**

Clonogenic survival/growth assays of A) RCC4 EV and B) 786-0 EV cells treated with rapamycin or BEZ235. Graphs show mean and SEM of three independent experiments. C). Table of $SF_{50}$ values for rapamycin and BEZ235 in RCC4 EV and 786-0 EV cells.

### 3.2.14 Testing the combination of rapamycin and BEZ235

Having seen that BEZ235 caused a greater inhibition of signalling downstream of mTORC1 by inhibiting both pS6 and p4E-BP1, but that it was less potent in terms of concentration required to cause these effects, it was of interest to see whether combining BEZ235 with rapamycin was able to cause greater growth inhibition than with either agent alone, and if so, which mTOR targets correlated with growth inhibition. A concentration of 10 nM BEZ235 was used for these experiments as this concentration caused only a partial decrease in p4E-BP1 and a partial decrease in cell viability (Figure 3-17 and Figure 3-18). This was tested with 0.3 nM rapamycin, a concentration that caused inhibition of pS6, and activation of pAKT S473, while the effects on p4E-BP1 were minor (Figure 3-17). The hypothesis was that rapamycin resistance was a result of failure to completely inhibit p4E-BP1, and that the addition of BEZ235 would cause a greater decrease in p4E-BP1 and greater inhibition of cell viability. Each drug individually caused a modest decrease in cell viability in RCC4EV and 786-0EV cells (Figure 3-20 A). The combination of 0.3 nM rapamycin and 10 nM BEZ235 caused a significantly greater decrease in viability than either drug alone in both cell lines.

Analysis of the effects of the two drugs singly, and in combination revealed differences in their effects on mTOR signalling (Figure 3-20 B). Results were similar for both RCC4 EV and 786-0 EV cells. Both 0.3 nM rapamycin and 10 nM BEZ235 caused similar inhibition of pS6, and the combination of the two drugs was no more effective. Rapamycin caused an increase in pAKT S473 in RCC4 EV but not in 786-0 EV cells, while BEZ235 did not, yet the two drugs caused the same degree of inhibition of viability (**Error! Reference source not found.**). Rapamycin caused only a very minor effect on p4E-BP1 (seen by the small degree of band shift rather than decrease in the intensity of the band, lane 2 and lane 6 in Figure 3-20 B). BEZ235 caused a greater effect, but the combination of rapamycin and BEZ235 caused the greatest inhibition of p4E-BP1, suggesting that inhibition of p4E-BP1 correlated most clearly with the degree of inhibition of cell viability (Figure 3-20 A).

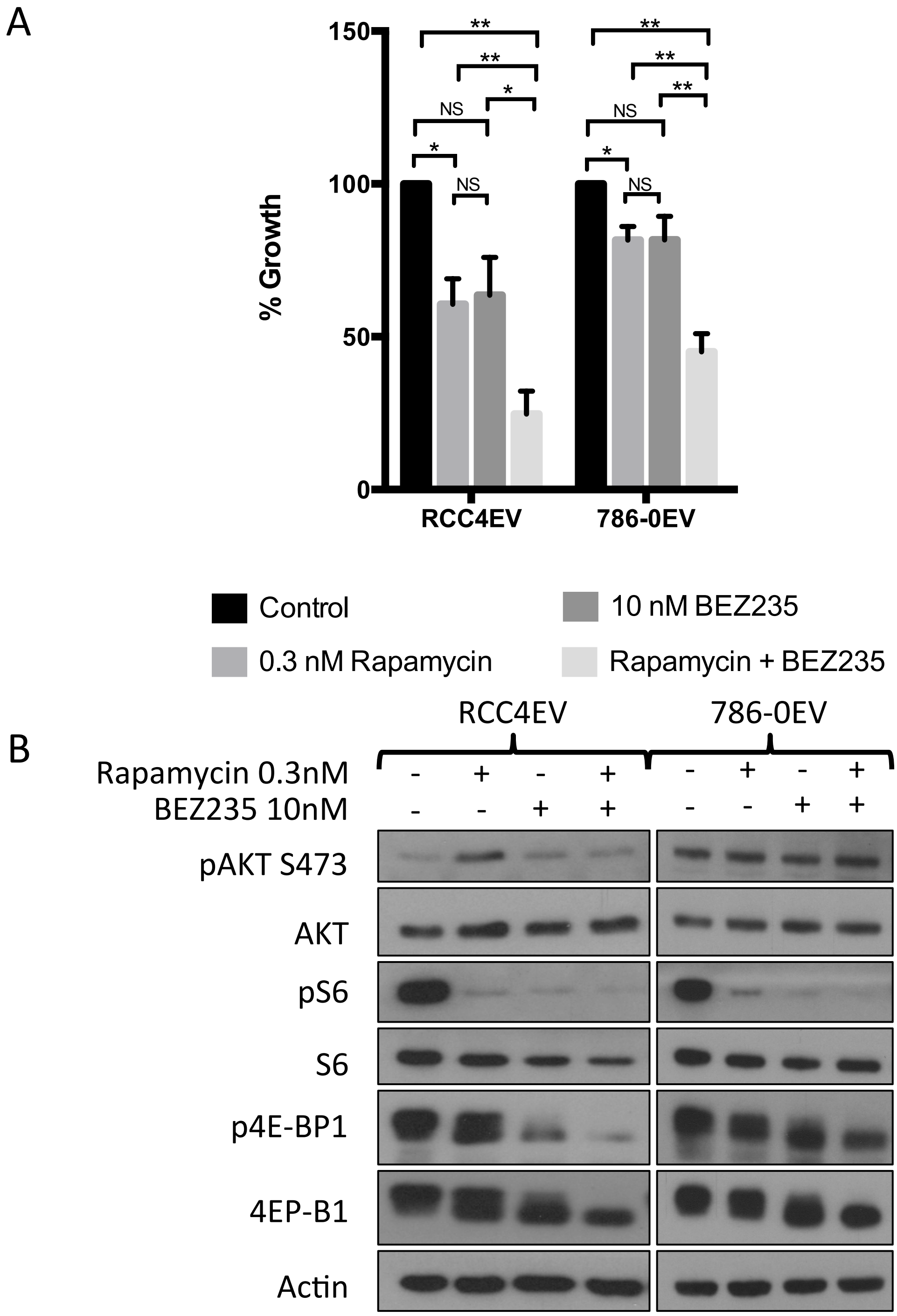


**Figure 3-20 BEZ235 at 10 nM sensitises CCRCC cells to rapamycin**

A) CTG viability assays of RCC4 EV and 786-0 EV cells treated with solvent, 0.3 nM rapamycin and solvent, 10 nM BEZ235 and solvent, or 0.3 nM rapamycin and 10 nM BEZ235. Graphs show mean and SEM of three independent assays. NS $p>0.05$, * $p<0.05$, ** $p<0.01$ by one way ANOVA. B) Monolayer RCC4 EV, or 786-0 EV cells were treated with solvent, 0.3 nM rapamycin, 10 nM BEZ235 or rapamycin and BEZ235 for 6 hours. Cell lysates were analysed by SDS-PAGE. Similar results seen in 3 independent similar experiments.

## 3.3 Discussion

The results presented here show that IGF-1R inhibition was not effective at inhibiting proliferation in RCC cells *in vitro*. The VHL status of the cells did not significantly affect this conclusion. Previous work in our lab using siRNA to deplete the IGF-1R in renal cancer cell lines suggested a greater effect on cell survival than was observed here using small molecule inhibitors (Yuen et al. 2009). There are a number of possible explanations for this difference. It is possible that the siRNA used in the previous work had some unidentified off target effect that accounted for the reduced survival. It is also possible that the small molecule inhibitors were incompletely blocking signalling via the IGF-1R. Certainly, inhibition of pAKT was less complete than the inhibition of pIGF-1R for any given concentration of OSI-906 (Figure 3-5), which raises the possibility that low levels of IGF-1R phosphorylation may persist and are undetectable by western blotting due to antibody insensitivity, but could be sufficient to maintain signalling to AKT.

The more specific reason to evaluate IGF-1R inhibitors in renal cancer was because IGF-1R may be involved in the feedback activation of AKT in response to rapamycin, which has been proposed as a potential resistance mechanism (Shi et al. 2005, O'Reilly et al. 2006, Wan et al. 2007). The data presented here however contradict this hypothesis in this *in vitro* model. Two different IGF-1R inhibitors were unable to sensitise to rapamycin, despite evidence of blockade of rapamycin induced AKT activation at 6 hours (Figure 3-7 C). AKT reactivation was seen during prolonged treatment with OSI-906, raising the possibility of alternative routes to AKT activation via alternative receptor tyrosine kinases. However, alternative strategies to block PI3K or AKT also proved ineffective in sensitising to rapamycin. Furthermore, the experiments using BEZ235 (Figure 3-20) suggested that the levels of pAKT S473 did not correlate with effects on viability. The conclusion of these experiments therefore was that AKT activation did not appear to contribute to resistance to mTOR inhibition in renal cancer.

There is conflicting evidence, in other cancers and with other drugs within the same classes, as to whether the AKT feedback pathway is indeed an important resistance mechanism.

Most pertinent to the current study, the humanized IGF-1R antibody hR1 was combined with the rapalogue temsirolimus in renal cancer cell lines, including 786-0 cells (Cardillo et al. 2013). This antibody depleted total levels of IGF-1R and was able to sensitise renal cancer cells to mTORC1 inhibition. Temsirolimus is a rapalogue, and has the same mechanism of action as rapamycin, but hR1 has a different mechanism of action to drugs such as OSI-906. While hR1 depletes levels of IGF-1R protein, (as does gene silencing, used in Yuen et al 2009) OSI-906 does not. It is possible that that this could account for the difference in the ability of these drugs to sensitise to mTORC1 inhibition. IGF-1R downregulation could result in a more complete inhibition of IGF-1R signalling than is possible with small molecule kinase inhibitors, as discussed above. Alternatively, it could suggest a non-kinase function of the IGF-1R, as reported in control of apoptosis and glucose homeostastis (Boucher et al. 2010, Janku et al. 2013).

Also of direct relevance to the current study, OSI-906 and been tested clinically in combination with everolimus in patients with refractory metastatic colorectal carcinoma. In this phase I trial, no disease response were seen in 18 patients (Bendell et al. 2015). No tumour samples were taken to assess the activity of the rapalogue-induced activation of AKT in these patients.

Others have seen that the PI3K inhibitor LY294002 increased sensitivity to rapamycin in renal cancer cell lines including 786-0 cells, but no evidence was presented directly linking this effect to the ability of LY294002 to block rapamycin induced AKT activation (Elfiky et al. 2011b).

A secondary hypothesis that was explored was that as IGF-1R expression has been reported to be regulated depending upon the VHL status of renal cancer cells, VHL status itself may alter the feedback response to activate AKT, and alter the response to IGF-1R inhibition in combination with rapamycin. There was no consistent evidence of a biologically significant effect to support this hypothesis. Others have suggested that VHL status may be predictive in other combination therapies. The synergy seen in the combination of gefitinib with rapamycin was linked to VHL wild type cellular models, where gefitinib was able to inhibit pERK (Gemmill et al. 2005). It has also been shown that VHL status may predict sensitivity to mTOR inhibition. VHL wild type renal cancer cells were more resistant to the rapalogue temsirolimus (Thomas et al. 2006). In the current study however, no predictive value in VHL status was seen. Possible explanations for this include that the effects are drug specific, rather than class specific or that there are differences in the model used here and in the assessment of temsirolimus. The 786-0 and RCC4 cells both harbour mutant VHL, and has been transfected with functional VHL to create an isogenic cell line pair. The SN12C cells used by Thomas et al. were VHL wild type, and VHL was knocked down with shRNA, so it is possible that these two models are not equivalent.

Testing of the dual mTORC kinase inhibitor BEZ235, showed that it caused a greater anti-proliferative effect than rapamycin, and that this correlated with reduction in p4E-BP1. This is consistent with findings of other groups, and in particular these two effects were seen in renal cancer by Cho et al. (Cho et al. 2010). Similar results have been seen with this drug, as well as with other mTORC kinase inhibitors, and in other cancer types, including breast cancer, glioma, lung cancer, multiple myeloma, and diffuse large B cell lymphoma (Serra et al. 2008, Breuleux et al. 2009, Feldman et al. 2009, Thoreen et al. 2009, Cho et al. 2010, Chresta et al. 2010, Nyfeler et al. 2012, Pike et al. 2013, Zhang et al. 2013).

Other evidence also points towards inhibition of p4E-BP1 as a determinant of sensitivity to mTORC inhibition. Of the two downstream mTORC1 targets, S6 and 4E-BP1, it is 4E-BP1 that has been shown to be important in controlling cell proliferation, rather than controlling cell size (Dowling et al. 2010). Inhibition of p4E-BP1 correlated with drug sensitivity in a panel of colorectal cancer cell lines treated with rapamycin or mTOR kinase inhibitors including BEZ235, and in a screen of 600 cell lines of mixed lineage using the mTORC kinase inhibitor PP242 (Zhang and Zheng 2012, Ducker et al. 2013).

In the current study, the combination of rapamycin and BEZ235 at low concentrations caused a greater reduction in p4E-BP1 levels and reduction in proliferation than either drug alone. The combination of a rapalogue and BEZ235 has also been of interest to others. In lung cancer, the combination of everolimus and BEZ235 decreased p4E-BP1 and was more effective than either drug alone at reducing levels of avian myelocytomatosis viral oncogene homologue (c-Myc) and cyclin D1 (Xu et al. 2011). Similarly, the combination of temsirolimus and BEZ235 caused synergistic growth inhibition in endometrial cancer (Yang et al. 2011). Novartis have completed a phase I trial of everolimus and BEZ235 (results awaited) following their discovery that low doses of the two drugs act synergistically to inhibit p4E-BP1 and proliferation (Nyfeler et al. 2012). Synergistic effects were only seen at low concentrations of the two drugs, and high concentrations of BEZ235 were able to produce maximal inhibition of p4E-BP1 and proliferation, which is consistent with the data shown here. The interest for Novartis in the combination lies in the potential to use low doses of drugs to alleviate side effects.

There was no evidence to support the further investigation of the combination of rapamycin and inhibitors of the IGF-1R – AKT pathway in these models of renal cancer. The mTORC kinase inhibitor BEZ235 showed promise as a more effective treatment strategy in renal cancer and warranted further research. Initial observations presented here correlated well with the findings of other groups that inhibition of 4E-BP1 correlated with sensitivity to mTOR inhibition, while pAKT activation did not.

# 4 Results 2: The creation and screening of BEZ235 resistant CCRCC cells

## 4.1 Introduction

Data shown in the previous chapter suggested that mTORC kinase inhibitors were more effective than rapamycin in inhibiting proliferation and survival of renal cancer cells. Attention then turned to understanding mechanisms of resistance to this new class of drugs. There are two types of resistance seen in the treatment of cancer in the clinic. One is that of primary resistance, where the cancer never responds to treatment. The second is acquired resistance, where after an initial response to treatment, resistance develops and the cancer grows despite on-going exposure to drug. One approach to study primary resistance *in vitro*, is to assess a large panel of cell lines for drug sensitivity, and screen the cells for common mutations or expression patterns in genes or pathways, that correlate with resistance or sensitivity, and this approach has been taken by some groups (Zhang and Zheng 2012, Ducker et al. 2013, Yang et al. 2013). *In vitro* models of acquired resistance have also been shown to be feasible and of value. One such method is to culture cells continuously with the drug, starting at low concentrations that modestly inhibit growth, e.g. by 30%, and slowly increasing the concentration as proliferation recovers (Ricci et al. 2002, Engelman et al. 2006b). In this manner, it has been possible to create cancer cells with at least a log fold increase in $GI_{50}$ in cell viability assays. Using this approach, Engleman et al. were able to show that gefitinib sensitive non small cell lung cancer (NSCLC) cells, acquired a T790M mutation in the EGFR kinase domain, which was shown to confer resistance to gefitinib (Engelman et al. 2006b). This mutation is now well-recognised as occurring naturally in tumour samples taken from patients who had acquired resistance to gefitinib (Kobayashi et al. 2005a, Kobayashi et al. 2005b). These results show that this method of producing resistant cells is capable of revealing mechanisms of resistance that are clinically relevant.

A second approach to identify resistance mechanisms was used by Sharma et al. (Sharma et al. 2010) who noted that even when NSCLC cells were treated with the EGFR inhibitor erlotinib at concentrations well in excess of the $SF_{50}$, some colonies were still able survive. Cells from some of these colonies were able to proliferate for prolonged periods, had upregulated IGF-1R, and a proportion had stem cell like properties (Sharma et al. 2010).

The two approaches have the potential to identify different types of apparently acquired resistance. The method used by Engleman may be more likely to uncover adaptive mechanisms of resistance, e.g. through mutation. On the other hand, the method used by Sharma may uncover a subpopulation of cells that have primary drug resistance and are therefore able to survive the initial insult of treatment. This would be in keeping with the current views of cancer stem cells in human cancer cell lines *in vitro,* where there is heterogeneity within the cell population (Islam et al. 2015). Such heterogeneity is certainly found in human renal cancers (Gerlinger et al. 2012, Gerlinger et al. 2014) and renal cancers have been found to contain stem cell like cells (Bussolati et al. 2008). If the main bulk of a tumour is made up of sensitive cells at the start of treatment, an initial response of tumour volume shrinkage will be seen followed by regrowth, comprised of resistant cells. This *in vitro* model could therefore mimic clinical patterns of response and resistance, and uncover important resistance mechanisms. Both of these approaches were employed in this project, with a view to identifying novel mechanisms of resistance to mTOR inhibition in general, and BEZ235 specifically.

## 4.2 Results

### 4.2.1 Testing the duration of action of BEZ235

In order to create resistant cells by continuous culture in BEZ235, it was first necessary to establish the duration of action of BEZ235, so that the frequency of replenishment could be determined to ensure consistent mTOR blockade. The 786-0 EV cells were cultured in full medium containing 100nM BEZ235 for up to 7 days as indicated in Figure 4-1. Control cells were treated with solvent, and were collected at 2 time-points, 1 day, and 7 days. This experiment showed complete mTORC1 inhibition at all time-points as evidenced by absence of pS6 and p4E-BP1. BEZ235 also inhibited PI3K and mTORC2 as shown by reduction in phosphorylation of AKT on T308 and S473 respectively, but these effects were noted to be more transient, with return to baseline at 2 days. On the basis of mTORC1 inhibition, it was accepted that BEZ235 was active in culture for at least

7 days from a single application, and therefore in order to create resistant cells, media were exchanged for fresh BEZ235-containing media at least every 7 days.

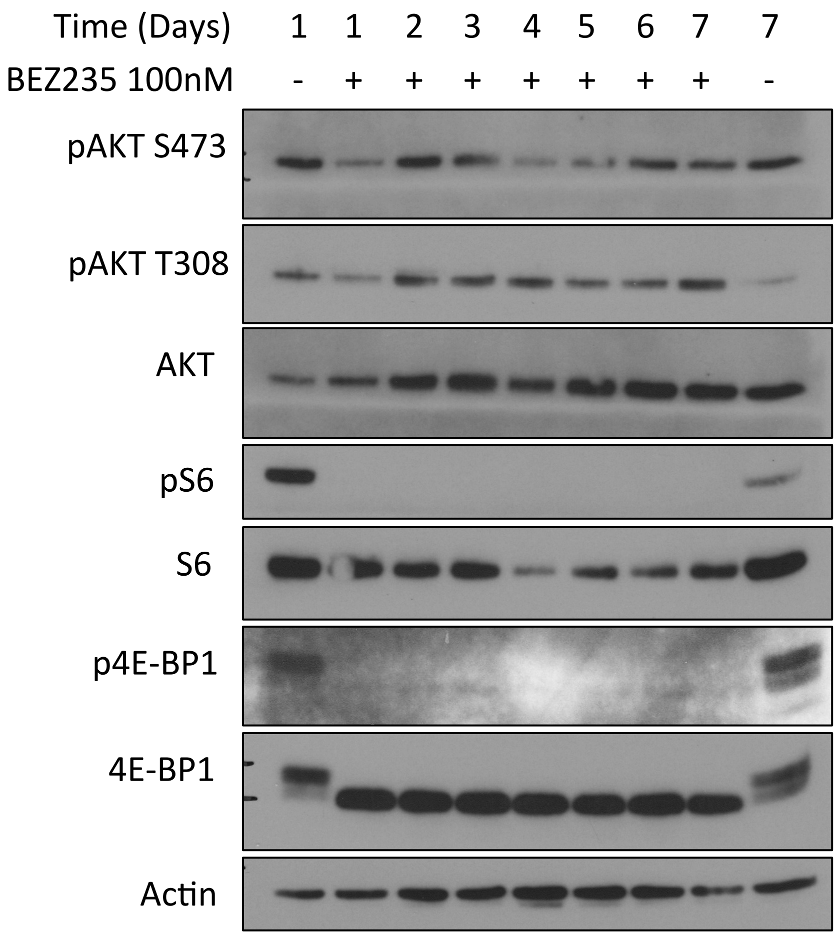


**Figure 4-1 BEZ235 inhibits mTOR *in vitro* for at least 7 days**

Monolayer 786-0 EV cells were treated with solvent, or 100 nM BEZ235 for the indicated length of time. Cell lysates were analysed by SDS-PAGE. BEZ235 inhibited pS6 and p4E-BP1 for the duration of the experiment. N=1.

### 4.2.2 Creation of BEZ235 resistant RCC4 cells

The subline cultured in BEZ235 was paired with a control culture of the same initial cell stock, but cultured in 0.1% DMSO solvent continuously for the same duration. These cells grew at the same rate as untreated cells, requiring the same standard passaging (1 in 30 split every 7 days). A representative image of these cells (called RCC4S hereafter) is show in Figure 4-2 A.

To begin the creation of BEZ235 resistant RCC4 cells, the medium was exchanged for medium containing 10 nM, 50 nM or 100 nM BEZ235. The lowest concentration was used with the intention of gradually increasing the concentration as per the method of Engleman (Ricci et al. 2002, Engelman et al. 2006b). The 50 and 100 nM concentrations were trialed in an attempt to mimic the approach of Sharma (Sharma et al. 2010). However, RCC4 cells did not tolerate culture in 50-100 nM BEZ235. Although some cells survived, they did not proliferate, and after 4 months these cultures were abandoned.

The RCC4 cells that were commenced in 10 nM BEZ235 grew well and the concentration was increased to 20 nM within the first month. After transfer to 20 nM BEZ235, cells grew very slowly, and initially took on a thin spindle like appearance (Figure 4-2 B). After three months of culture, the cells had not grown sufficiently to require passaging although the cells looked less spindle shaped and thin (Figure 4-2 B shows appearance on initial application of 20 nM BEZ235, C shows appearances after 3 months within the same flask). At this point, after 3 months of drug exposure, numerous dense, tightly packed colonies of cells became apparent (Figure 4-2 D and E). These cells had an apparently much faster rate of growth than the background cells. An attempt was made to isolate colonies of individual clones of these cells, but was unsuccessful. Instead, the rapidly-growing cells were allowed to overgrow the more slowly-growing cells over serial passages.

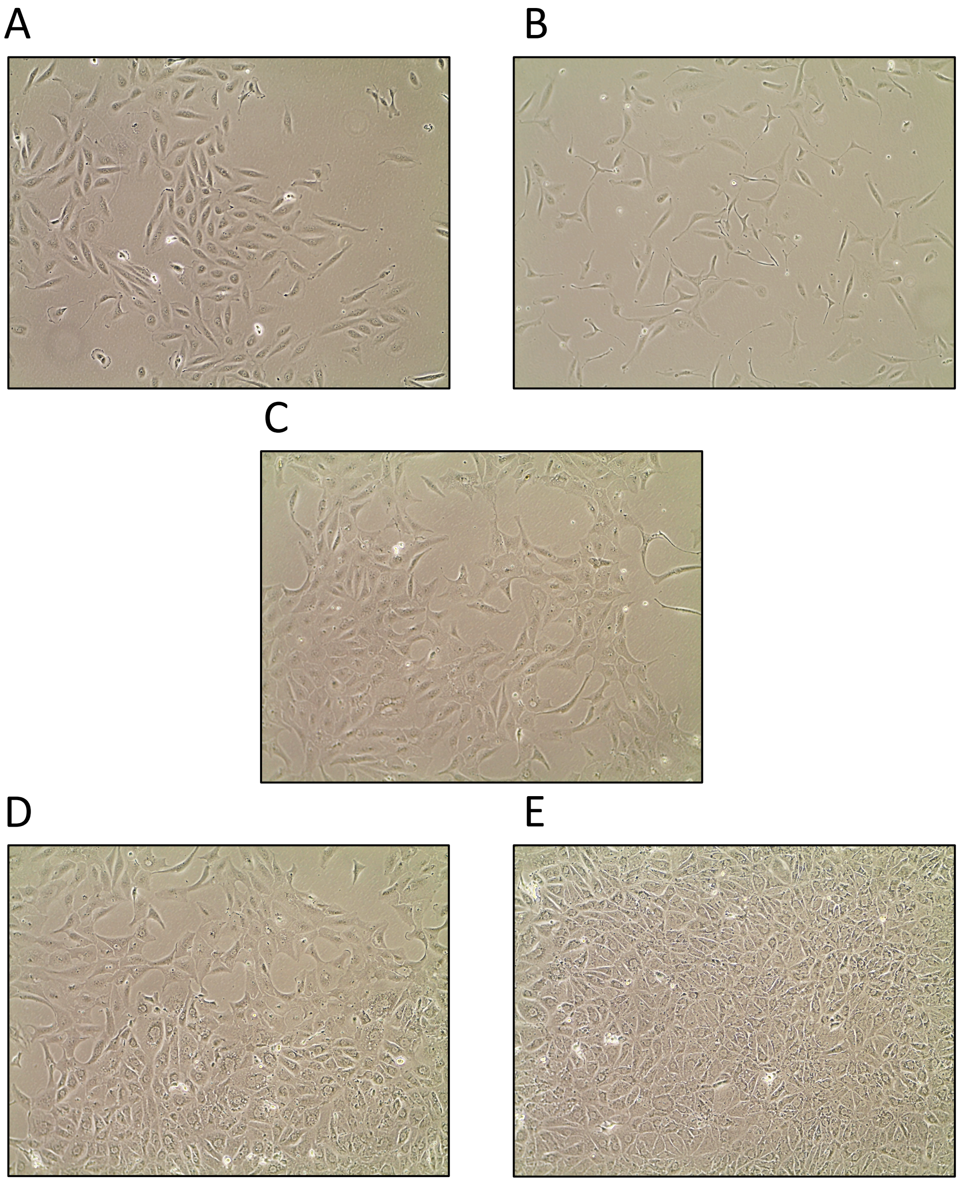

**Figure 4-2 RCC4 cells undergo morphological changes in response to treatment with BEZ235**

Light micrographs, original magnification x4, of A) RCC4 cells (sensitive to BEZ235) growing in solvent control, B) RCC4 cells after 1 week of treatment with 20 nM BEZ235, C) RCC4 cells after three months of treatment with 20 nM BEZ235. Cells had been slowly growing in the same flask for 3 months without need for passaging. D) Dense colonies appeared after 3 months treatment with 20 nM BEZ235. Border of a dense colony of fast growing cells (bottom right) within a background field of slow growing cells (top left). E) Centre of dense colony of cells shown in D).

Over serial passages following the appearance of the dense colonies, the proliferation rate of the RCC4 cells growing in 20 nM BEZ235 (hereafter called RCC4B20) progressively increased as evidenced by the need for more frequent passaging. The flask in which dense colonies appeared had been split 1:2, and took 3 months before requiring passage. Over the subsequent two months, 1:2 splits were required weekly initially, and 1:5 splits were required at two months. This remained the routine passaging split for these cells. During this time, serial viability assays were performed to test the sensitivity of the RCC4B20 cells. The resistance of these cells increased as seen in Figure 4-3 A and B, with rising $GI_{50}$ values and resistant populations. BEZ235 resistance plateaued at three months post the appearance of dense colonies, at which time the resistance of RCC4B20 cells compared to RCC4S cells revealed a 14 fold increase in $GI_{50}$ (Figure 4-3 C).

In order to test the sensitivity the following procedure was performed, and repeated for all subsequent cell viability and clonogenic survival/growth assays using these cells, and 786-0 resistant cells. A washout period of at least 72 hours without drug was performed prior to commencement of the assay. This was most commonly following passaging of cells such that rather than being seeded into 20 nM BEZ235, RCC4B20 cells were seeded into solvent control medium, or alternatively drug washout was performed by medium exchange for fresh, solvent control medium. After 72 hours, cells were seeded into the appropriate plate or dish for the assay in full medium (no solvent, no drug). After overnight incubation to allow cells to adhere, cells were treated with the indicated concentrations of drug, as in the cell viability assays and clonogenic cell survival/growth assays reported in the first results chapter. With each cell viability or clonogenic survival/growth assay performed on resistant cells, a duplicate assay was performed using the control BEZ235 sensitive parental cells (RCC4S).

Initial assays assessed clonogenicity using RCC4S and RCC4B20 cells that had undergone drug washout as described above. No treatments were applied to these clonogenic plates. Clonogenicity was tested by calculating the colonies formed as a percentage of cells seeded (Figure 4-4 A). This revealed that a lower percentage of cells formed colonies in RCC4B20 cells as compared to RCC4S cells and suggested that these cells did not posses stem cell like properties, where an increase in clonogenicity would have been expected.

Resistance to BEZ235 was next tested by clonogenic survival/growth assay. Due to the lower clonogenicity of RCC4B20 cells, the seeding number of these cells was doubled compared to RCC4S cells in order to give approximately the same total number of colonies in controls. This assay confirmed that RCC4B20 cells also showed resistance to BEZ235 in this assay format, with a six-fold increase in $SF_{50}$ (Figure 4-4 B and C).

A

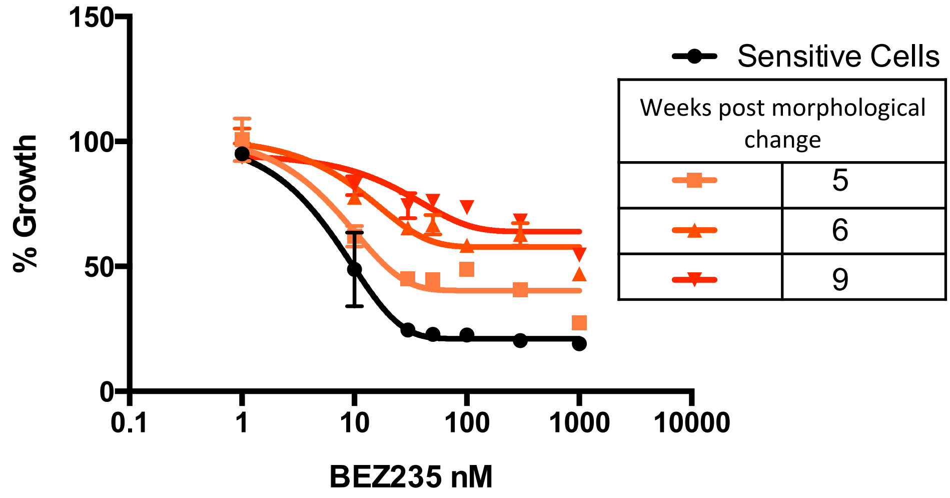


B

| Weeks post morphological change | $GI_{50}$ nM (95% CI) | Resistant Population % (95% CI) |
|---|---|---|
| Sensitive Cells (RCC4S) | 10 (8 – 12) | 21 (18 – 24) |
| 5 | 19 (13 – 26) | 40 (36 – 45) |
| 6 | >1000 | 58 (54 – 62) |
| 9 | >1000 | 64 (59 – 70) |

C

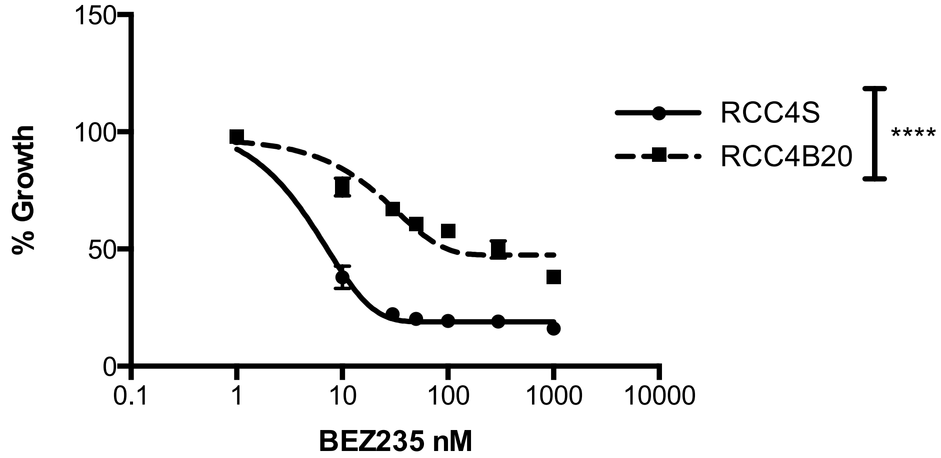


D

| Cell Line | $GI_{50}$ nM (95% CI) | Fold Change | Resistant Population % (95% CI) | Fold Change |
|---|---|---|---|---|
| RCC4S | 7 (6 – 8) | 14 (8.25 – >1000) | 19 (16 – 21) | 2.5 (2 – 3.3) |
| RCC4B20 | 99 (66 – >1000) | | 47 (42 – 53) | |

**Figure 4-3 Development of resistance to BEZ235 in RCC4 cells after undergoing morphological change**

A) Serial viability assays of RCC4 cells having undergone morphological change following growth in 20 nM BEZ235 for three months. Black line shows RCC4 cells grown in solvent control for the same length of time (RCC4S). Graph shows mean and SEM of triplicate values from one experiment on each occasion. B) Table showing $GI_{50}$ concentrations and resistant population from graph A). C) CTG viability assays of RCC4S and RCC4 resistant cells (hereafter called RCC4B20), treated with BEZ235, after stable resistance reached at 3 months post morphological change. Graph shows mean and SEM of three independent experiments. **** p<0.0001 by two way ANOVA. D) Table of BEZ235 $GI_{50}$ concentrations and resistant populations from graph C). Fold change calculated as ratio of these parameters in resistant/sensitive cells.

A

B

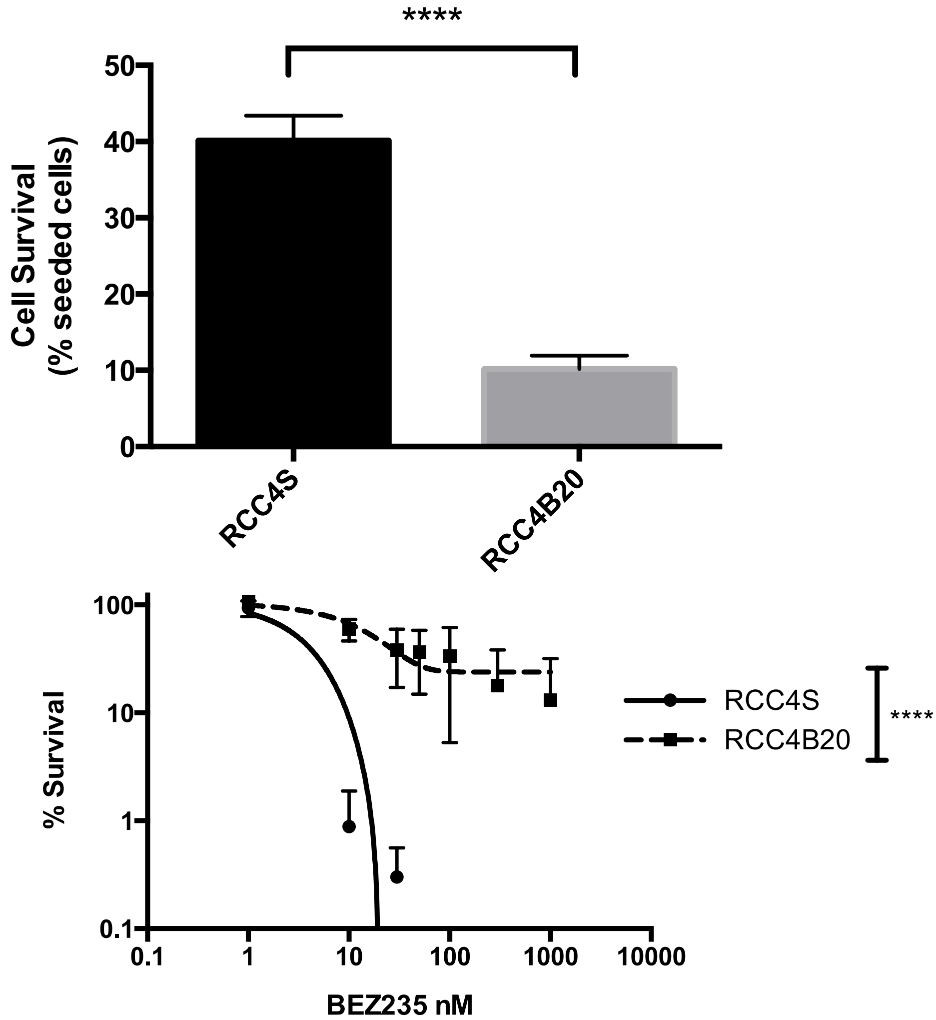


C

| Cell Line | $SF_{50}$ nM (95% CI) | Fold Change |
|---|---|---|
| RCC4S | 3 (2 – 4) | 6 (2.5 – 15) |
| RCC4B20 | 18 (10 – 30) | |

**Figure 4-4 Relative clonogenicity of RCC4S and RCC4B20 cells and cell survival/growth in response to BEZ235**

A) Colony formation of RCC4S and RCC4B20 cells expressed as % of cells seeded. Mean and SEM taken from 6 data points in two independent experiments. **** p< 0.0001 by t test. B) Clonogenic survival/growth assays of RCC4S and RCC4B20 treated with BEZ235. Graph shows mean and SEM of three independent experiments. **** p<0.0001 by two way ANOVA. C) Table of $SF_{50}$ concentration of BEZ235 from graph C). Fold change calculated as ratio of this parameter in resistant/sensitive cells.

### 4.2.3 Creation of BEZ235 resistant 786-0 cells

A solvent treated control culture of 786-0 cells was created in the same way as for RCC4 cells, and will be termed 786-0S hereafter. In order to create resistant cells, 786-0 cells were cultured in 100 nM, 300 nM or 500 nM BEZ235. These were all high concentrations, following the method of resistance creation of Sharma. Some cells remained viable in 300 and 500 nM BEZ235, but they failed to grow over a 5 month period, and these cultures were therefore abandoned. The 786-0 cells cultured in 100 nM BEZ235 showed similar changes in appearance on acute exposure to BEZ235 as that seen in RCC4 cells (Figure 4-2 B). They grew slowly, and were passaged by splitting 1:2 every 10-14 days. The proliferation rate gradually increased, and after three months a 1:5 split was required every 10-14 days. During this time the cells returned to a more normal appearance, but no dense colonies, or sudden changes in appearance were noted, unlike the emergence of BEZ235-resistant RCC4 cells. A sub-culture was split from cells growing in 100 nM BEZ235 at this point, and cultured in 200 nM BEZ235. Over the next 6 months, cells growing in 200 nM BEZ235 increased their proliferation rate to match the cells in 100 nM BEZ235. At this point, both cultures were requiring a 1:5 split every 10 days. The 786-0 cells growing in 200 nM BEZ235 (hereafter referred to as 786-0B200) were selected for further analysis because they were proliferating at the same rate as the 786-0 cells in 100 nM BEZ235 despite the higher concentration of drug, suggesting a higher level of resistance.

Resistance of the 786-0B200 cells was confirmed by cell viability assays (Figure 4-5 A) with greater than 55 fold increase in $GI_{50}$ compared to 786-0S controls. The 786-0B200 cells showed lower clonogenicity than the 786-0S, BEZ235 sensitive cells, in the same manner as RCC4B20 cells (Figure 4-5 B). Resistance to BEZ235 was confirmed by clonogenic survival/growth assays (Figure 4-5 C).

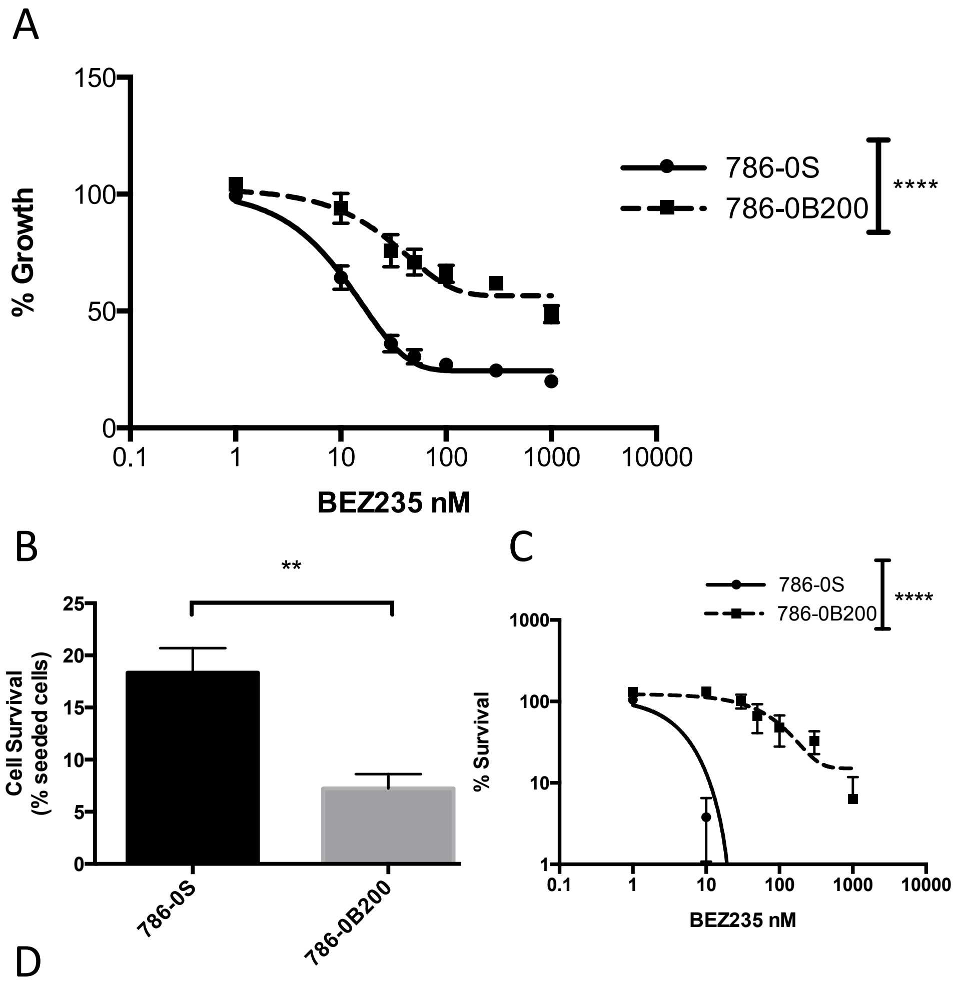


D

| Cell Line | $GI_{50}$ nM (95% CI) | Fold Change | Resistant Population % (95% CI) | Fold Change | $SF_{50}$ nM (95% CI) | Fold Change |
|---|---|---|---|---|---|---|
| **786-0S** | 18 (15 – 21) | >55.6 | 24 (21 – 27) | 2.4 (1.9 – 3) | 4 (3 – 5) | 26.8 (14.2 – 53.3) |
| **786-0B200** | >1000 | | 57 (50 – 63) | | 107 (71 – 160) | |

**Figure 4-5 Development of resistance to 200 nM BEZ235 in 786-0 cells**

A) Viability assay of 786-0 cells cultured continuously in solvent (786-0S) or 200 nM BEZ235 (786-0B200), exposed after a three day washout to BEZ235. Graph shows mean and SEM of three independent assays. **** $p<0.0001$ by two way ANOVA. B) Colony formation of 786-0S and 786-0B200 cells expressed as % of cells seeded. Mean and SEM taken from 6 data points in two independent experiments. ** $p< 0.01$ by t test. C) Clonogenic cell survival/growth assay of 786-0S and 786-0B200 cells treated with BEZ235. Graph shows mean and SEM of three independent experiments. **** $p<0.0001$ by two way ANOVA. D) Table of $GI_{50}$ concentrations and resistant populations to BEZ235 by cell viability assay, and $SF_{50}$ concentration by clonogenic assay.

### 4.2.4 Testing the cross resistance of BEZ235 resistant cell lines to inhibitors of the PI3K – AKT – mTOR pathway

After establishing resistance to BEZ235, RCC4B20 and 786-0B200 cells were assessed for cross-resistance to alternative inhibitors of the PI3K – AKT – mTOR pathway. The first drug tested was another mTORC kinase inhibitor, AZD2014 which has an $IC_{50}$ for mTOR of 0.0028 µM, pAKT S473 0.08 µM and pS6 0.2 µM and shows selectivity for mTOR over PI3K , with $IC_{50}$ concentrations for inhibition of PI3K α, β, γ ,δ, isoforms of 3.8, >30, >30 and >29 µM respectively (Pike et al. 2013). This is in contrast to BEZ235, which is a dual mTORC kinase and PI3K inhibitor. AZD2014 is in early phase clinical trial development. Consistent with its higher published $IC_{50}$ concentrations, $GI_{50}$ concentrations for AZD2014 were higher than for BEZ235 (Figure 3-18 and Figure 4-6). RCC4B20 cells showed cross-resistance to AZD2014, with 6.8 fold increase in $GI_{50}$, and 2 fold increase in the resistant population compared to RCC4S cells (Figure 4-6 A and Table 4-1). This effect was replicated in 786-0B200 cells, which showed a 18.5 fold increase in $GI_{50}$ and 2.8 fold increase in the resistant population compared to 786-0S cells (Figure 4-6 B and Table 4-1). These results suggested that resistance had developed to mTORC kinase inhibition, rather than specifically to BEZ235.

Statistically significant cross-resistance to rapamycin was demonstrated in RCC4B20 cells and 786-0B200 cells when assessed by two-way ANOVA (Figure 4-6 C and D), but the magnitude of this effect was very small. The rapamycin-resistant population of RCC4B20 cells was only 1.2 fold different from RCC4S cells, but this change meant that the $GI_{50}$ was not reached, and hence there was an apparent large fold change in $GI_{50}$. However, the overall responses of RCC4B20 and RCC4S cells to rapamycin look very similar, and the differences are unlikely to be of biological importance. A similar pattern was seen for 786-0B200 cells, although with a slightly larger fold change in resistant populations (Table 4-1).

RCC4B20 cells were not cross-resistant to the PI3K inhibitor BKM120 (Figure 4-6 E and Table 4-1), while 786-0B200 cells showed a small degree of cross-resistance, with a 2.8 fold change in $GI_{50}$, and 2.2 fold change in resistant population (Figure 4-6 F and Table 4-1). Both RCC4B20 and 786-0B200 showed a small degree of resistance to the AKT inhibitor AZD5363, with 2.4 and 1.9 fold changes in $GI_{50}$ respectively (Figure 4-6 G and H, and Table 4-1).

The patterns of cross-resistance were interesting, and informative of possible resistance mechanisms. RCC4B20 cells showed the greatest cross-resistance to mTORC kinase inhibition. They were not cross-resistant to allosteric mTORC1 inhibition, or PI3K inhibition, and only showed a small degree of cross-resistance to an inhibitor of AKT. This suggests that the resistance in these cells had developed primarily to kinase inhibition of mTORC1, as opposed to the alternative actions of BEZ235 on PI3K, or to allosteric mTORC1 inhibition.

In contrast, 786-0B200 cells showed a broader spectrum of cross-resistance. As well as a large degree of cross-resistance to the alternative mTORC kinase inhibitor AZD2014, they also showed some evidence of cross-resistance to PI3K, AKT, and allosteric mTORC1 inhibition. The magnitude of resistance to AZD2014, as compared to the other tested drugs, suggests that the resistance to BEZ235 was primarily to mTORC1 kinase inhibition, but with possible components of resistance to the additional actions of BEZ235.

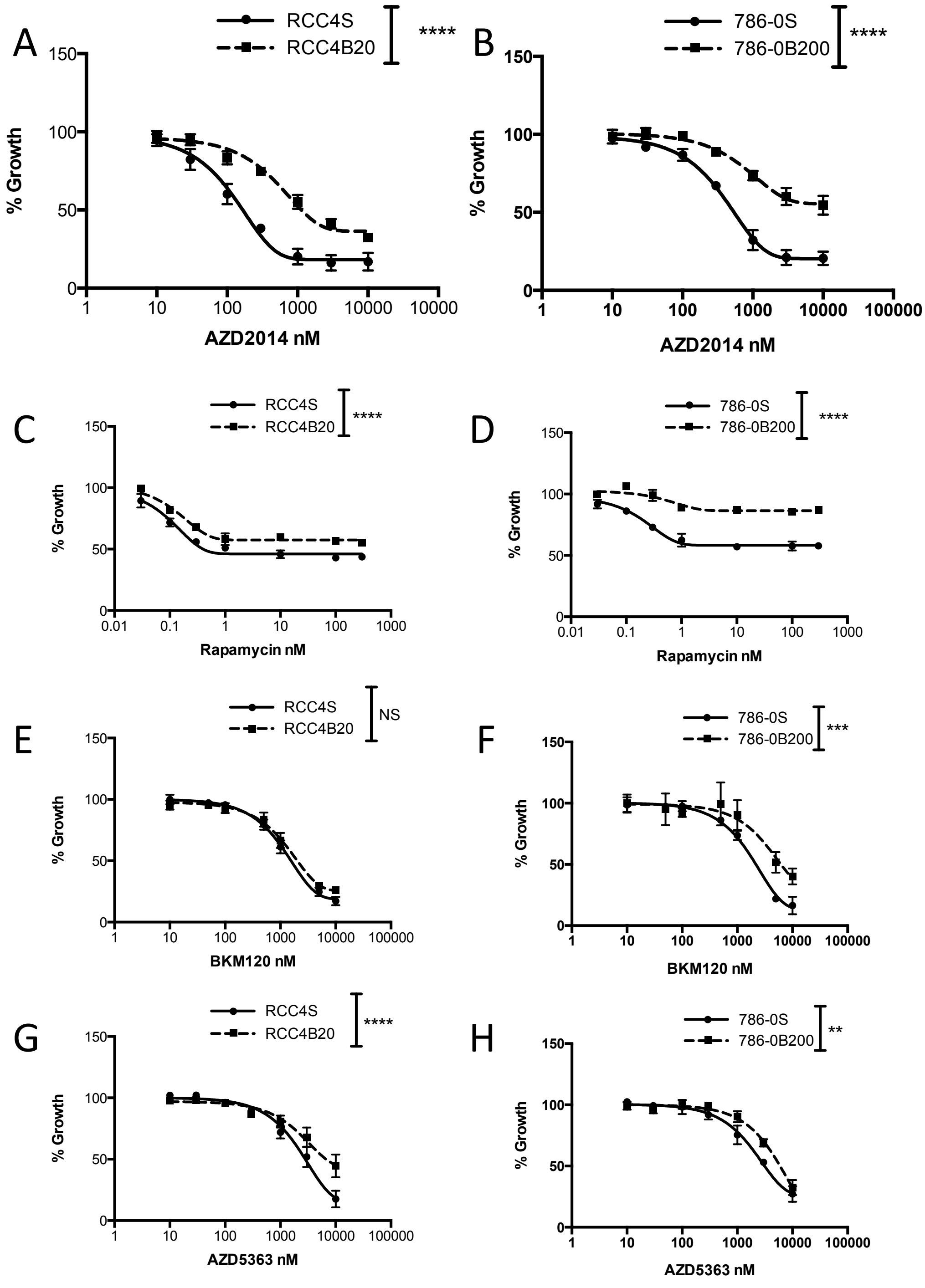


**Figure 4-6 BEZ235 resistant cells show cross resistance to the mTORC kinase inhibitor AZD2014**

After a three day drug washout, RCC4S and RCC4B20 cells were treated with A) AZD2014, C) rapamycin, E) BKM120 or G) AZD5363. Graphs show mean and SEM of three independent viability assays. NS $p>0.05$, **** $p<0.0001$ by two way ANOVA. CTG cell viability assay of 786-0S and 786-0B200 cells treated with B) AZD2014, D) rapamycin, F) BKM120 or H) AZD5363. Graphs show mean and SEM of three independent assays. ** $p=0.0013$, *** $p=0.0007$, **** $p<0.0001$ by two way ANOVA.

| Cell Line | AZD2014 | | Rapamycin | | BKM120 | | AZD5363 | |
|---|---|---|---|---|---|---|---|---|
| | **GI$_{50}$ nM (95% CI)** | **Fold Change (95% CI)** | **GI$_{50}$ nM (95% CI)** | **Fold Change (95% CI)** | **GI$_{50}$ nM (95% CI)** | **Fold Change (95% CI)** | **GI$_{50}$ nM (95% CI)** | **Fold Change (95% CI)** |
| **RCC4S** | 166 (129 – 216) | 6.8 (4.0 – 11.4) | 0.4 (0.3 – 0.6) | >750 | 1558 (1290 – 1888) | 1.3 (0.8 – 2.0) | 2810 (2237 – 3522) | 2.4 (1.2 - >2.8) |
| **RCC4B20** | 1131 (856 – 1468) | | >300 | | 2020 (1579 – 2571) | | 6686 (4381 - >10000) | |
| **786-0S** | 540 (479 – 611) | >18.5 | >300 | NE | 2176 (1879 – 2519) | 2.8 (1.6 - >4.4) | 3124 (2688 – 3618) | 1.9 (1.4 – 2.5) |
| **786-0B200** | >10000 | | >300 | | 6172 (4100 - <10000) | | 5958 (5237 – 6679) | |

| Cell Line | AZD2014 | | Rapamycin | | BKM120 | | AZD5363 | |
|---|---|---|---|---|---|---|---|---|
| | **Resistant Population % (95% CI)** | **Fold Change (95% CI)** | **Resistant Population % (95% CI)** | **Fold Change (95% CI)** | **Resistant Population % (95% CI)** | **Fold Change (95% CI)** | **Resistant Population % (95% CI)** | **Fold Change (95% CI)** |
| **RCC4S** | 18 (13 – 24) | 2 (1.3 – 3.2) | 46 (43 – 49) | 1.2 (1.1 – 1.4) | 19 (13 – 24) | 1.3 (0.8 – 2.5) | 15 (3 – 27) | 2.9 (1.1 – 18.7) |
| **RCC4B20** | 36 (31 – 42) | | 57 (55 – 60) | | 25 (19 – 32) | | 43 (29 – 56) | |
| **786-0S** | 20 (17 – 24) | 2.8 (2.2 – 3.5) | 58 (55 – 61) | 1.5 (1.4 – 1.6) | 13 (7 – 18) | 2.2 (0 – 9) | 26 (19 – 32) | 0.2 (0 – 1.7) |
| **786-0B200** | 56 (52 – 59) | | 86 (83 – 89) | | 28 (0 – 63) | | 6 (0 – 32) | |

**Table 4-1 Summary of cross resistance of BEZ235 resistant cells**

Table of GI50 concentrations and fold changes between sensitive to resistant cells taken from Figure 4-6 graphs A) – H). Table of resistant population of cells and fold changes from sensitive to resistant cells taken from Figure 4-6 graphs A) – H). NE, not evaluable.

### 4.2.5 Techniques to screen BEZ235 resistant cells for mediators of resistance

In order to investigate resistance mechanisms in BEZ235 resistant cells, it was decided to screen the resistant cells in an unbiased way. Thought was given to the nature of the screen to be undertaken, as numerous types of screen were available, to detect mutations in DNA, altered expression at the mRNA level, or changes in post-translational modifications, which either activate or inactivate the protein. These include proteolytic cleavage, phosphorylation, acetylation, methylation, glycosylation, ubiquitination, or SUMOylation (Mann and Jensen 2003).

Screening for altered gene transcription is accomplished by examining expressed mRNA. Microarrays using hybridisation technology with specific probes to known genes can give information on the relative expression of any gene for which there is a probe set on the microarray (Lin et al. 2015). This is a well-established technique that is relatively cheap. Alternatively, next generation sequencing allows for RNA sequencing, which is also quantitative, has lower background levels (due to no cross hybridisation) and has a greater dynamic range allowing detections of differences in genes with very low, or high expression levels. Furthermore, this approach can also detect alternatively spliced transcripts, and non-coding RNAs (Martin and Wang 2011, Mwenifumbo and Marra 2013)

Screening for altered translation can be accomplished by measuring ribosomal bound mRNA (Ingolia et al. 2009), which can quantify those mRNAs undergoing active translation. Alternatively, protein levels can be assessed by antibody microarray. This measure is affected not only by expression, but also by protein stability and degradation. A second advantage of this approach is that antibody arrays may include antibodies to phosphorylated, or unphosphorylated proteins. Antibody arrays, similarly to hybridisation based cDNA microarrays, can suffer from non-specific binding, increasing background signal and giving false positives. Secondly antibody arrays can give false negatives when non-denatured proteins are assessed, especially in proteins that exist in complexes, if a binding partner covers the antibody epitope (Alhamdani et al. 2009).

A final type of screen uses libraries of inhibitors, either small molecules or siRNAs to identify inhibitors that cause sensitisation, hence identifying that target protein or that pathway as a mediator of resistance (Mohr et al. 2014).

The primary role of mTORC1 is in controlling translation and therefore, it was decided to screen at the protein level by antibody array. Such arrays were commercially available, and also allowed screening of phosphorylation status of the proteins on the array. mTOR also has functions that affect transcription factors, and therefore an mRNA based screen was also conducted. These screens were conducted sequentially, with the protein level screen conducted first.

### 4.2.6 Antibody array screen of BEZ235 resistant RCC cells

To screen BEZ235 resistant cells at the protein level, the Phospho Explorer Array service was purchased from Full Moon Biosystems. The array included 1318 antibodies, which were directed at phospho-proteins, with corresponding antibodies to the non-phosphorylated epitopes of the same proteins. Due to the cost of the screen, only one cell pair could be screened. The RCC4S and RCC4B20 cell pair was selected for assessment. There were several reasons for this choice. Firstly, RCC4B20 cells appeared more robust than the 786-0B200 cells, with more rapid and reproducible proliferation including when seeded for viability or clonogenic assay. Secondly, the assessment of cross resistance suggested that 786-0B200 cells showed a greater range of cross resistance, including to PI3K and allosteric mTORC1 inhibition (Figure 4-6). It was felt therefore that investigation of RCC4B20 cells would be more likely to reveal resistance mechanisms specific to mTORC1 kinase inhibition, whereas testing of 786-0B200 cells would potentially uncover resistance mechanisms to other targets including PI3K. It would have been interesting to have screened the 786-0B200 cells as well, but as an alternative, it was decided to attempt validation of potential hits from the antibody array in both RCC4B20 cells and 786-0B200 cells, aiming to identify common factors in BEZ235 resistance.

Conditions were selected to enable evaluation of markers that changed between BEZ235 sensitive and resistant cells. To differentiate effects of acute vs. continuous BEZ235 treatment, an additional control of acutely treated RCC4S cells was used. As well as allowing the identification of acute effects of BEZ235, this allowed for the detection of a “return to baseline” mechanism of resistance, e.g. acute BEZ235 causes reduction in phospho-protein X in sensitive cells, but in resistant cells the level of phospho-protein X returns to that of untreated sensitive cells. RCC4S cells were treated with 20 nM BEZ235, or solvent control. RCC4B20 cells did not undergo drug washout, but had medium exchanged for fresh medium containing 20nM BEZ235. After one hour, cells were collected and cell pellets were snap frozen as described in 2.4.1. Cell pellets were couriered to Fullmoon Biosystems where the antibody array and data analysis was carried out by Fullmoon Biosystems staff as described in section 2.4.

The normalised data were filtered to exclude antibodies that did not meet the “ true signal” level, which was defined as an average signal intensity of replicate spots at least 3 times the level of background signal. Potential mediators of resistance were identified as a 2-fold change from RCC4S to RCC4B20 cells (Resistant:Sensitive) or a 2-fold change from BEZ235 treated RCC4S to RCC4B20 cells (Resistant:Acute), and are presented in Table 4-2. Values greater than 2 (i.e. 2-fold increase) and <0.5 (i.e. 2-fold decrease) were both considered. Potential candidates that showed changes between resistant and control treated sensitive cells were excluded from further assessment if the same change was induced by acute BEZ235 treatment of sensitive cells, e.g. nuclear factor kappa-light-chain-enhancer of activated B cells (NFκB) -p65 phospho S468 in Table 4-2.

| Protein | Fold Change | | |
|---|---|---|---|
| | **Resistant:Sensitive** | **Resistant:Acute** | **Acute:Sensitive** |
| Abl1 | 2.67 | 2.24 | 1.19 |
| CaMKII | 2.81 | 1.93 | 1.46 |
| Caspase 9 | 1.6 | 2.41 | 0.66 |
| CD4 | 1.47 | 2.16 | 0.68 |
| Integrin beta-1 | 2.05 | 1.6 | 1.28 |
| HSL | 1.58 | 2.36 | 0.67 |
| LIMK1/2 | 0.7 | 0.33 | 2.12 |
| MAPKAPK2 | 0.66 | 0.5 | 1.33 |
| MEK1 | 1.5 | 2.15 | 0.7 |
| MET Phospho Y1356 | 2.32 | 1.39 | 1.67 |
| NFκB-p65 Phospho S468 | 4.48 | 1.37 | 3.26 |
| Ras-GRF1 | 2.91 | 1.79 | 1.56 |
| Shc | 2.53 | 1.79 | 1.41 |
| Potential hits meeting secondary criteria | | | |
| Cyclin D1 Phospho T286 | 0.99 | 0.55 | 0.97 |
| IKK-a/b | 1.92 | 1.67 | 1.15 |
| SRF | 1.29 | 1.94 | 0.67 |

**Table 4-2 Potential hits from antibody array**

Potential hits from the Full Moon Biosystems phospho-explorer antibody array listed in alphabetical order. Top part of table shows hits with predicted fold change in expression levels ≥2 or ≤0.5 in RCC4B20 cells compared to acutely treated RCC4S cells, or RCC4B20 cells compared to RCC4S control treated cells. Bottom part of table shows potential hits meeting less stringent inclusion criteria of predicted fold changes of ≥1.9 or ≤0.55

The first part of the validation process was to confirm altered expression by western blotting. There were two significant differences in this validation in comparison to the screen. Firstly, whereas the antibody array was conducted on non-denatured proteins, western blotting is performed on denatured proteins. Secondly, the Full Moon Biosystems antibody array used proprietary antibodies, while western blotting was performed with commercially available antibodies. The second stage of the validation process was to investigate the possibility of a causal relationship between the potential hit and resistance to BEZ235, by use of small molecule inhibitors and siRNA. Results have been presented to show screen hits that were validated by western blot, followed by effects of targeting each hit, and finally those potential screen hits that failed to validate by western blot.

### 4.2.7 Validating potential hits by western blotting

Investigations focussed on the three druggable targets: MET, Abelson murine leukaemia viral oncogene homolog (Abl) and MEK. MET is the receptor tyrosine kinase that is activated by hepatocyte growth factor (HGF). MET exists as an α/β heterodimer, having been cleaved from its pro-receptor into its α and β chains (Bottaro et al. 1991). Upon ligand binding, MET undergoes homodimerisation and transphosphorylation. There are two phosphorylation sites in the kinase domain at tyrosine 1234 and 1235, which regulate kinase activity (Longati et al. 1994), and two in the carboxy terminus at tyrosine 1349 and 1356, which serve as docking sites for adaptor proteins (Ponzetto et al. 1993, Ponzetto et al. 1994).

Phosphorylation at tyrosine 1356 transduces signals required for cell motility and morphogenesis (Furge et al. 2000).

MET signals via multiple pathways including RAS – Raf – MEK, PI3K – AKT, signal transducer and activator of transcription (STAT) and nuclear factor κB inhibitor α (IκBα) – nuclear factor-κB (NF-κB) complex, to cause effects including proliferation, protection from apoptosis, motility and invasion, angiogenesis and epithelial to mesenchymal transition (Pelicci et al. 1995, Maroun et al. 1999, Sipeki et al. 1999, Canadas et al. 2014a, Canadas et al. 2014b).

MET and its ligand HGF are often overexpressed in cancer, and activating mutations of *MET* are described in hereditary and sporadic papillary renal cancer (Schmidt et al. 1997, Schmidt et al. 1998, Schmidt et al. 2004). The *MET* gene is often amplified, and this may be another marker alongside mutation, indicating susceptibility to MET inhibition (Smolen et al. 2006, McDermott et al. 2007). *MET* amplification, and increased HGF expression have been shown to mediate acquired resistance to EGFR inhibition in NSCLC in vitro and clinically, and inhibitors of MET were able to reverse this resistance (Engelman et al. 2007, Yano et al. 2011, Nakagawa et al. 2012).

MET is known to be over-expressed in some CCRCCs, and to be associated with a worse prognosis. MET was therefore seen as a credible potential mechanism of acquired resistance to BEZ235 in RCC (Gibney et al. 2013).

The Abelson murine leukaemia viral oncogene homolog 1 (Abl) is a non receptor tyrosine kinase that links extra-cellular signalling to downstream effects including cell growth, survival, migration and invasion. Abl has an auto-inhibitory confirmation, promoted by myristoylation and interaction between its SH3 and SH2 domains. Abl can be stabilised in its active form by phosphorylation, which is thought to be either transphosphorylation by Abl or phosphorylation by the related SRC family kinases. Abl is well-known for its role in the BCR-ABL1 fusion oncoprotein formed by the t(9;22)(q34;q11) chromosome translocation (the Philadelphia Chromosome) found in chronic myeloid leukaemia (CML), which results in constitutively active Abl function (Ben-Neriah et al. 1986). The Abl kinase inhibitor imatinib is regarded as the most successful targeted cancer treatment due to the duration of responses to treatment (O'Brien et al. 2003).

The role of Abl in solid tumours is not as well established, but there is emerging evidence of its importance in invasion and growth, and overexpression in a variety of cancer types, including breast cancer, lung cancer, ovarian serous cystadenocarcinoma, urothelial carcinoma, colorectal carcinoma and renal cancer, and has recently reviewed by Greuber, Smith-Pearson, Wang and Pendergast (Sos et al. 2009, Behbahani et al. 2012, Network. 2012, Greuber et al. 2013). Abl can be activated downstream of receptor tyrosine kinases such as HER2 in breast cancer, to stimulate invasion and by MET to promote proliferation (Srinivasan and Plattner 2006, Furlan et al. 2011).

Little is known about the role of Abl in renal cancer, but it is known to be over-expressed in some tumours including CCRCC (Behbahani et al. 2012). There is however clinical data concerning the efficacy of imatinib in renal cancer, based on the ability of imatinib to inhibit its other targets, namely PDGFR and KIT, which can be expressed by renal tumours (Castillo et al. 2004). However, a phase 2 trial of single agent imatinib in RCC of all types showed no partial or complete responses (Vuky et al. 2006). In another phase II study, imatininb was combined with anti VEGF antibody bevacizumab and EGFR inhibitor erlotinib, again on the hypothesis that inhibition of PDGFR could increase response rates. This trial did not select for any predictive biomarkers, showed no increased activity over that seen with bevacizumab/erlotinib, but did see increased toxicity (Hainsworth et al. 2007). A small phase II trial of imatinib with interferon α (IFN-α) saw a response rate of only 6%, and did not recommend the combination for further study (Polite et al. 2006). Finally, imatinib has been combined in a renal cancer Phase 2 trial with everolimus, the rationale being that PDGFR inhibition may sensitise to everolimus. The trial was closed early due to lack of efficacy (Ryan et al. 2011). These trials suggest that imatinib is unlikely to have significant activity in renal cancer, although the patients in these trials were unselected for biomarkers, or Abl expression. In the context of cells with acquired resistance to BEZ235, the possibility that increased Abl expression could mediate resistance was worthy of investigation.

Cells treated in the same manner as for the antibody array were collected and lysed for analysis by western blotting. Control cells were either treated with solvent or BEZ235 for 1 hour. Resistant cells were not given a drug washout period, but did have the medium exchanged for fresh BEZ235 containing medium (20 nM for RCC4B20 and 200 nM for 786-0B200) in order to control for the effects of replenishing serum in new medium. Two antibodies were tested for the detection of pY1356 MET (see Table 2-5), which had been identified in the screen, but neither gave signal. However, an antibody to pMET Y1234/1235 did show detectable signal, with a clear indication of MET activation in both RCC4B20 and 786-0B200 resistant cells (Figure 4-7 A and B), although the signal this antibody gave was inconsistent in a standard western blot. The levels of total MET were also increased in RCC4B20 cells (Figure 4-7 A and B). This change reached statistical significance between acutely treated control cells and resistant cells. Although increased MET activation was seen in 786-0B200 cells, total MET did not increase. Despite not being able to detect pMET Y1356, MET activation as characterised by phospho-Y1234 1245 was detected, and on this basis MET was taken forward as a potential mediator of resistance.

In RCC4B20 cells, but not 786-0B200 cells, there was evidence of increased expression of Abl (Figure 4-7 A and C). There was some variability in the magnitude of increase across three independent experiments, such that statistical significance was not reached when the blots were quantified. However, there was a clear trend towards increased expression in RCC4B20, and on this basis Abl was taken forward for further validation as a potential mediator of resistance to BEZ235.

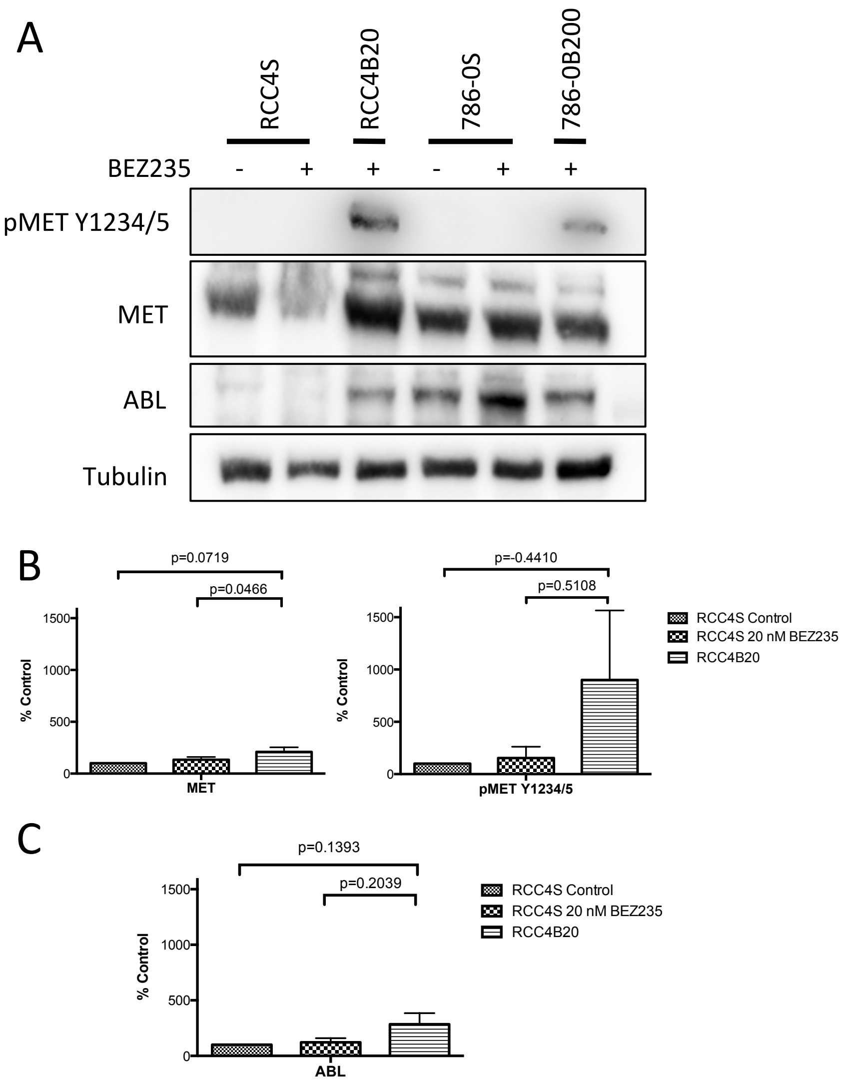


**Figure 4-7 ABL and MET show increased expression in RCC4B20 cells**

A) Monolayer RCC4S cells were treated with solvent or 20 nM BEZ235. RCC4B20 cells were treated with fresh 20 nM BEZ235. 786-0S cells were treated with solvent or 200 nM BEZ235 and 786-0B200 cells were treated with 200 nM BEZ235. One hour later cells were collected, lysed and analysed by SDS PAGE. B) Western blots of MET and pMET Y1234/5 were quantified using ImageJ, normalised to tubulin loading, and expressed as a percentage of control treated RCC4S cells. Graphs show mean and SEM of four independent experiments for MET (T test p values shown) and mean and range of two independent experiments for pMET Y1234/5. C) Western blots of ABL were quantified using ImageJ, normalised to tubulin loading, and expressed as a percentage of control treated RCC4S cells. Graphs show mean and SEM of three independent experiments. Student's T test p values shown.

Mitogen activated protein (MAP) kinase kinase (MEK) is an enzyme that forms part of the MAP kinase (ERK) signalling pathway. In response to stimulation by growth factors, a variety of growth factor receptors activate Ras, which in turn activates Raf. The most important form of Raf in cancer appears to be *BRAF,* which is mutated in 66% of melanomas and at lower frequencies in many other cancers, and when mutated is able to transform cells in culture (Davies et al. 2002). Raf phosphorylates and activates MEK, which phosphorylates and activates ERKs 1 and 2 (Ahn et al. 1991, Gomez and Cohen 1991, Kyriakis et al. 1992). MEK is highly specific for ERK as its target (Seger et al. 1992). ERK translocates to the nucleus and controls cell cycle and DNA replication through ELK-1 dependent gene transcription, to influence proliferation, differentiation, protection from apoptosis and adhesion/motility through its interaction with Paxilin (Ray and Sturgill 1988, Boulton et al. 1990, Brunet et al. 1999b, Pages et al. 1999, Scheid et al. 1999, Ku and Meier 2000, Allan et al. 2003).

The antibody array predicted an increase in total MEK in RCC4B20 cells over acutely treated RCC4S sensitive control cells. Using the same experimental design as for Figure 4-7, western blotting for MEK confirmed a trend towards increased total MEK in RCC4B20 cells. Changes in pMEK itself were less consistent, and although there was a trend towards increased pMEK in RCC4B20 cells compared to solvent treated controls, it was also noted that acute BEZ235 treatment induced increased pMEK (Figure 4-8 A and B). No consistent changes in total or phospho MEK were noted in 786-0B200 cells. The downstream MEK target ERK showed significantly up-regulated expression and a trend towards increased activation in RCC4B20 resistant cells compared to both solvent and BEZ235 treated control cells (Figure 4-8 A and C). The 786-0B200 cells, showed a minor increase in pERK over solvent treated controls, but a similar increase was induced by acute BEZ235 treatment of control cells. On the basis of the changes in MEK – ERK signalling in RCC4B20 cells, it was decided to investigate MEK/ERK as a potential mediator of BEZ235 resistance.

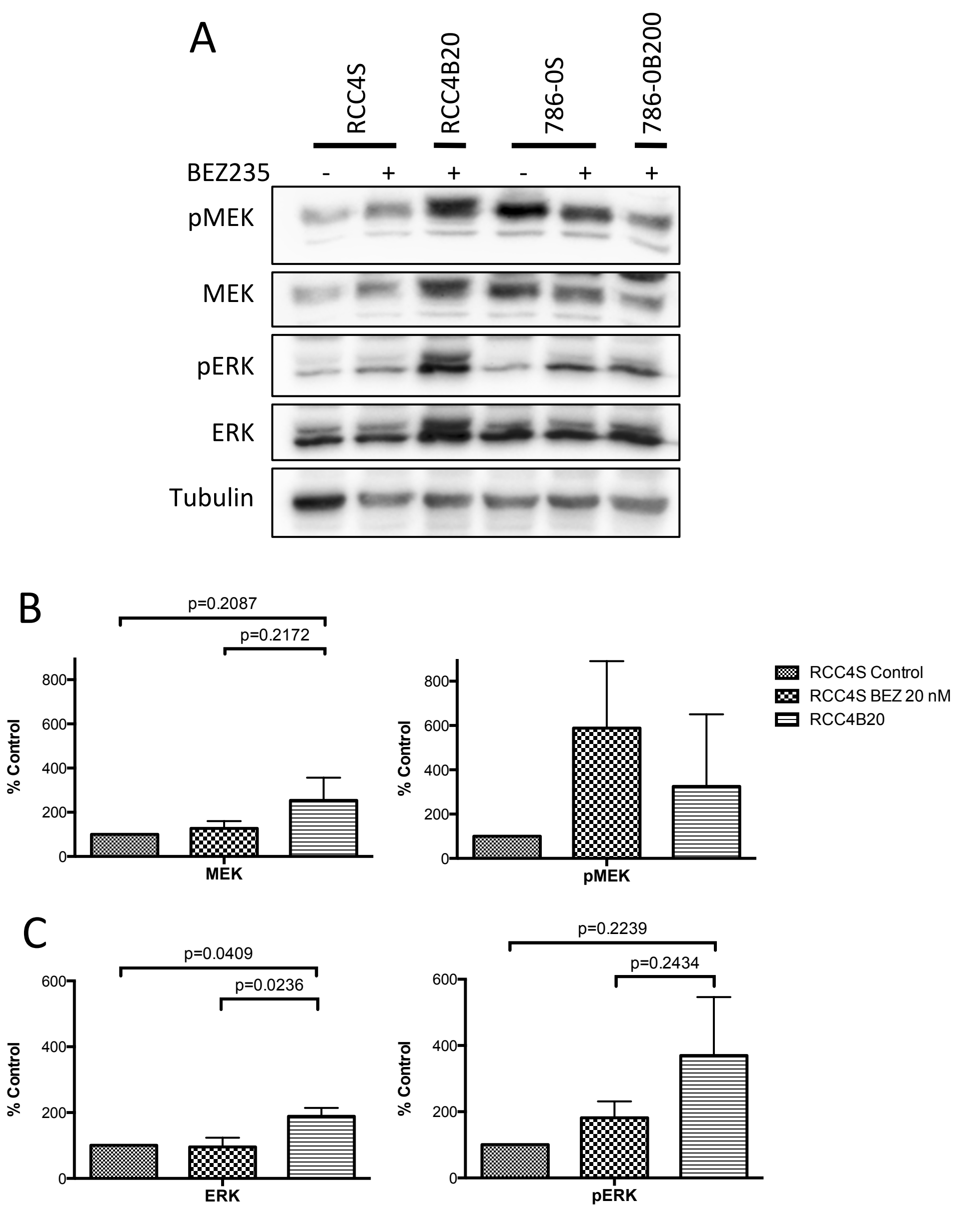


**Figure 4-8 MEK and ERK show increased expression and activation in RCC4B20 cells**

A) Monolayer RCC4S cells were treated with solvent or 20 nM BEZ235. RCC4B20 cells were treated with fresh 20 nM BEZ235. 786-0S cells were treated with solvent or 200 nM BEZ235 and 786-0B200 cells were treated with 200 nM BEZ235. After 1 hour of treatment cells were collected and lysed. Cell lysates were analysed by SDS PAGE. B) Western blots of MEK and pMEK were quantified using ImageJ, normalised to tubulin loading, and expressed as a percentage of control treated RCC4S cells. Graphs show mean and SEM of five independent experiments for MEK (Student's T test p values shown) and mean and range of two independent experiments for pMEK. C) Western blots of ERK and pERK were quantified using ImageJ, normalised to tubulin loading, and expressed as a percentage of control treated RCC4S cells. Graphs show mean and SEM of four independent experiments and T test p values.

### 4.2.8 Evaluation of the functional relevance of increased MET expression and activation in BEZ235 resistant RCC cells

In order to test whether MET was contributing to resistance to BEZ235, three different approaches were taken, using a small molecule MET inhibitor, INC280, MET depletion with siRNA, and stimulation of sensitive cells with the ligand HGF.

INC280 inhibits MET trans-phosphorylation *in vitro* with low nM $IC_{50}$ concentrations and shows high specificity to MET, with only 30% inhibition of activity of 56 other tested kinases when tested at a concentration of INC280 inhibiting 90% of MET activity (Liu et al. 2011). INC280 is currently undergoing early phase clinical testing (Bang et al. 2014).

INC280 was able to inhibit the constitutive activation of MET in RCC4B20 BEZ235 resistant cells (Figure 4-9 A). As described earlier, detection of pMET Y1234/1235 was inconsistent in western blot, and therefore INC280 inhibition was tested by immunoprecipitation of total MET, and probing for pMET Y1234/1235. Two concentrations were chosen and were tested at two time-points, to detect early inhibition of pMET (1 hour), and also to test the duration of Met inhibition over the same time-course as a cell viability assay (72 hours). This showed that both concentrations of INC280 inhibited pMET at both time-points.

Next the anti-proliferative effects of INC280 were tested by cell viability assay. RCC4B20 cells showed no increased sensitivity to INC280 in comparison to RCC4S cells despite showing increased MET activation (Figure 4-9 B) and in fact viability in neither RCC4 subline was altered by INC280. A similar lack of effect was seen in 786-0B200 and 786-0S cells (Figure 4-9 C).

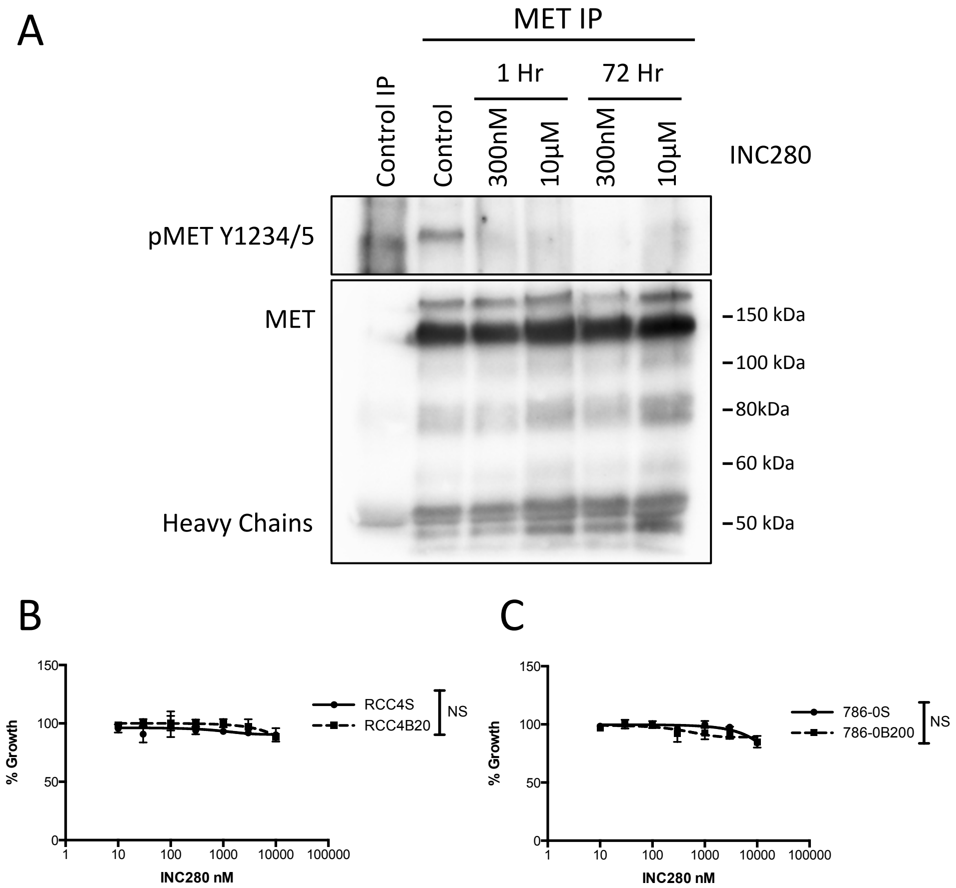


**Figure 4-9 INC280 inhibits MET phosphorylation but does not inhibit proliferation in BEZ235 sensitive or resistant cells**

A) Monolayer RCC4B20 cells were treated with solvent, 300 nM or 10 µM INC280 for the indicated time. Whole cell lysates were immunoprecipitated with MET antibody (CS #8198) or non specific IgG (control IP) and analysis performed by SDS PAGE and western blotting for phospho- and total MET. Similar results were seen in two other independent similar experiments. CTG cell viability assays of B) RCC4S and RCC4B20, and C) 786-0S and 786-0B200 treated with INC280. Graphs show mean and SEM of six data points from two independent experiments. NS P>0.05 by two way ANOVA.

Despite not being more sensitive to single agent INC280, it was still possible that MET activation was contributing to BEZ235 resistance. Therefore the combination of 10 μM INC280 and BEZ235 was tested. The higher concentration was used because the difficulty in detecting pMET could have been due to poor antibody sensitivity, and therefore it was possible that the lower concentration (300 nM, Figure 4-9 A) was incompletely inhibiting MET, but that this was below the detection threshold of the antibody. The 10 μM concentration was not expected to have significant off target effects because it did not influence proliferation (Figure 4-9 B and C).

The combination was tested in both BEZ235 resistant and sensitive control cells, with the hypothesis that if MET was mediating resistance to BEZ235 it would sensitise BEZ235 resistant cells, but not influence the control cells. In RCC4S cells (Figure 4-10 A) the predicted result was seen, and no alteration in BEZ235 sensitivity was detected (Table 4-3). BEZ235 resistant RCC4B20 cells however also showed no BEZ235 sensitisation when INC280 was added (Figure 4-10 A and Table 4-3), suggesting that MET activation was not mediating resistance in RCC4B20 cells. Clonogenic survival/growth assays confirmed these results, with no change in $SF_{50}$ in RCC4S cells with the addition of INC280 (Figure 4-10 C and Table 4-3). In RCC4B20 cells, a small shift in $SF_{50}$ was detected that reached statistical significance by two way ANOVA. However, this was an extremely small change, and rather than sensitising to BEZ235, MET inhibition slightly increased resistance (Figure 4-10 D and Table 4-3).

The same lack of effect was seen: In 786-0S and 786-0B200 cells INC280 did not sensitise resistant cells to BEZ235 in assays for viability (Figure 4-10 E and F and Table 4-3), or clonogenic survival/growth (Figure 4-10 G and H and Table 4-3).

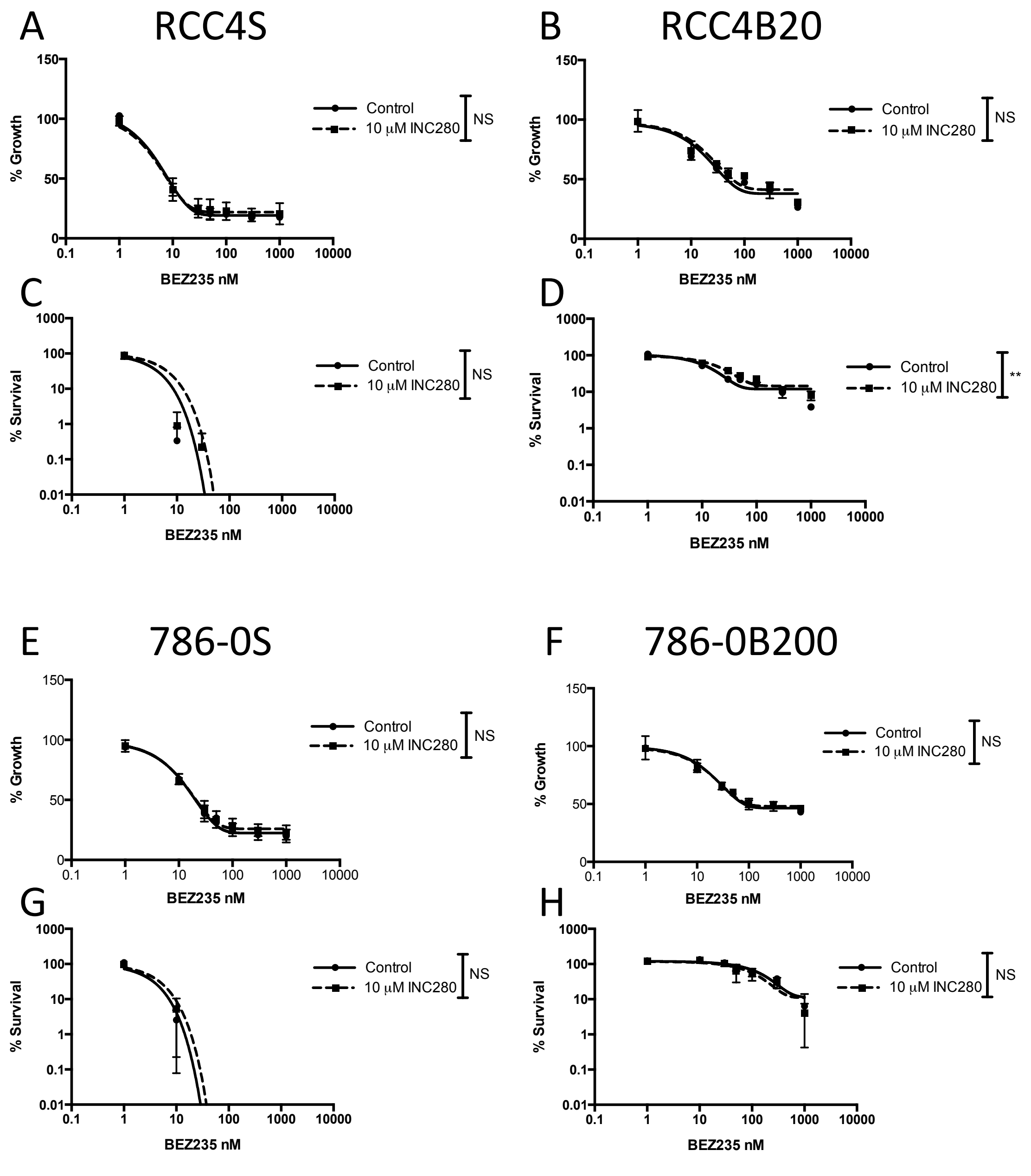


**Figure 4-10 INC280 does not sensitise BEZ235-resistant RCC cells to BEZ235**

CTG cell viability assays of A) RCC4S, B) RCC4B20, E) 786-0S and F) 786-0B200 cells treated with BEZ235 and solvent, or BEZ235 and 10 µM INC280. Graphs show mean and SEM of two independent experiments. NS P>0.05 by two way ANOVA. Clonogenic survival/growth assays of C) RCC4S, D) RCC4B20, G) 786-0S and H) 786-0B200 cells treated with BEZ235 and solvent, or BEZ235 and 10 µM INC280. Graphs show mean and SEM of two independent experiments. NS P>0.05, ** P=0.0042 by two way ANOVA.

| Cell Line | $GI_{50}$ nM (95% CI) | | Fold Sensitisation | $SF_{50}$ nM (95% CI) | | Fold Sensitisation |
|---|---|---|---|---|---|---|
| | BEZ235 | + INC280 | | BEZ235 | + INC280 | |
| **RCC4S** | 8 (7 – 10) | 8 (6 – 11) | 1 (0.6 – 1.7) | 3 (2 – 5) | 3 (2 – 4) | 1 (0.5 – 2.5) |
| **RCC4B20** | 46 (30 – 67) | 59 (40 – 88) | 0.8 (0.3 – 1.6) | 12 (9 – 15) | 19 (15 – 24) | 0.6 (0.4 – 1) |
| **786-0S** | 20 (17 – 24) | 21 (17 – 26) | 1 (0.7 – 1.4) | 4 (3 – 6) | 5 (3 – 5) | 1.3 (0.6 – 2) |
| **786-0B200** | 82 (62 – >1000) | 96 (76 – >1000) | 0.9 | 157 (98 – 257) | 117 (71 – 195) | 1.3 (0.5 – 3.6) |

**Table 4-3 Effect of MET inhibition on response to BEZ235**

$GI_{50}$ and $SF_{50}$ values taken from Figure 4-10. Fold sensitisation = control treated $GI_{50}$/INC280 treated $GI_{50}$, or control treated $SF_{50}$/INC280 treated $SF_{50}$.

MET has been shown to have ligand independent activity, which can be abrogated by depletion of total MET levels (Olwill et al. 2013). MET has been shown to cross activate with fibronectin and integrins, the EGFR and IR where it forms hybrid receptors (Dulak et al. 2011, Fafalios et al. 2011, Mitra et al. 2011). Similarly, other receptors, including the IGF-1R and the EGFR have been shown to have kinase independent function (Wright et al. 1995, Boucher et al. 2010, Janku et al. 2013). It was conceivable therefore that MET over-expression could influence resistance to BEZ235, even though abrogation of its kinase function was ineffective at sensitising BEZ235 resistant cells.

In order to address this possibility, MET depletion with siRNA was tested for its ability to sensitise to BEZ235. In both the RCC4 and 786-0 pairs of resistant and sensitive cell lines, siRNA to MET caused good detectable MET depletion at 48 and 72 hours post transfection (Figure 4-11 A). However, MET knockdown did not sensitise RCC4S, RCC4B20, 786-0S or 786-0B200 cells to treatment with BEZ235 in comparison to control siRNA transfected cells (Figure 4-11 B – E).

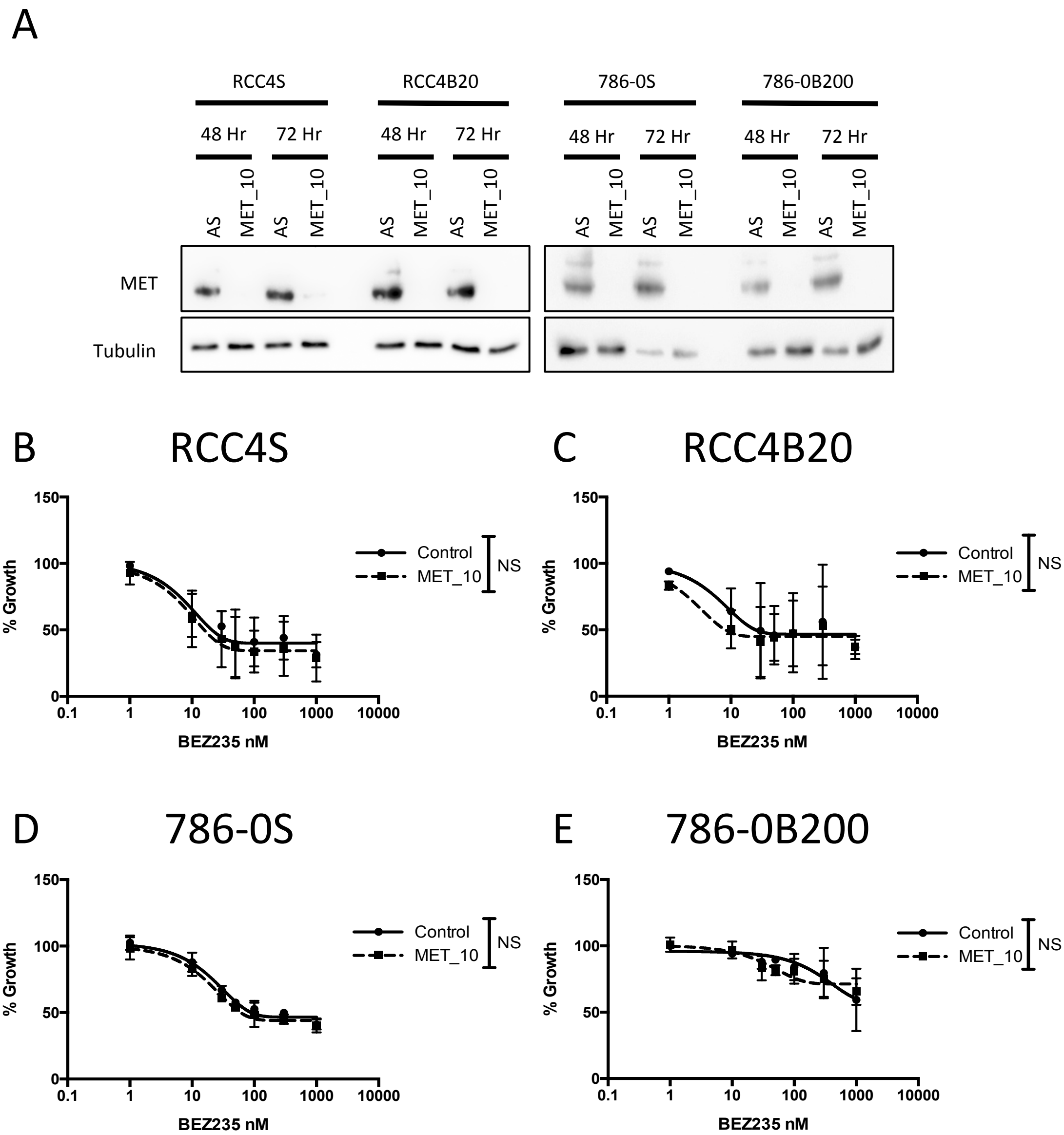


**Figure 4-11 MET knockdown does not sensitise BEZ235 resistant RCC cells to BEZ235**

Monolayer cells were reverse transfected with MET_10 siRNA or control (All Stars) siRNA. Cells were collected at the indicated times, and cell lysates analysed by SDS PAGE. Similar results were seen in an independently prepared set of cell lysates. CTG cell viability assay of B) RCC4S, C) RCC4B20, D) 786-0S and E) 786-0B200 cells reverse transfected with control siRNA or MET_10 siRNA and 48 hours later treated with BEZ235. Graphs show mean and SEM of 6 data points from two independent experiments. NS P>0.05 by two way ANOVA.

In a final test of the contribution of MET, HGF stimulation was evaluated, to determine whether this could induce resistance to BEZ235. It has been established that stimulation with high levels of growth factors, can confer resistance to small molecule inhibitors, e.g. HGF can induce vemurafenib resistance in *BRAF*-mutant melanoma models, so this approach was tested with HGF (Wilson et al. 2012). The hypothesis was that if MET was a potential resistance mediator, HGF could induce BEZ235 resistance in BEZ235 sensitive cells but should not alter the established resistance in BEZ235 resistant cells. A cell viability assay was performed as previously described for resistant cells, with the addition of 50 ng/ml HGF or solvent control applied simultaneously with BEZ235. HGF at 50 ng/ml was chosen as concentration reported in the literature to be capable of reversing resistance to vemurafenib in *BRAF*-mutant melanoma (Wilson et al. 2012). However, the addition of HGF did not affect the response to BEZ235 in any of the four cell lines tested (Figure 4-12 A – D).

This series of experiments showed that although MET expression and activation were correlated with resistance, these changes were not causative and therefore did not support further evaluation of combinations of mTORC kinase inhibitors and MET inhibitors in the treatment of renal cancer.

Other groups have observed more positive results when combining similar drugs. Recently, the RON/MET inhibitor BMS-777067 was combined with the mTORC kinase inhibitor AZD8055 and synergistic activity was seen in pancreatic cancer cells, including cancer stem cells (Zeng et al. 2014). In epithelioid sarcoma cell lines, the rapalogue everolimus has been noted to cause MET dependent AKT activation, and the MET inhibitor INC280 was able to block this signalling, and sensitise to everolimus (Imura et al. 2014). It is clear therefore that although the combination was ineffective in this model of renal cancer drug resistance, it may be effective in other cancers. The work in epithelioid sarcomas was interesting in that MET inhibition was combined with an allosteric inhibitor of mTORC1, and also that the cancer model was dependent on AKT activation for resistance. This is in contrast to the model presented here, in which resistance does not appear to be AKT dependent (Figure 4-6 G and H), and where an mTORC1/2 kinase inhibitor was combined with a MET inhibitor. It would be interesting to know whether the synergy observed in the sarcoma study would remain if an mTORC kinase inhibitor replaced everolimus (Imura et al. 2014).

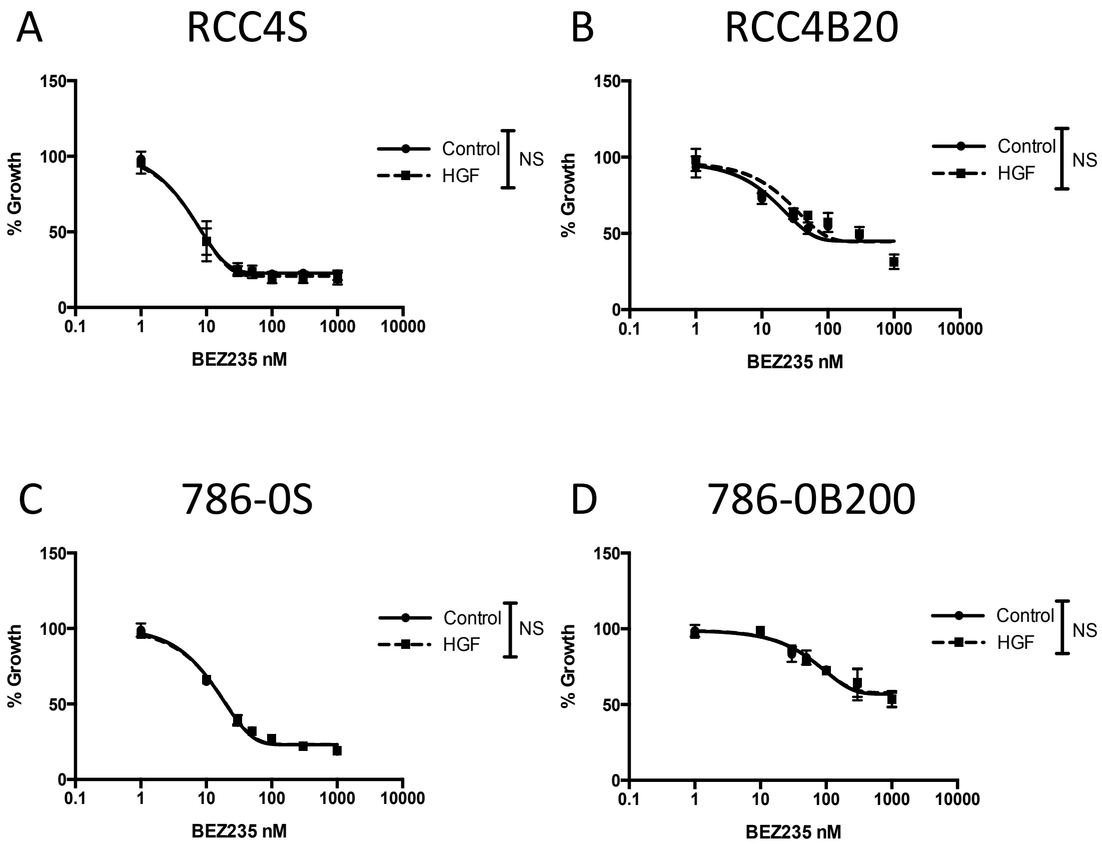


**Figure 4-12 HGF does not induce resistance to BEZ235 in BEZ235 sensitive control RCC cells**

CTG cell viability assays of A) RCC4S, B) RCC4B20, C) 786-0S and D) 786-0B200 cells treated with BEZ235 and solvent, or BEZ235 and 50 ng/ml HGF. Graphs show mean and SEM of two independent experiments. NS P>0.05 by two way ANOVA.

### 4.2.9 Evaluation of the functional relevance of increased MEK expression and activation in RCC resistant cells

The contribution of MEK/ERK to BEZ235 resistance was tested using AZD6244, a novel allosteric inhibitor that is highly specific for MEK and inhibits ERK phosphorylation at low nM concentrations (Yeh et al. 2007). AZD6244 is in early clinical trial development, particularly in melanoma where *BRAF* mutations are common, and result in MEK activation (Catalanotti et al. 2013).

First, the effects of AZD6244 on RCC cell lines was assessed. Cells were treated with either solvent, 100 nM, or 10 µM AZD6244, applied for 1 hour, to test acute inhibition, or 72 hours to test effects over the same time course as a cell viability assay. Phospho-ERK was used to assess inhibition of MEK as AZD6244 does not itself prevent MEK phosphorylation. In both RCC4S and 786-0S cells, 1 hour treatment with AZD6244 inhibited pERK at both 100 nM and 10 µM. At 72 hours, persistent ERK inhibition was seen at only 10 µM AZD6244, with both cell lines showing a degree of pERK reactivation in the presence of 100 nM AZD6244 (Figure 4-13 A). The two cell lines showed a different response to AZD6244 in terms of levels of pMEK. In 786-0S cells the levels of pMEK fell at both 1 and 72 hours. In RCC4S cells, however, pMEK increased in AZD6244-treated cells, particularly in cells treated for 72 hours, with 10 µM AZD6244, where there was also an increase in total MEK. AZD6244 has been noted to release feedback inhibition and result in an accumulation of pMEK in BRAF wild-type NSCLC, so it is possible that similar feedback is in effect here (Friday et al. 2008).

The next step was to investigate the sensitivity of BEZ235 resistant and sensitive cells to single agent AZD6244 in viability assays. Despite showing activation of MEK/ERK, RCC4B20 cells were more resistant to AZD6244 than sensitive control cells. Neither RCC4S nor RCC4B20 cells were sensitive to AZD6244, with the maximal amount of growth inhibition being less than 50% (Figure 4-13 B). In the 786-0 cell pair, the pattern was the same even though there was no clear difference in MEK/ERK signalling between 786-0S and 786-0B200 cells.

As for the MET inhibitor, the combination of AZD6244 and BEZ235 was assessed to determine whether MEK inhibition was able to reverse BEZ235 resistance. The concentration of 10 μM AZD6244 was selected as it showed complete inhibition of MEK activity for the duration of a cell viability assay. In RCC4S cells, no difference was noted in $GI_{50}$ or resistant population (Figure 4-13 D and Table 4-4), whilst in RCC4B20 cells, apparent large fold change was noted in $GI_{50}$, with AZD6244 treated cells being more resistant. This is very unlikely to be biologically significant, and is seen only because there was a minor difference in the resistant populations of cells, under 50% in control treated RCC4B20 cells, allowing calculation of a $GI_{50}$ concentration (41 nM BEZ235), and 51% in AZD6244 treated cells, giving a $GI_{50}$ of >1000 nM (Figure 4-13 D Table 4-4). In 786-0S and 786-0B200, AZD6244 did not affect response to BEZ235 in terms of $GI_{50}$ or resistant population (Figure 4-13 E and Table 4-4).

These results suggested that MEK/ERK activation was unlikely to contribute to BEZ235 resistance in RCC cells. In contrast, recent data in an *in vivo* model of gefitinib resistant non small cell lung cancer showed that combined treatment with AZD6244 and BEZ235 was more effective than either agent alone (Qu et al. 2014). In a rhabdomyosarcoma model, PI3K/mTOR inhibition resulted in increased ERK, and the combination of the mTOR inhibitor AZD8055 and the MEK inhibitor AZD6244 was more effective than either alone, although the combination of BEZ235 and AZD6244 was not more efficacious (Renshaw et al. 2013). Markers for response to this combination are not fully understood, but may include KRAS activation as the new mTORC kinase inhibitor Torin2 was ineffective in lung cancer models driven by KRAS, but when combined with AZD6244 induced significant growth inhibition in xenograft models (Liu et al. 2013b). In support of this, a study of *KRAS* mutant colorectal cancer showed that the combination of AZD8055 and AZD6244 was more effective than either agent alone and prevented tumour growth, but did not cause tumour regressions (Migliardi et al. 2012). The 786-0 cells do not harbour *RAS* mutations (http://cancer.sanger.ac.uk/cell_lines/sample/overview?id=905947) and although the mutation status of RCC4 cells has not been published, the rate of RAS mutations in renal cancer are low (Nanus et al. 1990, Rochlitz et al. 1992).

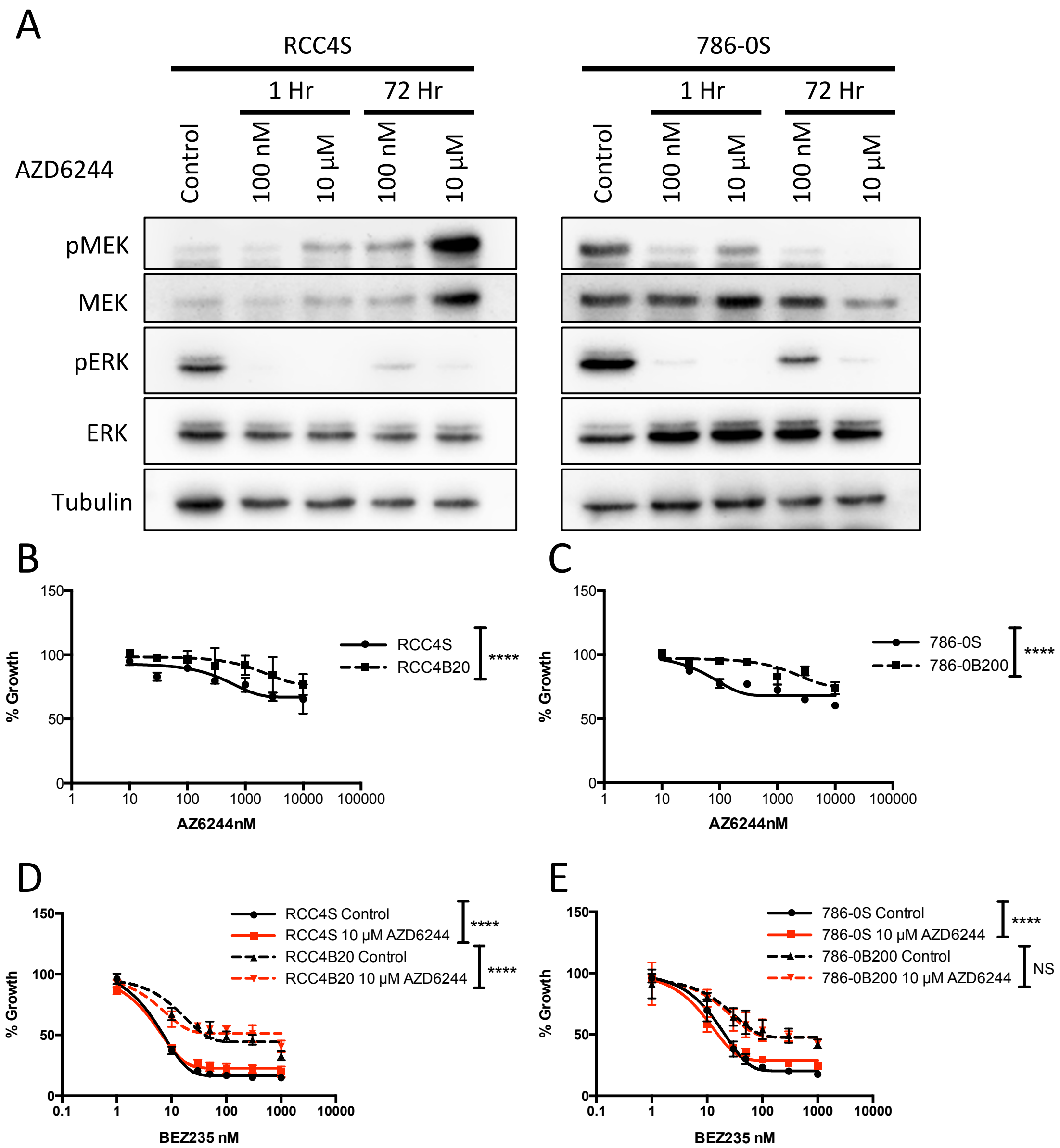


**Figure 4-13 MEK inhibition does not sensitise RCC cells to BEZ235**

A) RCC4S and 786-0S cells were treated with solvent or with the indicated concentration of AZD6244. After the indicated duration of treatment, cells were collected, lysed and lysates analysed by SDS PAGE and western blotting. Similar results were seen in two independent experiments. CTG cell viability assays of B) RCC4S and RCC4B20, and C) 786-0S and 786-0B200 cells treated with AZD6244. Graphs show mean and SEM of three independent experiments. **** P<0.0001 by two way ANOVA. CTG cell viability assays of D) RCC4S and RCC4B20, and E) 786-0S and 786-0B200 cells treated with BEZ235 and solvent, or BEZ235 and 10 µM AZD6244. Graphs show mean and SEM of three independent experiments. NS P>0.05, **** P<0.0001 by two way ANOVA.

| Cell Line | $GI_{50}$ nM (95% CI) | | Fold Sensitisation | Resistant Population % (95% CI) | | Fold Sensitisation |
|---|---|---|---|---|---|---|
| | BEZ235 | + 10 µM AZD6244 | | BEZ235 | + 10 µM AZD6244 | |
| **RCC4S** | 7 (6 – 8) | 7 (6 – 8) | 1 (0.8 – 1.3) | 16 (15 – 18) | 23 (21 – 26) | 0.7 (0.6 – 0.9) |
| **RCC4B20** | 41 (27 – 61) | >1000 | <0.04 * | 44 (40 – 49) | 51 (48 – 55) | 0.9 (0.7 – 1) |
| **786-0S** | 21 (18 – 24) | 16 (13 – 18) | 1.3 (1 – 1.8) | 20 (17 – 23) | 29 (26 – 32) | 0.7 (0.5 – 0.9) |
| **786-0B200** | 96 (61 – >1000) | 83 (48 – >1000) | 1.2 | 48 (42 – 53) | 48 (41 – 54) | 1 (0.8 – 1.3) |

**Table 4-4 Summary of effects of AZD6244 on response to BEZ235**

$GI_{50}$ and $SF_{50}$ values taken from Figure 4-10. Fold sensitisation = control treated $GI_{50}$/AZD6244 treated $GI_{50}$, or control treated resistant population/AZD6244 treated resistant population. * Apparent large shift in sensitivity by $GI_{50}$ is due to a small, non-statistically significant shift in the resistant population such that $GI_{50}$ is calculable in control, but not in AZD6244 treated cells. This is not thought to be a biologically significant difference.

### 4.2.10 Evaluation of the functional relevance of increased Abl expression in RCC resistant cells

The contribution of increased Abl expression was examined using the Abl kinase inhibitor imatinib. As well as inhibiting Abl, imatinib also inhibits c-KIT and PDGFR at nM concentrations (Buchdunger et al. 1995). Imatinib is licenced for use in CML where it targets the BCR-ABL fusion protein (O'Brien et al. 2003) and gastrointestinal stromal tumour (GIST), where gain of function c-KIT mutations are common (Demetri et al. 2002).

In order to test for Abl inhibition, a downstream target was identified that is phosphorylated by Abl. This was because Abl activity is controlled by myristoylation, and antibodies to detect direct activation of Abl were not available. The Abl target CT10 Regulator of Kinase (CrK) is phosphorylated by Abl on tyrosine 221 and is therefore a marker of Abl activity (Feller et al. 1994). The activity of imatinib was assessed at 1 and 72 hours, in cells treated with 1 and 10 μM imatinib. Results of western blots in RCC4S, 786-0S and 786-0B200 are shown (Figure 4-14 A). Western blots of pCRKII in RCC4B20 cells showed no signal. In 786-0 cells, it appeared that levels of phospho-CRKII were higher in 786-0B200 cells than the paired sensitive subline, suggesting increased Abl activity. There was evidence of Abl inhibition in RCC4S and 786-0S cells. It was noted that in 786-0B200 cells imatinib induced only a modest reduction in pCRKII, but this inhibition did persist at 72 hours.

The anti-proliferative effects of imatinib were compared between BEZ235 resistant and sensitive cells. There was no biologically significant difference in response between RCC4S and RCC4B20 cells (Figure 4-14 B) or between 786-0S and 786-0B200 cells (Figure 4-14 C). On the grounds that the highest concentration of imatinib was required to see reduction in pCRKII in 786-0B200 cells, and that the anti-proliferative effects at this high concentration were modest, the concentration of 10 μM imatinib was chosen to combine with BEZ235. In BEZ235 sensitive cells RCC4S and 786-0S there was no change in $GI_{50}$ or resistant population in the presence of 10 μM imatinib (Figure 4-14 D and E and Table 4-5). In the BEZ235 resistant cells RCC4B20 and 786-0B200, the addition of 10 μM imatinib (Figure 4-14 D and E and Table 4-5) made the cells appear more resistant. The modest shift in the dose-response curves resulted in inability to calculate $GI_{50}$ values in imatinib-treated RCC4B20 and 786-0B200 cells, making the fold change in $GI_{50}$ appear very large, but this small shift is unlikely to be biologically significant.

Abl has been linked to resistance to targeted treatments in other sold tumours, particularly breast cancer, where clinical data suggest that Abl overexpression is found in breast cancers that have progressed on aromatase inhibitors (Weigel et al. 2013). Pre clinical data, also in breast cancer, link Abl activity to lapatinib resistance (Lo et al. 2011). There is some evidence that in prostate cancer cells imatinib enhances the anti-proliferative effects of rapamycin, although this was not shown to be through Abl inhibition, but could have been mediated by one of the other actions of imatinib (Masiello et al. 2007). Conversely, studies have focused on the role of mTOR in resistance to imatinib and other Abl kinase inhibitors in CML. In this context, mTOR inhibitors including BEZ235 have shown efficacy in increasing apoptosis, decreasing colony formation and inhibiting growth both *in vitro* and *in vivo* (Okabe et al. 2014).

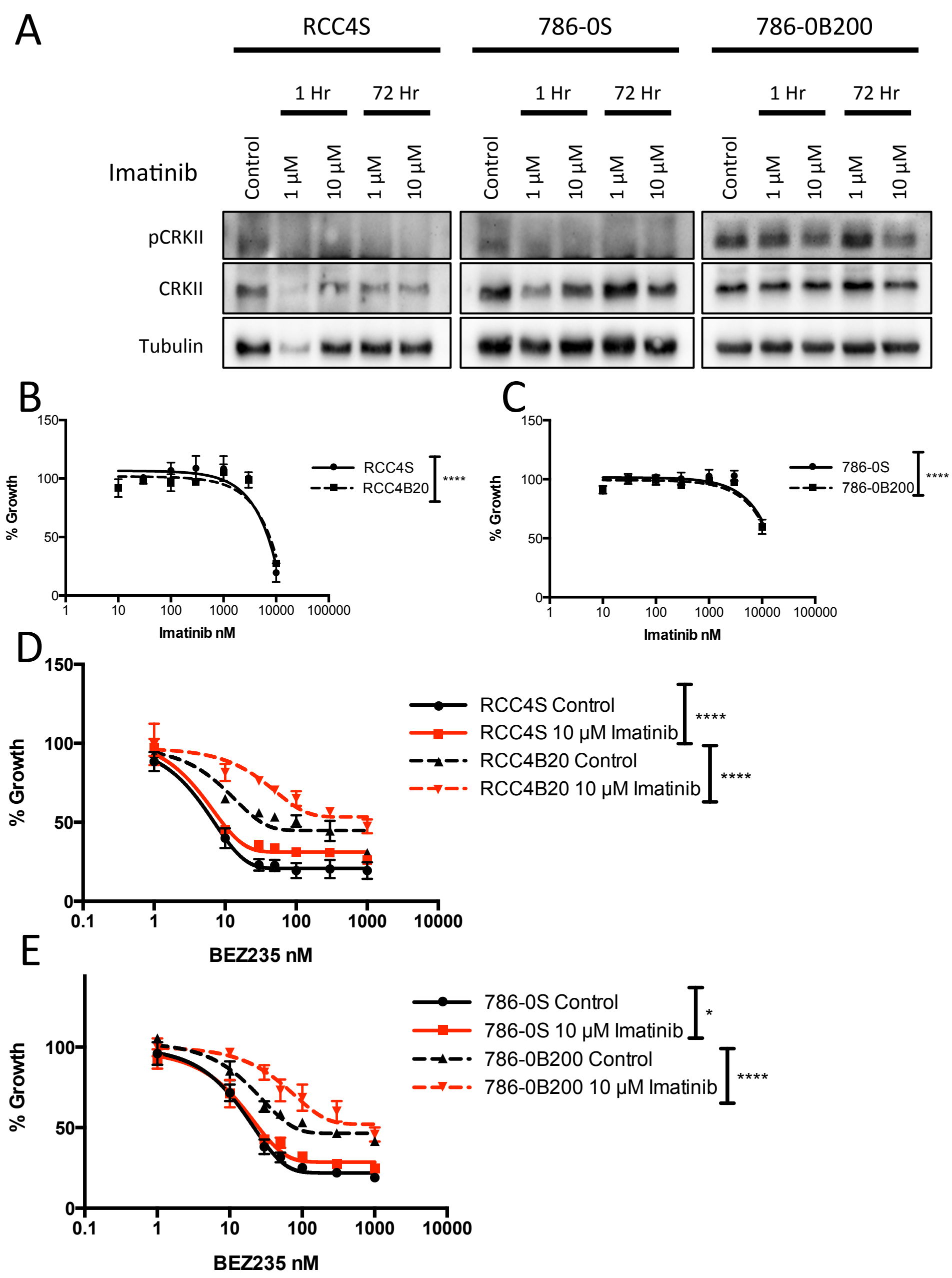


**Figure 4-14 Effects of imatinib on Abl activation and response to BEZ235**

A) Monolayer RCC4S, 786-0S and 786-0B200 cells were treated with solvent or the indicated concentrations of imatinib for 1 hour or 72 hours. Cell lysates were analysed by SDS PAGE and western blotting for phospho-CRKII (tyrosine 221) to test for Abl inhibition by imatinib. Similar results were seen in another independent experiment. CTG cell viability assays of B) RCC4S and RCC4B20, and C) 786-0S and 786-0B200 cells treated with imatinib. Graphs show mean and SEM of six data points from two independent experiments. **** P<0.0001. CTG cell viability assay of D) RCC4S and RCC4B20, and E) 786-0S and 786-0B200 cells treated with BEZ235 and solvent, or BEZ235 and 10 μM imatinib. Graphs show mean and SEM of six data points from two independent experiments. *P=0.0337, **** P<0.0001 by two way ANOVA.

| Cell Line | GI50 nM (95% CI) | | Fold Sensitisation | Resistant Population % (95% CI) | | Fold Sensitisation |
|---|---|---|---|---|---|---|
| | BEZ235 | + 10 µM imatinib | | BEZ235 | + 10 µM imatinib | |
| **RCC4S** | 7 (6 – 9) | 9 (7 – 11) | 0.8 (0.5 – 1.3) | 21 (18 – 24) | 31 (28 – 34) | 1.5 (1.2 – 1.9) |
| **RCC4B20** | 32 (18 – >1000) | >1000 | <0.03 * | 45 (39 – 51) | 53 (46 – 60) | 0.8 (0.7 – 1.1) |
| **786-0S** | 22 (19 – 25) | 25 (20 – 31) | 0.9 (0.6 – 1.3) | 22 (19 – 25) | 29 (25 – 33) | 0.8 (0.6 – 1) |
| **786-0B200** | 78 (59 – >1000) | >1000 | <0.08 * | 46 (42 – 50) | 52 (45 – 59) | 0.9 (0.7 – 1.1) |

**Table 4-5 Summary of effects of imatinib on response to BEZ235**

$GI_{50}$ and $SF_{50}$ values taken from Figure 4-14. Fold sensitisation = control treated $GI_{50}$/imatinib treated $GI_{50}$, or control treated resistant population/imatinib treated resistant population. * Apparent large shift in sensitivity by $GI_{50}$ is due to a small, non-statistically significant shift in the resistant population such that $GI_{50}$ is calculable in control, but not in imatinib treated cells. This is not thought to be a biologically significant difference.

### 4.2.11 Several potential hits from the antibody array could not be validated

Several potential mediators of resistance could not be validated in independent samples by western blotting of denatured proteins. The Ras guanine release factor 1 (RasGRF1) activates Ras through GDP/GTP exchange (Cen et al. 1993) and can increase proliferation, particularly when targeted to the cell membrane (Quilliam et al. 1994). RasGRF1 is predominantly expressed in the nervous system but has been identified in some melanoma cell lines (Zhu et al. 2007). The antibody array predicted a 2.91 fold increase in RCC4B20 BEZ235 resistant cells (Table 4-2), but western blotting did not confirm this (Figure 4-15 A).

Mitogen activated protein kinase activated protein kinase 2 (MAPKAPK2) is a serine threonine protein kinase that is part of the p38 MAP kinase pathway. Population cohort studies in China have linked MAPKAPK2 gene copy number and protein expression with risk of lung cancer (Liu et al. 2012), and MAPKAPK2 expression has been linked with the cancer stem cell phenotype and protection from apoptosis in colorectal cancer (Lin et al. 2012). One of the roles uncovered for MAPKAPK2 is in stress induced cytoskeletal rearrangements, and VEGF induced migration, where it phosphorylates LIM domain kinase (LIMK1), which was also a candidate hit from the antibody array screen (Kobayashi et al. 2006). Both of these proteins were chosen for validation and were predicted to show increased expression in RCC4B20 resistant cells in comparison to acutely BEZ235 treated control cells. Western blotting however showed a minor, non significant increase in MAPKAPK2, and no change in LIMK1 their levels (Figure 4-15 A).

Cyclin D1 associates with and activates cyclin dependent kinases 4 and 6 which phosphorylates retinoblastoma protein (Rb), and through doing so promotes cell cycle progression and proliferation (Casimiro et al. 2014). The complex of Cyclin D and CDK4/6 is able to phosphorylate and inactivate the negative regulator of mTOR TSC1/2 thus promoting protein translation (Zacharek et al. 2005). Cyclin D1 is phosphorylated on threonine 286, which leads to its nuclear export and degradation (Diehl et al. 1998, Guo et al. 2005). The level of pT286 -cyclin D1 was predicted to fall in RCC4B20 cells to approximately half the level seen in acutely treated control cells according to the antibody array (Table 4-2). Western blotting however showed a non-statistically significant increase in phospho-cyclin D1 (Figure 4-15 B).

Hormone sensitive lipase (HSL) hydrolises the first fatty acid from a triglyceride molecule, releasing a fatty acid and diglyceride, and thus forms part of the pathway by which fat stores are mobilised (Casimiro et al. 2014). Cancers have altered metabolism, and cancer cachexia is associated with increased HSL (Das and Hoefler 2013). In prostate cancer, the activity of HSL may also be associated with the production of androgens (Locke et al. 2010). The level of HSL was predicted to rise in RCC4B20 cells to over twice the levels seen in acutely treated control cells. Western blotting for HSL however showed that HSL is not expressed at detectable levels in RCC4B20 or RCC4S cells (Figure 4-15 C). In this experiment, adipose tissue lysate (a gift from Ulrike Harjes, Adrian Harris lab) was used as a positive control to confirm ability to detect HSL in western blotting.

Finally, calcium calmodulin dependent protein kinase II (CaMKII) is activated when calcium binds to calmodulin, leading to autophosphorylation. CaMKII is involved in several signalling cascades, and has been shown to be able to phosphorylate AKT and protect from apoptosis in prostate cancer (Rokhlin et al. 2007). The antibody array predicted an increase in CaMKII levels in RCC4B20 cells to almost three times the levels seen in control cells. In western blotting, the level of CaMKII in RCC4B20 cells varied in comparison to RCC4S cells, and although there was a trend towards increased expression, this did not reach statistical significance (Figure 4-15 C).

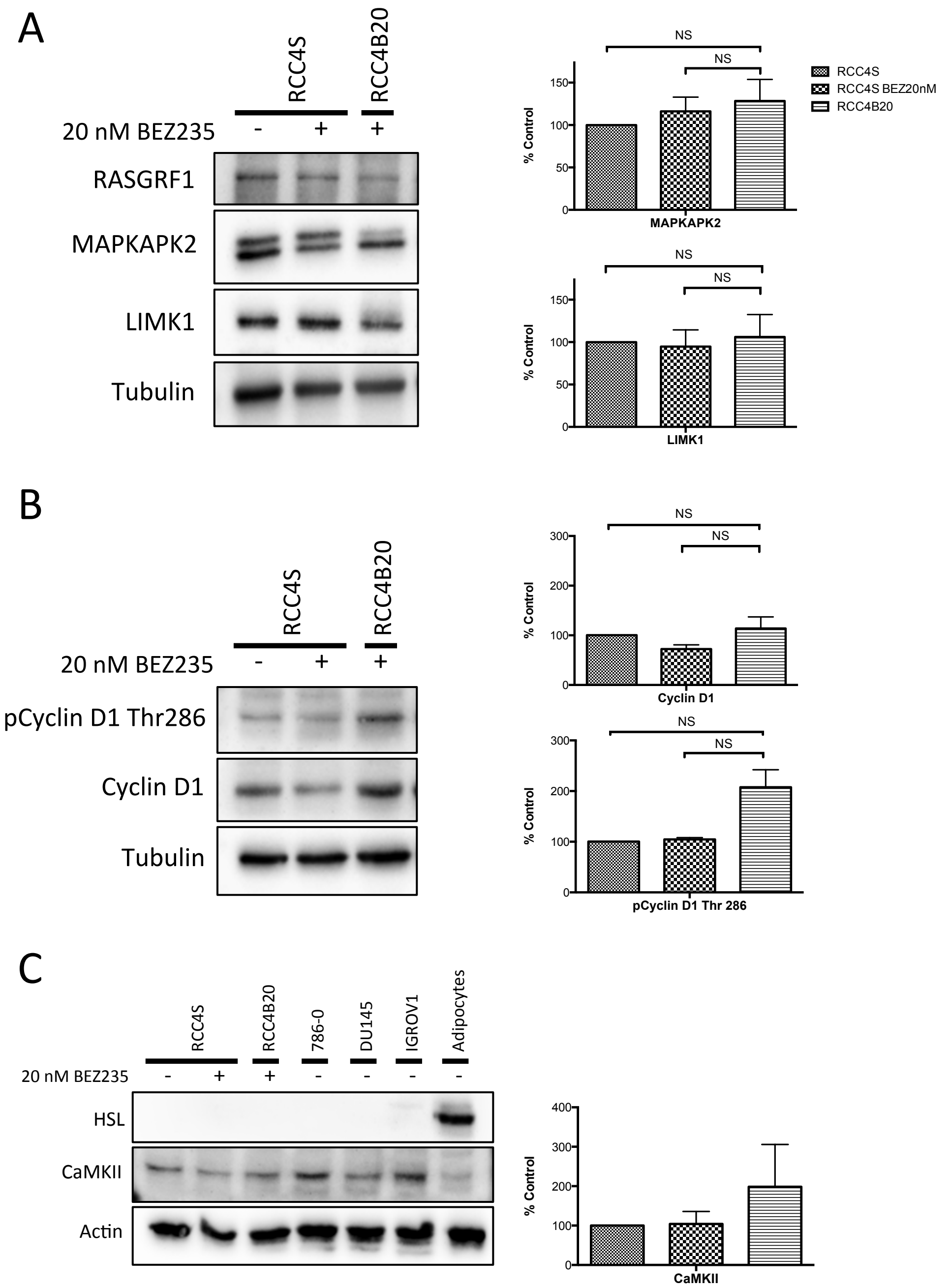


**Figure 4-15 Potential hits identified by antibody array that failed to validate by western blot**

Monolayer RCC4S and RCC4B20 cells were treated with solvent, or 20 nM BEZ235 for 1 hour. Adipocytes were solvent treated for 1 hour and served as control for HSL. DU145 and IGROV1 were used as control cell lines during the testing of the antibodies used in validation of the antibody array hits. They have been included in the displayed blot to maintain the integrity of the HSL control. Cell lysates were analysed by SDS PAGE and western blotted for A) RASGRF1, MAPKAPK2 and LIMK1, B) p cyclin D1 Thr 286 and total cyclin D1, and C) HSL and CaMKII. Graphs show quantifications of western blots using ImageJ, normalised to loading control (tubulin or actin) and expressed as a percentage of control treated RCC4S cells. Mean and SEM shown of 5 independent experiments (MAPKAPK2, LIMK1) and 3 independent experiments (cyclin D1 and p cyclin D1). NS P>0.05 by student's T test. Graph shows mean and range of 2 independent experiments for CaMKII.

### 4.2.12 Screening BEZ235 resistant RCC4B20 cell by microarray

As well as screening BEZ235 resistant RCC4B20 cells at the protein level by antibody array, they were also screened for altered expression at the RNA level. The same conditions were selected as for the antibody array screen: RCC4S BEZ235 sensitive cells were treated for one hour with solvent, or 20 nM BEZ235. RCC4B20 cells were not given a drug washout, but were treated with fresh medium with 20 nM BEZ235 for one hour. Triplicate samples of each condition were analysed by microarray, at the Cancer Research UK microarray facility, Manchester.

Prior to analysis correlations between replicate samples were visualised on a dendrogram. Replicate samples would be expected to have similar expression profiles, and hence cluster on the dendrogram as a sub-tree. This revealed one of the RCC4B20 samples to be an outlier compared to the two other samples, and therefore was excluded from further analysis. Results were expressed as $\log_2$ fold changes between RCC4B20 and solvent treated RCC4S cells (signal intensity RCC4B20 / signal intensity RCC4S control) and between RCC4B20 and BEZ235 treated RCC4S cells (signal intensity RCC4B20 / signal intensity RCC4S BEZ235). An interquartile range filter was applied to enrich the list of potential hits for genes that were highly expressed, and then results were filtered for hits with a p value ≤ 0.05. The data from these comparisons were loaded into Metacore (http://thomsonreuters.com/metacore/), which is an online tool that allows analysis of data sets such as microarrays to identify pathways or signalling networks that are significantly altered between the different conditions being tested. In both comparisons, the “Notch – epithelial mesenchymal transition (EMT)” pathway was identified as being significantly altered in resistant cells (Figure 4-16). The Notch ligand Jagged 1 was predicted to increase 1.2 $\log_2$ fold in RCC4B20 cells compared to RCC4S control treated cells (and 1 $\log_2$ fold, i.e. a doubling, between RCC4B20 and BEZ235 treated RCC4S cells). The Notch 1 transcriptionally-regulated target hairy/enhancer of split related with YRPW motif (HEY1) was predicted to increase ~1.75 fold compared to control treated RCC4S cells (1.1 $\log_2$ fold compared to BEZ235 treated RCC4S cells). Fibronectin was predicted to decrease 0.9 $\log_2$ fold, i.e. by half, compared to control treated RCC4S (1.1 $\log_2$ fold compared to BEZ235 treated RCC4S cells). In addition to these genes identified as being part of this pathway, another Notch regulated gene, hairy and enhancer of split 1 (HES1) was also identified as being increased by 1.1 $\log_2$ fold compared to control treated RCC4S cells (1.5 $\log_2$ fold compared to BEZ235 treated RCC4S cells). Although none of these changes was large, the identification of multiple members of the Notch family suggested that changes in this pathway could be associated with BEZ235 resistance. Identification of pathways in this manner is an advantage of using Metacore.

The Notch family of receptors consist of Notch 1 – Notch 4. They are single pass transmembrane receptors that bind to membrane bound Delta like (DLL) or Serrate homolog ligands (DLL1 – 4 or Jagged 1 – 2). Upon ligand binding, the ligand expressing cell endocytoses the ligand/receptor complex, and the extracellular domain of Notch is cleaved by a disintegrin and metalloproteinase (ADAM) at S2 (Brou et al. 2000, Mumm et al. 2000). The receptor is then further cleaved by gamma secretase at valine 1794, to remove the transmembrane portion of Notch (Schroeter et al. 1998). This releases the Notch intracellular domain (NICD), which translocates to the nucleus, where it converts the suppressor of hair-less/Lag-1 to an activator and promotes the transcription of genes including *HES1*, *HES5*, *HES7*, *HEY1*, *HEY2* and *HEYL*.

Notch signalling has been implicated in the control of cell fate, maintenance of stem cells, as well as controlling EMT through expression of Twist and Snail transcription factors, both during normal development, and cancer development (Mani et al. 2008). EMT is characterised by cells taking on a fibroblast-like appearance, downregulating epithelial markers such as E-cadherin, and upregulating mesenchymal markers such as N-cadherin, vimentin and fibronectin (Mani et al. 2008). EMT in cancer has been described as an important step during metastasis (Yang et al. 2004), and is associated with drug resistance (Wang et al. 2009, Xie et al. 2012). Notch also plays a role in angiogenesis as evidenced by the severe vascular abnormalities seen in *Notch 1* homozygous mutant mice (Krebs et al. 2000). Notch 1 and Jagged 1 expression are associated with poor prognosis in breast cancer (Reedijk et al. 2005), and are associated with metastasis and high grade in prostate cancer (Zhu et al. 2013).

In the kidney, Notch plays a role in embryogenesis, and has been linked to renal cancer, where it and its ligand Jagged 1 show increased expression compared to adjacent normal tissue, and Notch inhibition *in vitro* and *in vivo* inhibited RCC proliferation (Sjolund et al. 2008). *In vitro* in renal cancer cell lines, Notch signalling decreases PTEN expression, and consequently leads to increased AKT phosphorylation levels (Liu et al. 2013c). These results make this pathway an interesting candidate as a mediator of resistance to mTORC inhibition.

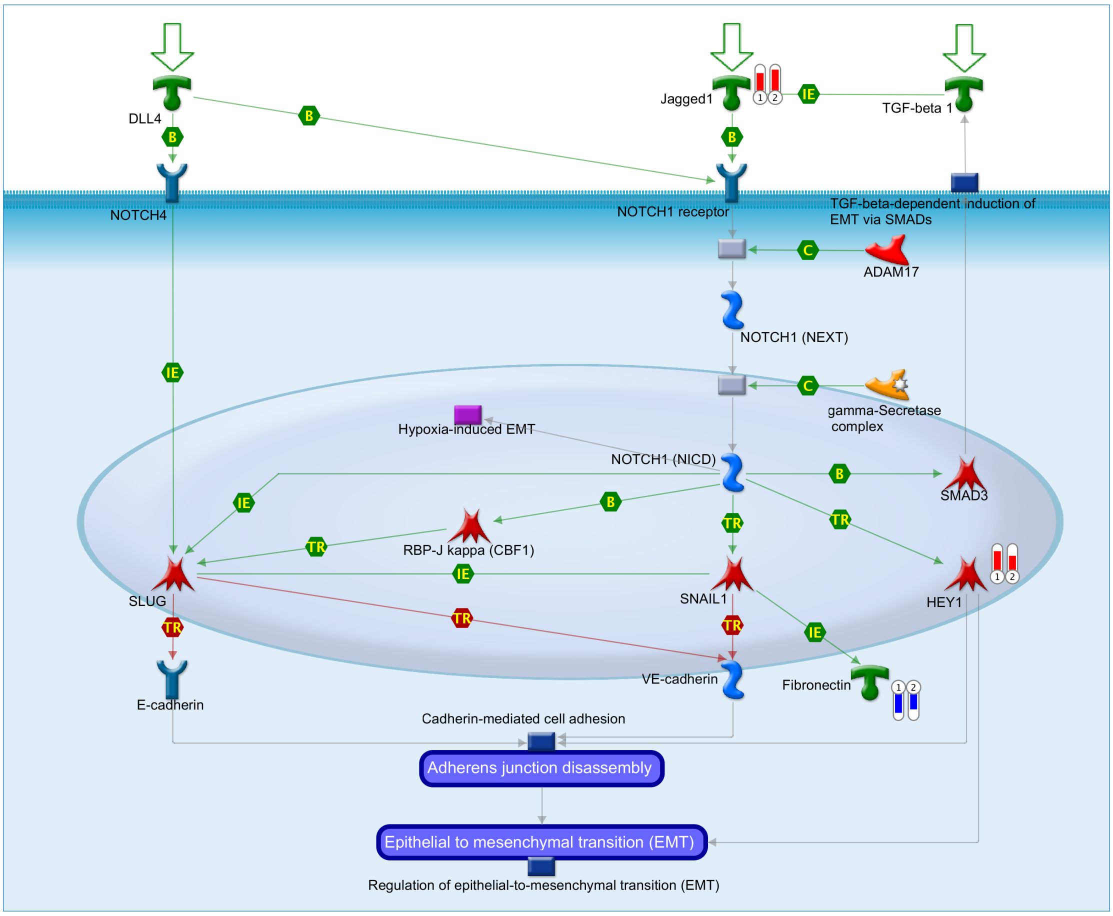


**Figure 4-16 Microarray analysis suggests alteration of the Notch pathway**

The raw microarray data were analysed to quantify changes in gene expression in RCC4B20 cells relative to solvent treated control cells, and for levels in RCC4B20 cells relative to BEZ235 treated control cells. An interquartile range (IQR) filter was applied to remove genes with low expression values, or low variance between samples, and results were filtered for P value <0.05. The $\log_2$ fold change data were uploaded to Metacore ([http://thomsonreuters.com/metacore/](http://thomsonreuters.com/metacore/)) for pathway analysis. The "Notch epithelial-to-mesenchymal transition (EMT)" pathway was identified in both analyses of RCC4B20 compared to solvent treated control cells (P=0.0001463) and RCC4B20 compared to BEZ235 treated control cells (P=0.0003752). Red bars indicate increased gene expression, and blue bars indicate reduced gene expression in RCC4B20. Each bar represents one sample pair.

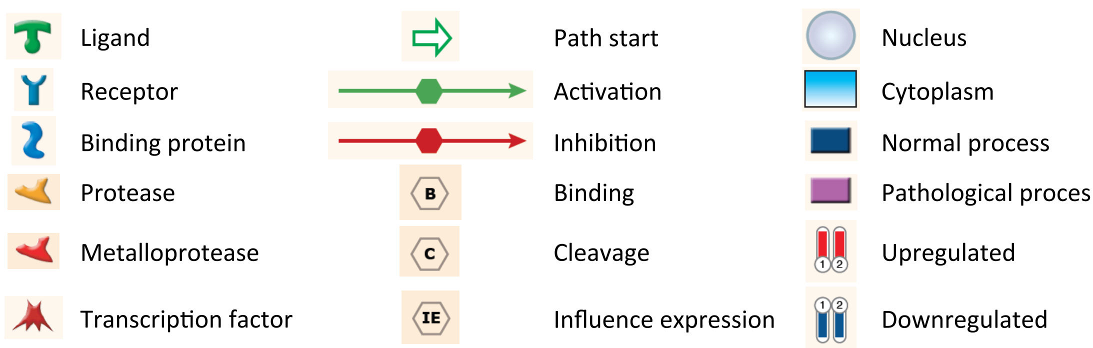

## 4.2.13 Validation of increased expression of Notch pathway members

The first stage in investigating the Notch pathway as a mediator of BEZ235 resistance was to validate the results of the microarray by qRT-PCR (Figure 4-17 A and B). This confirmed that in comparison to solvent or BEZ235-treated RCC4S cells, HEY1 was up-regulated and fibronectin was down-regulated. HES1 was statistically significantly up-regulated compared to BEZ235 treated control cells, but not compared to solvent treated control cells, whereas Jagged 1 showed the reverse pattern, with significant up-regulation seen compared to solvent treated control cells, while the apparent upregulation compared with BEZ235 treated control cells failed to reach statistical significance (Figure 4-17 A and B). Increased Jagged 1 expression was confirmed at the protein level by western blotting, and this was associated with increased cleaved Notch 1 (NICD) (Figure 4-17 C). The antibody used for this study, CS #4147, recognises Notch 1 only when cleaved by gamma secretase at valine 1744. This result suggested that Jagged 1 was upregulated in BEZ235 resistant RCC4B20 cells, resulting in increased signalling via Notch 1.

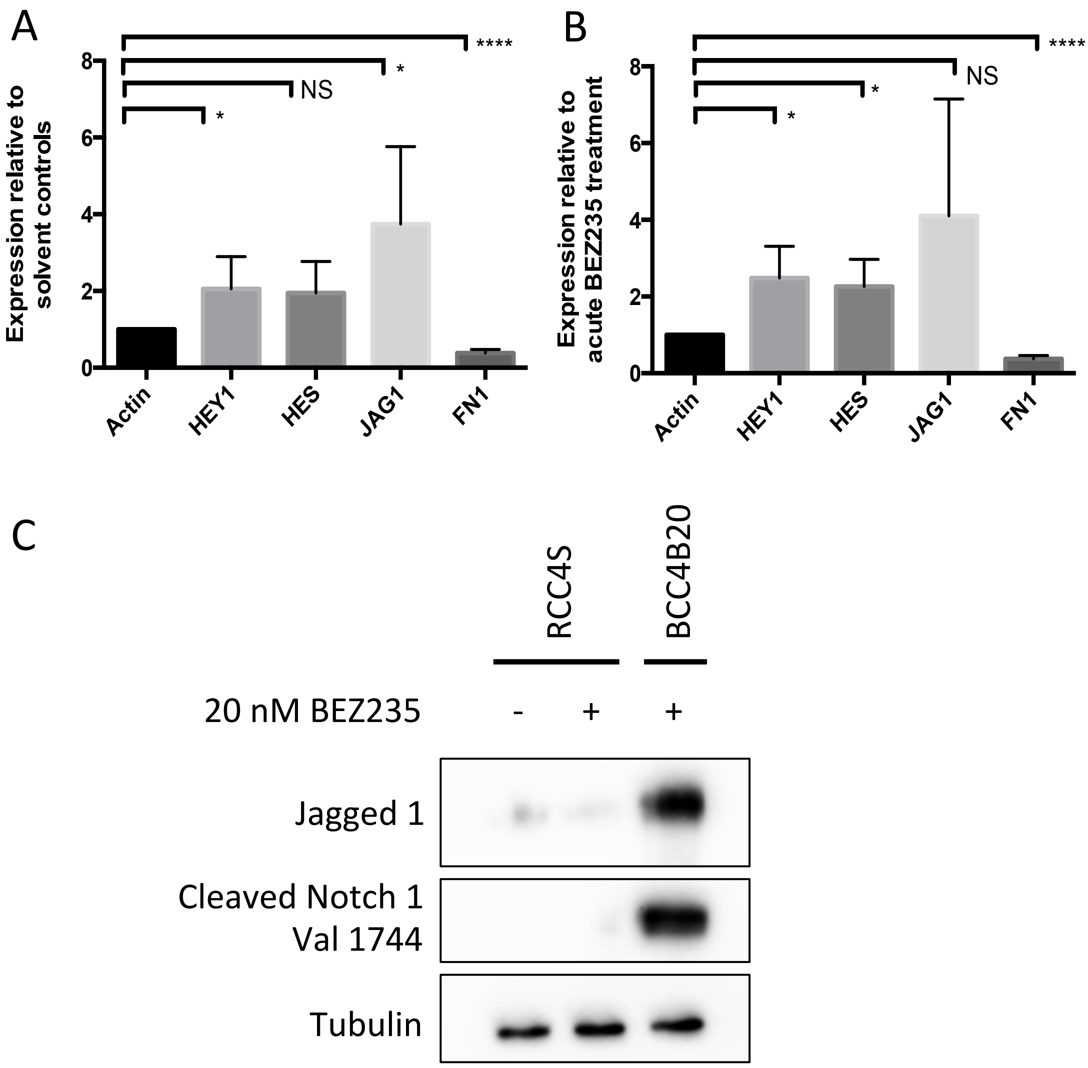


**Figure 4-17 qRT-PCR validation of microarray Notch pathway hits and confirmation that increased Jagged 1 led to increased Notch activation**

Monolayer RCC4S cells were treated for 1 hour with solvent or 20 nM BEZ235. RCC4B20 cells were treated with fresh 20 nM BEZ235 for 1 hour. Cells were collected, RNA extracted and cDNA made by reverse transcription. qRT-PCR was performed for the indicated genes and expression normalised to actin for each sample. Graphs show expression of selected genes in RCC4B20 cells relative to A) solvent-treated control cells, and B) BEZ235 treated control cells. Mean and SEM of 4 independent experiments. NS P>0.05, * P<0.05, **** P<0.0001 by students T test. C) Monolayer RCC4S cells were treated with solvent or 20 nM BEZ235 and RCC4B20 cells were treated with fresh 20 nM BEZ235 (with no drug washout). One hour later cells were lysed and analysed by SDS PAGE. Wet transfer was performed overnight onto PVDF membrane, which was activated with methanol before western blotting for Jagged 1, Cleaved Notch 1 val 1744 and tubulin. Similar results were seen in an independently prepared set of lysates.

The functional consequences of Notch pathway activation by Jagged 1 were assessed by using the gamma secretase inhibitor dibenzazepine (DBZ). This prevents the release of NICD, and therefore inhibits the transcriptional activity of Notch activation. On acute treatment with DBZ for 1 hour, no clear inhibition of Notch signalling was seen in RCC4S cells either by reduction in NICD, or by reduction of the transcriptional target HES1 (Figure 4-18 A). In RCC4B20 cells, a small degree of inhibition of Notch 1 was seen as judged by a reduction of NICD, and HES1, particularly at the higher concentration of 100 nM DBZ (Figure 4-18 A). Membranes were probed with a second Notch antibody that recognised full length Notch, as well as notch cleaved by ADAM. This showed the specificity of DBZ to inhibit only the second cleavage event that produces NICD, not the ADAM mediated cleavage that removes the extracellular domain of Notch.

Due to the poor inhibition of Notch 1 after 1 hour, a longer duration of exposure was tested. At 24 hours, DBZ clearly inhibited formation of NICD in both RCC4S and RCC4B20 cells. In RCC4S cells, that had a lower basal level of HES1, both tested concentrations of DBZ completely inhibited HES1 expression. In RCC4B20 cells however, the lower concentration of 10 nM DBZ caused incomplete inhibition of HES1 expression as seen on the longer exposure (Figure 4-18 B).

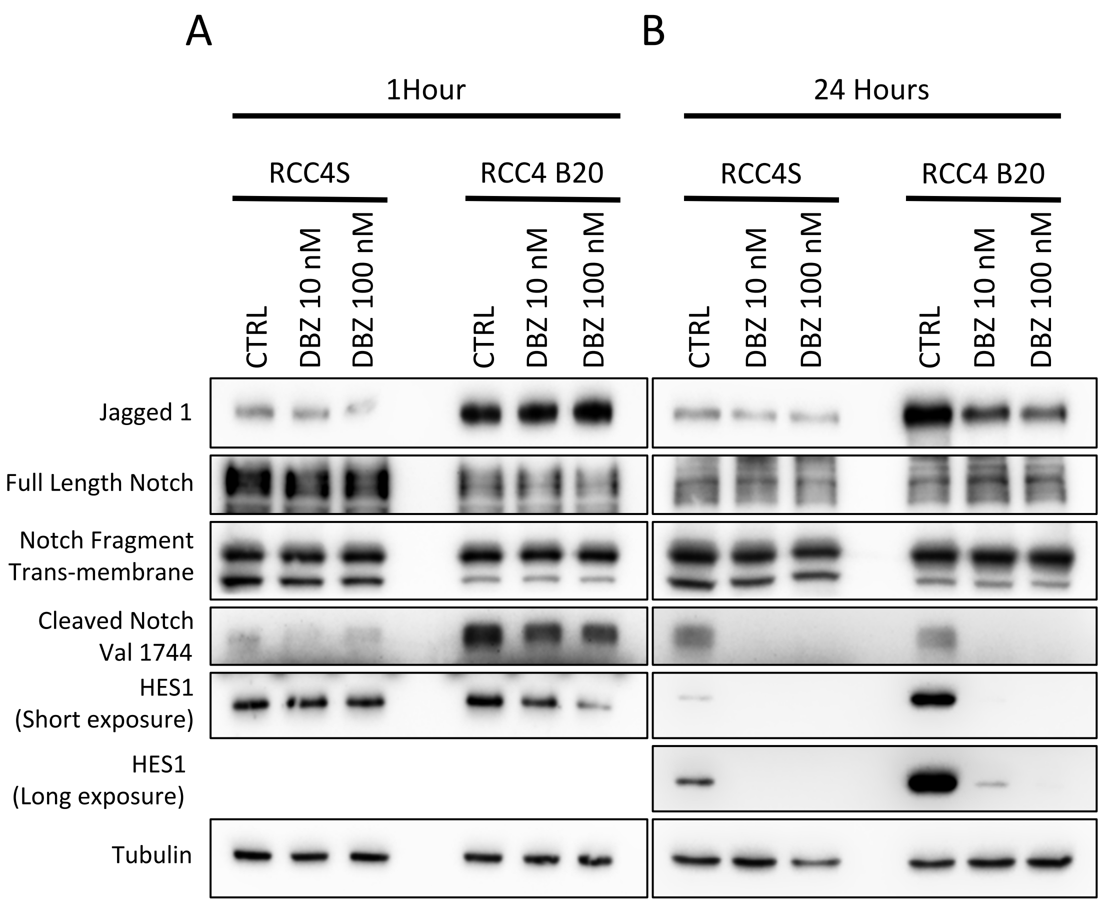


**Figure 4-18 The effects of DBZ on BEZ235 resistant cells**

Monolayer RCC4S and RCC4B20 cells, after a drug washout, were treated with solvent, or the indicated concentration of the gamma secretase inhibitor DBZ for A) 1 hour and B) 24 hours. Cells were lysed, analysed by SDS PAGE, transferred to PVDF membrane by overnight wet transfer and analysed by western blotting. Membranes were probed with two Notch antibodies to assess for action of DBZ. The first detected full length Notch 1 and cleaved fragments including the trans-membrane region. The second antibody recognised Notch 1 cleaved at Val 1744 only (the Notch intra-cellular domain). HES 1 was probed for as a downstream Notch regulated gene. Similar results were seen in another independent experiment.

In order to test whether increased Jagged 1 expression acting via the Notch pathway was responsible for BEZ235 resistance, RCC4 cells were treated with DBZ in combination with BEZ235. The higher concentration of 100 nM DBZ was chosen because it caused greater inhibition of the Notch pathway (Figure 4-18). In previous drug combination tests, the two treatments had been applied simultaneously because both BEZ235 and the second drug had been shown to inhibit their respective targets within one hour. However, DBZ showed complete inhibition only after 24 hours, likely because the downstream events that were being assessed were transcriptional. As well as inhibiting the creation of new HES1, any pre-existing HES1 would also have to be degraded. To account for this lag in effects, the cell viability assays were performed with a 24 hour pre treatment of DBZ before the application of BEZ235.

The gamma secretase inhibitor DBZ had no effect on the response to BEZ235 in RCC4S BEZ235 sensitive cells (Figure 4-19 A). In BEZ235 resistant RCC4B20 cells, there was a statistically significant shift in the response curve by two way ANOVA, with the DBZ treated cells being slightly more resistant. The magnitude of effect however was small, and likely not biologically relevant (Figure 4-19 B). In these BEZ235 resistant cells, it appears that Jagged 1 expression and Notch pathway activation are correlates of resistance, but are not mediators of resistance.

A

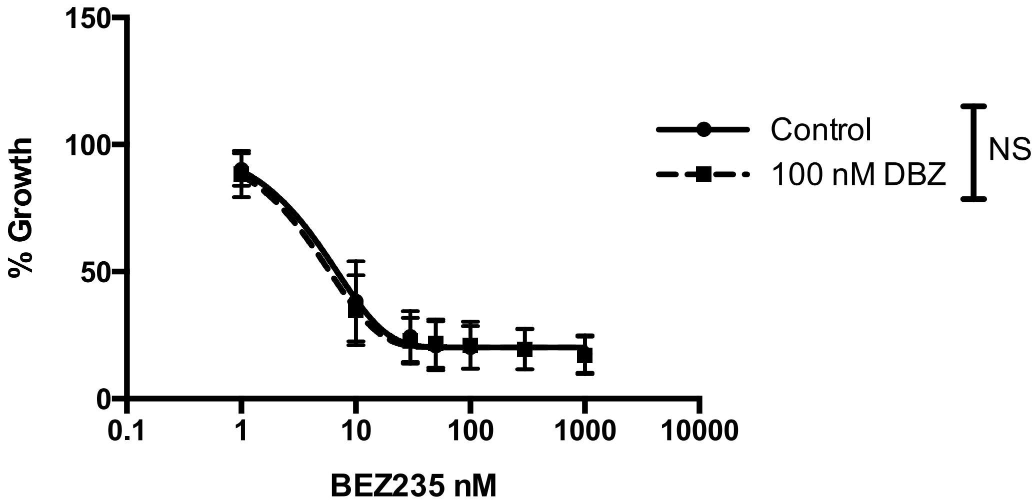


B

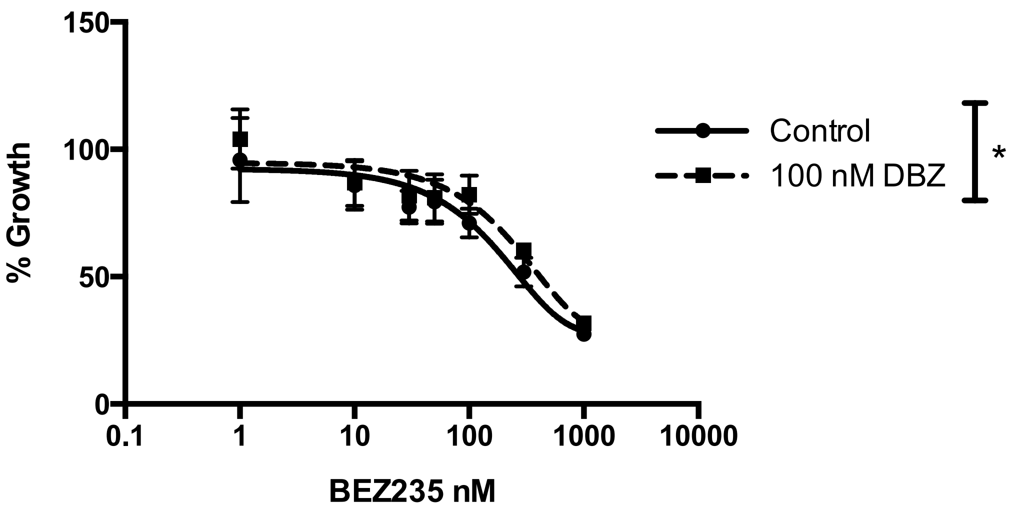


**Figure 4-19 DBZ does not sensitise BEZ235 resistant RCC cells**

CTG cell viability assays of A) RCC4S and B) RCC4B20 cells. After seeding 500 cells per well into 96 well plates, cells were left to adhere overnight, and 24 hours later solvent or 100 nM DBZ was applied. Following 24 hours incubation, the indicated concentration of BEZ235 was added. Graphs show mean and SEM of six data points from two independent assays. NS $P>0.05$, * $P=0.0324$ by two way ANOVA.

Notch 1 has been suggested as a potential mediator of resistance to mTORC1 inhibition on the basis that in renal cancer Notch signalling has been shown to decrease PTEN expression and increase pAKT (Liu et al. 2013c, Santoni et al. 2014). The data presented here would not support the hypothesis as a mediator of resistance to mTOR inhibition and the microarray did not show increased PTEN expression. There is other evidence that mTOR inhibition alters the expression of Notch pathway members, where in colorectal cancer, the use of the mTORC kinase inhibitor Torin 1 decreased mRNA levels of Notch and DLL4 (Francipane and Lagasse 2013). However, in this study in renal cancer, there was no change in Notch or DLL4 mRNA level on acute treatment with BEZ235. There is interest in mTOR and Notch inhibition as a treatment combination in leukaemia, where mTOR inhibition has been noted to influence Notch expression (Ono et al. 2013), and the reverse relationship has been seen in acute myeloblastic leukaemia, where Notch increases the expression of mTOR (Okuhashi et al. 2013). It appears clear therefore that the two pathways are linked such that Notch signalling can increase mTOR, and mTOR can decrease Notch expression, but functional relevance of this link is not clear.

In this study, experiments using DBZ suggested that suppressing Notch pathway activity did not influence BEZ235 resistance. It is possible that the increased expression of Jagged 1 seen in RCC4B20 cells was not part of a resistance mechanism, but rather a response to chronic BEZ235 exposure. This could be assessed by investigating Jagged 1 levels in BEZ235 sensitive cells over more prolonged exposure to BEZ235, e.g. 24 - 72 hours. An alternative explanation for the inability of DBZ to sensitise to BEZ235 could be that DBZ was not active for the duration of the viability assays, as this was not tested beyond 24 hours. Although it is possible that this could influence the response or lack of it, even if DBZ were only active for a part of the duration of a cell viability assay, there may still be some effect on total cell viability.

## 4.3 Discussion

RCC4 and 786-0 BEZ235 resistant cells were successfully created by continuous culture in BEZ235. Both cell lines showed cross-resistance to an alternative mTOR kinase inhibitor AZD2014, adding weight to the hypothesis that the resistance was directed to mTORC kinase inhibition rather than specifically to BEZ235. This increases the potential clinical impact of this work. The 786-0B200 subline showed some evidence of cross resistance to alternative inhibitors of the PI3-K – mTOR pathway. In contrast, the resistance in RCC4B20 appeared to be more specific to mTOR kinase.

Two large scale screens, at the level of protein expression and activation, and at the mRNA level, failed to identify resistance mechanisms, although correlates of resistance were noted in MET, Abl, MEK/ERK and the Notch pathway. It is interesting that the protein level screen was performed because it was hypothesised that mTOR inhibition could alter protein levels via effects on translation, without affecting gene transcription, and in fact none of the potential hits on the antibody array were identified as potential hits in the microarray screen.

It would be interesting to make further effort to achieve more robust Abl inhibition in 786-0B200 cells, and to confirm Abl inhibition in RCC4B20 cells in order to more robustly characterise the potential role of Abl in BEZ235 resistance in CCRCC.

The Full Moon antibody array did not detect any mediators of resistance to BEZ235. Furthermore, the array did not identify numerous expected changes in acutely treated sensitive cells, e.g. reduction in pAKT S473, pS6 and p4E-BP1, which were routinely detected by western blotting. This raised questions about the sensitivity and specificity of the antibody array to detect significant changes. All the antibodies on the array were proprietary and not independently validated in my work. It may have been that the antibodies themselves lacked sensitivity and specificity for the epitopes they were claimed to recognise. It was also possible that results in antibodies to non-denatured proteins differ to antibodies against denatured proteins by western blotting. Full Moon Biosystems claim that results by western blotting to validate the antibody array often have a larger magnitude of change, which would further support the lack of sensitivity of their system. Finally, the prospect of antibody array false negatives, whereby a protein binding-partner obscures the epitope recognised by the Full Moon antibody, is a very real possibility that may have further reduced the sensitivity of the screen.

The microarray screen produced a much larger number of differentially expressed potential mediators of resistance, and only the Notch pathway members were investigated. Therefore, it is entirely possible that genuine mediators of resistance may have been identified in that screen, and await validation. It would be of interest to assess Notch pathway upregulation in the second model of BEZ235 resistance, the 786-0B200 cells.

It was worth noting that inhibitors of some of the hits from these screens have been tested with mTOR inhibitors in other cancers or cellular contexts and have shown functional relevance (Masiello et al. 2007, Migliardi et al. 2012, Liu et al. 2013b, Renshaw et al. 2013, Imura et al. 2014, Qu et al. 2014, Zeng et al. 2014). The reasons why these same targets do not appear to show the same relevance in this RCC model remain elusive, and biomarkers that predict for successful combinations of drugs are very much still needed.

The breadth of the potential hits, and the failure of numerous attempts to sensitise to BEZ235 with the addition of single target compounds raises the distinct possibility that great redundancy exists with the pathways that mediate proliferation and protect from apoptosis.

# 5 Results 3: mTOR kinase resistance was associated with increased p4E-BP1 and partially mediated by RAPTOR upregulation

## 5.1 Introduction

The unbiased screens of BEZ235 resistant cells identified correlates, but not mediators of resistance. In addition to this approach, a hypothesis led approach was also taken. In order to generate hypotheses, the BEZ235 resistant cells were further characterised.

When Sharma reported "drug tolerant persister" cells surviving high concentrations of erlotinib, and showing resistance to re-challenge with erlotinib, the cells were shown to express cancer stem cell markers CD133 and CD24 (Sharma et al. 2010). When these cells were removed from culture in erlotinib, they quickly regained their erlotinib sensitivity. The resistant cells were found to have upregulated histone demethylase KDM5A and manipulation of KDM5A expression by knockdown or overexpression altered drug sensitivity and the development of resistance. Because KDM5A associates with histone deacetylases (DHAC)(Klose et al. 2007), they tested the ability of the HDAC inhibitor (HDACi) trichostatin to influence resistance. Trichostatin was able to reverse established resistance, and prevent the development of resistance, while not affecting the growth of parental (non-resistant) cells (Sharma et al. 2010).

Based on these observations, the next experiments tested for persistence of BEZ235 resistance after removal from drug. If the BEZ235 resistant cells were to lose their resistance, the implications would be two-fold: a potential mechanism for resistance would be suggested in the form of epigenetic modification as seen by Sharma et al., and the re-sensitised cells would provide an additional, useful control with which to examine signalling changes along the PI3K – AKT – mTOR pathway. Any signalling changes seen in BEZ235 resistant cells would only be considered possible contributors to BEZ235 resistance if they were not seen in BEZ235 re-sensitised cells.

## 5.2 Results

### 5.2.1 Withdrawal of BEZ235 from resistant cells

The BEZ235 resistant cells were created by continuous culture in drug, and their resistance was maintained by culture in BEZ235, but it was unknown whether it was necessary to continue this process to retain resistance. The previous work in chapter 4 showed that RCC4B20 and 786-0B200 cells retained their resistance during the 72 hour washout period that was necessary in order to retest their resistance, but it was unknown whether the resistance phenotype would be maintained if this period was extended.

Therefore, RCC4B20 cells had their medium exchanged for solvent control containing medium, and their resistance to BEZ235 was tested over the following weeks. These cells were termed RCC4B20-S. Over 8 weeks RCC4B20-S cell progressively lost their resistance to BEZ235, both in terms of $GI_{50}$ and resistant population (Figure 5-1 A). During this time there was an increase in the baseline proliferation rate as evidenced by routine splits during passaging. Whereas RCC4B20 cells were split 1:5 every week, RCC4B20-S cells increased their proliferation rate to require a 1:20 split every week after approximately 3 months growing in control medium.

After three months growing in solvent, RCC4B20-S cells were also tested for cross-resistance to AZD2014. This showed that as well as losing resistance to BEZ235, RCC4B20-S cells had also lost their resistance to AZD2014 (Figure 5-1 B).

A

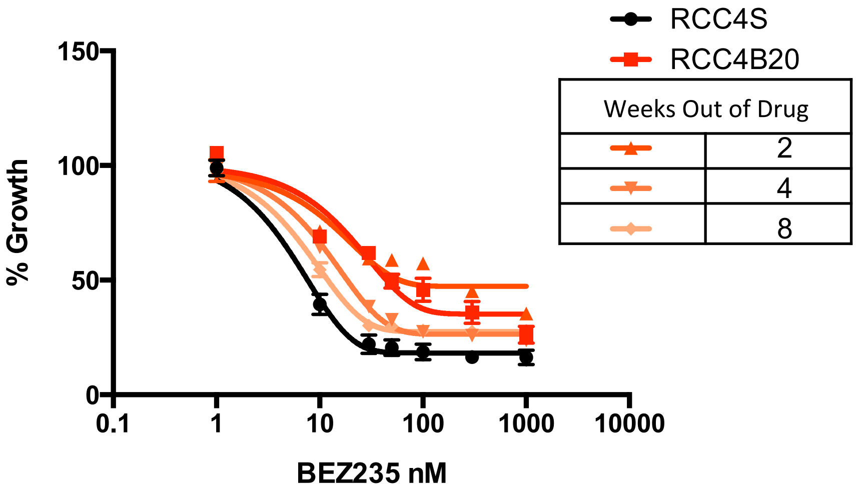


| Weeks out of drug | $GI_{50}$ nM (95% CI) | Resistant Population % (95% CI) |
|---|---|---|
| **RCC4S** | 8 (7 – 9) | 18 (16 – 21) |
| **RCC4B20** | 44 (33 – 58) | 35 (29 – 41) |
| **2** | 59 (37 – >1000) | 47 (42 – 53) |
| **4** | 18 (17 – 20) | 26 (25 – 28) |
| **8** | 12 (11 – 13) | 28 (26 – 29) |

B

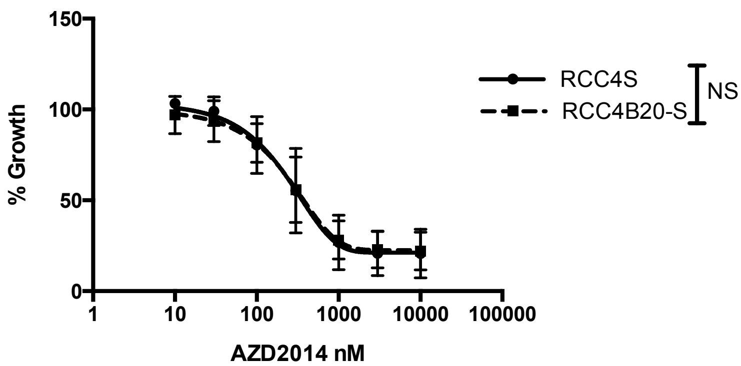


| Cell Line | $GI_{50}$ nM (95% CI) | Resistant Population % (95% CI) |
|---|---|---|
| **RCC4S** | 359 (235 – 548) | 21 (11 – 32) |
| **RCC4B20-S** | 376 (258 – 549) | 23 (14 – 31) |

**Figure 5-1 RCC4B20 cells lose BEZ235 resistance after withdrawal of BEZ235**

A) RCC4B20 cells were removed from 20 nM BEZ235 and grown in solvent control medium (RCC4B20-S). At the indicated number of weeks post removal from drug, sensitivity was tested by CTG cell viability assay. Graph shows serial CTG cell viability assays with mean and SEM of triplicate wells shown, table shows $GI_{50}$ and resistant populations. B) CTG cell viability assay of RCC4S and RCC4B20-S, after at least 3 months growing in solvent, treated with AZD2014. Graph shows mean and SEM of three independent experiments. NS $p>0.05$ by two way ANOVA. Table shows $GI_{50}$ and resistant populations of cells.

The same experiment was conducted in 786-0B200 cells, withdrawing BEZ235 and replacing it with solvent control (cells termed 786-0B200-S). Serial cell viability tests over the following weeks showed that these 786-0B200-S cells retained their resistance to BEZ235, both in terms of $GI_{50}$ and the resistant population (Figure 5-2 A). This was a different response from that seen in RCC4B20 cells. However, the response to BEZ235 withdrawal in terms of baseline proliferation rate was similar between the two cell lines: 786-0B200-S cells also increased their proliferation rate in culture. While 786-0B200 were passaged weekly, with a 1:5 split, 786-0B200-S cells increased their proliferation rate, and after three months required a weekly 1:30 split.

After at least six months of culture in solvent control medium, 786-0B200-S cells were tested to determine whether they had also retained resistance to AZD2014. Cell viability assays revealed that while 786-0B200-S cells were still resistant to AZD2014, the magnitude of resistance in terms of $GI_{50}$ and resistant population was less than in 786-0B200 cells (Figure 4-6 B and Table 4-1 compared to Figure 5-2 B). This variation in the retention of resistance to BEZ235 and AZD2014 is interesting to note. Resistance to BEZ235 remained the same at 5 months after withdrawal of BEZ235, while AZD2014 resistance was assessed at 6 months post withdrawal of BEZ235. Given the stability in retention of BEZ235 (Figure 5-2 A) it seems unlikely that this difference in resistance of 786-0B200-S cells could be due to the one month interval between testing resistance to BEZ235 and AZD2014.

A

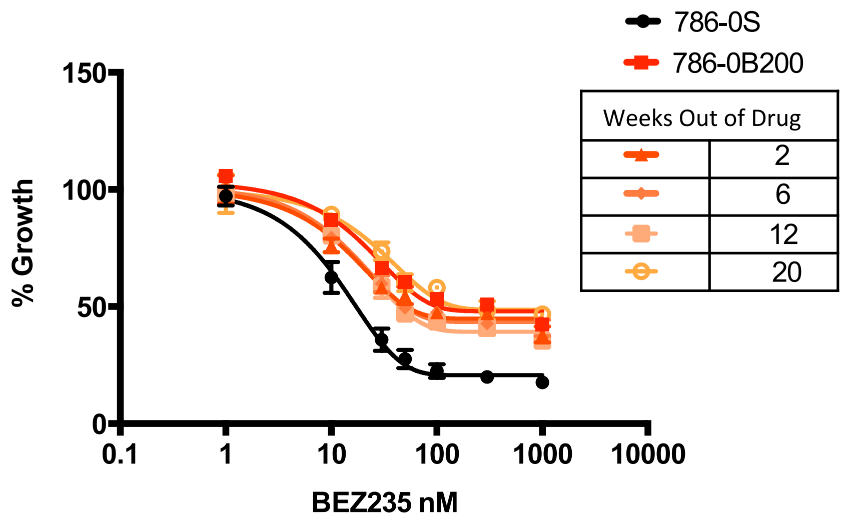


| Weeks out of drug | $GI_{50}$ nM (95% CI) | Resistant Population % (95% CI) |
|---|---|---|
| **786-0S** | 17 (16 – 19) | 21 (19 – 23) |
| **786-0B200** | 101 (19 – >1000) | 48 (45 – 51) |
| **2** | 51 (41 – 66) | 45 (42 – 48) |
| **6** | 50 (42 – 59) | 43 (41 – 46) |
| **12** | 45 (38 – 52) | 39 (36 – 42) |
| **20** | 149 ( 107 – >1000) | 49 (43 – 52) |

B

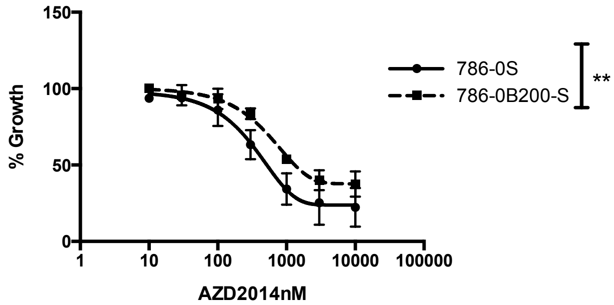


| Cell Line | $GI_{50}$ nM (95% CI) | Resistant Population % (95% CI) |
|---|---|---|
| **786-0S** | 517 (370 – 723) | 24 (16 – 32) |
| **786-0B200-S** | 1320 (1023 – 1680) | 38 (32 – 43) |

**Figure 5-2 786-0B200 cells retain BEZ235 resistance after withdrawal of BEZ235**

A) 786-0B200 cells were removed from 200 nM BEZ235 and grown in solvent control medium (786-0B200-S). At the indicated number of weeks post removal from drug, sensitivity was tested by CTG cell viability assay. Graph shows serial CTG cell viability assays with mean and SEM of triplicate wells, table shows $GI_{50}$ and resistant populations. B) CTG cell viability assay of 786-0S and 786-0B200-S, after at least 6 months growing in solvent, treated with AZD2014. Graph shows mean and SEM of three independent experiments. ** p=0.0023 by two way ANOVA. Table shows $GI_{50}$ and resistant populations of cells.

### 5.2.2 BEZ235 resistant CCRCC cells show differences in signalling in the mTOR pathway

After the characterisation of their resistance and cross-resistance patterns, and re-sensitisation, the next experiments examined signalling along the PI3K – AKT – mTOR pathway to identify any changes that may be associated with the resistance. The acute effect of BEZ235 in the control RCC4S and 786-0S cells was compared to the signalling in RCC4B20 and 786-0B200 cells that were cultured in continuous BEZ235. Acute treatment was conducted over 1 hour, by medium exchange, to match the previous experiments with BEZ235 (Figure 3-13). In order to examine the signalling of the resistant cells cultured in continuous BEZ235, no drug washout period was used, but in order to match the conditions of control cells, fresh medium containing BEZ235 was applied to cells, one hour pre-harvest, to match the controls in terms of supplying fresh medium with growth factors, and nutrients. This experiment showed that there was evidence of persistent mTORC1 blockade of pS6 in both RCC4B20 and 786-0B200 cells (Figure 5-3 A). This is important, as it suggests that BEZ235 was still active within the resistant cells, and suggested that drug export was an unlikely contributor to resistance. The other mTORC1 target, 4E-BP1, showed different patterns in the two cell lines. In 786-0B200 cells, 4E-BP1 phosphorylation followed the pS6 pattern and remained suppressed. However, in the RCC4B20 cells there was evidence of increased 4E-BP1 phosphorylation to a level intermediate between the high basal level and the acutely treated level seen in RCC4S cells (Figure 5-3 A).

There were minor differences in mTORC2 activity between the two resistant cell lines. The RCC4B20 cells showed increase in S473 AKT phosphorylation, above baseline levels in RCC4S cells, indicating not just re-activation, but a level of activation above baseline. The resistant 786-0B200 cells, showed some evidence of re-phosphorylation of AKT S473, although this did not reach the levels seen in untreated 786-0S cells.

Similar responses were seen to the alternative mTORC kinase inhibitor AZD2014 (Figure 5-3 B). For this experiment, both of the resistant cell lines were given a 72 hour washout period from BEZ235 in order to assess the effects of AZD2014 alone, without being complicated by residual effects of BEZ235. In both resistant cell lines AZD2014 induced complete suppression of pS6, but in RCC4B20 cells there was evidence of moderate re-phosphorylation of 4E-BP1, suggesting that the effects on mTORC1 were broadly the same in response to both mTORC kinase inhibitors. The effects of AZD2014 were different from those of BEZ235 on mTORC2 activity when examined in RCC4B20 cells, with AZD2014 blocking re-phosphorylation of S473 on AKT. In 786-0B200 cells there was less of a reduction in pAKT S473 in response to acute AZD2014 than in 786-0S cells.

The previous experiments in chapter 4 testing patterns of cross-resistance had shown that 786-0B200 cells were more sensitive to the AKT inhibitor AZD5363 (fold change of $GI_{50}$ 1.9). RCC4B20 cells were also more sensitive to the AKT inhibitor AZD5363 (fold change in $GI_{50}$ 2.4). This suggested that the increased level of pAKT S473 possibly contributed to resistance to mTORC inhibition. The relatively minor ~ 2-fold sensitisation to AKT inhibition suggested that this mechanism was unlikely to be a significant contributor to the resistance phenotype seen in RCC4B20 and 786-0B200 cells (Figure 4-6 G and H).

The RCC4B20-S cells that had regained sensitivity to BEZ235 and AZD2014 were assessed, in an attempt to identify changes that tracked with the acquisition and loss of resistance. While not providing proof of a causative relationship between the observed change and resistance, if the change were to persist in the re-sensitised RCC4B20-S cells, then that would constitute evidence against the hypothesis of a causative relationship. The next experiment assessed RCC4B20-S cells treated for one hour with solvent or 20 nM BEZ235, comparing with RCC4S cells treated with the same drugs, and RCC4B20 cells treated with fresh 20 nM BEZ235 (with medium change, but no prior drug washout). It was observed that RCC4B20-S cells had reverted to the low level of p4E-BP1 seen in RCC4S cells in response to mTOR inhibition (Figure 5-3 C). It was also noted that the levels of pAKT S473 had reverted to the sensitive RCC4S pattern. As discussed above, the contribution of AKT to mTOR kinase inhibition was thought to be minor, but the contribution of 4E-BP1 warranted further investigation.

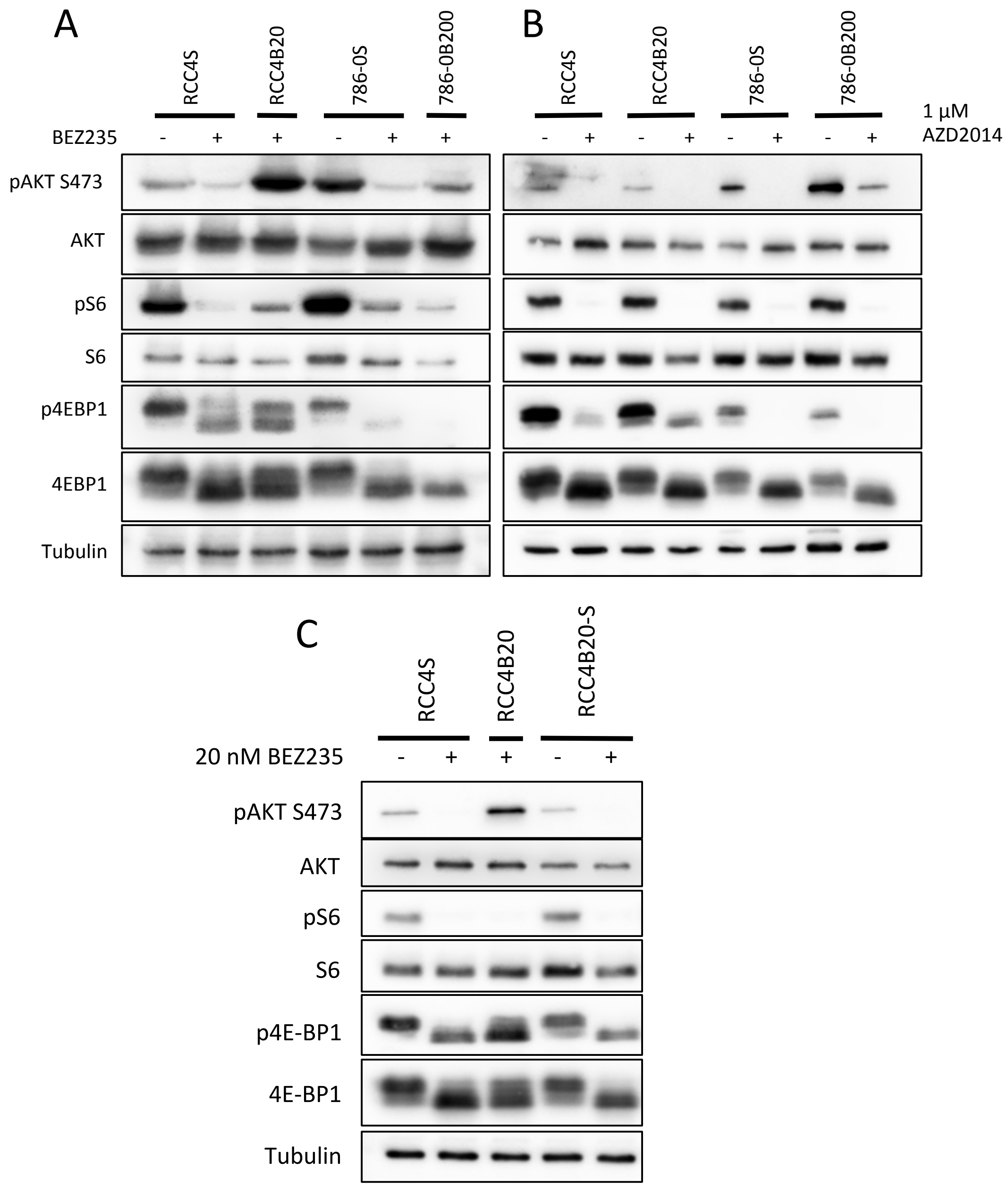


**Figure 5-3 Levels of p4E-BP1 track with resistance and re-sensitisation in RCC4 cells**

A) Monolayer RCC4S cells were treated with 20 nM BEZ235 or solvent control for 1 hour. RCC4B20 cells were treated with fresh 20 nM BEZ235 for 1 hour (there was no drug washout period). 786-0S cells were treated with 200 nM BEZ235 or solvent control for 1 hour. 786-0B200 cells were treated with fresh 200 nM BEZ235 for 1 hour (there was no drug washout period). Cell lysates were analysed by SDS PAGE. Similar results were seen in two independently prepared sets of lysates. B) RCC4B20 and 786-0B200 cells were grown in drug free media for at least 72 hours before being treated with solvent or 1 µM AZD2014 for 1 hour. RCC4S and 786-0S cells were treated with solvent or 1 µM AZD2014 for 1 hour. Cell lysates were analysed by SDS PAGE. Similar results were seen in an independently prepared set of cell lysates. C) RCC4S and RCC4B20-S were treated with solvent or 20 nM BEZ235 for 1 hour. RCC4B20 cells were treated with fresh 20 nM BEZ235 for 1 hour (there was no drug washout period). Cell lysates were analysed by SDS PAGE. Similar results were seen in two independently prepared sets of cell lysates.

### 5.2.3 Investigating the re-phosphorylation of 4E-BP1

It was interesting to note that in RCC4B20 cells, phosphorylation of the mTORC1 substrate 4E-BP1 correlates with resistance in this model of acquired resistance in renal cancer, as p4E-BP1 has also previously been shown to correlate with primary resistance to mTOR inhibition in a variety of cancer cell lines including the colorectal cell lines SW620, COLO205, HCT116, HCT15 and SW48 (Zhang and Zheng 2012, Ducker et al. 2013). The 786-0B200 cells in contrast do no not show, increased p4E-BP1, but knowledge of the mechanism of action of 4E-BP1 suggests that resistance could still be through downstream activation of this pathway. It is known that 4E-BP1 binds and sequesters the initiation of translation factor 4E (eIF4E) thus reducing cap-dependent translation. When 4E-BP1 is phosphorylated, this binding is inhibited, and cap dependent translation proceeds (Pause et al. 1994, Tait et al. 2010) (Figure 1-2). The extent to which 4E-BP1 is dephosphorylated by mTOR inhibition is therefore a marker of the extent to which translation is inhibited. However, the degree of phosphorylation of 4E-BP1 is not the sole determinant of eIF4E activity, which can also be influenced by the relative abundance of 4E-BP1 and eIF4E. This was shown in a model of induced resistance to the mTORC kinase inhibitor PP242, where liver cancer cell lines became drug-resistant through decreased expression of total 4E-BP1, which, even when unphosphorylated, was insufficient to bind all eIF4E and was therefore unable to prevent translation. Furthermore, manipulating the ratio of 4E-BP1 to eIF4E altered sensitivity to multiple mTORC kinase inhibitors (Alain et al. 2012).

Both eIF4e and 4E-BP1 have been linked to tumour progression in human cancers, as has the ratio of eIF4E to 4E-BP1. In breast cancer, increased p4E-BP1 correlates with higher grade and stage as well as independently correlating with a worse prognosis (Armengol et al. 2007). Interestingly, the ratio of p4E-BP1 to total 4E-BP1 also correlated with tumour grade, and it was noted that in grade 3 tumours that lacked 4E-BP1 phosphorylation, eIF4E was over expressed with respect to 4E-BP1 as measured by immunohistochemistry. In human prostate, areas of high grade prostatic neoplasia in situ with high p4E-BP1 were more likely to progress to invasive prostate cancer (Armengol et al. 2007).

eIF4E has been shown to have an important role in tumorogenesis both *in vitro* and clinically, being capable of causing malignant transformation of rodent fibroblasts and human mammary epithelial cells (Lazaris-Karatzas et al. 1990, Avdulov et al. 2004). eIF4E is overexpressed in many cancer types, and has been associated with worse prognosis, or lymph node metastasis in cancers of the stomach, colon, breast, penis, bladder, head and neck, lung and cervix (Nathan et al. 1997a, Nathan et al. 1997b, Crew et al. 2000, Seki et al. 2002, Lee et al. 2005, Ferrandiz-Pulido et al. 2013, Heikkinen et al. 2013, Niu et al. 2014, Tapia et al. 2014).

In light of the established data on the importance of eIF4E expression and the ratio of 4E-BP1 to eIF4E, RCC4B20 and 786-0B200 cells were assessed for the expression of eIF4E. In neither cell line was increased eIF4E observed, and there were no convincing differences in total 4E-BP1 (Figure 5-4).

Other groups have noted increases in eIF4E in models of mTORC kinase inhibition, including a colon cancer model resistant to AZD8055 where resistance was caused by increased expression and phosphorylation of eIF4E (Cope et al. 2014). BEZ235 resistance in human mammary epithelial cells was associated with *eIF4E* amplification and resistance induced by introduction of mutant *PIK3CA* was associated with *MYC* amplification, known to induce expression of eIF4E (Jones et al. 1996, Ilic et al. 2011). The lack of change in eIF4E and 4E-BP1 expression suggests that the mechanism of resistance in RCC4B20 and 786-0B200 cells appears to be different from that found other models.

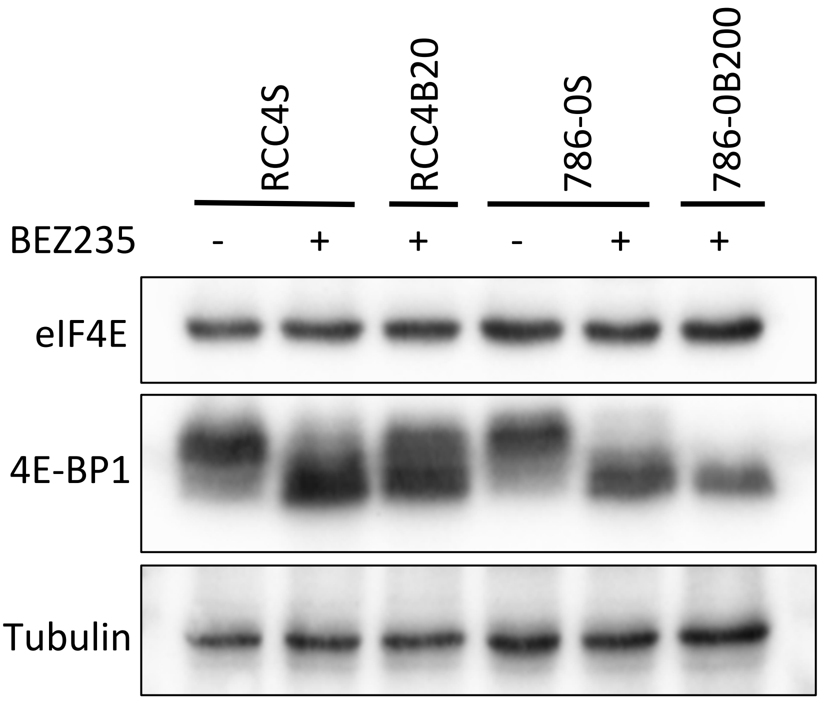


**Figure 5-4 The Levels of 4E-BP1 and eIF4E do not change in BEZ235 resistant cells**

RCC4S cells were treated with solvent, or 20 nM BEZ235 for 1 hour. RCC4B20 cells were treated with fresh 20 nM BEZ235 for 1 hour (no drug washout). 786-0S cells were treated with solvent or 200 nM BEZ235 for 1 hour. 786-0B200 cells were treated with fresh 200 nM BEZ235 (no drug washout). Cell lysates were analysed by SDS PAGE. Similar results were seen in another set of independently prepared cell lysates.

There are a number of mechanisms shown to regulate activation of cap dependent translation via control of the 4E-BP1 – eIF4E interaction, and they were worthy of consideration as to whether they could contribute to resistance in RCC4B20 and 786-0B200 cells. The first is through the alteration in the 4E-BP1:eIF4E ratio as discussed above, as this could explain resistance in 786-0B200 cells despite on-going suppression of p4E-BP1. Secondly it is worth considering that the phosphorylation of 4E-BP1 results from the balance between kinase and phosphatase activity. It is possible that changing expression or activity of phosphatases of 4E-BP1 could allow maintenance of p4E-BP1 in RCC4B20 cells. It is also worth considering the kinase. mTOR is the best characterised kinase to phosphorylate 4E-BP1, but the potential for other kinases to take over this role was worthy of consideration.

A recent report identified the metal-dependent protein phosphatase 1G (PPM 1G) as a phosphatase capable of dephosphorylating 4E-BP1 (Liu et al. 2013a). A second phosphatase that is capable of de-phosphorylating 4E-BP1 is the serine/threonine protein phosphatase 2A (PP2A) (Pham et al. 2000, Guan et al. 2007, Michlewski et al. 2008). PP2A exists as a heterotrimer, consisting of a catalytic C subunit, a structural A subunit and a regulatory B subunit (Schonthal 2001, Seshacharyulu et al. 2013). While A and C subunits are ubiquitously expressed, B subunits are expressed in a tissue and developmental stage specific manner (McCright et al. 1996). PP2A acts as a serine threonine phosphatase for numerous targets including AKT (Kuo et al. 2008, Li et al. 2012a), and may have tumour suppressor qualities, as in HEK293 cells, its depletion was transforming (Chen et al. 2005).

To pursue the possibility of altered expression of phosphatases, levels of PPM1G and the C subunit of PP2A were assessed by western blot. However, levels did not change in either RCC4B20 or 786-0B200 cells compared to their parental sensitive cell line pairs (Figure 5-5).

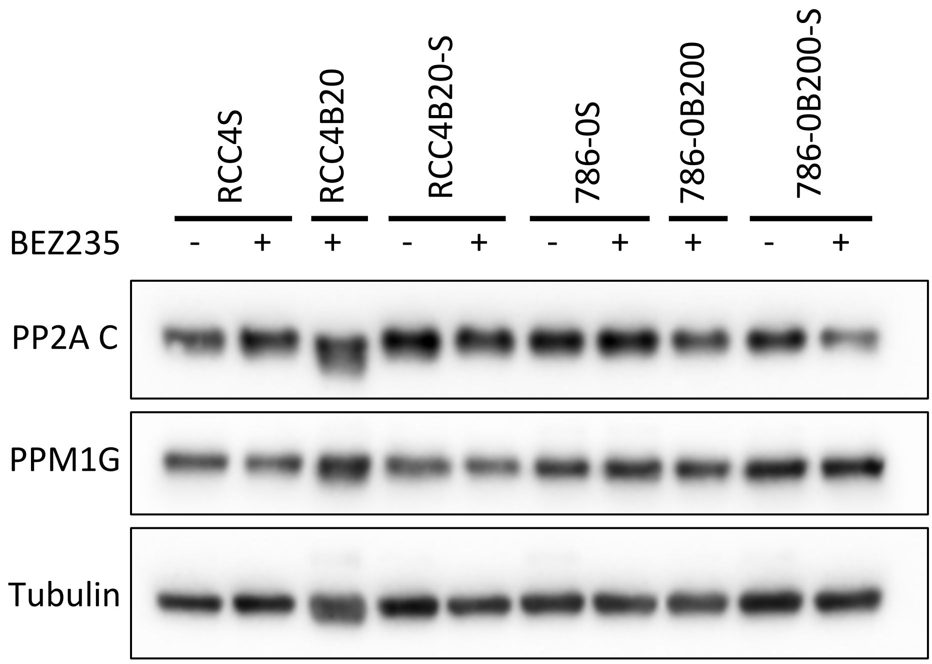


**Figure 5-5 The levels of 4E-BP1 phosphatases PP2A C and PPM1G do not change in BEZ235 resistant cells**

RCC4S cells were treated with solvent, or 20 nM BEZ235 for 1 hour. RCC4B20 cells were treated with fresh 20 nM BEZ235 for 1 hour (no drug washout). 786-0S cells were treated with solvent or 200 nM BEZ235 for 1 hour. 786-0B200 cells were treated with fresh 200 nM BEZ235 (no drug washout). RCC4B20-S cells were treated as RCC4S cells and 786-0B200-S cells were treated as 786-0S cells. Cell lysates were analysed by SDS PAGE. Similar results were seen in another set of independently prepared cell lysates.

The next experiments aimed to identify whether mTOR was the kinase responsible for the increased 4E-BP1 phosphorylation seen in RCC4B20 cells. Assessment of the abundance of the mTOR complex 1, could not be done by detecting relative levels of mTOR protein, because mTOR can be present in both mTORC1 and mTORC2 complexes. Instead, the unique binding partner regulatory-associated protein of mTOR (RAPTOR) was quantified to assess the relative abundance of mTORC1. Initial use of the RAPTOR antibody CS #2280 (Cell Signalling Technology) did not produce a clean band, so to verify that RAPTOR was being detected, a knockdown experiment was performed, which confirmed the presence of a band at the predicted 150 kDa in control (Allstars) transfectants that was reduced by RAPTOR siRNA. This revealed that RCC4B20 cells expressed higher levels of RAPTOR than the sensitive RCC4S cells (Figure 5-6).

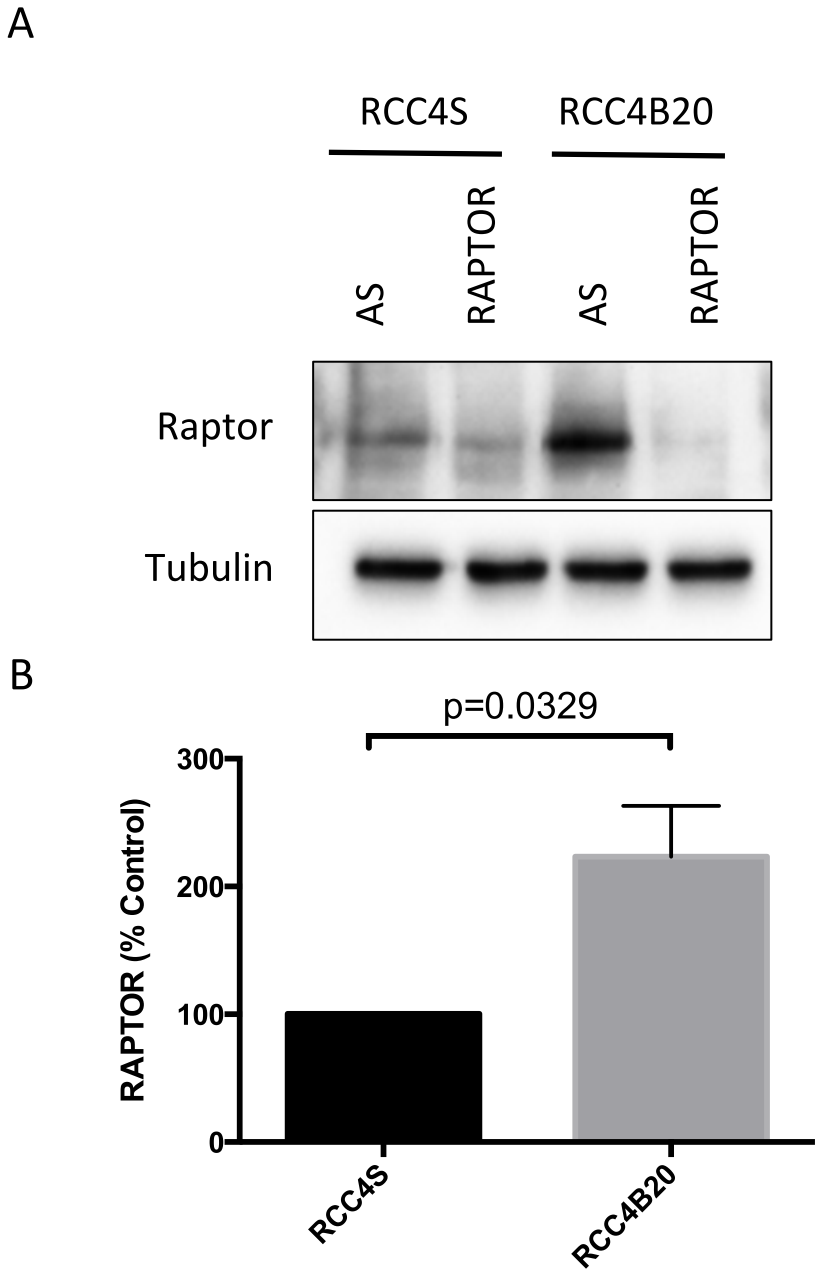


**Figure 5-6 The level of RAPTOR increases in resistant cells**

A) RCC4S cells were reverse transfected with allstars (AS) control siRNA or Raptor siRNA. After 72 hour drug washout, RCC4 B20 cells were transfected with the same siRNA. Cell lysates were collected after 60 hours and analysed by SDS PAGE. B) RAPTOR levels were quantified using ImageJ and corrected for tubulin loading, then expressed as a percentage of RCC4S levels. Graph shows mean and SEM for three independent sets of lysates and t-test p value.

The increased expression of RAPTOR suggested that more cellular mTOR protein could be contained in mTORC1 complexes and raised the possibility that mTOR itself was phosphorylating 4E-BP1 in RCC4B20 cells despite its activity towards S6 remaining blocked. It was also possible that increased RAPTOR was a passenger rather than a driver of resistance, and as postulated above, an alternative kinase could be taking over the role. Several other candidate 4E-BP1 kinases have been proposed including cyclin dependent kinase cdc2 (Heesom et al. 2001), ERK (Herbert et al. 2002), ataxia telangiectasia mutated (ATM) (Yang and Kastan 2000), and leucine-rich repeat kinase 2 (LRRK2) (Imai et al. 2008). It is worth noting that ERK was not shown to directly phosphorylate 4E-BP1 *in vitro*, and has known mTOR-stimulating function via the phosphorylation and inhibition of TSC2 (Ma et al. 2005). This raises doubt as to whether ERK activation could be causing phosphorylation of 4E-BP1 independently of mTORC1.

Several approaches were taken to address this question of the contribution of mTORC1 in phosphorylating 4E-BP1. If it could be shown that targeting mTORC1 in an alternative manner was able to decrease p4E-BP1 in BEZ235-treated RCC4B20 cells, then it would be less likely that another kinase was involved. This approach could also assess the contribution of p4E-BP1 to resistance.

The first approach was to deplete cells of RAPTOR through siRNA knockdown. This would disrupt the mTORC1 complex and had the potential to block the kinase activity of mTOR by doing so. In RCC4S cells RAPTOR depletion was detected at 48-72 hours after siRNA transfection (Figure 5-7 A). There was a small reduction in p4E-BP1 levels, only at the 72 hour time-point. In RCC4B20 cells, the siRNA transfection was conducted in the absence of BEZ235, and 20nM BEZ235 was included in the medium exchange at 6 hours, in order to detect any effect of RAPTOR knockdown on p4E-BP1 phosphorylation in the presence of BEZ235. As in control cells, RAPTOR was depleted in RCC4B20 cells at 48-72 hours (Figure 5-7 A). At 48 and 72 hours there was a small reduction in p4E-BP1 compared to control knockdown. In contrast, pAKT levels in RCC4B20 were increased by at 24-48 hours by RAPTOR knockdown, suggesting that RAPTOR knockdown was not inhibiting mTORC2 function. It is possible that this increase in pAKT could be due to relief of the feedback loops between mTOR, S6 and AKT that were examined in chapter three (Figure 3-2, Figure 3-7, Figure 3-15 and Figure 3-17).

Having seen that RAPTOR knockdown had at least some effect on 4E-BP1 phosphorylation in BEZ235-treated RCC4B20 cells, the effects on sensitivity to BEZ235 were assessed by cell viability assay (Figure 5-7 B and C). In RCC4S cells RAPTOR depletion induced minor sensitisation to BEZ235, with a 2 fold change in BEZ235 $GI_{50}$, not reaching statistical significance by two way ANOVA. RCC4B20 cells however showed a more marked shift in the BEZ235 response curve, with a 20 fold reduction in $GI_{50}$, which is very close to the degree of resistance that was present between RCC4S and RCC4B20 cells. The resistant population of cells however did not shift with RAPTOR knockdown, and the maximal growth inhibition that was achieved was to 45% of untreated controls (Figure 5-7 C and D).

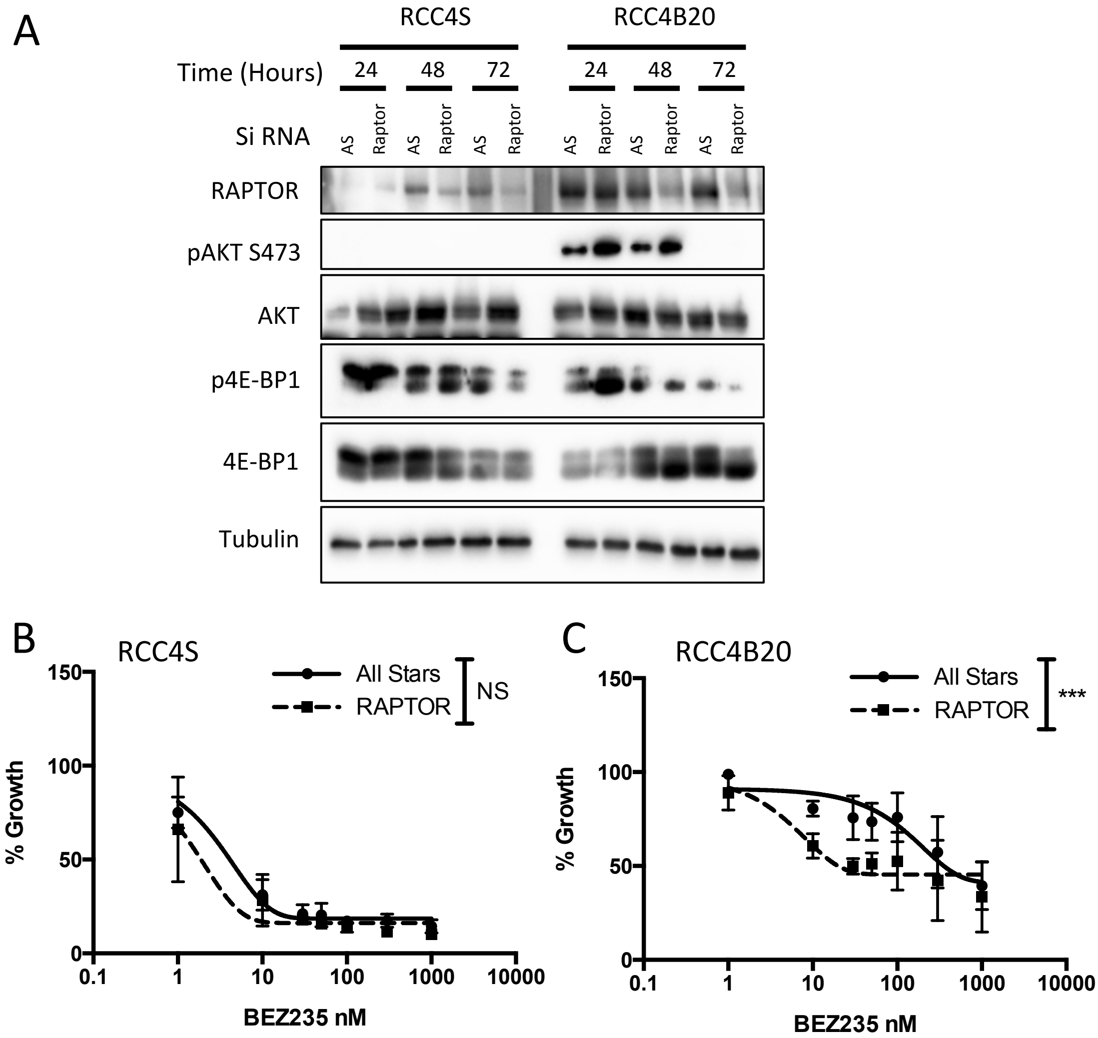


D

| Cell Line | $GI_{50}$ AS nM (95% CI) | $GI_{50}$ RAPTOR nM (95% CI) | Fold Sensitisation (95% CI) |
|---|---|---|---|
| RCC4S | 4 (3 – 5) | 2 (1 – 3) | 2 (1 – 5) |
| RCC4B20 | 355 (190 – >1000) | 18 (8 – >1000) | 20 (<5.2 – >125) |

**Figure 5-7 Raptor knockdown sensitizes BEZ235 resistant but not sensitive control RCC4 cells to BEZ235**

A) RCC4S and RCC4B20 cells were reverse transfected with RAPTOR or control siRNA. After 6 hour incubation with siRNA, solvent control medium was added to RCC4S cells, and 20 nM BEZ235 was added to RCC4B20 cells. Cells were collected and lysed at the indicated times and analysed by SDS-PAGE. Similar results were seen in three independently prepared sets of lysates. CTG cell viability assays of B) RCC4S and C) RCC4B20 cells treated with BEZ235. Cells were reverse transfected in 96 well plates with either control siRNA(All Stars) or RAPTOR siRNA. After 48 hours to allow RAPTOR depletion, BEZ235 was added at the indicated concentrations. Graphs show mean and SEM of three independent experiments. NS p>0.05, *** p=0.005 by two way ANOVA. D) Table of $GI_{50}$ concentrations for BEZ235 with control Allstars (AS) siRNA or RAPTOR knockdown.

These initial data from RAPTOR knockdowns suggested that mTORC1 was responsible for the sustained phosphorylation of 4E-BP1 in RCC4B20 cells, and that RAPTOR depletion could reverse some of the resistance that was seen. A second approach to target mTORC1 was made, using the allosteric mTOR inhibitor rapamycin. In BEZ235 sensitive cells it had previously been noted that rapamycin and BEZ235 together were better able to inhibit p4E-BP1, and that this caused greater growth inhibition (Figure 3-20 A and B). This may have been because the mechanisms of mTOR inhibition are different between rapamycin and BEZ235 (allosteric and kinase inhibitor respectively). Therefore the next step tested whether the same effects could be seen in BEZ235 resistant cells.

The first experiment assessed whether rapamycin could reduce BEZ235 resistant p4E-BP1 in RCC4B20 cells. RCC4B20 cells were given a 72-hour drug washout period before being treated with solvent, 20 nM BEZ235, 0.3 nM rapamycin, or the combination of rapamycin and BEZ235. RCC4S cells were given the same treatment, with the exception of not requiring a drug washout period. This revealed that in RCC4B20 cells, just as in RCC4S cells, rapamycin alone was ineffective at reducing p4E-BP1. As seen previously (Figure 5-3), BEZ235 caused a greater reduction in the levels of p4E-BP1 in RCC4S than in RCC4B20 cells. The combination of rapamycin and BEZ235 was effective in both cell lines at reducing p4E-BP1 to lower levels than either drug alone (Figure 5-8 A). This confirmed the results seen with RAPTOR knockdown (Figure 5-7 A), and strongly suggested that mTORC1 remained the primary kinase phosphorylating 4E-BP1.

Cell viability assays were performed of RCC4S and RCC4B20 cells, treating with BEZ235 alone or with 0.3 nM rapamycin. These assays revealed that rapamycin was able to sensitise cells to BEZ235 (Figure 5-8 B and C). In RCC4S cells, this was a relatively modest effect, showing a 4-fold sensitisation, but the response curves were not statistically significant by two way ANOVA. However, RCC4B20 cells were sensitised considerably with a 28-fold change in $GI_{50}$. Despite this change in $GI_{50}$, the total reduction in viability (i.e. the resistant population) was not affected by rapamycin. Therefore, these results mirror those of RAPTOR knockdown, and support the suggestion that regain of mTORC1 function is responsible for phosphorylation of 4E-BP1 in resistant cells, despite evidence that other functions of mTORC1 remain blocked, and that this accounts for some of the resistance that is seen. However, since neither rapamycin, nor RAPTOR depletion reversed BEZ235 resistance completely, it follows that there may be other mechanisms at work that contribute to the resistance, and experiments to address this were in presented in chapter 4, and the remainder of chapter 5.

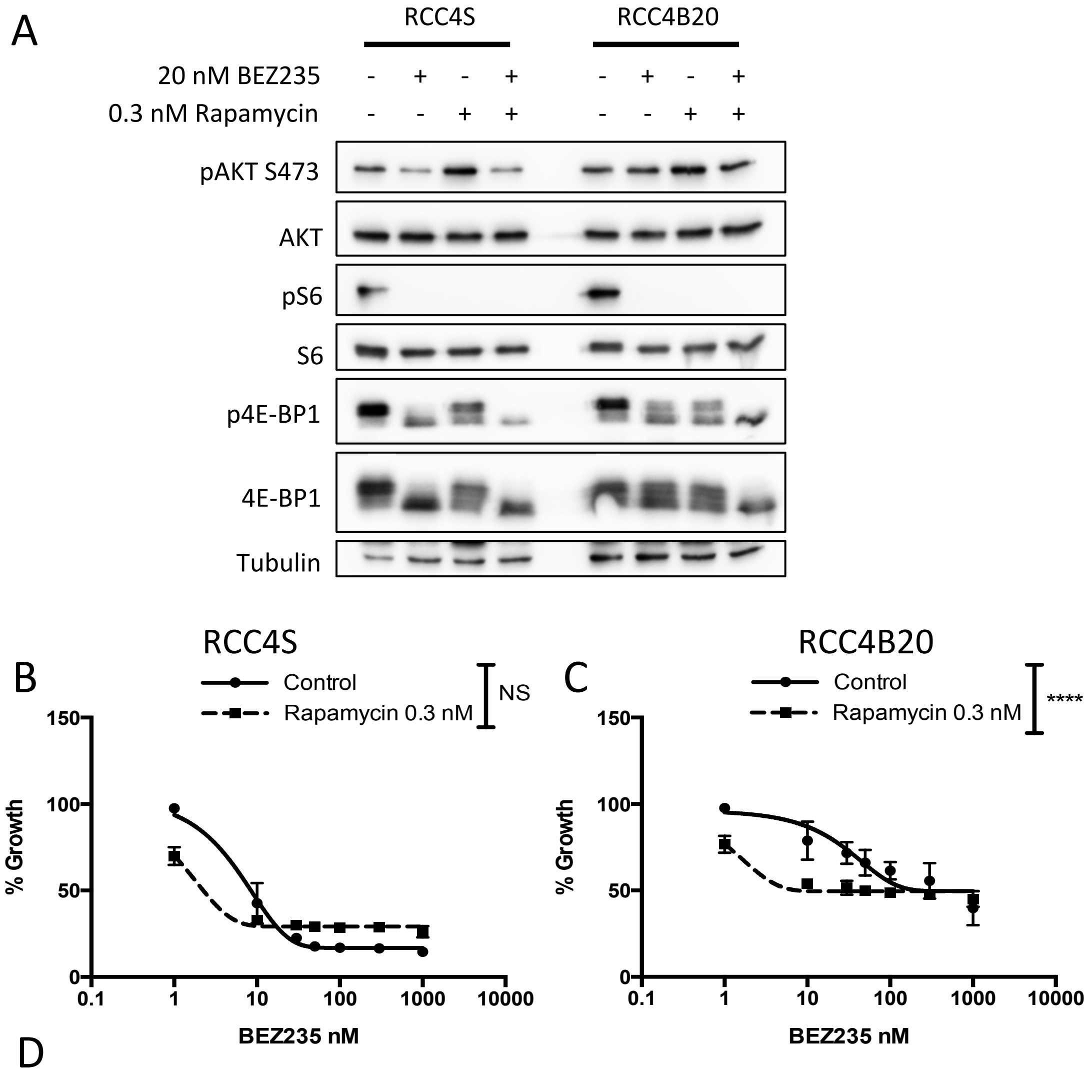


D

| Cell Line | GI50 Control nM (95% CI) | GI50 Rapamycin nM (95% CI) | Fold Sensitisation (95% CI) |
|---|---|---|---|
| **RCC4S** | 8 (7 – 10) | 2 (2 – 3) | 4 (3.5 – 5) |
| **RCC4B20** | 225 (81 – >1000) | 8 (4 – >1000) | 28 (12 – >250) |

**Figure 5-8 The addition of rapamycin to BEZ235 sensitizes resistant RCC4 cells to BEZ235**

A) Monolayer RCC4S and RCC4B20 cells were treated with solvent, 20 nM BEZ235, 0.3 nM rapamycin or the combination of BEZ235 and rapamycin. After 6 hours cells were collected, and lysates were analysed by SDS-PAGE and western blotting. Similar results were seen in another independent experiment. CTG cell viability assay of B) RCC4S and C) RCC4B20 cells treated with BEZ235 and solvent, or BEZ235 and rapamycin. Graphs show mean and SEM of six individual data points from two independent experiments. NS $p>0.05$, **** $p<0.0001$ by two way ANOVA. D) Table of BEZ235 $GI_{50}$ values with and without 0.3 nM rapamycin.

One of the main pathways that activates mTOR is the IGF-1R, and it has already been shown that it is involved in feedback loops from mTORC1 (O'Reilly et al. 2006, Wan et al. 2007). The levels of IGF-1R and IR were therefore examined in the resistant cells to assess the likelihood of their involvement in resistance. This revealed that the IGF-1R and the IR receptor were upregulated in RCC4B20 cells compared to control RCC4S cells (Figure 5-9 A and B). The 786-0B200 cells did not show the same upregulation in IGF-1R, and did not express IR.

Cell viability assays were performed to assess the contribution of these proteins to resistance, using the IGF-1R/IR inhibitor OSI-906, at the concentration of 3 μM as was used in the first results chapter. The addition of OSI-906 to BEZ235 did not sensitise RCC4S cells, as expected from the results seen in previously in Figure 3-7, but also did not sensitise RCC4B20 cells despite the upregulated levels of IGF-1R and IR (Figure 5-9 C). Similarly, 786-0S cells were not affected by the addition of OSI-906 (as seen previously in Figure 3-8), and neither were 786-0B200 cells.

It appeared therefore that the upregulation of IGF-1R and IR was not contributing to BEZ235 resistance, and was likely a passenger effect, or an entirely redundant resistance pathway.

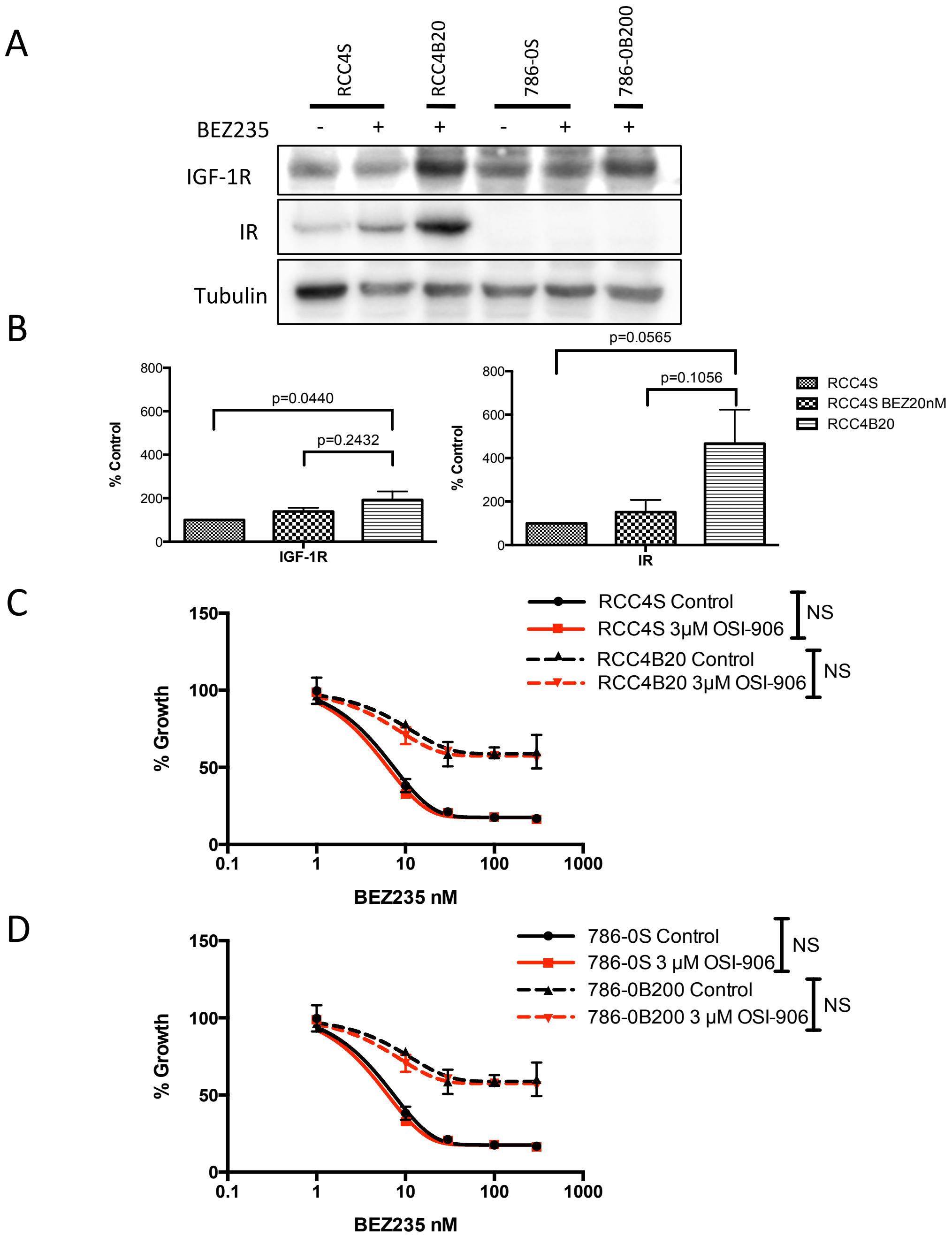


**Figure 5-9 RCC4B20 cells upregulate IGF-1R and IR but their inhibition by OSI-906 does not sensitise to BEZ235**

A) Monolayer RCC4S cells were treated with 20 nM BEZ235 or solvent control for 1 hour. RCC4B20 cells were treated with fresh 20 nM BEZ235 for 1 hour. 786-0S cells were treated with 200 nM BEZ235 or solvent control for 1 hour. 786-0B200 cells were treated with fresh 200 nM BEZ235 for 1 hour. Cell lysates were analysed by SDS PAGE. B) Western blots of IGF-1R and IR were quantified using ImageJ, normalised to tubulin loading, and expressed as a percentage of control treated RCC4S cells. Graphs show mean and SEM of five independent experiments for IGF-1R and 4 four independent experiments for IR. Student's T test p values shown. CTG cell viability assay of C) RCC4S and RCC4B20, and D) 786-0S and 786-0B200 cells treated with BEZ235 and solvent or BEZ235 and 3 μM OSI-906. Graphs show mean and SEM of two independent experiments. NS p>0.05 by two way ANOVA.

### 5.2.4 Histone modification as a mechanism of resistance

The BEZ235 resistant RCC4B20 and 786-0B200 cells did not suggest stem cell like properties based on their clonogenicity (Figure 4-4), but they did show a reversal of their resistance on withdrawal of BEZ235. This reversibility suggests that an epigenetic modification could contribute to BEZ235 resistance so this possibility was investigated.

Histones undergo multiple modifications, including acetylation, and the acetylation status is dependent upon the balance of activity between histone acetyltransferases (HATs) and HDACs, which remove acetyl groups from lysine residues in the amino termini of histones. Hyperacetylation of histones results in chromatin adopting a more open configuration, which allows gene transcription, while hypoacetylation results in a more closed conformation, and reduced transcription. There are four classes of HDACs, with classes I, II and IV being zinc dependent and inhibited by current HDACi's, while class III HDACs are zinc independent (Glozak and Seto 2007).

The acetylation of histones has been linked to cancer development where the loss of specific acetylations has been documented in multiple cancer types (Fraga et al. 2005). HDACs show altered expression in gastric, colorectal, breast, lung, hepatocellular, prostate, and renal cancer, as well as cutaneous T cell lymphoma, Hodgkin's lymphoma, and acute lymphoblastic leukaemia (Krusche et al. 2005, Rikimaru et al. 2007, Marquard et al. 2008, Weichert et al. 2008a, Weichert et al.

2008b, Weichert et al. 2008c, Cha et al. 2009, Adams et al. 2010, Moreno et al. 2010, Minamiya et al. 2011, West and Johnstone 2014).

There are numerous HDACi in clinical development, and two that are licensed for the treatment of cutaneous T cell lymphoma, vorinostat, and romidepsin (Olsen et al. 2007, Coiffier et al. 2012). One of the drugs in development is panobinostat which is a pan-HDAC inhibitor that is more potent than vorinostat, showing low nM $IC_{50}$ concentrations against class I, II and IV HDACs (Shao et al. 2008, Atadja 2009). Panobinostat is in early clinical trials in renal cancer, and in a variety of other solid tumours including breast cancer, gliomas, prostate cancer, colorectal cancer, pancreatic cancer and small cell lung cancer (Conte et al. 2009, Rathkopf et al. 2010, Hainsworth et al. 2011, Drappatz et al. 2012, Gold et al. 2012, Shapiro et al. 2012, Wang et al. 2012, de Marinis et al. 2013).

The activity of panobinostat was assessed in the paired BEZ235 sensitive and resistant cell lines. After drug washout for 72 hours in the resistant cells, treatments of solvent, or 20 nM panobinostat were applied and acetylated histone H3 levels assessed by western blotting (Figure 5-10 A). This revealed that the two resistant cell lines had the same basal levels of acetylated histone H3 as their sensitive counterparts, and that panobinostat was active in all cell lines as evidenced by increased acetyl histone H3 levels. The major signalling components of the AKT – mTOR pathway were assessed as well, revealing that panobinostat had no direct effects on mTOR signalling (Figure 5-10 A). Next, the sensitivity of BEZ235 resistant cells to panobinostat was compared to their parental counterparts. Both RCC4B20 (Figure 5-10 B) and 786-0B200 (Figure

5-10 C) showed the same sensitivity to single agent panobinostat as the sensitive control cells. This shows that BEZ235 resistance did not induce sensitivity to HDAC inhibition.

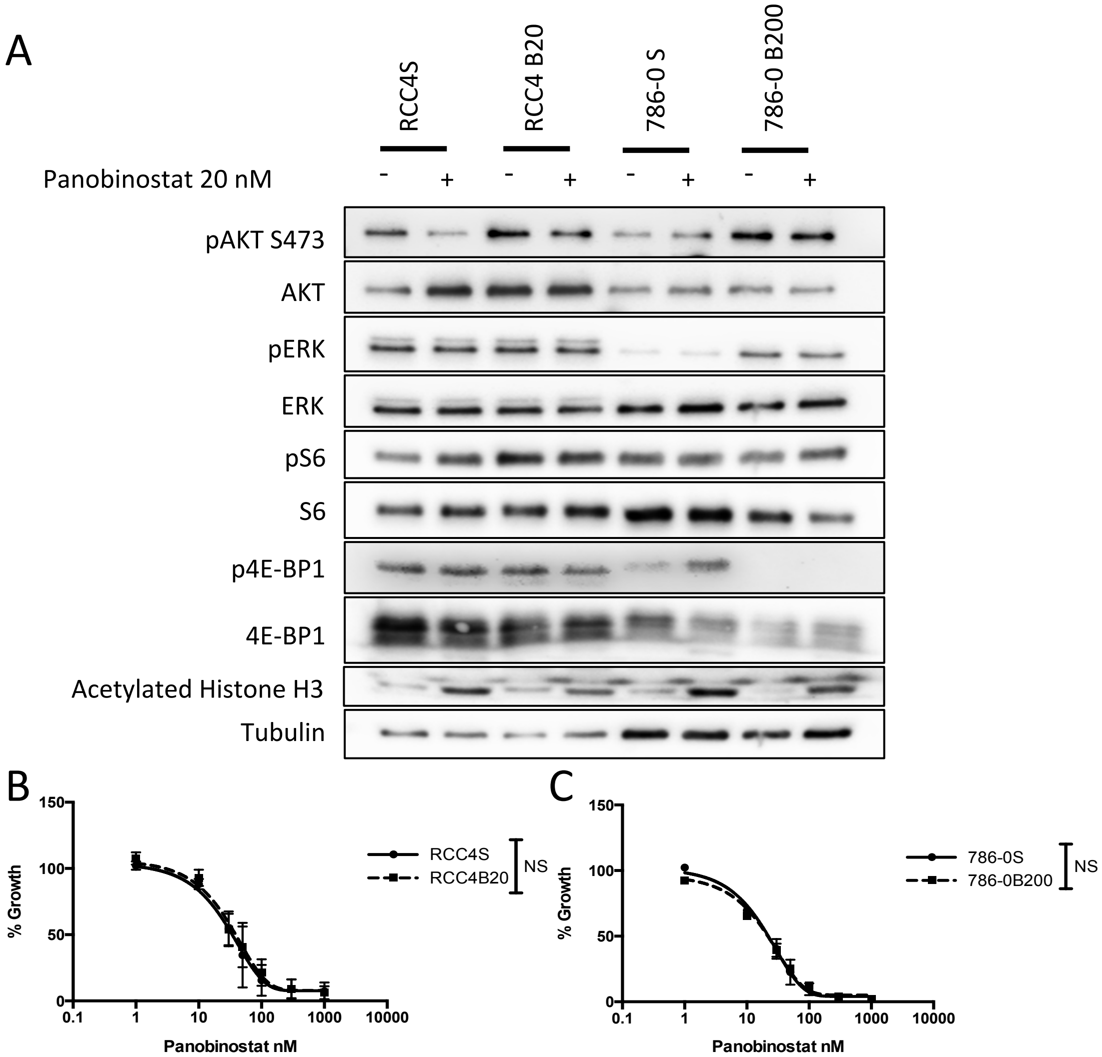


D

| Cell Line | $GI_{50}$ nM (95% CI) |
|---|---|
| **RCC4S** | 34 (27 – 44) |
| **RCC4B20** | 39 (31 – 48) |
| **786-0S** | 22 (19 – 25) |
| **786-0B200** | 22 (19 – 24) |

**Figure 5-10 Panobinostat inhibits histone deacetylase but does not alter mTORC1 signalling**

A) Monolayer RCC4S, RCC4B20, 786-0S and 786-0B200 cells were treated with 20 nM panobinostat for 1 hour. Cell lysates were analysed by SDS-PAGE and blotted with the indicated antibodies. Similar results were seen in an independently prepared set of cell lysates. CTG viability assay of B) RCC4S and RCC4B20 and C) 786-0S and 786-0B200 cells treated with panobinostat. Graphs show mean and SEM of three independent experiments. NS $p>0.05$ by two way ANOVA. D) Table of panobinostat $GI_{50}$ concentrations.

Panobinostat was combined with BEZ235 to see whether HDAC inhibition sensitised BEZ235 resistant cells. Cell viability assays in RCC4S cells showed that the addition of 20 nM panobinostat had no effect on the dose-response curve for BEZ235 (Figure 5-11 A). In BEZ235 resistant RCC4B20 cells however, 20 nM panobinostat significantly altered the response to BEZ235 both in terms of $GI_{50}$ concentrations and the resistant population (Figure 5-11 B and Table 5-1). The partial reversal of resistance in RCC4B20 cells was confirmed by clonogenic survival/growth assay, as was the lack of effect in RCC4S cells (Figure 5-11 C).

A similar pattern was seen in the other cell pair: 786-0S cells showed no shift in response to BEZ235 with the addition of 20 nM panobinostat (Figure 5-11 D) whereas the addition of panobinostat to the resistant 786-0B200 cells caused a partial reversal of BEZ235 resistance (Figure 5-11 E and Table 5-1). Once again, this was confirmed by clonogenic cell survival/growth assay (Figure 5-11 F).

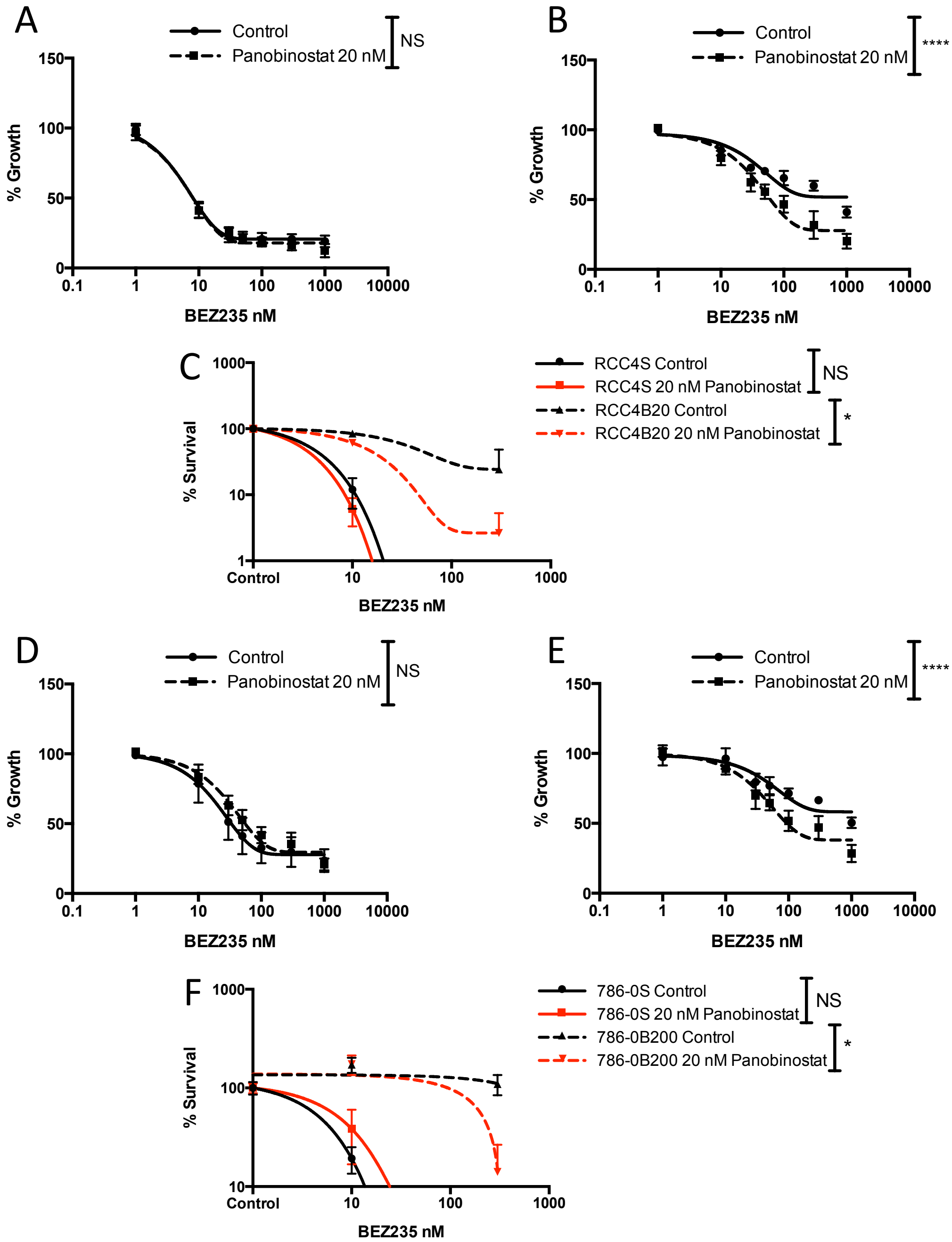


**Figure 5-11 The addition of 20 nM panobinostat reverses resistance to BEZ235**

CTG cell viability assay for A) RCC4S and B) RCC4B20 cells treated with BEZ235 and solvent, or BEZ235 and 20 nM panobinostat. Graph shows mean and SEM of three independent assays. NS p>0.05, **** p<0.0001 by two way ANOVA. C) Clonogenic cell survival/growth assay of RCC4S and RCC4B20 cells treated with solvent, BEZ235, 20 nM panobinostat or the combination of BEZ235 and panobinostat. Graph shows mean and SEM of six data points from two independent experiments. NS P>0.05, * P=0.0274 by two way ANOVA. CTG cell viability assay for D) 786-0S and E) 786-0B200 cells treated with BEZ235 and solvent, or BEZ235 and 20 nM panobinostat. Graph shows mean and SEM of three independent assays. NS p>0.05, **** p<0.0001 by two way ANOVA. F) Clonogenic cell survival/growth assay of 786-0S and 786-0B200 cells treated with solvent, BEZ235, 20 nM panobinostat or the combination of BEZ235 and panobinostat. Graph shows mean and SEM of six data points from two independent experiments. NS P>0.05, * P=0.0283 by two way ANOVA.

| Cell Line | $GI_{50}$ nM (95% CI) | | Fold Sensitisation (95% CI) | Resistant Population % (95% CI) | | Fold Sensitisation (95% CI) |
|---|---|---|---|---|---|---|
| | Control | 20 nM panobinostat | | Control | 20 nM panobinostat | |
| **RCC4S** | 8<br>(7 – 10) | 8<br>(7 – 10) | 1<br>(1 – 1) | 21<br>(18 – 23) | 18<br>(15 – 21) | 1.2<br>(0.9 – 1.5) |
| **RCC4B20** | >1000 | 61<br>(49 – 77) | >16 | 52<br>(46 – 58) | 28<br>(21 – 34) | 1.9<br>(1.4 – 2.8) |
| **786-0S** | 33<br>(25 – 44) | 55<br>(45 – 67) | 0.5<br>(0.4 – 1) | 28<br>(21 – 35) | 30<br>(24 – 35) | 0.9<br>(0.6 – 1.4) |
| **786-0B200** | >1000 | 93<br>(71 – 124) | >11 | 58<br>(52 – 64) | 38<br>(31 – 45) | 1.5<br>(1.1 – 2.1) |

**Table 5-1 $GI_{50}$ and resistant populations and fold sensitisation for BEZ235 and BEZ235 with 20 nM panobinostat**

Table summarises data from Figure 5-11 A, B, D and E

In order to understand the mechanism by which HDAC inhibition sensitises to BEZ235 in resistant cells, it is necessary to consider the known effects of HDAC inhibitors. HDAC inhibitors are known to induce apoptosis and this is at least in part through altered expression of proteins that regulate the extrinsic and intrinsic pathways of apoptosis induction. HDAC inhibitors including trichostatin and vorinostat have been shown in increase expression of death receptor 5 (DR5) (Nakata et al. 2004), and pro-apoptotic proteins such as Bim, Bax and Bac, and to decrease expression of anti apoptotic proteins BCL-XL and BCL2 (Peart et al. 2005). HDAC inhibitors also influence cell cycle progression, possibly not just through histone modification, but by directly altering the acetylation of p53. The DNA binding activity of p53 is increased by acetylation, and HDACs are involved in its deacteylation and deactivation (Gu and Roeder 1997, Luo et al. 2000, Luo et al. 2004).

Of particular relevance to this project, several studies have tested combinations of mTOR inhibitors and HDAC inhibitors. In human renal cancer cells *in vitro*, the combination of panobinostat and rapamycin was able to reduce the level of pAKT, including rapamycin induced pAKT and was more effective than either agent alone at reducing colony formation *in vitro* and xenograft growth *in vivo* (Verheul et al. 2008). Similar AKT inhibition has been seen in head and neck squamous cancer cells following treatment with panobinostat and a variety of PI3K/mTOR inhibitors including BKM120 and BEZ235 and in pancreatic cancer with the combination of BEZ235 and panobinostat (Erlich et al. 2012, Venkannagari et al. 2012). In diffuse large B cell lymphomas, HDACi induced decrease in pAKT has been linked to the expression of the phosphatase PP1 (Gupta et al. 2009). In contrast, the same drug combination in prostate cancer cell lines did not inhibit pAKT S473, but did inhibit pERK (Ellis et al. 2013). In breast cancer cell lines, the combination of the mTORC kinase inhibitor MLN0128 and trichostatin not only decreased phosphorylation of S473 AKT, but also of 4E-BP1 (Wilson-Edell et al. 2014).

Given the evidence suggesting that the co-inhibition of HDAC and mTOR could decrease mTORC1 and mTORC2 signalling, the next experiments tested effects of the combination of panobinostat and BEZ235 on BEZ235 resistant and BEZ235 sensitive cells. It had already been seen that panobinostat as a single agent had no effect on pAKT, pERK, pS6 or p4E-BP1 (Figure 5-10 A). Two concentrations of BEZ235 were tested in combination with 20 nM panobinostat in RCC4S, RCC4B20, 786-0S and 786-0B200 cells (Figure 5-12). The addition of panobinostat did not influence the phosphorylation of AKT S473, S6, 4E-BP1 or ERK in either of the BEZ235 resistant cell lines, or their parental BEZ235 sensitive pairs.

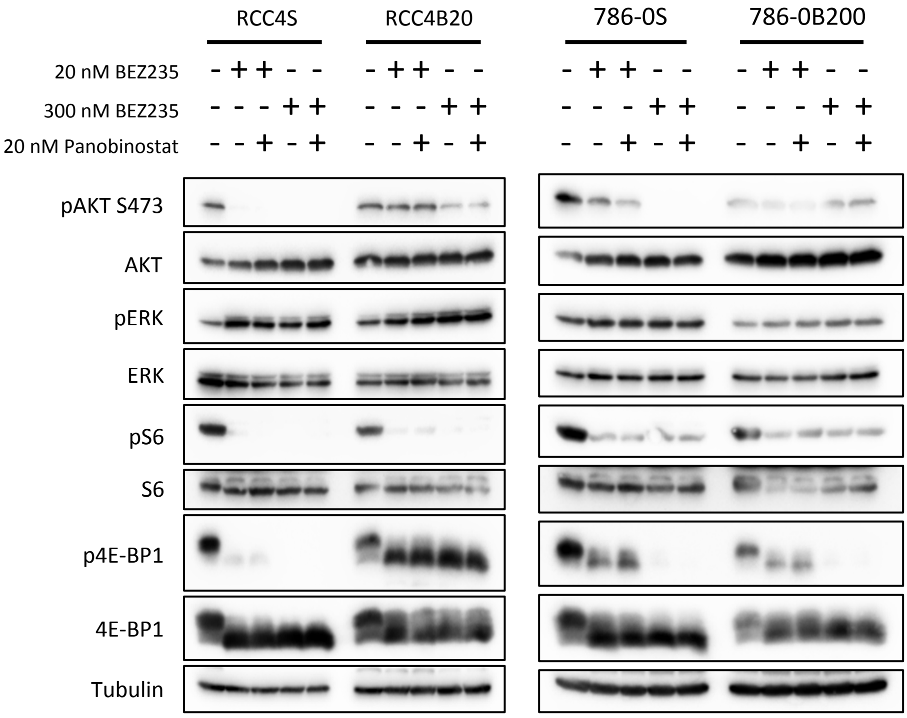


**Figure 5-12 The addition of panobinostat to BEZ235 does not acutely alter mTOR signalling**

Monolayer RCC4S, RCC4B20, 786-0S and 786-0B200 cells were grown in drug free media for 72 hours before seeding into dishes. After 24 hours, cells were treated for 1 hour with solvent or the indicated concentrations of BEZ235 and solvent, or BEZ235 and 20 nM panobinostat. Cell lysates were analysed by SDS PAGE and western blotting. Similar results were seen in an independent experiment.

Since no direct effects on mTORC signalling were observed, the known property of HDAC inhibition to induce apoptosis was examined. In addition to inducing apoptosis as a single agent, the combination of mTORC and HDAC inhibition has been shown to synergise in inducing apoptosis in breast and pancreatic cancer cell lines (Venkannagari et al. 2012, Wilson-Edell et al. 2014). Apoptosis was assayed using CaspaseGlo caspase 3/7 activity assay, described in section 2.6. Caspase 3 and 7 are two key effector caspases that lie downstream of the extrinsic and intrinsic (mitochondrial) apoptotic pathways. They exist as pro-enzymes, which are activated by other caspases in the apoptotic caspase cascade. Caspase 3 is cleaved and activated by caspase 8 and 9, and itself cleaves and activates caspase 7. The activity of caspase 3 and 7 therefore give an indication of the amount of apoptosis taking place in a cell population. RCC4S and RCC4B20 cells were treated with solvent, 300 nM BEZ235, 20 nM panobinostat, or BEZ235 and panobinostat for either 24 or 48 hours and caspase activity assays were performed (Figure 5-13 A and B). These time points were chosen based on reports that BEZ235 has been shown to induce apoptosis at 24 hours in renal cancer cells, and 48 hours in lung cancer (Xu et al. 2011, Li et al. 2012b). The most apparent finding was that at both 24 hours and 48 hours, there was a non statistically significant trend towards untreated RCC4B20 cells having a higher basal rate of apoptosis than the solvent treated controls. In both the BEZ235 sensitive and resistant RCC4 cell lines, at both time-points, BEZ235 had minimal effect on apoptosis, with a trend to decreasing caspase activity especially at 48 hours. Panobinostat did show the expected increase in apoptosis in RCC4S cells, particularly at 48 hours, but this was not seen in RCC4B20 cells. The combination of BEZ235 and panobinostat caused a non-statistically significant increase in apoptosis compared to BEZ235 or panobinostat alone at both 24 and 48 hours, in both BEZ235 resistant and BEZ235 sensitive cells. The increase in apoptosis from combination treatment was a relatively modest ~50% increase over RCC4B20 control cells.

In 786-0S and 786-0B200 cells a similar pattern was seen with a particularly striking increase in basal levels of apoptosis in the BEZ235-resistant subline compared to the sensitive parental cells. However, large variability in the inter-assay replicates of the two assays performed hindered statistical significance (Figure 5-13 C and D). In 786-0S cells as in RCC4S, BEZ235 appeared to suppress apoptosis and there was a trend towards increased apoptosis in the BEZ235 and panobinostat combination compared to BEZ235 alone at both time-points. In 786-0B200 cells, there was a trend towards increased apoptosis with the BEZ235 and panobinostat combination at 24 hours, but not at 48 hours.

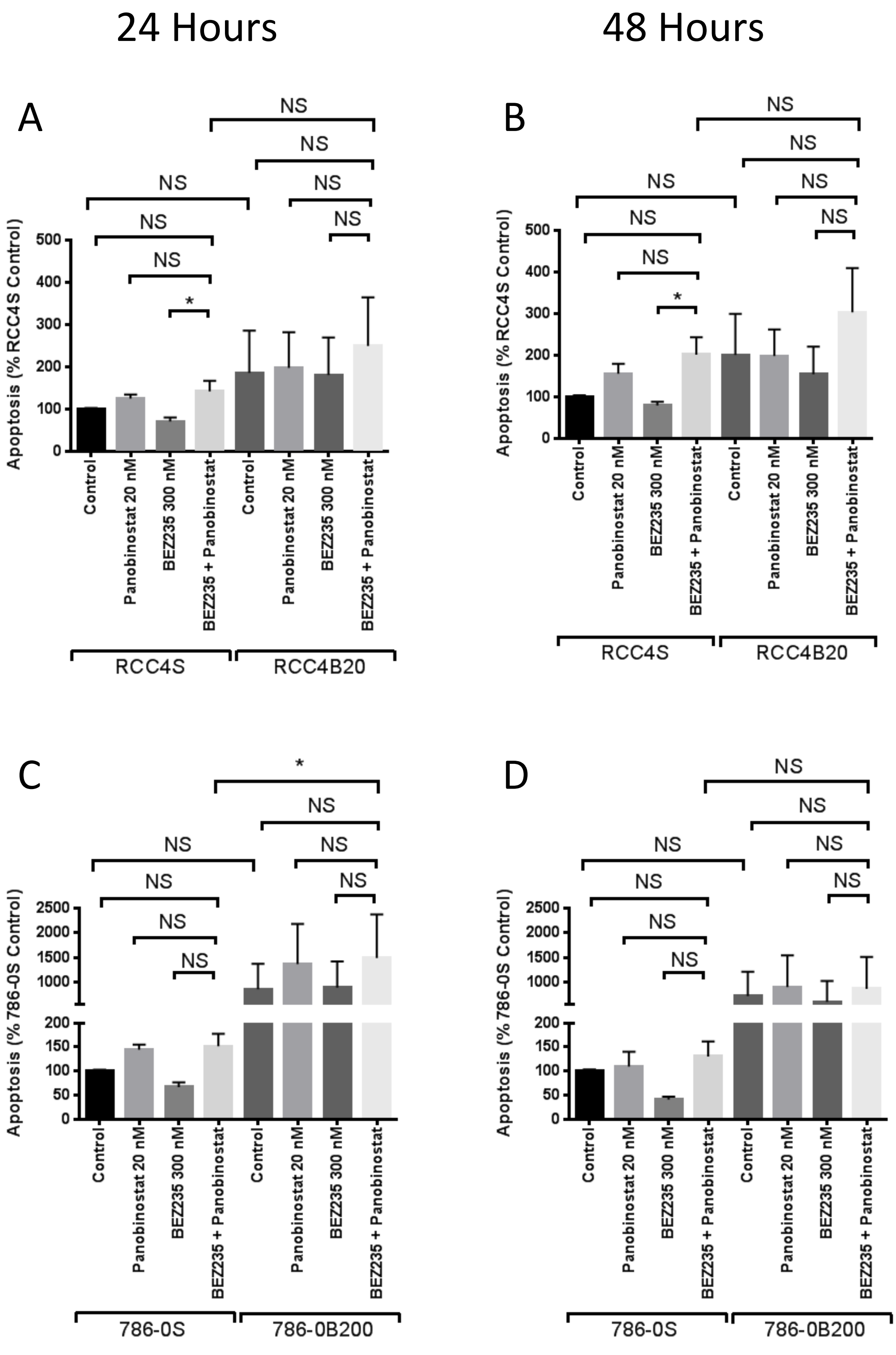


**Figure 5-13 The addition of panobinostat to BEZ235 causes a trend towards increased apoptosis**

CaspaseGlo Caspase 3/7 activity assays of RCC4S, RCC4B20, 786-0S and 786-0B200 cells. Cells were treated with the indicated concentrations of drugs, or solvent for 24 hours, A) and C) or 48 hrs, B) and D). Graphs show mean and SEM of six data points from 2 independent experiments. NS P>0.05 and * 0.05<P<0.01 by Friedman Test with Dunn's multiple comparisons test.

Although not reaching statistical significance, there was a trend towards both the resistant sublines, RCC4B20 and 786-0B200 cells having higher basal levels of apoptosis than the sensitive cell line pairs. This is unlikely to be explained simply by cell numbers, because identical numbers of cells were seeded at the start of each experiment, and in each cell line pair, the BEZ235-sensitive cells were the more rapidly proliferating. The 786-0B200 cells were noted to be larger than 786-0S cells, and this could contribute to the increased caspase activity, if more caspase is present within each cell undergoing apoptosis. If this were the case, however, a western blot for cleaved poly ADP ribose polymerase (PARP), which is a caspase target during apoptosis would show no difference between 786-0B200 and 786-0S cells, because loading would be normalised for protein concentration. As can be seen in Figure 5-14, this was not seen to be the case: 786-0B200 cells showed detectable PARP cleavage, indicating higher levels of caspase activity, while PARP cleavage was not detected in the BEZ235-sensitive cells.

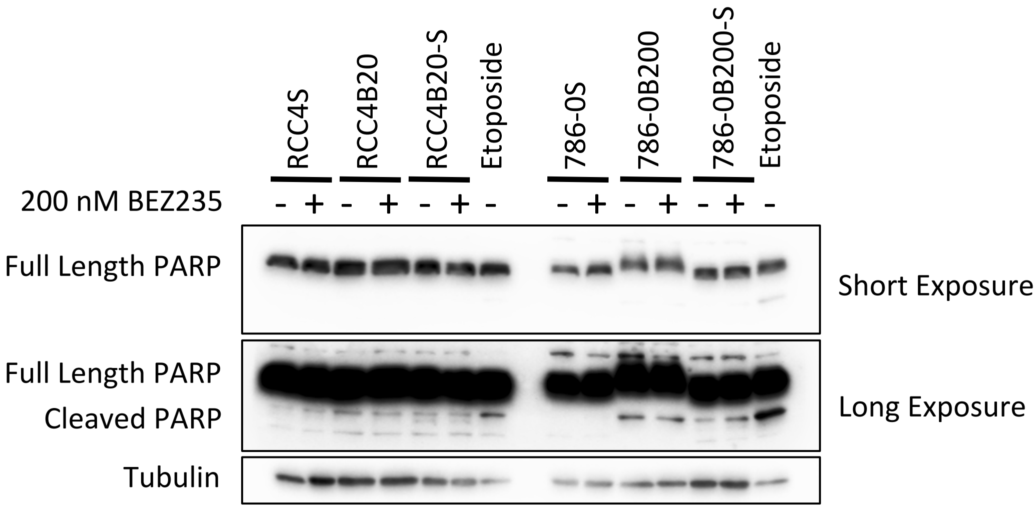


**Figure 5-14 BEZ235 resistant cells show increased basal apoptotic activity**

Resistant cells were given a 72 hour drug washout. The indicated cell lines were treated with solvent or 200 nM BEZ235 RCC4S or with 34 µM etoposide as a positive control for 24 hours. Similar results seen in a second independent experiment.

## 5.3 Discussion

Hypothesis led investigation of BEZ235 resistant cells was successful in discovering factors contributing to resistance. There was evidence for reactivation of 4E-BP1, which appeared to remain mTORC1-dependent, and may in part be related to increased RAPTOR expression. Consistent with this hypothesis, targeting of mTORC1 with RAPTOR knockdown or rapamycin partially reversed BEZ235 resistance. Whilst there are reports that resistance to mTORC kinase inhibition can be associated with altered eIF4E:4E-BP1 ratios downstream of mTORC1 (Alain et al. 2012, Cope et al. 2014), there are no reports that increased RAPTOR expression can be associated with the same resistance phenotype. RAPTOR is known to bind directly to 4E-BP1, and facilitates mTOR dependent phosphorylation of 4E-BP1 (Hara et al. 2002). Paradoxically, overexpression of wild type RAPTOR in HEK293 cells was shown to cause a decrease in p4E-BP1, possibly through sequestration of 4E-BP1 or other important scaffolding proteins. In HEK293 cells and mouse embryonic fibroblasts, RAPTOR knockdown or knockout was shown to sensitise to rapamycin-induced retardation in 5' terminal oliogopyrimidine (5'TOP) mRNA translation (Patursky-Polischuk et al. 2009). In renal cancer, RAPTOR has been found to show altered expression in 241 of 401 renal cancers (57.5%), and was significantly associated with higher stage, grade, and venous thrombosis. As part of a multi biomarker panel, altered RAPTOR expression was associated with a poor prognosis (Darwish et al. 2013). Similarly, in breast cancer RAPTOR was reported to show increased expression over adjacent normal tissue, and to be associated with higher tumour grade (Wazir et al. 2013). Therefore, it is conceivable that increased RAPTOR expression could contribute to resistance to mTORC kinase inhibition. Indeed, increased expression of the mTORC2 companion protein RICTOR has been correlated with paclitaxel resistance in ovarian cancer (Foster et al. 2010a). RAPTOR upregulation might indicate that more mTOR kinase was present in RCC4B20 BEZ235 resistant cells in mTORC1 complexes and this could be tested for by co-precipitating mTOR and RAPTOR. RAPTOR itself has been implicated in other roles that could help explain its association with resistance to mTORC kinase inhibition. During mitosis, protein translation is decreased and activators of mTOR are generally inactive. RAPTOR phosphorylation has been show to promote G2/M transition by maintaining mTOR activity and internal ribosome entry site (IRES) translation (Ramirez-Valle et al. 2010). In future, it would be interesting to investigate this role further, and in the first instance test for altered RAPTOR expression in samples of human renal cancer from patients treated with mTOR inhibitors to investigate correlations between RAPTOR expression and response or resistance to treatment.

The effect of HDAC inhibitors is also intriguing, given reports that HDAC inhibition has been reported to sensitise to mTORC inhibition in other cancer models. In this RCC model, HDAC inhibition did not sensitise parental cells to BEZ235, but in the cells that had developed BEZ235 resistance there was significant sensitisation. The mechanism of this sensitisation has not been uncovered here, but it does not appear to be a direct effect on mTORC signalling or on apoptosis, in contrast to other reports (Verheul et al. 2008, Venkannagari et al. 2012, Ellis et al. 2013, Wilson-Edell et al. 2014). Other possible mechanisms that could contribute to the effects of HDAC inhibition include effects on cell cycle distribution, given the G1 arrest seen in breast cancer models (Wilson-Edell et al. 2014), effects on the DNA damage response, such as the reduction in ATM seen in prostate cancer cell models (Ellis et al. 2013), or the decreased expression of HIF1α seen in renal cancer models (Verheul et al. 2008). In addition to these hypothesis driven routes of investigation, an unbiased screen to uncover alterations in gene transcription could be performed in cells co-treated with BEZ235 and panobinostat, and the results compared to a similar screen conducted in BEZ235 resistant cells, to investigate reciprocally regulated genes.

It was of interest that BEZ235 cells showed higher basal rates of apoptosis as evidenced by Caspase activity assay and PARP cleavage (Figure 5-13 and Figure 5-14) One possibility to explain this apparently paradoxical elevation in apoptosis is that RCC4B20 and 786-0B200 cells may have become dependent on BEZ235. This could be analogous to dependence on BRAF inhibitors that has recently been shown in a melanoma model of induced resistance to the BRAF inhibitor vemurafenib. Resistant cells were shown to overexpress BRAF, consequently, when the inhibitor was removed the cells were subjected to ERK hyperactivation, leading to cell cycle arrest, apoptosis and tumour regression (Das Thakur et al. 2013). No direct evidence of such hyperactivation was detected in RCC4B20 or 786-0B200 cells on BEZ235 withdrawal, but it is worth noting that when seeded into clonogenic assays, 786-0B200 cells consistently showed increased clonogenicity when treated at low concentrations of BEZ235 (Figure 5-11 F). It would be interesting to investigate the possibility of signalling hyperactivation upon BEZ235 withdrawal.

# 6 Conclusions and Future Directions

This project has taken several different approaches to investigate resistance mechanisms to mTOR inhibition in renal cancer. Initial work focused on the testing of hypotheses developed previously in this group. In the previous study, IGF-1R knockdown was found to suppress rapamycin induced AKT activation and sensitise VHL null cells to rapamycin (Yuen et al. 2009). Furthermore, as VHL null renal cancer was previously shown to have increased IGF-1R expression (Yuen et al. 2007), VHL was hypothesised to act as a biomarker for: response to IGF-1R inhibition, and the ability of IGF-1R inhibition to sensitise to mTOR inhibition by rapamycin. This project found no evidence that sensitivity to rapamycin was induced by IGF-1R tyrosine kinase inhibitors OSI-906 or AZ12253801 (Figure 3-7, Figure 3-8 and Figure 3-10). It was noted that OSI-906 only transiently inhibited AKT, which may account in part for OSI-906's inability to sensitise to rapamycin (Figure 3-11).

Evidence presented earlier in section 3.3 showed that other groups had found evidence in renal cancer that the IGF-1R inhibitor hR1 or the PI3K inhibitor LY294002 were able to sensitise to mTOR inhibition in preclinical models (Elfiky et al. 2011a, Cardillo et al. 2013). However, in a clinical study the combination OSI-906 and everolimus was ineffective, causing no tumour responses in colorectal cancer (Bendell et al. 2015). There is also contradictory evidence from different cancer types concerning the ability of IGF-1R inhibition to sensitise to rapamycin. In brief, other studies have tested panels of cells lines with the rapalogue everolimus and feedback release of AKT activation was seen, but did not correlate with sensitivity to rapamycin, whereas basal levels of AKT activation did (Breuleux et al. 2009). Others however have seen that the small molecule IGF-1R inhibitor NVP-AEW541 sensitised breast cancer and prostate cancer cell lines to everolimus (Garcia-Echeverria et al. 2004, O'Reilly et al. 2006). The addition of the AKT inhibitor MK-2206 sensitised castrate resistant prostate cancer models to the mTOR inhibitor MK-8669 (ridaforolimus). This result was partly attributed to blockade of AKT activation, but also partly to decrease of phosphorylation of Rb, which inhibited progression through the cell cycle (Floc'h et al. 2012). The therapeutic IGF-1R antibody CP-751,871 (Figitumumab) when combined with rapamycin prevented AKT activation and inhibited growth of osteo- and Ewings sarcoma (Kurmasheva et al. 2009). Similar effects were seen with the use of rapamycin and the PI3K inhibitor IC87114 in acute myeloid leukaemia, with blockade of mTORC1 induced AKT activation, and increased anti-proliferative effects (Tamburini et al. 2008).

Thus there is some evidence that rapamycin-induced AKT activation occurs clinically, but its functional relevance remains inconclusive. In patients with glioblastoma who had previously undergone debulking surgery, patients were treated on progression with short duration (median 7 days) of rapamycin followed by further debulking surgery, followed by rapamycin until next progression (Cloughesy et al. 2008). Evidence of AKT activation was found in 7 of 14 patients, which was associated with a shorter time to progression on rapamycin post second debulking surgery. However, there was no correlation between markers of mTORC1 inhibition, decrease in pS6 levels, or in decrease in Ki67 staining (a marker of proliferation), and progression free survival. A phase I trial of the rapalogue everolimus, examined levels of pAKT in tumour samples as well as in skin biopsies. Increases in pAKT were seen in 50% of patients, but there were insufficient clinical responses for correlations to be made. Increases in pAKT were not always sustained, and in some patients decreased AKT phosphorylation was observed (Tabernero et al. 2008). In patients with breast cancer however, decreases in pAKT have been correlated with response to everolimus (Sabine et al. 2010).

Because of the preclinical data supporting the combination of IGF-1R inhibition and mTOR inhibition, a number of early phase clinical trials have been conducted. Everolimus was combined with figutumumab in 21 patients with sarcomas and other solid tumours, with one response by RECIST criteria and prolonged disease stabilisation in additional patients (Quek et al. 2011). Ridaforolimus was combined with the IGF-1R antibody dalotozumab in patients with mixed solid tumours, and 3 of 62 patients had confirmed partial responses (Di Cosmio et al. 2010). Cixutumumab has been combined with temsirolimus in mixed solid tumours, breast cancer, Ewing's Sarcoma and adrenocortical carcinomas, and some responses and prolonged stable disease was seen (Naing et al. 2011, Naing et al. 2012b, Ma et al. 2013, Naing et al. 2013). No pre and post treatment tumour samples were taken to investigate AKT activation and there were no comparator arms of mTOR inhibitor alone. It is therefore unclear from these results to what extent the feedback loop from mTOR to the IGF-1R was active, clinically important, and suppressed by IGF-1R inhibition.

A phase II study of temsirolimus and cixutumumab in patients with IGF-1R expressing sarcomas suggested activity of the drug combination on the basis of progression free survival at 12 weeks (Schwartz et al. 2013). Paired pre and post treatment tumour biopsies were taken from some patients and the majority showed reduction in pAKT suggesting that AKT activation from temsirolimus was blocked. However, only 32 patients underwent biopsy, and there was no correlation reported between changes in pAKT or pS6 with response to treatment, or progression free survival.

Thus there is limited support for the concept that IGF-1R inhibition can suppress rapamycin/rapalogue induced AKT activation in some cancers. However in the current study, OSI-906 only transiently inhibited AKT, and did not sensitise to rapamycin.

Subsequent work in this project focussed on the next generation of mTOR inhibitors, which are direct ATP competitive kinase inhibitors of mTOR. This work was primarily carried out using BEZ235, but was relevant also to AZD2014, supporting the wider implication of this work to this class of mTOR inhibitors. The data presented here confirm other studies showing that mTOR kinase inhibitors cause more complete blockade of mTORC1 function and greater *in vitro* anti-proliferative effects than allosteric mTOR inhibitors (Serra et al. 2008, Breuleux et al. 2009, Feldman et al. 2009, Thoreen et al. 2009, Cho et al. 2010, Chresta et al. 2010, Nyfeler et al. 2012, Pike et al. 2013, Zhang et al. 2013).

The main focus of this project was to investigate mediators of resistance to mTOR kinase inhibition using RCC cells made resistant to BEZ235 *in vitro*. The goals of this research were three-fold: to identify potential biomarkers predicting sensitivity or resistance, to identify drivers of resistance, and to use this information to propose drug combinations to enhance sensitivity to mTOR inhibition.

Large scale screens were performed at the protein and mRNA levels, identifying potential biomarkers of BEZ235 resistance, including MET, MEK – ERK, Abl and the Notch pathway. These proteins and pathways were chosen for testing based upon their known roles in CCRCC and roles in drug resistance. MET is overexpressed in some CCRCCs and confers a poor prognosis (Gibney et al. 2013), and has been implicated in resistance to EGFR inhibition in NSCLC (Engelman et al. 2007, Yano et al. 2011, Nakagawa et al. 2012). Recently, the results of the phase 3 trial comparing cabozantinib to everolimus was reported showing higher response rates and prolonged progression free survival and overall survival with cabozantinib (Choueiri et al. 2015). Cabozantinib is an inhibitor of VEGFR as well as MET and AXL, both of which have been implicated in resistance to VEGFR targeted therapy in RCC. It is interesting to note that inhibition of MET by cabozantinib in VEGFR inhibition resistance proved efficacious, whereas in mTOR inhibitor resistance in this model it did not. Abl is known to be over-expressed in renal cancer (Behbahani et al. 2012). MEK and ERK have previously been shown to mediate resistance to targeted agents including mTOR inhibitors (Renshaw et al. 2013, Qu et al. 2014). The Notch pathway is associated with epithelial – mesenchymal – transition and is therefore associated with drug resistance (Wang et al. 2009, Xie et al. 2012). Furthermore, Notch and Jagged are overexpressed in renal cancer (Sjolund et al. 2008), and associated with poor prognosis in breast cancer (Reedijk et al. 2005). Inhibition of the Notch pathway as with inhibition of MET, Abl or MEK did not reverse the BEZ235 resistance phenotype. This suggests that these changes may be passengers, not drivers of resistance. However, they could still be valid biomarkers of resistance. Were clinical material available from patients who have received mTOR kinase inhibitors, it would then be possible to assess the clinical application of such biomarkers. Tumour material from patients treated with allosteric mTOR inhibitors is much more widely available as everolimus and temsirolimus are licensed for use, so this may represent a more pragmatic way to test clinical relevance. However, it should be noted that the BEZ235 resistant cells did not show a marked cross-resistance to allosteric mTOR inhibitors in this study, so this may not be a good test of these biomarkers' clinical validity.

Two potential drivers of resistance were identified: RAPTOR upregulation, and acetylation (of histones or other proteins). BEZ235 resistant RCC4B20 cells showed clear upregulation of RAPTOR, and partial reversal of resistance upon RAPTOR depletion. Furthermore, these phenotypic effects were associated with alteration in phospho-4E-BP1 levels, which correlated with the anti-proliferative effects of mTOR inhibition in BEZ235 sensitive cells. Combining the allosteric mTOR inhibitor rapamycin with BEZ235 closely mimicked the effects of RAPTOR knockdown, and indeed rapamycin has been shown to disrupt mTOR complexes (Oshiro et al. 2004, Sarbassov et al. 2006), supporting the hypothesis that RAPTOR upregulation was contributing to regain of mTORC1 function in BEZ235 resistant RCC cells. It remains to be determined whether increased transcription, increased translation, or increased protein stability accounts for RAPTOR upregulation. It would be of interest, in future work, to determine whether other members of the mTORC1 complex including mTOR and PRAS40 also showed altered expression in BEZ235 resistant cells. It may also be informative to test for RAPTOR expression in tumour tissue of patients treated with mTOR inhibitors. Experiments to investigate these questions would certainly strengthen the work presented here.

It would be of great interest to test the two identified modifiers of resistance, rapamycin and panobinostat, in combination with alternative mTOR kinase inhibitors. The obvious choice would be AZD2014 given the pre-existing data presented here showing cross resistance of BEZ235 resistant RCC cells to AZD2014 (Figure 4-6). If this were to show that the addition of rapamycin and or panobinostat were to sensitise to alternative mTOR inhibitors, this would extend the potential clinical impact of the research. This may be an important area to address because BEZ235 is not being actively pursued in further clinical testing by Novartis largely because of toxicity, whereas alternative mTOR kinase inhibitors including AZD2014 are still undergoing further testing.

The same arguments could be made for testing alternative HDAC inhibitors. Panobinostat did not alter signalling along the PI3K – mTOR pathway, or the MAPK – ERK pathway, and did not alter apoptosis induction. The mechanism through which HDAC inhibition sensitised to BEZ235 therefore remains undefined. This is an area of research that would be worth pursuing, but the controversy around the mechanism by which HDAC inhibitors cause their anti cancer effects suggests that this course of research could be fraught with difficulty (West and Johnstone 2014).

One key way to increase the impact of this work would be through *in vivo* and clinical data. It may be possible to get access to archival, i.e. pre treatment tissue, but it is not clear to what extent the biomarkers identified here in a model of induced resistance are also relevant to primary resistance. Ideally, post treatment tissue would be tested as well, but accessing this material is very difficult. The number of patients treated with mTOR kinase inhibitors is still small, so obtaining any appropriate tissue and clinical data would be very difficult. Another way to obtain *in vivo* data would be to create mouse xenograft models using the BEZ235-resistant cells. Successful establishment of such an *in vivo* model would allow testing of the ability of rapamycin and or HDAC inhibition to reverse BEZ235 resistance. This was attempted with both 786-0B200 and RCC4B20 cell lines, but unfortunately was unsuccessful with no tumours forming (data not shown).

The final results of a phase 2 trial comparing AZD2014 to everolimus have very recently been reported showing that outcomes were worse with the mTORC kinase inhibitor with progression free survival of 1.8 months vs. 4.6 months for the allosteric mTOR inhibitor (Powles et al. 2015). This result, and the similar results of another mTOR kinase inhibitor GDC-0980 make it highly unlikely that mTOR kinase inhibition will be pursued in renal cancer. The work here does not directly address the reasons behind this unexpected result. RAPTOR upregulation was seen with long term mTOR kinase inhibitor treatment, and has been noted to have poor prognostic effects in renal cancer which could go some way to explaining the results. It would be interesting to test for RAPTOR upregulation on long term allosteric mTOR inhibition.

Nevertheless, this project has uncovered several potential biomarkers of response to mTOR inhibition that are worthy of further evaluation, and two potential mediators of resistance that could provide the rationale for combination trials. Biomarkers of mTOR inhibition sensitivity are greatly needed. Recent work has identified activating mTOR mutations in human cancers including kidney, lung, stomach, endometrial and melanoma, some of which conferred hypersensitivity to rapamycin *in vitro* and *in vivo* (Grabiner et al. 2014). Further evidence points to the clinical relevance of activating mTOR mutations: a patient with metastatic urothelial cancer obtained a 14 month complete response to everolimus in a phase I trial was found to have two activating mTOR mutations (Wagle et al. 2014b). The first report of an mTOR mutation resulting in resistance to an mTOR inhibitor has also been made. A patient with anaplastic thyroid cancer achieved an almost complete response to everolimus with an 18 month duration of response. Analysis of pre and post treatment tissue revealed that the appearance of resistance was associated with a mutation in mTOR in the FKBP-rapamycin binding region, which conferred resistance to rapalogues, but not mTOR kinase inhibitors *in vitro* (Wagle et al. 2014a). It is unlikely that a mutation in mTOR accounted for the BEZ235 resistance seen in RCC4B20 cells because the resistance was reversible on withdrawal of BEZ235 (Figure 5-1). However, the 786-0B200 cells did not lose resistance after 5 months of BEZ235 withdrawal. It is possible that a mutation in mTOR accounted for this resistance, and it would be interesting to test for this.

These new discoveries of the role of mTOR mutations as mediators of response and resistance open up the prospect of biomarker directed clinical trials. Work remains to elucidate the role of these mutations in the context of mTOR kinase inhibitors. There is already evidence that mTORC kinase inhibitors can overcome mTOR mutation mediated rapalogue resistance (Wagle et al. 2014a). In this context, the RCC model of BEZ235 resistance created in this project warrants further investigation and may shed light on the key clinical questions of biomarker identification and design of treatment combinations in the field of mTOR inhibition.

# 7 Bibliography

(NCIN), N. C. I. N. (2010). One, five and ten-year cancer prevalence by cancer network, UK, 2006. *NCIN*.

Abern, M. R., E. Scosyrev, M. Tsivian, E. M. Messing, T. J. Polascik and A. Z. Dudek (2014). Survival of patients undergoing cytoreductive surgery for metastatic renal cell carcinoma in the targeted-therapy era. *Anticancer Res* **34**(5): 2405-2411.

Adams, H., F. R. Fritzsche, S. Dirnhofer, G. Kristiansen and A. Tzankov (2010). Class I histone deacetylases 1, 2 and 3 are highly expressed in classical Hodgkin's lymphoma. *Expert Opin Ther Targets* **14**(6): 577-584.

Adams, T. E., V. C. Epa, T. P. Garrett and C. W. Ward (2000). Structure and function of the type 1 insulin-like growth factor receptor. *Cell Mol Life Sci* **57**(7): 1050-1093.

Ahmad, N., C. A. Keehn and D. Coppola (2004a). The expression of insulin-like growth factor-I receptor correlates with Fuhrman grading of renal cell carcinomas. *Hum Pathol* **35**(9): 1132-1136.

Ahmad, N., C. A. Keehn and D. Coppola (2004b). The expression of insulin-like growth factor-I receptor correlates with Fuhrman grading of renal cell carcinomas. *Human pathology* **35**(9): 1132-1136.

Ahn, N. G., R. Seger, R. L. Bratlien, C. D. Diltz, N. K. Tonks and E. G. Krebs (1991). Multiple components in an epidermal growth factor-stimulated protein kinase cascade. In vitro activation of a myelin basic protein/microtubule-associated protein 2 kinase. *J Biol Chem* **266**(7): 4220-4227.

Alain, T., M. Morita, B. D. Fonseca, A. Yanagiya, N. Siddiqui, M. Bhat, D. Zammit, V. Marcus, P. Metrakos, L. A. Voyer, V. Gandin, Y. Liu, I. Topisirovic and N. Sonenberg (2012). eIF4E/4E-BP Ratio Predicts the Efficacy of mTOR Targeted Therapies. *Cancer research*.

Aleksic, T., M. M. Chitnis, O. V. Perestenko, S. Gao, P. H. Thomas, G. D. Turner, A. S. Protheroe, M. Howarth and V. M. Macaulay (2010). Type 1 insulin-like growth factor receptor translocates to the nucleus of human tumor cells. *Cancer research* **70**(16): 6412-6419.

Aleksic, T. and S. M. Feller (2008). Gamma-secretase inhibition combined with platinum compounds enhances cell death in a large subset of colorectal cancer cells. *Cell Commun Signal* **6**: 8.

Alhamdani, M. S., C. Schroder and J. D. Hoheisel (2009). Oncoproteomic profiling with antibody microarrays. *Genome Med* **1**(7): 68.

Allan, L. A., N. Morrice, S. Brady, G. Magee, S. Pathak and P. R. Clarke (2003). Inhibition of caspase-9 through phosphorylation at Thr 125 by ERK MAPK. *Nat Cell Biol* **5**(7): 647-654.

Alt, A. L., S. A. Boorjian, C. M. Lohse, B. A. Costello, B. C. Leibovich and M. L. Blute (2011). Survival after complete surgical resection of multiple metastases from renal cell carcinoma. *Cancer* **117**(13): 2873-2882.

Andre, F., R. O'Regan, M. Ozguroglu, M. Toi, B. Xu, G. Jerusalem, N. Masuda, S. Wilks, F. Arena, C. Isaacs, Y. S. Yap, Z. Papai, I. Lang, A. Armstrong, G. Lerzo, M. White, K. Shen, J. Litton, D. Chen, Y. Zhang, S. Ali, T. Taran and L. Gianni (2014). Everolimus for women with trastuzumab-resistant, HER2-positive, advanced breast cancer (BOLERO-3): a randomised, double-blind, placebo-controlled phase 3 trial. *Lancet Oncol* **15**(6): 580-591.

Antonelli, A., R. Tardanico, P. Balzarini, N. Arrighi, L. Perucchini, T. Zanotelli, A. Cozzoli, D. Zani, S. C. Cunico and C. Simeone (2010). Cytogenetic features, clinical significance and prognostic impact of type 1 and type 2 papillary renal cell carcinoma. *Cancer Genet Cytogenet* **199**(2): 128-133.

Arkenau, H. T., S. F. Jones, C. Kurkjian, J. R. Infante, S. Pant, H. A. Burris, K. N. Moore, D. S. McMeeken, F. A. Greco, S. Ramsey and J. C. Bendell (2012). The PI3K/mTOR inhibitor BEZ235 given twice daily for the treatment of patients (pts) with advanced solid tumors. *Journal of clinical oncology : official journal of the American Society of Clinical Oncology* **30**(Suppl): Abstr 3097.

Armengol, G., F. Rojo, J. Castellvi, C. Iglesias, M. Cuatrecasas, B. Pons, J. Baselga and S. Ramon y Cajal (2007). 4E-binding protein 1: a key molecular "funnel factor" in human cancer with clinical implications. *Cancer Res* **67**(16): 7551-7555.

Atadja, P. (2009). Development of the pan-DAC inhibitor panobinostat (LBH589): successes and challenges. *Cancer Lett* **280**(2): 233-241.

Avdulov, S., S. Li, V. Michalek, D. Burrichter, M. Peterson, D. M. Perlman, J. C. Manivel, N. Sonenberg, D. Yee, P. B. Bitterman and V. A. Polunovsky (2004). Activation of translation complex eIF4F is essential for the genesis and maintenance of the malignant phenotype in human mammary epithelial cells. *Cancer Cell* **5**(6): 553-563.

Banerji, U., E. J. Dean, M. Gonzalez, A. P. Greystoke, B. Basu, M. Krebs, M. Puglisi, L. Grinsted, E. Oelmann, W. Burke, E. Harrington, S. Green and M. Ranson (2012). First-in-human phase I trial of the dual mTORC1 and mTORC2 inhibitor AZD2014 in solid tumors.

. *Journal of clinical oncology : official journal of the American Society of Clinical Oncology* **30**(Suppl.): Abstr 3004.

Bang, Y.-J., W.-C. Su, D.-H. Nam, W.-T. Lim, T. M. Bauer, I. Brana, R. T.-P. Poon, D. S. Hong, C.-C. Lin, B. Peng, Y. Zhang, S. Zhao, A. Kumar, M. Akimov and B. Ma (2014).

Phase I study of the safety and efficacy of INC280 in patients with advanced MET-dependent solid tumors. *Journal of clinical oncology : official journal of the American Society of Clinical Oncology* **32**(5s): suppl; abstr 2520.

Baselga, J., M. Campone, M. Piccart, H. A. Burris, 3rd, H. S. Rugo, T. Sahmoud, S. Noguchi, M. Gnant, K. I. Pritchard, F. Lebrun, J. T. Beck, Y. Ito, D. Yardley, I. Deleu, A. Perez, T. Bachelot, L. Vittori, Z. Xu, P. Mukhopadhyay, D. Lebwohl and G. N. Hortobagyi (2012). Everolimus in postmenopausal hormone-receptor-positive advanced breast cancer. *N Engl J Med* **366**(6): 520-529.

Behbahani, T. E., C. Thierse, C. Baumann, D. Holl, P. J. Bastian, A. von Ruecker, S. C. Muller, J. Ellinger and S. Hauser (2012). Tyrosine kinase expression profile in clear cell renal cell carcinoma. *World J Urol* **30**(4): 559-565.

Belfiore, A., F. Frasca, G. Pandini, L. Sciacca and R. Vigneri (2009). Insulin receptor isoforms and insulin receptor/insulin-like growth factor receptor hybrids in physiology and disease. *Endocr Rev* **30**(6): 586-623.

Bellmunt, J. and J. Dutcher (2013). Targeted therapies and the treatment of non-clear cell renal cell carcinoma. *Ann Oncol* **24**(7): 1730-1740.

Ben-Neriah, Y., G. Q. Daley, A. M. Mes-Masson, O. N. Witte and D. Baltimore (1986). The chronic myelogenous leukemia-specific P210 protein is the product of the bcr/abl hybrid gene. *Science* **233**(4760): 212-214.

Bendell, J. C., S. F. Jones, L. Hart, D. R. Spigel, C. M. Lane, C. Earwood, J. R. Infante, J. Barton and H. A. Burris (2015). A phase Ib study of linsitinib (OSI-906), a dual inhibitor of IGF-1R and IR tyrosine kinase, in combination with everolimus as treatment for patients with refractory metastatic colorectal cancer. *Invest New Drugs* **33**(1): 187-193.

Bendell, J. C., J. Rodon, H. A. Burris, M. de Jonge, J. Verweij, D. Birle, D. Demanse, S. S. De Buck, Q. C. Ru, M. Peters, M. Goldbrunner and J. Baselga (2012). Phase I, dose-escalation study of BKM120, an oral pan-Class I PI3K inhibitor, in patients with advanced solid tumors. *Journal of clinical oncology : official journal of the American Society of Clinical Oncology* **30**(3): 282-290.

Beretta, L., A. C. Gingras, Y. V. Svitkin, M. N. Hall and N. Sonenberg (1996). Rapamycin blocks the phosphorylation of 4E-BP1 and inhibits cap-dependent initiation of translation. *Embo j* **15**(3): 658-664.

Biswas, S., P. J. Charlesworth, G. D. Turner, R. Leek, P. T. Thamboo, L. Campo, H. Turley, P. Dildey, A. Protheroe, D. Cranston, K. C. Gatter, F. Pezzella and A. L. Harris (2012). CD31 angiogenesis and combined expression of HIF-1alpha and HIF-2alpha are prognostic in primary clear-cell renal cell carcinoma (CC-RCC), but HIFalpha transcriptional products are not: implications for antiangiogenic trials and HIFalpha biomarker studies in primary CC-RCC. *Carcinogenesis* **33**(9): 1717-1725.

Bottaro, D. P., J. S. Rubin, D. L. Faletto, A. M. Chan, T. E. Kmiecik, G. F. Vande Woude and S. A. Aaronson (1991). Identification of the hepatocyte growth factor receptor as the c-met proto-oncogene product. *Science* **251**(4995): 802-804.

Boucher, J., Y. Macotela, O. Bezy, M. A. Mori, K. Kriauciunas and C. R. Kahn (2010). A kinase-independent role for unoccupied insulin and IGF-1 receptors in the control of apoptosis. *Sci Signal* **3**(151): ra87.

Boulay, A., S. Zumstein-Mecker, C. Stephan, I. Beuvink, F. Zilbermann, R. Haller, S. Tobler, C. Heusser, T. O'Reilly, B. Stolz, A. Marti, G. Thomas and H. A. Lane (2004). Antitumor efficacy of intermittent treatment schedules with the rapamycin derivative RAD001 correlates with prolonged inactivation of ribosomal protein S6 kinase 1 in peripheral blood mononuclear cells. *Cancer Res* **64**(1): 252-261.

Boulton, T. G., G. D. Yancopoulos, J. S. Gregory, C. Slaughter, C. Moomaw, J. Hsu and M. H. Cobb (1990). An insulin-stimulated protein kinase similar to yeast kinases involved in cell cycle control. *Science* **249**(4964): 64-67.

Brauch, H., G. Weirich, M. A. Hornauer, S. Storkel, T. Wohl and T. Bruning (1999). Trichloroethylene exposure and specific somatic mutations in patients with renal cell carcinoma. *J Natl Cancer Inst* **91**(10): 854-861.

Breuleux, M., M. Klopfenstein, C. Stephan, C. A. Doughty, L. Barys, S. M. Maira, D. Kwiatkowski and H. A. Lane (2009). Increased AKT S473 phosphorylation after mTORC1 inhibition is rictor dependent and does not predict tumor cell response to PI3K/mTOR inhibition. *Molecular cancer therapeutics* **8**(4): 742-753.

Britten, C. D., A. A. Adjei, R. Millham, B. E. Houk, G. Borzillo, K. Pierce, Z. A. Wainberg and P. M. LoRusso (2014). Phase I study of PF-04691502, a small-molecule, oral, dual inhibitor of PI3K and mTOR, in patients with advanced cancer. *Invest New Drugs* **32**(3): 510-517.

Brou, C., F. Logeat, N. Gupta, C. Bessia, O. LeBail, J. R. Doedens, A. Cumano, P. Roux, R. A. Black and A. Israel (2000). A novel proteolytic cleavage involved in Notch signaling: the role of the disintegrin-metalloprotease TACE. *Mol Cell* **5**(2): 207-216.

Brown, E. J., M. W. Albers, T. B. Shin, K. Ichikawa, C. T. Keith, W. S. Lane and S. L. Schreiber (1994). A mammalian protein targeted by G1-arresting rapamycin-receptor complex. *Nature* **369**(6483): 756-758.

Brugarolas, J., K. Lei, R. L. Hurley, B. D. Manning, J. H. Reiling, E. Hafen, L. A. Witters, L. W. Ellisen and W. G. Kaelin, Jr. (2004). Regulation of mTOR function in response to hypoxia by REDD1 and the TSC1/TSC2 tumor suppressor complex. *Genes Dev* **18**(23): 2893-2904.

Brunet, A., A. Bonni, M. J. Zigmond, M. Z. Lin, P. Juo, L. S. Hu, M. J. Anderson, K. C. Arden, J. Blenis and M. E. Greenberg (1999a). Akt promotes cell survival by phosphorylating and inhibiting a Forkhead transcription factor. *Cell* **96**(6): 857-868.

Brunet, A., D. Roux, P. Lenormand, S. Dowd, S. Keyse and J. Pouyssegur (1999b). Nuclear translocation of p42/p44 mitogen-activated protein kinase is required for growth factor-induced gene expression and cell cycle entry. *Embo j* **18**(3): 664-674.

Buchdunger, E., J. Zimmermann, H. Mett, T. Meyer, M. Muller, U. Regenass and N. B. Lydon (1995). Selective inhibition of the platelet-derived growth factor signal transduction pathway by a protein-tyrosine kinase inhibitor of the 2-phenylaminopyrimidine class. *Proc Natl Acad Sci U S A* **92**(7): 2558-2562.

Buck, E., A. Eyzaguirre, E. Brown, F. Petti, S. McCormack, J. D. Haley, K. K. Iwata, N. W. Gibson and G. Griffin (2006). Rapamycin synergizes with the epidermal growth factor receptor inhibitor erlotinib in non-small-cell lung, pancreatic, colon, and breast tumors. *Mol Cancer Ther* **5**(11): 2676-2684.

Buck, E., A. Eyzaguirre, M. Rosenfeld-Franklin, S. Thomson, M. Mulvihill, S. Barr, E. Brown, M. O'Connor, Y. Yao, J. Pachter, M. Miglarese, D. Epstein, K. K. Iwata, J. D. Haley, N. W. Gibson and Q. S. Ji (2008). Feedback mechanisms promote cooperativity for small molecule inhibitors of epidermal and insulin-like growth factor receptors. *Cancer Res* **68**(20): 8322-8332.

Buck, E., P. C. Gokhale, S. Koujak, E. Brown, A. Eyzaguirre, N. Tao, M. Rosenfeld-Franklin, L. Lerner, M. I. Chiu, R. Wild, D. Epstein, J. A. Pachter and M. R. Miglarese (2010). Compensatory insulin receptor (IR) activation on inhibition of insulin-like growth factor-1 receptor (IGF-1R): rationale for cotargeting IGF-1R and IR in cancer. *Molecular cancer therapeutics* **9**(10): 2652-2664.

Buck, E. and M. Mulvihill (2011). Small molecule inhibitors of the IGF-1R/IR axis for the treatment of cancer. *Expert opinion on investigational drugs* **20**(5): 605-621.

Budanov, A. V. and M. Karin (2008). p53 target genes sestrin1 and sestrin2 connect genotoxic stress and mTOR signaling. *Cell* **134**(3): 451-460.

Burris, H., J. Rodon, S. Sharma, R. S. Herbst, J. Tabernero, J. R. Infante, A. Silva, D. Demanse, W. Hacki and J. Baselga (2010). First-in-human phase I study of the oral PI3K inhibitor BEZ235 in patients (pts) with advanced solid tumors. *Journal of clinical oncology : official journal of the American Society of Clinical Oncology* **28**(15s): Abstr 3005.

Bussolati, B., S. Bruno, C. Grange, U. Ferrando and G. Camussi (2008). Identification of a tumor-initiating stem cell population in human renal carcinomas. *The FASEB Journal* **22**(10): 3696-3705.

Cairns, P. (2010). Renal cell carcinoma. *Cancer Biomark* **9**(1-6): 461-473.

Canadas, I., F. Rojo, A. Taus, O. Arpi, M. Arumi-Uria, L. Pijuan, S. Menendez, S. Zazo, M. Domine, M. Salido, S. Mojal, A. Garcia de Herreros, A. Rovira, J. Albanell and E. Arriola (2014a). Targeting epithelial-to-mesenchymal transition with Met inhibitors reverts chemoresistance in small cell lung cancer. *Clin Cancer Res* **20**(4): 938-950.

Canadas, I., A. Taus, I. Gonzalez, X. Villanueva, J. Gimeno, L. Pijuan, M. Domine, A. Sanchez-Font, I. Vollmer, S. Menendez, O. Arpi, S. Mojal, F. Rojo, A. Rovira, J. Albanell and E. Arriola (2014b). High circulating hepatocyte growth factor levels associate with epithelial to mesenchymal transition and poor outcome in small cell lung cancer patients. *Oncotarget* **5**(14): 5246-5256.

Cangiano, T., J. Liao, J. Naitoh, F. Dorey, R. Figlin and A. Belldegrun (1999). Sarcomatoid renal cell carcinoma: biologic behavior, prognosis, and response to combined surgical resection and immunotherapy. *J Clin Oncol* **17**(2): 523-528.

Carden, C. P., E. S. Kim, R. L. Jones, S. Alam, F. Jognson, A. W. Stephens, S. Poondru, R. Gedrich, S. M. Lippman and S. B. Kaye (2010). Phase I study of intemittent dosing of OSI-906, a dual tyrosine kinase inhibitor of insulin-like growfactor-1 receptor (IGF-1R) and insulin receptor (IR) in patients with advanced solid tumors. *Journal of clinical oncology : official journal of the American Society of Clinical Oncology* **28**(15s): abstr 2530.

Cardillo, T. M., P. Trisal, R. Arrojo, D. M. Goldenberg and C. H. Chang (2013). Targeting both IGF-1R and mTOR synergistically inhibits growth of renal cell carcinoma in vitro. *BMC Cancer* **13**: 170.

Carracedo, A., L. Ma, J. Teruya-Feldstein, F. Rojo, L. Salmena, A. Alimonti, A. Egia, A. T. Sasaki, G. Thomas, S. C. Kozma, A. Papa, C. Nardella, L. C. Cantley, J. Baselga and P. P. Pandolfi (2008). Inhibition of mTORC1 leads to MAPK pathway activation through a PI3K-dependent feedback loop in human cancer. *J Clin Invest* **118**(9): 3065-3074.

Casimiro, M. C., M. Velasco-Velazquez, C. Aguirre-Alvarado and R. G. Pestell (2014). Overview of cyclins D1 function in cancer and the CDK inhibitor landscape: past and present. *Expert Opin Investig Drugs* **23**(3): 295-304.

Castillo, M., A. Petit, B. Mellado, A. Palacin, J. B. Alcover and C. Mallofre (2004). C-kit expression in sarcomatoid renal cell carcinoma: potential therapy with imatinib. *The Journal of urology* **171**(6 Pt 1): 2176-2180.

Catalanotti, F., D. B. Solit, M. P. Pulitzer, M. F. Berger, S. N. Scott, T. Iyriboz, M. E. Lacouture, K. S. Panageas, J. D. Wolchok, R. D. Carvajal, G. K. Schwartz, N. Rosen and P. B. Chapman (2013). Phase II trial of MEK inhibitor selumetinib (AZD6244, ARRY-142886) in patients with BRAFV600E/K-mutated melanoma. *Clin Cancer Res* **19**(8): 2257-2264.

Cen, H., A. G. Papageorge, W. C. Vass, K. E. Zhang and D. R. Lowy (1993). Regulated and constitutive activity by CDC25Mm (GRF), a Ras-specific exchange factor. *Mol Cell Biol* **13**(12): 7718-7724.

Cha, T. L., M. J. Chuang, S. T. Wu, G. H. Sun, S. Y. Chang, D. S. Yu, S. M. Huang, S. K. Huan, T. C. Cheng, T. T. Chen, P. L. Fan and P. W. Hsiao (2009). Dual degradation of aurora A and B kinases by the histone deacetylase inhibitor LBH589 induces G2-M arrest and apoptosis of renal cancer cells. *Clin Cancer Res* **15**(3): 840-850.

Chalhoub, N. and S. J. Baker (2009). PTEN and the PI3-kinase pathway in cancer. *Annu Rev Pathol* **4**: 127-150.

Chandarlapaty, S., A. Sawai, M. Scaltriti, V. Rodrik-Outmezguine, O. Grbovic-Huezo, V. Serra, P. K. Majumder, J. Baselga and N. Rosen (2011). AKT inhibition relieves feedback suppression of receptor tyrosine kinase expression and activity. *Cancer cell* **19**(1): 58-71.

Chang, X., F. Zhang, T. Liu, C. Ji, X. Zhao, R. Yang, X. Yan, W. Wang and H. Guo (2014). Radiofrequency ablation versus partial nephrectomy for clinical T1b renal cell carcinoma: long-term clinical and oncologic outcomes. *J Urol*.

Chen, N. and J. Debnath (2010). Autophagy and tumorigenesis. *FEBS Lett* **584**(7): 1427-1435.

Chen, W., J. D. Arroyo, J. C. Timmons, R. Possemato and W. C. Hahn (2005). Cancer-associated PP2A Aalpha subunits induce functional haploinsufficiency and tumorigenicity. *Cancer Res* **65**(18): 8183-8192.

Chitnis, M. M., K. A. Lodhia, T. Aleksic, S. Gao, A. S. Protheroe and V. M. Macaulay (2013). IGF-1R inhibition enhances radiosensitivity and delays double-strand break repair by both non-homologous end-joining and homologous recombination. *Oncogene*.

Chitnis, M. M., J. S. Yuen, A. S. Protheroe, M. Pollak and V. M. Macaulay (2008). The type 1 insulin-like growth factor receptor pathway. *Clinical cancer research : an official journal of the American Association for Cancer Research* **14**(20): 6364-6370.

Chiu, C. W., H. Nozawa and D. Hanahan (2010). Survival benefit with proapoptotic molecular and pathologic responses from dual targeting of mammalian target of rapamycin and epidermal growth factor receptor in a preclinical model of pancreatic neuroendocrine carcinogenesis. *J Clin Oncol* **28**(29): 4425-4433.

Cho, D. C., M. B. Cohen, D. J. Panka, M. Collins, M. Ghebremichael, M. B. Atkins, S. Signoretti and J. W. Mier (2010). The efficacy of the novel dual PI3-kinase/mTOR inhibitor NVP-BEZ235 compared with rapamycin in renal cell carcinoma. *Clinical cancer research : an official journal of the American Association for Cancer Research* **16**(14): 3628-3638.

Choueiri, T. K., B. Escudier, T. Powles, P. N. Mainwaring, B. I. Rini, F. Donskov, H. Hammers, T. E. Hutson, J. L. Lee, K. Peltola, B. J. Roth, G. A. Bjarnason, L. Geczi, B. Keam, P. Maroto, D. Y. Heng, M. Schmidinger, P. W. Kantoff, A. Borgman-Hagey, C. Hessel, C. Scheffold, G. M. Schwab, N. M. Tannir and R. J. Motzer (2015). Cabozantinib versus Everolimus in Advanced Renal-Cell Carcinoma. *N Engl J Med*.

Choueiri, T. K., A. Plantade, P. Elson, S. Negrier, A. Ravaud, S. Oudard, M. Zhou, B. I. Rini, R. M. Bukowski and B. Escudier (2008). Efficacy of sunitinib and sorafenib in metastatic papillary and chromophobe renal cell carcinoma. *J Clin Oncol* **26**(1): 127-131.

Chresta, C. M., B. R. Davies, I. Hickson, T. Harding, S. Cosulich, S. E. Critchlow, J. P. Vincent, R. Ellston, D. Jones, P. Sini, D. James, Z. Howard, P. Dudley, G. Hughes, L. Smith, S. Maguire, M. Hummersone, K. Malagu, K. Menear, R. Jenkins, M. Jacobsen, G. C. Smith, S. Guichard and M. Pass (2010). AZD8055 is a potent, selective, and orally bioavailable ATP-competitive mammalian target of rapamycin kinase inhibitor with in vitro and in vivo antitumor activity. *Cancer Res* **70**(1): 288-298.

Christensen, J. G. (2007). A preclinical review of sunitinib, a multitargeted receptor tyrosine kinase inhibitor with anti-angiogenic and antitumour activities. *Ann Oncol* **18 Suppl 10**: x3-10.

Clark, J. I., M. B. Atkins, W. J. Urba, S. Creech, R. A. Figlin, J. P. Dutcher, L. Flaherty, J. A. Sosman, T. F. Logan, R. White, G. R. Weiss, B. G. Redman, C. P. Tretter, D. McDermott, J. W. Smith, M. S. Gordon and K. A. Margolin (2003). Adjuvant high-dose bolus interleukin-2 for patients with high-risk renal cell carcinoma: a cytokine working group randomized trial. *J Clin Oncol* **21**(16): 3133-3140.

Cloughesy, T. F., K. Yoshimoto, P. Nghiemphu, K. Brown, J. Dang, S. Zhu, T. Hsueh, Y. Chen, W. Wang, D. Youngkin, L. Liau, N. Martin, D. Becker, M. Bergsneider, A. Lai, R. Green, T. Oglesby, M. Koleto, J. Trent, S. Horvath, P. S. Mischel, I. K. Mellinghoff and C. L. Sawyers (2008). Antitumor activity of rapamycin in a Phase I trial for patients with recurrent PTEN-deficient glioblastoma. *PLoS Med* **5**(1): e8.

Cohick, W. S. and D. R. Clemmons (1993). The insulin-like growth factors. *Annu Rev Physiol* **55**: 131-153.

Coiffier, B., B. Pro, H. M. Prince, F. Foss, L. Sokol, M. Greenwood, D. Caballero, P. Borchmann, F. Morschhauser, M. Wilhelm, L. Pinter-Brown, S. Padmanabhan, A. Shustov, J. Nichols, S. Carroll, J. Balser, B. Balser and S. Horwitz (2012). Results from a pivotal, open-label, phase II study of romidepsin in relapsed or refractory peripheral T-cell lymphoma after prior systemic therapy. *J Clin Oncol* **30**(6): 631-636.

Conte, P., M. Campone, P. Pronzato, D. Amadori, R. Frank, F. Schuetz, D. Rea, A. Wardley, C. Britten and A. Elias (2009). Phase I trial of panobinostat (LBH589) in combination with trastuzumab in pretreated HER2-positive metastatic breast cancer (mBC): Preliminary safety and tolerability results. *Journal of clinical oncology : official journal of the American Society of Clinical Oncology* **27**(15s): Abstr 1081.

Cope, C. L., R. Gilley, K. Balmanno, M. J. Sale, K. D. Howarth, M. Hampson, P. D. Smith, S. M. Guichard and S. J. Cook (2014). Adaptation to mTOR kinase inhibitors by amplification of eIF4E to maintain cap-dependent translation. *J Cell Sci* **127**(Pt 4): 788-800.

Courtney, K. D., R. B. Corcoran and J. A. Engelman (2010). The PI3K pathway as drug target in human cancer. *J Clin Oncol* **28**(6): 1075-1083.

Crew, J. P., S. Fuggle, R. Bicknell, D. W. Cranston, A. de Benedetti and A. L. Harris (2000). Eukaryotic initiation factor-4E in superficial and muscle invasive bladder cancer and its correlation with vascular endothelial growth factor expression and tumour progression. *Br J Cancer* **82**(1): 161-166.

Crino, P. B., K. L. Nathanson and E. P. Henske (2006). The tuberous sclerosis complex. *N Engl J Med* **355**(13): 1345-1356.

Dabydeen, D. A., J. P. Jagannathan, N. Ramaiya, K. Krajewski, F. A. Schutz, D. C. Cho, I. Pedrosa and T. K. Choueiri (2012). Pneumonitis associated with mTOR inhibitors therapy in patients with metastatic renal cell carcinoma: incidence, radiographic findings and correlation with clinical outcome. *European journal of cancer* **48**(10): 1519-1524.

Dansen, T. B. and B. M. Burgering (2008). Unravelling the tumor-suppressive functions of FOXO proteins. *Trends Cell Biol* **18**(9): 421-429.

Darwish, O. M., P. Kapur, R. F. Youssef, A. Bagrodia, M. Belsante, F. Alhalabi, A. I. Sagalowsky, Y. Lotan and V. Margulis (2013). Cumulative number of altered biomarkers in mammalian target of rapamycin pathway is an independent predictor of outcome in patients with clear cell renal cell carcinoma. *Urology* **81**(3): 581-586.

Das, S. K. and G. Hoefler (2013). The role of triglyceride lipases in cancer associated cachexia. *Trends Mol Med* **19**(5): 292-301.

Das Thakur, M., F. Salangsang, A. S. Landman, W. R. Sellers, N. K. Pryer, M. P. Levesque, R. Dummer, M. McMahon and D. D. Stuart (2013). Modelling vemurafenib resistance in melanoma reveals a strategy to forestall drug resistance. *Nature* **494**(7436): 251-255.

Davies, B. R., H. Greenwood, P. Dudley, C. Crafter, D. H. Yu, J. Zhang, J. Li, B. Gao, Q. Ji, J. Maynard, S. A. Ricketts, D. Cross, S. Cosulich, C. C. Chresta, K. Page, J. Yates, C. Lane, R. Watson, R. Luke, D. Ogilvie and M. Pass (2012). Preclinical pharmacology of AZD5363, an inhibitor of AKT: pharmacodynamics, antitumor activity, and correlation of monotherapy activity with genetic background. *Mol Cancer Ther* **11**(4): 873-887.

Davies, H., G. R. Bignell, C. Cox, P. Stephens, S. Edkins, S. Clegg, J. Teague, H. Woffendin, M. J. Garnett, W. Bottomley, N. Davis, E. Dicks, R. Ewing, Y. Floyd, K. Gray, S. Hall, R. Hawes, J. Hughes, V. Kosmidou, A. Menzies, C. Mould, A. Parker, C. Stevens, S. Watt, S. Hooper, R. Wilson, H. Jayatilake, B. A. Gusterson, C. Cooper, J. Shipley, D. Hargrave, K. Pritchard-Jones, N. Maitland, G. Chenevix-Trench, G. J. Riggins, D. D. Bigner, G. Palmieri, A. Cossu, A. Flanagan, A. Nicholson, J. W. Ho, S. Y. Leung, S. T. Yuen, B. L. Weber, H. F. Seigler, T. L. Darrow, H. Paterson, R. Marais, C. J. Marshall, R. Wooster, M. R. Stratton and P. A. Futreal (2002). Mutations of the BRAF gene in human cancer. *Nature* **417**(6892): 949-954.

de Marinis, F., A. Atmaca, M. Tiseo, L. Giuffreda, A. Rossi, V. Gebbia, C. D'Antonio, L. Dal Zotto, S. E. Al-Batran, S. Marsoni and M. Wolf (2013). A phase II study of the histone deacetylase inhibitor panobinostat (LBH589) in pretreated patients with small-cell lung cancer. *J Thorac Oncol* **8**(8): 1091-1094.

De Meyts, P., B. Wallach, C. T. Christoffersen, B. Urso, K. Gronskov, L. J. Latus, F. Yakushiji, M. M. Ilondo and R. M. Shymko (1994). The insulin-like growth factor-I receptor. Structure, ligand-binding mechanism and signal transduction. *Horm Res* **42**(4-5): 152-169.

Delahunt, B. and J. N. Eble (1997). Papillary renal cell carcinoma: a clinicopathologic and immunohistochemical study of 105 tumors. *Mod Pathol* **10**(6): 537-544.

Demetri, G. D., M. von Mehren, C. D. Blanke, A. D. Van den Abbeele, B. Eisenberg, P. J. Roberts, M. C. Heinrich, D. A. Tuveson, S. Singer, M. Janicek, J. A. Fletcher, S. G. Silverman, S. L. Silberman, R. Capdeville, B. Kiese, B. Peng, S. Dimitrijevic, B. J. Druker, C. Corless, C. D. Fletcher and H. Joensuu (2002). Efficacy and safety of imatinib mesylate in advanced gastrointestinal stromal tumors. *N Engl J Med* **347**(7): 472-480.

Desbois-Mouthon, C., A. Baron, M. J. Blivet-Van Eggelpoel, L. Fartoux, C. Venot, F. Bladt, C. Housset and O. Rosmorduc (2009). Insulin-like growth factor-1 receptor inhibition induces a resistance mechanism via the epidermal growth factor receptor/HER3/AKT signaling pathway: rational basis for cotargeting insulin-like growth factor-1 receptor and epidermal growth factor receptor in hepatocellular carcinoma. *Clin Cancer Res* **15**(17): 5445-5456.

Di Cosmio, S., J. C. Bendell, a. Cervantes-Ruiperez, D. Roda, L. Prudkin, M. N. Stein, A. Leighton-Swayze, Y. H. Song, S. Ebbinghaus and J. Baselga (2010). A phase I study of the oral mTOR inhibitor ridaforolimus (RIDA) in combination with the IGF-1R antibody dalotozumab (DALO) in patients (pts) with advanced solid tumors. *Journal of clinical oncology : official journal of the American Society of Clinical Oncology* **28**(15s): Abstr 3008.

Di Lorenzo, G., C. Buonerba, P. Federico, P. Rescigno, M. Milella, C. Ortega, M. Aieta, C. D'Aniello, N. Longo, A. Felici, E. M. Ruggeri, G. Palmieri, C. Imbimbo, M. Aglietta, S. De Placido and V. Mirone (2010). Third-line sorafenib after sequential therapy with sunitinib and mTOR inhibitors in metastatic renal cell carcinoma. *Eur Urol* **58**(6): 906-911.

Di Lorenzo, G., G. Carteni, R. Autorino, G. Bruni, M. Tudini, M. Rizzo, M. Aieta, A. Gonnella, P. Rescigno, S. Perdona, G. Giannarini, S. Pignata, N. Longo, G. Palmieri, C. Imbimbo, M. De Laurentiis, V. Mirone, C. Ficorella and S. De Placido (2009). Phase II study of sorafenib in patients with sunitinib-refractory metastatic renal cell cancer. *J Clin Oncol* **27**(27): 4469-4474.

Diehl, J. A., M. Cheng, M. F. Roussel and C. J. Sherr (1998). Glycogen synthase kinase-3beta regulates cyclin D1 proteolysis and subcellular localization. *Genes Dev* **12**(22): 3499-3511.

Dorrello, N. V., A. Peschiaroli, D. Guardavaccaro, N. H. Colburn, N. E. Sherman and M. Pagano (2006). S6K1- and betaTRCP-mediated degradation of PDCD4 promotes protein translation and cell growth. *Science* **314**(5798): 467-471.

Doublet, J. D., M. N. Peraldi, B. Gattegno, P. Thibault and J. D. Sraer (1997). Renal cell carcinoma of native kidneys: prospective study of 129 renal transplant patients. *J Urol* **158**(1): 42-44.

Dowling, R. J., I. Topisirovic, T. Alain, M. Bidinosti, B. D. Fonseca, E. Petroulakis, X. Wang, O. Larsson, A. Selvaraj, Y. Liu, S. C. Kozma, G. Thomas and N. Sonenberg (2010). mTORC1-mediated cell proliferation, but not cell growth, controlled by the 4E-BPs. *Science* **328**(5982): 1172-1176.

Drappatz, J., E. Q. Lee, S. Hammond, S. A. Grimm, A. D. Norden, R. Beroukhim, M. Gerard, D. Schiff, A. S. Chi, T. T. Batchelor, L. M. Doherty, A. S. Ciampa, D. C. Lafrankie, S. Ruland, S. M. Snodgrass, J. J. Raizer and P. Y. Wen (2012). Phase I study of panobinostat in combination with bevacizumab for recurrent high-grade glioma. *J Neurooncol* **107**(1): 133-138.

Ducker, G. S., C. E. Atreya, J. P. Simko, Y. K. Hom, M. R. Matli, C. H. Benes, B. Hann, E. K. Nakakura, E. K. Bergsland, D. B. Donner, J. Settleman, K. M. Shokat and R. S. Warren (2013). Incomplete inhibition of phosphorylation of 4E-BP1 as a mechanism of primary resistance to ATP-competitive mTOR inhibitors. *Oncogene*.

Dulak, A. M., C. T. Gubish, L. P. Stabile, C. Henry and J. M. Siegfried (2011). HGF-independent potentiation of EGFR action by c-Met. *Oncogene* **30**(33): 3625-3635.

Dutcher, J. P., P. de Souza, D. McDermott, R. A. Figlin, A. Berkenblit, A. Thiele, M. Krygowski, A. Strahs, J. Feingold and G. Hudes (2009). Effect of temsirolimus versus interferon-alpha on outcome of patients with advanced renal cell carcinoma of different tumor histologies. *Med Oncol* **26**(2): 202-209.

Duvel, K., J. L. Yecies, S. Menon, P. Raman, A. I. Lipovsky, A. L. Souza, E. Triantafellow, Q. Ma, R. Gorski, S. Cleaver, M. G. Vander Heiden, J. P. MacKeigan, P. M. Finan, C. B. Clish, L. O. Murphy and B. D. Manning (2010). Activation of a metabolic gene regulatory network downstream of mTOR complex 1. *Mol Cell* **39**(2): 171-183.

Elfiky, A. A., S. A. Aziz, P. J. Conrad, S. Siddiqui, W. Hackl, M. Maira, C. L. Robert and H. M. Kluger (2011a). Characterization and targeting of phosphatidylinositol-3 kinase (PI3K) and mammalian target of rapamycin (mTOR) in renal cell cancer. *Journal of translational medicine* **9**: 133.

Elfiky, A. A., S. A. Aziz, P. J. Conrad, S. Siddiqui, W. Hackl, M. Maira, C. L. Robert and H. M. Kluger (2011b). Characterization and targeting of phosphatidylinositol-3 kinase (PI3K) and mammalian target of rapamycin (mTOR) in renal cell cancer. *J Transl Med* **9**: 133.

Ellis, L., S. Y. Ku, S. Ramakrishnan, E. Lasorsa, G. Azabdaftari, A. Godoy and R. Pili (2013). Combinatorial antitumor effect of HDAC and the PI3K-Akt-mTOR pathway inhibition in a Pten defecient model of prostate cancer. *Oncotarget* **4**(12): 2225-2236.

Engelman, J. A., J. Luo and L. C. Cantley (2006a). The evolution of phosphatidylinositol 3-kinases as regulators of growth and metabolism. *Nature reviews. Genetics* **7**(8): 606-619.

Engelman, J. A., T. Mukohara, K. Zejnullahu, E. Lifshits, A. M. Borras, C. M. Gale, G. N. Naumov, B. Y. Yeap, E. Jarrell, J. Sun, S. Tracy, X. Zhao, J. V. Heymach, B. E. Johnson, L. C. Cantley and P. A. Janne (2006b). Allelic dilution obscures detection of a biologically significant resistance mutation in EGFR-amplified lung cancer. *The Journal of clinical investigation* **116**(10): 2695-2706.

Engelman, J. A., K. Zejnullahu, T. Mitsudomi, Y. Song, C. Hyland, J. O. Park, N. Lindeman, C. M. Gale, X. Zhao, J. Christensen, T. Kosaka, A. J. Holmes, A. M. Rogers, F. Cappuzzo, T. Mok, C. Lee, B. E. Johnson, L. C. Cantley and P. A. Janne (2007). MET amplification leads to gefitinib resistance in lung cancer by activating ERBB3 signaling. *Science* **316**(5827): 1039-1043.

Erlich, R. B., Z. Kherrouche, D. Rickwood, L. Endo-Munoz, S. Cameron, A. Dahler, M. Hazar-Rethinam, L. M. de Long, K. Wooley, A. Guminski and N. A. Saunders (2012). Preclinical evaluation of dual PI3K-mTOR inhibitors and histone deacetylase inhibitors in head and neck squamous cell carcinoma. *Br J Cancer* **106**(1): 107-115.

Escudier, B., J. Bellmunt, S. Negrier, E. Bajetta, B. Melichar, S. Bracarda, A. Ravaud, S. Golding, S. Jethwa and V. Sneller (2010). Phase III trial of bevacizumab plus interferon alfa-2a in patients with metastatic renal cell carcinoma (AVOREN): final analysis of overall survival. *J Clin Oncol* **28**(13): 2144-2150.

Escudier, B., T. Eisen, W. M. Stadler, C. Szczylik, S. Oudard, M. Siebels, S. Negrier, C. Chevreau, E. Solska, A. A. Desai, F. Rolland, T. Demkow, T. E. Hutson, M. Gore, S. Freeman, B. Schwartz, M. Shan, R. Simantov and R. M. Bukowski (2007a). Sorafenib in advanced clear-cell renal-cell carcinoma. *N Engl J Med* **356**(2): 125-134.

Escudier, B., T. Eisen, W. M. Stadler, C. Szczylik, S. Oudard, M. Staehler, S. Negrier, C. Chevreau, A. A. Desai, F. Rolland, T. Demkow, T. E. Hutson, M. Gore, S. Anderson, G. Hofilena, M. Shan, C. Pena, C. Lathia and R. M. Bukowski (2009a). Sorafenib for treatment of renal cell carcinoma: Final efficacy and safety results of the phase III treatment approaches in renal cancer global evaluation trial. *J Clin Oncol* **27**(20): 3312-3318.

Escudier, B., A. Pluzanska, P. Koralewski, A. Ravaud, S. Bracarda, C. Szczylik, C. Chevreau, M. Filipek, B. Melichar, E. Bajetta, V. Gorbunova, J. O. Bay, I. Bodrogi, A. Jagiello-Gruszfeld and N. Moore (2007b). Bevacizumab plus interferon alfa-2a for treatment of metastatic renal cell carcinoma: a randomised, double-blind phase III trial. *Lancet* **370**(9605): 2103-2111.

Escudier, B., C. Szczylik, T. E. Hutson, T. Demkow, M. Staehler, F. Rolland, S. Negrier, N. Laferriere, U. J. Scheuring, D. Cella, S. Shah and R. M. Bukowski (2009b). Randomized phase II trial of first-line treatment with sorafenib versus interferon Alfa-2a in patients with metastatic renal cell carcinoma. *J Clin Oncol* **27**(8): 1280-1289.

Evans, T., C. Lindsay, E. Chan, B. Tait, S. Michael, S. Day, A. Stephens, A. Franke, S. Poondru and I. Puzanov (2010). Phase I dose-escalation study of continuous oral dosing of OSI-906, a dual tyrosine kinase inhibitor of insulin-like growth factor-1 receptor (IGF-1R) and insulin receptor (IR), in patients with advanced solid tumors. *Journal of clinical oncology : official journal of the American Society of Clinical Oncology* **28**(15s): abstr 2531.

Fafalios, A., J. Ma, X. Tan, J. Stoops, J. Luo, M. C. Defrances and R. Zarnegar (2011). A hepatocyte growth factor receptor (Met)-insulin receptor hybrid governs hepatic glucose metabolism. *Nat Med* **17**(12): 1577-1584.

Feldman, M. E., B. Apsel, A. Uotila, R. Loewith, Z. A. Knight, D. Ruggero and K. M. Shokat (2009). Active-site inhibitors of mTOR target rapamycin-resistant outputs of mTORC1 and mTORC2. *PLoS Biol* **7**(2): e38.

Feller, S. M., B. Knudsen and H. Hanafusa (1994). c-Abl kinase regulates the protein binding activity of c-Crk. *Embo j* **13**(10): 2341-2351.

Feng, Z., H. Zhang, A. J. Levine and S. Jin (2005). The coordinate regulation of the p53 and mTOR pathways in cells. *Proc Natl Acad Sci U S A* **102**(23): 8204-8209.

Ferrandiz-Pulido, C., E. Masferrer, A. Toll, J. Hernandez-Losa, S. Mojal, R. M. Pujol, S. Ramon y Cajal, I. de Torres and V. Garcia-Patos (2013). mTOR signaling pathway in penile squamous cell carcinoma: pmTOR and peIF4E over expression correlate with aggressive tumor behavior. *J Urol* **190**(6): 2288-2295.

Floc'h, N., C. W. Kinkade, T. Kobayashi, A. Aytes, C. Lefebvre, A. Mitrofanova, R. D. Cardiff, A. Califano, M. M. Shen and C. Abate-Shen (2012). Dual targeting of the Akt/mTOR signaling pathway inhibits castration-resistant prostate cancer in a genetically engineered mouse model. *Cancer Res* **72**(17): 4483-4493.

Foster, H., H. M. Coley, A. Goumenou, G. Pados, A. Harvey and E. Karteris (2010a). Differential expression of mTOR signalling components in drug resistance in ovarian cancer. *Anticancer Res* **30**(9): 3529-3534.

Foster, K. G., H. A. Acosta-Jaquez, Y. Romeo, B. Ekim, G. A. Soliman, A. Carriere, P. P. Roux, B. A. Ballif and D. C. Fingar (2010b). Regulation of mTOR complex 1 (mTORC1) by raptor Ser863 and multisite phosphorylation. *J Biol Chem* **285**(1): 80-94.

Fraga, M. F., E. Ballestar, A. Villar-Garea, M. Boix-Chornet, J. Espada, G. Schotta, T. Bonaldi, C. Haydon, S. Ropero, K. Petrie, N. G. Iyer, A. Perez-Rosado, E. Calvo, J. A. Lopez, A. Cano, M. J. Calasanz, D. Colomer, M. A. Piris, N. Ahn, A. Imhof, C. Caldas, T. Jenuwein and M. Esteller (2005). Loss of acetylation at Lys16 and trimethylation at Lys20 of histone H4 is a common hallmark of human cancer. *Nat Genet* **37**(4): 391-400.

Francipane, M. G. and E. Lagasse (2013). Selective targeting of human colon cancer stem-like cells by the mTOR inhibitor Torin-1. *Oncotarget* **4**(11): 1948-1962.

Friday, B. B., C. Yu, G. K. Dy, P. D. Smith, L. Wang, S. N. Thibodeau and A. A. Adjei (2008). BRAF V600E disrupts AZD6244-induced abrogation of negative feedback pathways between extracellular signal-regulated kinase and Raf proteins. *Cancer Res* **68**(15): 6145-6153.

Fukuda, R., K. Hirota, F. Fan, Y. D. Jung, L. M. Ellis and G. L. Semenza (2002). Insulin-like growth factor 1 induces hypoxia-inducible factor 1-mediated vascular endothelial growth factor expression, which is dependent on MAP kinase and phosphatidylinositol 3-kinase signaling in colon cancer cells. *J Biol Chem* **277**(41): 38205-38211.

Furge, K. A., Y. W. Zhang and G. F. Vande Woude (2000). Met receptor tyrosine kinase: enhanced signaling through adapter proteins. *Oncogene* **19**(49): 5582-5589.

Furlan, A., V. Stagni, A. Hussain, S. Richelme, F. Conti, A. Prodosmo, A. Destro, M. Roncalli, D. Barila and F. Maina (2011). Abl interconnects oncogenic Met and p53 core pathways in cancer cells. *Cell Death Differ* **18**(10): 1608-1616.

Garcia, J. A., T. E. Hutson, P. Elson, C. L. Cowey, T. Gilligan, C. Nemec, R. Dreicer, R. M. Bukowski and B. I. Rini (2010). Sorafenib in patients with metastatic renal cell carcinoma refractory to either sunitinib or bevacizumab. *Cancer* **116**(23): 5383-5390.

Garcia-Echeverria, C., M. A. Pearson, A. Marti, T. Meyer, J. Mestan, J. Zimmermann, J. Gao, J. Brueggen, H. G. Capraro, R. Cozens, D. B. Evans, D. Fabbro, P. Furet, D. G. Porta, J. Liebetanz, G. Martiny-Baron, S. Ruetz and F. Hofmann (2004). In vivo antitumor activity of NVP-AEW541-A novel, potent, and selective inhibitor of the IGF-IR kinase. *Cancer cell* **5**(3): 231-239.

Garcia-Martinez, J. M. and D. R. Alessi (2008). mTOR complex 2 (mTORC2) controls hydrophobic motif phosphorylation and activation of serum- and glucocorticoid-induced protein kinase 1 (SGK1). *Biochem J* **416**(3): 375-385.

Gemmill, R. M., M. Zhou, L. Costa, C. Korch, R. M. Bukowski and H. A. Drabkin (2005). Synergistic growth inhibition by Iressa and Rapamycin is modulated by VHL mutations in renal cell carcinoma. *Br J Cancer* **92**(12): 2266-2277.

Gerlinger, M., S. Horswell, J. Larkin, A. J. Rowan, M. P. Salm, I. Varela, R. Fisher, N. McGranahan, N. Matthews, C. R. Santos, P. Martinez, B. Phillimore, S. Begum, A. Rabinowitz, B. Spencer-Dene, S. Gulati, P. A. Bates, G. Stamp, L. Pickering, M. Gore, D. L. Nicol, S. Hazell, P. A. Futreal, A. Stewart and C. Swanton (2014). Genomic architecture and evolution of clear cell renal cell carcinomas defined by multiregion sequencing. *Nat Genet* **46**(3): 225-233.

Gerlinger, M., A. J. Rowan, S. Horswell, J. Larkin, D. Endesfelder, E. Gronroos, P. Martinez, N. Matthews, A. Stewart, P. Tarpey, I. Varela, B. Phillimore, S. Begum, N. Q. McDonald, A. Butler, D. Jones, K. Raine, C. Latimer, C. R. Santos, M. Nohadani, A. C. Eklund, B. Spencer-Dene, G. Clark, L. Pickering, G. Stamp, M. Gore, Z. Szallasi, J. Downward, P. A. Futreal and C. Swanton (2012). Intratumor heterogeneity and branched evolution revealed by multiregion sequencing. *N Engl J Med* **366**(10): 883-892.

Gibney, G. T., S. A. Aziz, R. L. Camp, P. Conrad, B. E. Schwartz, C. R. Chen, W. K. Kelly and H. M. Kluger (2013). c-Met is a prognostic marker and potential therapeutic target in clear cell renal cell carcinoma. *Annals of oncology : official journal of the European Society for Medical Oncology / ESMO* **24**(2): 343-349.

Gill, I. S., S. F. Matin, M. M. Desai, J. H. Kaouk, A. Steinberg, E. Mascha, J. Thornton, M. H. Sherief, B. Strzempkowski and A. C. Novick (2003). Comparative analysis of laparoscopic versus open partial nephrectomy for renal tumors in 200 patients. *J Urol* **170**(1): 64-68.

Gleave, M. E., M. Elhilali, Y. Fradet, I. Davis, P. Venner, F. Saad, L. H. Klotz, M. J. Moore, V. Paton and A. Bajamonde (1998). Interferon gamma-1b compared with placebo in metastatic renal-cell carcinoma. Canadian Urologic Oncology Group. *N Engl J Med* **338**(18): 1265-1271.

Glozak, M. A. and E. Seto (2007). Histone deacetylases and cancer. *Oncogene* **26**(37): 5420-5432.

Gnarra, J. R., K. Tory, Y. Weng, L. Schmidt, M. H. Wei, H. Li, F. Latif, S. Liu, F. Chen, F. M. Duh and et al. (1994). Mutations of the VHL tumour suppressor gene in renal carcinoma. *Nature genetics* **7**(1): 85-90.

Gold, P. J., D. A. Smith, D. Iriarte, B. Boatman and H. G. Kaplan (2012). Phase II trial of panobinostat (LBH589) in patients (pts) with refractory metastatic colorectal cancer (MCRC). *Journal of clinical oncology : official journal of the American Society of Clinical Oncology* **30**(suppl 4): Abstr 582.

Gomez, N. and P. Cohen (1991). Dissection of the protein kinase cascade by which nerve growth factor activates MAP kinases. *Nature* **353**(6340): 170-173.

Grabiner, B. C., V. Nardi, K. Birsoy, R. Possemato, K. Shen, S. Sinha, A. Jordan, A. H. Beck and D. M. Sabatini (2014). A diverse array of cancer-associated MTOR mutations are hyperactivating and can predict rapamycin sensitivity. *Cancer Discov* **4**(5): 554-563.

Greuber, E. K., P. Smith-Pearson, J. Wang and A. M. Pendergast (2013). Role of ABL family kinases in cancer: from leukaemia to solid tumours. *Nature reviews. Cancer* **13**(8): 559-571.

Gross, J. D., N. J. Moerke, T. von der Haar, A. A. Lugovskoy, A. B. Sachs, J. E. McCarthy and G. Wagner (2003). Ribosome loading onto the mRNA cap is driven by conformational coupling between eIF4G and eIF4E. *Cell* **115**(6): 739-750.

Gu, W. and R. G. Roeder (1997). Activation of p53 sequence-specific DNA binding by acetylation of the p53 C-terminal domain. *Cell* **90**(4): 595-606.

Guan, L., K. Song, M. A. Pysz, K. J. Curry, A. A. Hizli, D. Danielpour, A. R. Black and J. D. Black (2007). Protein Kinase C-mediated Down-regulation of Cyclin D1 Involves Activation of the Translational Repressor 4E-BP1 via a Phosphoinositide 3-Kinase/Akt-independent, Protein Phosphatase 2A-dependent Mechanism in Intestinal Epithelial Cells. *Journal of Biological Chemistry* **282**(19): 14213-14225.

Guertin, D. A. and D. M. Sabatini (2009). The pharmacology of mTOR inhibition. *Science signaling* **2**(67): pe24.

Guertin, D. A., D. M. Stevens, C. C. Thoreen, A. A. Burds, N. Y. Kalaany, J. Moffat, M. Brown, K. J. Fitzgerald and D. M. Sabatini (2006). Ablation in mice of the mTORC components raptor, rictor, or mLST8 reveals that mTORC2 is required for signaling to Akt-FOXO and PKCalpha, but not S6K1. *Dev Cell* **11**(6): 859-871.

Guevara-Aguirre, J., P. Balasubramanian, M. Guevara-Aguirre, M. Wei, F. Madia, C. W. Cheng, D. Hwang, A. Martin-Montalvo, J. Saavedra, S. Ingles, R. de Cabo, P. Cohen and V. D. Longo (2011). Growth hormone receptor deficiency is associated with a major reduction in pro-aging signaling, cancer, and diabetes in humans. *Sci Transl Med* **3**(70): 70ra13.

Guo, Y., K. Yang, J. Harwalkar, J. M. Nye, D. R. Mason, M. D. Garrett, M. Hitomi and D. W. Stacey (2005). Phosphorylation of cyclin D1 at Thr 286 during S phase leads to its proteasomal degradation and allows efficient DNA synthesis. *Oncogene* **24**(16): 2599-2612.

Gupta, M., S. M. Ansell, A. J. Novak, S. Kumar, S. H. Kaufmann and T. E. Witzig (2009). Inhibition of histone deacetylase overcomes rapamycin-mediated resistance in diffuse large B-cell lymphoma by inhibiting Akt signaling through mTORC2. *Blood* **114**(14): 2926-2935.

Gwinn, D. M., D. B. Shackelford, D. F. Egan, M. M. Mihaylova, A. Mery, D. S. Vasquez, B. E. Turk and R. J. Shaw (2008). AMPK phosphorylation of raptor mediates a metabolic checkpoint. *Mol Cell* **30**(2): 214-226.

Hainsworth, J. D., J. R. Infante, D. R. Spigel, E. R. Arrowsmith, R. V. Boccia and H. A. Burris (2011). A phase II trial of panobinostat, a histone deacetylase inhibitor, in the treatment of patients with refractory metastatic renal cell carcinoma. *Cancer Invest* **29**(7): 451-455.

Hainsworth, J. D., D. R. Spigel, J. A. Sosman, H. A. Burris, 3rd, C. Farley, H. Cucullu, K. Yost, L. L. Hart, L. Sylvester, D. M. Waterhouse and F. A. Greco (2007). Treatment of advanced renal cell carcinoma with the combination bevacizumab/erlotinib/imatinib: a phase I/II trial. *Clinical genitourinary cancer* **5**(7): 427-432.

Haluska, P., H. M. Shaw, G. N. Batzel, D. Yin, J. R. Molina, L. R. Molife, T. A. Yap, M. L. Roberts, A. Sharma, A. Gualberto, A. A. Adjei and J. S. de Bono (2007). Phase I dose escalation study of the anti insulin-like growth factor-I receptor monoclonal antibody

CP-751,871 in patients with refractory solid tumors. *Clin Cancer Res* **13**(19): 5834-5840.

Hanahan, D. and R. A. Weinberg (2000). The hallmarks of cancer. *Cell* **100**(1): 57-70.

Hanahan, D. and R. A. Weinberg (2011). Hallmarks of cancer: the next generation. *Cell* **144**(5): 646-674.

Hankinson, S. E., W. C. Willett, G. A. Colditz, D. J. Hunter, D. S. Michaud, B. Deroo, B. Rosner, F. E. Speizer and M. Pollak (1998). Circulating concentrations of insulin-like growth factor-I and risk of breast cancer. *Lancet* **351**(9113): 1393-1396.

Hara, K., Y. Maruki, X. Long, K. Yoshino, N. Oshiro, S. Hidayat, C. Tokunaga, J. Avruch and K. Yonezawa (2002). Raptor, a binding partner of target of rapamycin (TOR), mediates TOR action. *Cell* **110**(2): 177-189.

Heesom, K. J. and R. M. Denton (1999). Dissociation of the eukaryotic initiation factor-4E/4E-BP1 complex involves phosphorylation of 4E-BP1 by an mTOR-associated kinase. *FEBS Lett* **457**(3): 489-493.

Heesom, K. J., A. Gampel, H. Mellor and R. M. Denton (2001). Cell cycle-dependent phosphorylation of the translational repressor eIF-4E binding protein-1 (4E-BP1). *Curr Biol* **11**(17): 1374-1379.

Heikkinen, T., T. Korpela, R. Fagerholm, S. Khan, K. Aittomaki, P. Heikkila, C. Blomqvist, O. Carpen and H. Nevanlinna (2013). Eukaryotic translation initiation factor 4E (eIF4E) expression is associated with breast cancer tumor phenotype and predicts survival after anthracycline chemotherapy treatment. *Breast Cancer Res Treat* **141**(1): 79-88.

Heitman, J., N. R. Movva and M. N. Hall (1991). Targets for cell cycle arrest by the immunosuppressant rapamycin in yeast. *Science* **253**(5022): 905-909.

Heng, D. Y., J. C. Wells, B. I. Rini, B. Beuselinck, J. L. Lee, J. J. Knox, G. A. Bjarnason, S. K. Pal, C. K. Kollmannsberger, T. Yuasa, S. Srinivas, F. Donskov, A. Bamias, L. A. Wood, D. S. Ernst, N. Agarwal, U. N. Vaishampayan, S. Y. Rha, J. J. Kim and T. K. Choueiri (2014). Cytoreductive Nephrectomy in Patients with Synchronous Metastases from Renal Cell Carcinoma: Results from the International Metastatic Renal Cell Carcinoma Database Consortium. *Eur Urol*.

Herbert, T. P., A. R. Tee and C. G. Proud (2002). The extracellular signal-regulated kinase pathway regulates the phosphorylation of 4E-BP1 at multiple sites. *The Journal of biological chemistry* **277**(13): 11591-11596.

Herman, J. G., F. Latif, Y. Weng, M. I. Lerman, B. Zbar, S. Liu, D. Samid, D. S. Duan, J. R. Gnarra, W. M. Linehan and et al. (1994). Silencing of the VHL tumor-suppressor gene by DNA methylation in renal carcinoma. *Proceedings of the National Academy of Sciences of the United States of America* **91**(21): 9700-9704.

Ho, A. L., S. D. Vasudeva, M. Lae, T. Saito, V. Barbashina, C. R. Antonescu, M. Ladanyi and G. K. Schwartz (2012). PDGF receptor alpha is an alternative mediator of rapamycin-induced Akt activation: implications for combination targeted therapy of synovial sarcoma. *Cancer Res* **72**(17): 4515-4525.

Holt, L. J. and K. Siddle (2005). Grb10 and Grb14: enigmatic regulators of insulin action--and more? *Biochem J* **388**(Pt 2): 393-406.

Hosokawa, N., T. Hara, T. Kaizuka, C. Kishi, A. Takamura, Y. Miura, S. Iemura, T. Natsume, K. Takehana, N. Yamada, J. L. Guan, N. Oshiro and N. Mizushima (2009). Nutrient-dependent mTORC1 association with the ULK1-Atg13-FIP200 complex required for autophagy. *Mol Biol Cell* **20**(7): 1981-1991.

Hsu, P. P., S. A. Kang, J. Rameseder, Y. Zhang, K. A. Ottina, D. Lim, T. R. Peterson, Y. Choi, N. S. Gray, M. B. Yaffe, J. A. Marto and D. M. Sabatini (2011). The mTOR-regulated phosphoproteome reveals a mechanism of mTORC1-mediated inhibition of growth factor signaling. *Science* **332**(6035): 1317-1322.

Huang, J., C. C. Dibble, M. Matsuzaki and B. D. Manning (2008). The TSC1-TSC2 complex is required for proper activation of mTOR complex 2. *Mol Cell Biol* **28**(12): 4104-4115.

Hudes, G., M. Carducci, P. Tomczak, J. Dutcher, R. Figlin, A. Kapoor, E. Staroslawska, J. Sosman, D. McDermott, I. Bodrogi, Z. Kovacevic, V. Lesovoy, I. G. Schmidt-Wolf, O. Barbarash, E. Gokmen, T. O'Toole, S. Lustgarten, L. Moore and R. J. Motzer (2007). Temsirolimus, interferon alfa, or both for advanced renal-cell carcinoma. *The New England journal of medicine* **356**(22): 2271-2281.

Hudson, C. C., M. Liu, G. G. Chiang, D. M. Otterness, D. C. Loomis, F. Kaper, A. J. Giaccia and R. T. Abraham (2002). Regulation of hypoxia-inducible factor 1alpha expression and function by the mammalian target of rapamycin. *Mol Cell Biol* **22**(20): 7004-7014.

Hutson, T. E., B. Escudier, E. Esteban, G. A. Bjarnason, H. Y. Lim, K. B. Pittman, P. Senico, A. Niethammer, D. R. Lu, S. Hariharan and R. J. Motzer (2014). Randomized phase III trial of temsirolimus versus sorafenib as second-line therapy after sunitinib in patients with metastatic renal cell carcinoma. *J Clin Oncol* **32**(8): 760-767.

Ikenoue, T., K. Inoki, Q. Yang, X. Zhou and K. L. Guan (2008). Essential function of TORC2 in PKC and Akt turn motif phosphorylation, maturation and signalling. *Embo j* **27**(14): 1919-1931.

Ilic, N., T. Utermark, H. R. Widlund and T. M. Roberts (2011). PI3K-targeted therapy can be evaded by gene amplification along the MYC-eukaryotic translation initiation factor 4E (eIF4E) axis. *Proc Natl Acad Sci U S A* **108**(37): E699-708.

Iliopoulos, O., A. Kibel, S. Gray and W. G. Kaelin, Jr. (1995). Tumour suppression by the human von Hippel-Lindau gene product. *Nat Med* **1**(8): 822-826.

Imai, Y., S. Gehrke, H. Q. Wang, R. Takahashi, K. Hasegawa, E. Oota and B. Lu (2008). Phosphorylation of 4E-BP by LRRK2 affects the maintenance of dopaminergic neurons in Drosophila. *The EMBO journal* **27**(18): 2432-2443.

Imura, Y., H. Yasui, H. Outani, T. Wakamatsu, K. Hamada, T. Nakai, S. Yamada, A. Myoui, N. Araki, T. Ueda, K. Itoh, H. Yoshikawa and N. Naka (2014). Combined targeting of mTOR and c-MET signaling pathways for effective management of epithelioid sarcoma. *Mol Cancer* **13**(1): 185.

Ingolia, N. T., S. Ghaemmaghami, J. R. Newman and J. S. Weissman (2009). Genome-wide analysis in vivo of translation with nucleotide resolution using ribosome profiling. *Science* **324**(5924): 218-223.

Inoki, K., Y. Li, T. Xu and K. L. Guan (2003a). Rheb GTPase is a direct target of TSC2 GAP activity and regulates mTOR signaling. *Genes Dev* **17**(15): 1829-1834.

Inoki, K., Y. Li, T. Zhu, J. Wu and K. L. Guan (2002). TSC2 is phosphorylated and inhibited by Akt and suppresses mTOR signalling. *Nat Cell Biol* **4**(9): 648-657.

Inoki, K., T. Zhu and K. L. Guan (2003b). TSC2 mediates cellular energy response to control cell growth and survival. *Cell* **115**(5): 577-590.

Islam, F., B. Qiao, R. A. Smith, V. Gopalan and A. K. Lam (2015). Cancer stem cell: Fundamental experimental pathological concepts and updates. *Exp Mol Pathol*.

Jacinto, E., V. Facchinetti, D. Liu, N. Soto, S. Wei, S. Y. Jung, Q. Huang, J. Qin and B. Su (2006). SIN1/MIP1 maintains rictor-mTOR complex integrity and regulates Akt phosphorylation and substrate specificity. *Cell* **127**(1): 125-137.

Jacinto, E., R. Loewith, A. Schmidt, S. Lin, M. A. Ruegg, A. Hall and M. N. Hall (2004). Mammalian TOR complex 2 controls the actin cytoskeleton and is rapamycin insensitive. *Nat Cell Biol* **6**(11): 1122-1128.

Janiszewska, A. D., S. Poletajew and A. Wasiutyński (2013). Spontaneous regression of renal cell carcinoma. *Contemp Oncol (Pozn)* **17**(2): 123-127.

Janku, F., H. J. Huang, L. S. Angelo and R. Kurzrock (2013). A kinase-independent biological activity for insulin growth factor-1 receptor (IGF-1R) : implications for inhibition of the IGF-1R signal. *Oncotarget* **4**(3): 463-473.

Janowitz, T., S. J. Welsh, K. Zaki, P. Mulders and T. Eisen (2013). Adjuvant therapy in renal cell carcinoma-past, present, and future. *Semin Oncol* **40**(4): 482-491.

Jonasch, E., P. Corn, L. C. Pagliaro, C. L. Warneke, M. M. Johnson, P. Tamboli, C. Ng, A. Aparicio, R. G. Ashe, J. J. Wright and N. M. Tannir (2010). Upfront, randomized, phase 2 trial of sorafenib versus sorafenib and low-dose interferon alfa in patients with advanced renal cell carcinoma: clinical and biomarker analysis. *Cancer* **116**(1): 57-65.

Jonasch, E., J. Gao and W. K. Rathmell (2014). Renal cell carcinoma. *Bmj* **349**: g4797.

Jones, R. M., J. Branda, K. A. Johnston, M. Polymenis, M. Gadd, A. Rustgi, L. Callanan and E. V. Schmidt (1996). An essential E box in the promoter of the gene encoding the mRNA cap-binding protein (eukaryotic initiation factor 4E) is a target for activation by c-myc. *Mol Cell Biol* **16**(9): 4754-4764.

Kaizuka, T., T. Hara, N. Oshiro, U. Kikkawa, K. Yonezawa, K. Takehana, S. Iemura, T. Natsume and N. Mizushima (2010). Tti1 and Tel2 are critical factors in mammalian target of rapamycin complex assembly. *J Biol Chem* **285**(26): 20109-20116.

Kantidakis, T., B. A. Ramsbottom, J. L. Birch, S. N. Dowding and R. J. White (2010). mTOR associates with TFIIIC, is found at tRNA and 5S rRNA genes, and targets their repressor Maf1. *Proc Natl Acad Sci U S A* **107**(26): 11823-11828.

Katz, M., I. Amit and Y. Yarden (2007). Regulation of MAPKs by growth factors and receptor tyrosine kinases. *Biochim Biophys Acta* **1773**(8): 1161-1176.

Kavolius, J. P., D. P. Mastorakos, C. Pavlovich, P. Russo, M. E. Burt and M. S. Brady (1998). Resection of metastatic renal cell carcinoma. *J Clin Oncol* **16**(6): 2261-2266.

Kim, D. H., D. D. Sarbassov, S. M. Ali, J. E. King, R. R. Latek, H. Erdjument-Bromage, P. Tempst and D. M. Sabatini (2002). mTOR interacts with raptor to form a nutrient-sensitive complex that signals to the cell growth machinery. *Cell* **110**(2): 163-175.

Kim, D. H., D. D. Sarbassov, S. M. Ali, R. R. Latek, K. V. Guntur, H. Erdjument-Bromage, P. Tempst and D. M. Sabatini (2003). GbetaL, a positive regulator of the rapamycin-sensitive pathway required for the nutrient-sensitive interaction between raptor and mTOR. *Mol Cell* **11**(4): 895-904.

King, H., T. Aleksic, P. Haluska and V. M. Macaulay (2014). Can we unlock the potential of IGF-1R inhibition in cancer therapy? *Cancer Treat Rev*.

Klose, R. J., Q. Yan, Z. Tothova, K. Yamane, H. Erdjument-Bromage, P. Tempst, D. G. Gilliland, Y. Zhang and W. G. Kaelin, Jr. (2007). The retinoblastoma binding protein RBP2 is an H3K4 demethylase. *Cell* **128**(5): 889-900.

Knight, Z. A., B. Gonzalez, M. E. Feldman, E. R. Zunder, D. D. Goldenberg, O. Williams, R. Loewith, D. Stokoe, A. Balla, B. Toth, T. Balla, W. A. Weiss, R. L. Williams and K. M. Shokat (2006). A pharmacological map of the PI3-K family defines a role for p110alpha in insulin signaling. *Cell* **125**(4): 733-747.

Kobayashi, M., M. Nishita, T. Mishima, K. Ohashi and K. Mizuno (2006). MAPKAPK-2-mediated LIM-kinase activation is critical for VEGF-induced actin remodeling and cell migration. *Embo j* **25**(4): 713-726.

Kobayashi, S., T. J. Boggon, T. Dayaram, P. A. Janne, O. Kocher, M. Meyerson, B. E. Johnson, M. J. Eck, D. G. Tenen and B. Halmos (2005a). EGFR mutation and resistance of non-small-cell lung cancer to gefitinib. *N Engl J Med* **352**(8): 786-792.

Kobayashi, S., H. Ji, Y. Yuza, M. Meyerson, K. K. Wong, D. G. Tenen and B. Halmos (2005b). An alternative inhibitor overcomes resistance caused by a mutation of the epidermal growth factor receptor. *Cancer Res* **65**(16): 7096-7101.

Koh, Y., H. Y. Lim, J. H. Ahn, J. L. Lee, S. Y. Rha, Y. J. Kim, T. M. Kim and S. H. Lee (2013). Phase II trial of everolimus for the treatment of nonclear-cell renal cell carcinoma. *Ann Oncol* **24**(4): 1026-1031.

Kontovinis, L., K. Laschos, A. Karadimou, C. Andreadis, A. Bamias, P. Paraskevopoulos, M. Dimopoulos and K. Papazisis (2012). Sequential treatment with sorafenib and sunitinib in metastatic renal cell carcinoma: clinical outcomes from a retrospective clinical study. *Med Oncol* **29**(2): 750-754.

Krebs, L. T., Y. Xue, C. R. Norton, J. R. Shutter, M. Maguire, J. P. Sundberg, D. Gallahan, V. Closson, J. Kitajewski, R. Callahan, G. H. Smith, K. L. Stark and T. Gridley (2000). Notch signaling is essential for vascular morphogenesis in mice. *Genes Dev* **14**(11): 1343-1352.

Krueger, D. A., M. M. Care, K. Holland, K. Agricola, C. Tudor, P. Mangeshkar, K. A. Wilson, A. Byars, T. Sahmoud and D. N. Franz (2010). Everolimus for subependymal giant-cell astrocytomas in tuberous sclerosis. *N Engl J Med* **363**(19): 1801-1811.

Krusche, C. A., P. Wulfing, C. Kersting, A. Vloet, W. Bocker, L. Kiesel, H. M. Beier and J. Alfer (2005). Histone deacetylase-1 and -3 protein expression in human breast cancer: a tissue microarray analysis. *Breast Cancer Res Treat* **90**(1): 15-23.

Ku, H. and K. E. Meier (2000). Phosphorylation of paxillin via the ERK mitogen-activated protein kinase cascade in EL4 thymoma cells. *J Biol Chem* **275**(15): 11333-11340.

Kuo, Y. C., K. Y. Huang, C. H. Yang, Y. S. Yang, W. Y. Lee and C. W. Chiang (2008). Regulation of phosphorylation of Thr-308 of Akt, cell proliferation, and survival by the B55alpha regulatory subunit targeting of the protein phosphatase 2A holoenzyme to Akt. *J Biol Chem* **283**(4): 1882-1892.

Kurmasheva, R. T., L. Dudkin, C. Billups, L. V. Debelenko, C. L. Morton and P. J. Houghton (2009). The insulin-like growth factor-1 receptor-targeting antibody, CP-751,871, suppresses tumor-derived VEGF and synergizes with rapamycin in models of childhood sarcoma. *Cancer Res* **69**(19): 7662-7671.

Kyriakis, J. M., H. App, X. F. Zhang, P. Banerjee, D. L. Brautigan, U. R. Rapp and J. Avruch (1992). Raf-1 activates MAP kinase-kinase. *Nature* **358**(6385): 417-421.

Langer, C. J., S. Novello, K. Park, M. Krzakowski, D. D. Karp, T. Mok, R. J. Benner, J. R. Scranton, A. J. Olszanski and J. Jassem (2014). Randomized, phase III trial of first-line figitumumab in combination with paclitaxel and carboplatin versus paclitaxel and carboplatin alone in patients with advanced non-small-cell lung cancer. *J Clin Oncol* **32**(19): 2059-2066.

Laplante, M. and D. M. Sabatini (2012). mTOR signaling in growth control and disease. *Cell* **149**(2): 274-293.

Latif, F., K. Tory, J. Gnarra, M. Yao, F. M. Duh, M. L. Orcutt, T. Stackhouse, I. Kuzmin, W. Modi, L. Geil and et al. (1993). Identification of the von Hippel-Lindau disease tumor suppressor gene. *Science* **260**(5112): 1317-1320.

Lazaris-Karatzas, A., K. S. Montine and N. Sonenberg (1990). Malignant transformation by a eukaryotic initiation factor subunit that binds to mRNA 5' cap. *Nature* **345**(6275): 544-547.

Lee, J. W., J. J. Choi, K. M. Lee, C. H. Choi, T. J. Kim, J. H. Lee, B. G. Kim, G. Ahn, S. Y. Song and D. S. Bae (2005). eIF-4E expression is associated with histopathologic grades in cervical neoplasia. *Hum Pathol* **36**(11): 1197-1203.

Li, G., X. D. Ji, H. Gao, J. S. Zhao, J. F. Xu, Z. J. Sun, Y. Z. Deng, S. Shi, Y. X. Feng, Y. Q. Zhu, T. Wang, J. J. Li and D. Xie (2012a). EphB3 suppresses non-small-cell lung cancer metastasis via a PP2A/RACK1/Akt signalling complex. *Nat Commun* **3**: 667.

Li, H., X. Jin, Z. Zhang, Y. Xing and X. Kong (2012b). Inhibition of autophagy enhances apoptosis induced by the PI3K/AKT/mTor inhibitor NVP-BEZ235 in renal cell carcinoma cells. *Cell Biochem Funct*.

Li, J., C. Yen, D. Liaw, K. Podsypanina, S. Bose, S. I. Wang, J. Puc, C. Miliaresis, L. Rodgers, R. McCombie, S. H. Bigner, B. C. Giovanella, M. Ittmann, B. Tycko, H. Hibshoosh, M. H. Wigler and R. Parsons (1997). PTEN, a putative protein tyrosine phosphatase gene mutated in human brain, breast, and prostate cancer. *Science* **275**(5308): 1943-1947.

Lin, S. P., Y. T. Lee, J. Y. Wang, S. A. Miller, S. H. Chiou, M. C. Hung and S. C. Hung (2012). Survival of cancer stem cells under hypoxia and serum depletion via decrease in PP2A activity and activation of p38-MAPKAPK2-Hsp27. *PLoS One* **7**(11): e49605.

Lin, T. C., Y. P. Liu, Y. C. Chan, C. Y. Su, Y. F. Lin, S. L. Hsu, C. S. Yang and M. Hsiao (2015). Ghrelin promotes renal cell carcinoma metastasis via Snail activation and is associated with poor prognosis. *J Pathol*.

Linehan, W. M., R. Srinivasan and J. A. Garcia (2013). Non-clear cell renal cancer: disease-based management and opportunities for targeted therapeutic approaches. *Semin Oncol* **40**(4): 511-520.

Liu, B., L. Yang, B. Huang, M. Cheng, H. Wang, Y. Li, D. Huang, J. Zheng, Q. Li, X. Zhang, W. Ji, Y. Zhou and J. Lu (2012). A functional copy-number variation in MAPKAPK2 predicts risk and prognosis of lung cancer. *Am J Hum Genet* **91**(2): 384-390.

Liu, J., P. D. Stevens, N. E. Eshleman and T. Gao (2013a). Protein phosphatase PPM1G regulates protein translation and cell growth by dephosphorylating 4E binding protein 1 (4E-BP1). *The Journal of biological chemistry* **288**(32): 23225-23233.

Liu, Q., C. Xu, S. Kirubakaran, X. Zhang, W. Hur, Y. Liu, N. P. Kwiatkowski, J. Wang, K. D. Westover, P. Gao, D. Ercan, M. Niepel, C. C. Thoreen, S. A. Kang, M. P. Patricelli, Y. Wang, T. Tupper, A. Altabef, H. Kawamura, K. D. Held, D. M. Chou, S. J. Elledge, P. A. Janne, K. K. Wong, D. M. Sabatini and N. S. Gray (2013b). Characterization of Torin2, an ATP-competitive inhibitor of mTOR, ATM, and ATR. *Cancer Res* **73**(8): 2574-2586.

Liu, S., X. Ma, Q. Ai, Q. Huang, T. Shi, M. Zhu, B. Wang and X. Zhang (2013c). NOTCH1 functions as an oncogene by regulating the PTEN/PI3K/AKT pathway in clear cell renal cell carcinoma. *Urol Oncol* **31**(6): 938-948.

Liu, X., Q. Wang, G. Yang, C. Marando, H. K. Koblish, L. M. Hall, J. S. Fridman, E. Behshad, R. Wynn, Y. Li, J. Boer, S. Diamond, C. He, M. Xu, J. Zhuo, W. Yao, R. C. Newton and P. A. Scherle (2011). A novel kinase inhibitor, INCB28060, blocks c-MET-dependent signaling, neoplastic activities, and cross-talk with EGFR and HER-3. *Clinical cancer research : an official journal of the American Association for Cancer Research* **17**(22): 7127-7138.

Livingstone, M. and M. Bidinosti (2012). Rapamycin-insensitive mTORC1 activity controls eIF4E:4E-BP1 binding. *F1000Res* **1**: 4.

Ljungberg, B., S. C. Campbell, H. Y. Choi, D. Jacqmin, J. E. Lee, S. Weikert and L. A. Kiemeney (2011). The epidemiology of renal cell carcinoma. *Eur Urol* **60**(4): 615-621.

Ljungberg, B., N. C. Cowan, D. C. Hanbury, M. Hora, M. A. Kuczyk, A. S. Merseburger, J. J. Patard, P. F. Mulders and I. C. Sinescu (2010). EAU guidelines on renal cell carcinoma: the 2010 update. *Eur Urol* **58**(3): 398-406.

Lo, Y. H., P. C. Ho, H. Zhao and S. C. Wang (2011). Inhibition of c-ABL sensitizes breast cancer cells to the dual ErbB receptor tyrosine kinase inhibitor lapatinib (GW572016). *Anticancer Res* **31**(3): 789-795.

Locke, J. A., E. S. Guns, M. L. Lehman, S. Ettinger, A. Zoubeidi, A. Lubik, K. Margiotti, L. Fazli, H. Adomat, K. M. Wasan, M. E. Gleave and C. C. Nelson (2010). Arachidonic acid activation of intratumoral steroid synthesis during prostate cancer progression to castration resistance. *Prostate* **70**(3): 239-251.

Longati, P., A. Bardelli, C. Ponzetto, L. Naldini and P. M. Comoglio (1994). Tyrosines1234-1235 are critical for activation of the tyrosine kinase encoded by the MET proto-oncogene (HGF receptor). *Oncogene* **9**(1): 49-57.

Luo, J., M. Li, Y. Tang, M. Laszkowska, R. G. Roeder and W. Gu (2004). Acetylation of p53 augments its site-specific DNA binding both in vitro and in vivo. *Proc Natl Acad Sci U S A* **101**(8): 2259-2264.

Luo, J., F. Su, D. Chen, A. Shiloh and W. Gu (2000). Deacetylation of p53 modulates its effect on cell growth and apoptosis. *Nature* **408**(6810): 377-381.

Lynch, T. J., D. W. Bell, R. Sordella, S. Gurubhagavatula, R. A. Okimoto, B. W. Brannigan, P. L. Harris, S. M. Haserlat, J. G. Supko, F. G. Haluska, D. N. Louis, D. C.

Christiani, J. Settleman and D. A. Haber (2004). Activating mutations in the epidermal growth factor receptor underlying responsiveness of non-small-cell lung cancer to gefitinib. *N Engl J Med* **350**(21): 2129-2139.

Ma, C. X., V. J. Suman, M. Goetz, P. Haluska, T. Moynihan, R. Nanda, O. Olopade, T. Pluard, Z. Guo, H. X. Chen, C. Erlichman, M. J. Ellis and G. F. Fleming (2013). A phase I trial of the IGF-1R antibody Cixutumumab in combination with temsirolimus in patients with metastatic breast cancer. *Breast cancer research and treatment* **139**(1): 145-153.

Ma, L., Z. Chen, H. Erdjument-Bromage, P. Tempst and P. P. Pandolfi (2005). Phosphorylation and functional inactivation of TSC2 by Erk implications for tuberous sclerosis and cancer pathogenesis. *Cell* **121**(2): 179-193.

Macaulay, V. M., M. R. Middleton, S. G. Eckardt, R. A. Juergens, C. A. Rudin, A. Manukyants, S. Gogov, S. Poondru, R. Gedrich and S. M. Gadgeel (2011). Phase I study of OSI-906, dual tyrosine kinase inhibitor of insulin-like growth factor-1 receptor (IGF-1R) and insulin receptor (IR) in combination with erlotinib (E) in patients with advanced solid tumours. *Journal of clinical oncology : official journal of the American Society of Clinical Oncology* **29**(suppl).

Maira, S. M., S. Pecchi, A. Huang, M. Burger, M. Knapp, D. Sterker, C. Schnell, D. Guthy, T. Nagel, M. Wiesmann, S. Brachmann, C. Fritsch, M. Dorsch, P. Chene, K. Shoemaker, A. De Pover, D. Menezes, G. Martiny-Baron, D. Fabbro, C. J. Wilson, R. Schlegel, F. Hofmann, C. Garcia-Echeverria, W. R. Sellers and C. F. Voliva (2012). Identification and characterization of NVP-BKM120, an orally available pan-class I PI3-kinase inhibitor. *Molecular cancer therapeutics* **11**(2): 317-328.

Maira, S. M., F. Stauffer, J. Brueggen, P. Furet, C. Schnell, C. Fritsch, S. Brachmann, P. Chene, A. De Pover, K. Schoemaker, D. Fabbro, D. Gabriel, M. Simonen, L. Murphy, P. Finan, W. Sellers and C. Garcia-Echeverria (2008). Identification and characterization of NVP-BEZ235, a new orally available dual phosphatidylinositol 3-kinase/mammalian target of rapamycin inhibitor with potent in vivo antitumor activity. *Molecular cancer therapeutics* **7**(7): 1851-1863.

Mani, S. A., W. Guo, M. J. Liao, E. N. Eaton, A. Ayyanan, A. Y. Zhou, M. Brooks, F. Reinhard, C. C. Zhang, M. Shipitsin, L. L. Campbell, K. Polyak, C. Brisken, J. Yang and R. A. Weinberg (2008). The epithelial-mesenchymal transition generates cells with properties of stem cells. *Cell* **133**(4): 704-715.

Mann, M. and O. N. Jensen (2003). Proteomic analysis of post-translational modifications. *Nat Biotechnol* **21**(3): 255-261.

Manning, B. D., A. R. Tee, M. N. Logsdon, J. Blenis and L. C. Cantley (2002). Identification of the tuberous sclerosis complex-2 tumor suppressor gene product tuberin as a target of the phosphoinositide 3-kinase/akt pathway. *Mol Cell* **10**(1): 151-162.

Markman, B., J. Tabernero, I. Krop, G. I. Shapiro, L. Siu, L. C. Chen, M. Mita, M. Melendez Cuero, S. Stutvoet, D. Birle, O. Anak, W. Hackl and J. Baselga (2012). Phase I safety, pharmacokinetic, and pharmacodynamic study of the oral phosphatidylinositol-3-kinase and mTOR inhibitor BGT226 in patients with advanced solid tumors. *Ann Oncol* **23**(9): 2399-2408.

Maroun, C. R., M. Holgado-Madruga, I. Royal, M. A. Naujokas, T. M. Fournier, A. J. Wong and M. Park (1999). The Gab1 PH domain is required for localization of Gab1 at sites of cell-cell contact and epithelial morphogenesis downstream from the met receptor tyrosine kinase. *Mol Cell Biol* **19**(3): 1784-1799.

Marquard, L., L. M. Gjerdrum, I. J. Christensen, P. B. Jensen, M. Sehested and E. Ralfkiaer (2008). Prognostic significance of the therapeutic targets histone deacetylase 1, 2, 6 and acetylated histone H4 in cutaneous T-cell lymphoma. *Histopathology* **53**(3): 267-277.

Martin, J. A. and Z. Wang (2011). Next-generation transcriptome assembly. *Nat Rev Genet* **12**(10): 671-682.

Masiello, D., M. G. Mohi, N. C. McKnight, B. Smith, B. G. Neel, S. P. Balk and G. J. Bubley (2007). Combining an mTOR antagonist and receptor tyrosine kinase inhibitors for the treatment of prostate cancer. *Cancer Biol Ther* **6**(2): 195-201.

Maxwell, P. H., M. S. Wiesener, G. W. Chang, S. C. Clifford, E. C. Vaux, M. E. Cockman, C. C. Wykoff, C. W. Pugh, E. R. Maher and P. J. Ratcliffe (1999). The tumour suppressor protein VHL targets hypoxia-inducible factors for oxygen-dependent proteolysis. *Nature* **399**(6733): 271-275.

McCright, B., A. M. Rivers, S. Audlin and D. M. Virshup (1996). The B56 family of protein phosphatase 2A (PP2A) regulatory subunits encodes differentiation-induced phosphoproteins that target PP2A to both nucleus and cytoplasm. *J Biol Chem* **271**(36): 22081-22089.

McDermott, U., S. V. Sharma, L. Dowell, P. Greninger, C. Montagut, J. Lamb, H. Archibald, R. Raudales, A. Tam, D. Lee, S. M. Rothenberg, J. G. Supko, R. Sordella, L. E. Ulkus, A. J. Iafrate, S. Maheswaran, C. N. Njauw, H. Tsao, L. Drew, J. H. Hanke, X. J. Ma, M. G. Erlander, N. S. Gray, D. A. Haber and J. Settleman (2007). Identification of genotype-correlated sensitivity to selective kinase inhibitors by using high-throughput tumor cell line profiling. *Proc Natl Acad Sci U S A* **104**(50): 19936-19941.

Mellemgaard, A., G. Engholm, J. K. McLaughlin and J. H. Olsen (1994). Risk factors for renal cell carcinoma in Denmark. I. Role of socioeconomic status, tobacco use, beverages, and family history. *Cancer Causes Control* **5**(2): 105-113.

Messing, E. M., J. Manola, G. Wilding, K. Propert, J. Fleischmann, E. D. Crawford, J. E. Pontes, R. Hahn and D. Trump (2003). Phase III study of interferon alfa-NL as adjuvant treatment for resectable renal cell carcinoma: an Eastern Cooperative Oncology Group/Intergroup trial. *J Clin Oncol* **21**(7): 1214-1222.

Michlewski, G., J. R. Sanford and J. F. Caceres (2008). The splicing factor SF2/ASF regulates translation initiation by enhancing phosphorylation of 4E-BP1. *Molecular cell* **30**(2): 179-189.

Mickisch, G. H., A. Garin, H. van Poppel, L. de Prijck and R. Sylvester (2001). Radical nephrectomy plus interferon-alfa-based immunotherapy compared with interferon alfa alone in metastatic renal-cell carcinoma: a randomised trial. *Lancet* **358**(9286): 966-970.

Migliardi, G., F. Sassi, D. Torti, F. Galimi, E. R. Zanella, M. Buscarino, D. Ribero, A. Muratore, P. Massucco, A. Pisacane, M. Risio, L. Capussotti, S. Marsoni, F. Di Nicolantonio, A. Bardelli, P. M. Comoglio, L. Trusolino and A. Bertotti (2012). Inhibition of MEK and PI3K/mTOR suppresses tumor growth but does not cause tumor regression in patient-derived xenografts of RAS-mutant colorectal carcinomas. *Clin Cancer Res* **18**(9): 2515-2525.

Minamiya, Y., T. Ono, H. Saito, N. Takahashi, M. Ito, M. Mitsui, S. Motoyama and J. Ogawa (2011). Expression of histone deacetylase 1 correlates with a poor prognosis in patients with adenocarcinoma of the lung. *Lung Cancer* **74**(2): 300-304.

Mitra, A. K., K. Sawada, P. Tiwari, K. Mui, K. Gwin and E. Lengyel (2011). Ligand-independent activation of c-Met by fibronectin and alpha(5)beta(1)-integrin regulates ovarian cancer invasion and metastasis. *Oncogene* **30**(13): 1566-1576.

Mohr, S. E., J. A. Smith, C. E. Shamu, R. A. Neumuller and N. Perrimon (2014). RNAi screening comes of age: improved techniques and complementary approaches. *Nat Rev Mol Cell Biol* **15**(9): 591-600.

Moreno, D. A., C. A. Scrideli, M. A. Cortez, R. de Paula Queiroz, E. T. Valera, V. da Silva Silveira, J. A. Yunes, S. R. Brandalise and L. G. Tone (2010). Differential expression of HDAC3, HDAC7 and HDAC9 is associated with prognosis and survival in childhood acute lymphoblastic leukaemia. *Br J Haematol* **150**(6): 665-673.

Moschos, S. J. and C. S. Mantzoros (2002). The role of the IGF system in cancer: from basic to clinical studies and clinical applications. *Oncology* **63**(4): 317-332.

Motzer, R. J., J. Bacik, B. A. Murphy, P. Russo and M. Mazumdar (2002). Interferon-alfa as a comparative treatment for clinical trials of new therapies against advanced renal cell carcinoma. *J Clin Oncol* **20**(1): 289-296.

Motzer, R. J., B. Escudier, S. Oudard, T. E. Hutson, C. Porta, S. Bracarda, V. Grunwald, J. A. Thompson, R. A. Figlin, N. Hollaender, A. Kay and A. Ravaud (2010). Phase 3 trial of everolimus for metastatic renal cell carcinoma : final results and analysis of prognostic factors. *Cancer* **116**(18): 4256-4265.

Motzer, R. J., B. Escudier, S. Oudard, T. E. Hutson, C. Porta, S. Bracarda, V. Grunwald, J. A. Thompson, R. A. Figlin, N. Hollaender, G. Urbanowitz, W. J. Berg, A. Kay, D. Lebwohl and A. Ravaud (2008). Efficacy of everolimus in advanced renal cell carcinoma: a double-blind, randomised, placebo-controlled phase III trial. *Lancet* **372**(9637): 449-456.

Motzer, R. J., B. Escudier, P. Tomczak, T. E. Hutson, M. D. Michaelson, S. Negrier, S. Oudard, M. E. Gore, J. Tarazi, S. Hariharan, C. Chen, B. Rosbrook, S. Kim and B. I. Rini (2013a). Axitinib versus sorafenib as second-line treatment for advanced renal cell carcinoma: overall survival analysis and updated results from a randomised phase 3 trial. *Lancet Oncol* **14**(6): 552-562.

Motzer, R. J., T. E. Hutson, D. Cella, J. Reeves, R. Hawkins, J. Guo, P. Nathan, M. Staehler, P. de Souza, J. R. Merchan, E. Boleti, K. Fife, J. Jin, R. Jones, H. Uemura, U. De Giorgi, U. Harmenberg, J. Wang, C. N. Sternberg, K. Deen, L. McCann, M. D. Hackshaw, R. Crescenzo, L. N. Pandite and T. K. Choueiri (2013b). Pazopanib versus sunitinib in metastatic renal-cell carcinoma. *N Engl J Med* **369**(8): 722-731.

Motzer, R. J., T. E. Hutson, P. Tomczak, M. D. Michaelson, R. M. Bukowski, S. Oudard, S. Negrier, C. Szczylik, R. Pili, G. A. Bjarnason, X. Garcia-del-Muro, J. A. Sosman, E. Solska, G. Wilding, J. A. Thompson, S. T. Kim, I. Chen, X. Huang and R. A. Figlin (2009). Overall survival and updated results for sunitinib compared with interferon alfa in patients with metastatic renal cell carcinoma. *Journal of clinical oncology : official journal of the American Society of Clinical Oncology* **27**(22): 3584-3590.

Motzer, R. J., T. E. Hutson, P. Tomczak, M. D. Michaelson, R. M. Bukowski, O. Rixe, S. Oudard, S. Negrier, C. Szczylik, S. T. Kim, I. Chen, P. W. Bycott, C. M. Baum and R. A. Figlin (2007). Sunitinib versus interferon alfa in metastatic renal-cell carcinoma. *The New England journal of medicine* **356**(2): 115-124.

Motzer, R. J., D. Nosov, T. Eisen, I. Bondarenko, V. Lesovoy, O. Lipatov, P. Tomczak, O. Lyulko, A. Alyasova, M. Harza, M. Kogan, B. Y. Alekseev, C. N. Sternberg, C. Szczylik, D. Cella, C. Ivanescu, A. Krivoshik, A. Strahs, B. Esteves, A. Berkenblit and T. E. Hutson (2013c). Tivozanib versus sorafenib as initial targeted therapy for patients with metastatic renal cell carcinoma: results from a phase III trial. *J Clin Oncol* **31**(30): 3791-3799.

Motzer, R. J., C. Porta, N. J. Vogelzang, C. N. Sternberg, C. Szczylik, J. Zolnierek, C. Kollmannsberger, S. Y. Rha, G. A. Bjarnason, B. Melichar, U. De Giorgi, V. Grunwald, I. D. Davis, J. L. Lee, E. Esteban, G. Urbanowitz, C. Cai, M. Squires, M. Marker, M. M. Shi and B. Escudier (2014). Dovitinib versus sorafenib for third-line targeted treatment of patients with metastatic renal cell carcinoma: an open-label, randomised phase 3 trial. *Lancet Oncol* **15**(3): 286-296.

Mukherjee, B., N. Tomimatsu, K. Amancherla, C. V. Camacho, N. Pichamoorthy and S. Burma (2012). The dual PI3K/mTOR inhibitor NVP-BEZ235 is a potent inhibitor of ATM- and DNA-PKCs-mediated DNA damage responses. *Neoplasia* **14**(1): 34-43.

Mulvihill, M. J., A. Cooke, M. Rosenfeld-Franklin, E. Buck, K. Foreman, D. Landfair, M. O'Connor, C. Pirritt, Y. Sun, Y. Yao, L. D. Arnold, N. W. Gibson and Q. S. Ji (2009). Discovery of OSI-906: a selective and orally efficacious dual inhibitor of the IGF-1 receptor and insulin receptor. *Future medicinal chemistry* **1**(6): 1153-1171.

Mumm, J. S., E. H. Schroeter, M. T. Saxena, A. Griesemer, X. Tian, D. J. Pan, W. J. Ray and R. Kopan (2000). A ligand-induced extracellular cleavage regulates gamma-secretase-like proteolytic activation of Notch1. *Mol Cell* **5**(2): 197-206.

Munster, P. N., R. van der Noll, E. E. Voest, E. C. Dees, A. R. Tan, J. M. Specht, G. S. Falchook, A. Daud, M. P. Lolkema, J. E. Grilley-Olsen, Y. Yu, S. Fu, E. K. Bergsland, J. Kleha, S. Peng, D. A. Smith, T. A. Lampkin, J. H. Schellens, S. R. Morris and R. Kurzrock (2011). Phase I first-in-human study of the PI3 kinase inhibitor GSK2126458 (GSK458) in patients with advanced solid tumors (study P3K112826). *Journal of clinical oncology : official journal of the American Society of Clinical Oncology* **29**(suppl.): abstr 3018.

Murakami, N., L. V. Riella and T. Funakoshi (2014). Risk of Metabolic Complications in Kidney Transplantation After Conversion to mTOR Inhibitor: A Systematic Review and Meta-Analysis. *Am J Transplant*.

Mwenifumbo, J. C. and M. A. Marra (2013). Cancer genome-sequencing study design. *Nat Rev Genet* **14**(5): 321-332.

Naing, A., C. Aghajanian, E. Raymond, D. Olmos, G. Schwartz, E. Oelmann, L. Grinsted, W. Burke, R. Taylor, S. Kaye, R. Kurzrock and U. Banerji (2012a). Safety, tolerability, pharmacokinetics and pharmacodynamics of AZD8055 in advanced solid tumours and lymphoma. *Br J Cancer* **107**(7): 1093-1099.

Naing, A., R. Kurzrock, A. Burger, S. Gupta, X. Lei, N. Busaidy, D. Hong, H. X. Chen, L. A. Doyle, L. K. Heilbrun, E. Rohren, C. Ng, C. Chandhasin and P. LoRusso (2011). Phase I trial of cixutumumab combined with temsirolimus in patients with advanced cancer. *Clin Cancer Res* **17**(18): 6052-6060.

Naing, A., P. Lorusso, S. Fu, D. Hong, H. X. Chen, L. A. Doyle, A. T. Phan, M. A. Habra and R. Kurzrock (2013). Insulin growth factor receptor (IGF-1R) antibody cixutumumab combined with the mTOR inhibitor temsirolimus in patients with metastatic adrenocortical carcinoma. *British journal of cancer* **108**(4): 826-830.

Naing, A., P. LoRusso, S. Fu, D. S. Hong, P. Anderson, R. S. Benjamin, J. Ludwig, H. X. Chen, L. A. Doyle and R. Kurzrock (2012b). Insulin growth factor-receptor (IGF-1R) antibody cixutumumab combined with the mTOR inhibitor temsirolimus in patients with refractory Ewing's sarcoma family tumors. *Clinical cancer research : an official journal of the American Association for Cancer Research* **18**(9): 2625-2631.

Nakagawa, T., S. Takeuchi, T. Yamada, S. Nanjo, D. Ishikawa, T. Sano, K. Kita, T. Nakamura, K. Matsumoto, K. Suda, T. Mitsudomi, Y. Sekido, T. Uenaka and S. Yano (2012). Combined therapy with mutant-selective EGFR inhibitor and Met kinase inhibitor for overcoming erlotinib resistance in EGFR-mutant lung cancer. *Mol Cancer Ther* **11**(10): 2149-2157.

Nakata, S., T. Yoshida, M. Horinaka, T. Shiraishi, M. Wakada and T. Sakai (2004). Histone deacetylase inhibitors upregulate death receptor 5/TRAIL-R2 and sensitize apoptosis induced by TRAIL/APO2-L in human malignant tumor cells. *Oncogene* **23**(37): 6261-6271.

Nanus, D. M., I. R. Mentle, R. J. Motzer, N. H. Bander and A. P. Albino (1990). Infrequent ras oncogene point mutations in renal cell carcinoma. *J Urol* **143**(1): 175-178.

Nathan, C. O., P. Carter, L. Liu, B. D. Li, F. Abreo, A. Tudor, S. G. Zimmer and A. De Benedetti (1997a). Elevated expression of eIF4E and FGF-2 isoforms during vascularization of breast carcinomas. *Oncogene* **15**(9): 1087-1094.

Nathan, C. O., L. Liu, B. D. Li, F. W. Abreo, I. Nandy and A. De Benedetti (1997b). Detection of the proto-oncogene eIF4E in surgical margins may predict recurrence in head and neck cancer. *Oncogene* **15**(5): 579-584.

Neshat, M. S., I. K. Mellinghoff, C. Tran, B. Stiles, G. Thomas, R. Petersen, P. Frost, J. J. Gibbons, H. Wu and C. L. Sawyers (2001). Enhanced sensitivity of PTEN-deficient tumors to inhibition of FRAP/mTOR. *Proc Natl Acad Sci U S A* **98**(18): 10314-10319.

Network., C. G. A. (2012). Comprehensive molecular portraits of human breast tumours. *Nature* **490**(7418): 61-70.

Nickerson, M. L., M. B. Warren, J. R. Toro, V. Matrosova, G. Glenn, M. L. Turner, P. Duray, M. Merino, P. Choyke, C. P. Pavlovich, N. Sharma, M. Walther, D. Munroe, R. Hill, E. Maher, C. Greenberg, M. I. Lerman, W. M. Linehan, B. Zbar and L. S. Schmidt (2002). Mutations in a novel gene lead to kidney tumors, lung wall defects, and benign tumors of the hair follicle in patients with the Birt-Hogg-Dube syndrome. *Cancer Cell* **2**(2): 157-164.

Niu, Z., J. Wang, S. Muhammad, W. Niu, E. Liu, C. Peng, B. Liang, Q. Sun, S. Obo, Z. He, S. Liu, X. Zou and J. Niu (2014). Protein expression of eIF4E and integrin alphavbeta6 in colon cancer can predict clinical significance, reveal their correlation and imply possible mechanism of interaction. *Cell Biosci* **4**: 23.

Nyfeler, B., Y. Chen, X. Li, M. Pinzon-Ortiz, Z. Wang, A. Reddy, E. Pradhan, R. Das, J. Lehar, R. Schlegel, P. M. Finan, Z. A. Cao, L. O. Murphy and A. Huang (2012). RAD001 Enhances the Potency of BEZ235 to Inhibit mTOR Signaling and Tumor Growth. *PLoS One* **7**(11): e48548.

O'Brien, S. G., F. Guilhot, R. A. Larson, I. Gathmann, M. Baccarani, F. Cervantes, J. J. Cornelissen, T. Fischer, A. Hochhaus, T. Hughes, K. Lechner, J. L. Nielsen, P. Rousselot, J. Reiffers, G. Saglio, J. Shepherd, B. Simonsson, A. Gratwohl, J. M. Goldman, H. Kantarjian, K. Taylor, G. Verhoef, A. E. Bolton, R. Capdeville and B. J. Druker (2003). Imatinib compared with interferon and low-dose cytarabine for newly diagnosed chronic-phase chronic myeloid leukemia. *N Engl J Med* **348**(11): 994-1004.

O'Reilly, K. E., F. Rojo, Q. B. She, D. Solit, G. B. Mills, D. Smith, H. Lane, F. Hofmann, D. J. Hicklin, D. L. Ludwig, J. Baselga and N. Rosen (2006). mTOR inhibition induces upstream receptor tyrosine kinase signaling and activates Akt. *Cancer research* **66**(3): 1500-1508.

Ogan, K., J. A. Cadeddu and M. D. Stifelman (2003). Laparoscopic radical nephrectomy: oncologic efficacy. *The Urologic clinics of North America* **30**(3): 543-550.

Ohh, M., C. W. Park, M. Ivan, M. A. Hoffman, T. Y. Kim, L. E. Huang, N. Pavletich, V. Chau and W. G. Kaelin (2000). Ubiquitination of hypoxia-inducible factor requires direct binding to the beta-domain of the von Hippel-Lindau protein. *Nat Cell Biol* **2**(7): 423-427.

Okabe, S., T. Tauchi, Y. Tanaka, T. Kitahara, S. Kimura, T. Maekawa and K. Ohyashiki (2014). Efficacy of the dual PI3K and mTOR inhibitor NVP-BEZ235 in combination with nilotinib against BCR-ABL-positive leukemia cells involves the ABL kinase domain mutation. *Cancer Biol Ther* **15**(2): 207-215.

Okuhashi, Y., M. Itoh, N. Nara and S. Tohda (2013). NOTCH knockdown affects the proliferation and mTOR signaling of leukemia cells. *Anticancer Res* **33**(10): 4293-4298.

Olmos, D., S. Postel-Vinay, L. R. Molife, S. H. Okuno, S. M. Schuetze, M. L. Paccagnella, G. N. Batzel, D. Yin, K. Pritchard-Jones, I. Judson, F. P. Worden, A. Gualberto, M. Scurr, J. S. de Bono and P. Haluska (2010). Safety, pharmacokinetics, and preliminary activity of the anti-IGF-1R antibody figitumumab (CP-751,871) in patients with sarcoma and Ewing's sarcoma: a phase 1 expansion cohort study. *Lancet Oncol* **11**(2): 129-135.

Olsen, E. A., Y. H. Kim, T. M. Kuzel, T. R. Pacheco, F. M. Foss, S. Parker, S. R. Frankel, C. Chen, J. L. Ricker, J. M. Arduino and M. Duvic (2007). Phase IIb multicenter trial of vorinostat in patients with persistent, progressive, or treatment refractory cutaneous T-cell lymphoma. *J Clin Oncol* **25**(21): 3109-3115.

Olwill, S. A., C. Joffroy, H. Gille, E. Vigna, G. Matschiner, A. Allersdorfer, B. M. Lunde, J. Jaworski, J. F. Burrows, C. Chiriaco, H. J. Christian, M. Hulsmeyer, S. Trentmann, K. Jensen, A. M. Hohlbaum and L. Audoly (2013). A highly potent and specific MET therapeutic protein antagonist with both ligand-dependent and ligand-independent activity. *Mol Cancer Ther* **12**(11): 2459-2471.

Ono, A., R. Oike, Y. Okuhashi, Y. Takahashi, M. Itoh, N. Nara and S. Tohda (2013). Comparative effects of PP242 and rapamycin on mTOR signalling and NOTCH signalling in leukemia cells. *Anticancer Res* **33**(3): 809-813.

ONS, O. f. N. S. (2014). Cancer Registration Statistics, England, 2012. *Statistical Bulletin*.

Oshiro, N., K. Yoshino, S. Hidayat, C. Tokunaga, K. Hara, S. Eguchi, J. Avruch and K. Yonezawa (2004). Dissociation of raptor from mTOR is a mechanism of rapamycin-induced inhibition of mTOR function. *Genes Cells* **9**(4): 359-366.

Pages, G., S. Guerin, D. Grall, F. Bonino, A. Smith, F. Anjuere, P. Auberger and J. Pouyssegur (1999). Defective thymocyte maturation in p44 MAP kinase (Erk 1) knockout mice. *Science* **286**(5443): 1374-1377.

Pan, M., M. Santamaria and D. B. Wollman (2007). CNS response after erlotinib therapy in a patient with metastatic NSCLC with an EGFR mutation. *Nat Clin Pract Oncol* **4**(10): 603-607.

Papadopoulos, K. P., J. Tabernero, B. Markman, A. Patnaik, A. W. Tolcher, J. Baselga, W. Shi, C. Egile, R. Ruiz-Soto, A. D. Laird, D. Miles and P. M. Lorusso (2014). Phase I safety, pharmacokinetic, and pharmacodynamic study of SAR245409 (XL765), a novel, orally administered PI3K/mTOR inhibitor in patients with advanced solid tumors. *Clin Cancer Res* **20**(9): 2445-2456.

Parker, A. S., J. C. Cheville, M. L. Blute, T. Igel, C. M. Lohse and J. R. Cerhan (2004). Pathologic T1 clear cell renal cell carcinoma: insulin-like growth factor-I receptor expression and disease-specific survival. *Cancer* **100**(12): 2577-2582.

Patursky-Polischuk, I., M. Stolovich-Rain, M. Hausner-Hanochi, J. Kasir, N. Cybulski, J. Avruch, M. A. Ruegg, M. N. Hall and O. Meyuhas (2009). The TSC-mTOR pathway mediates translational activation of TOP mRNAs by insulin largely in a raptor- or rictor-independent manner. *Mol Cell Biol* **29**(3): 640-649.

Pause, A., G. J. Belsham, A. C. Gingras, O. Donze, T. A. Lin, J. C. Lawrence, Jr. and N. Sonenberg (1994). Insulin-dependent stimulation of protein synthesis by phosphorylation of a regulator of 5'-cap function. *Nature* **371**(6500): 762-767.

Pavel, M. E., J. D. Hainsworth, E. Baudin, M. Peeters, D. Horsch, R. E. Winkler, J. Klimovsky, D. Lebwohl, V. Jehl, E. M. Wolin, K. Oberg, E. Van Cutsem and J. C. Yao (2011). Everolimus plus octreotide long-acting repeatable for the treatment of advanced neuroendocrine tumours associated with carcinoid syndrome (RADIANT-2): a randomised, placebo-controlled, phase 3 study. *Lancet* **378**(9808): 2005-2012.

Peart, M. J., G. K. Smyth, R. K. van Laar, D. D. Bowtell, V. M. Richon, P. A. Marks, A. J. Holloway and R. W. Johnstone (2005). Identification and functional significance of genes regulated by structurally different histone deacetylase inhibitors. *Proc Natl Acad Sci U S A* **102**(10): 3697-3702.

Pelicci, G., S. Giordano, Z. Zhen, A. E. Salcini, L. Lanfrancone, A. Bardelli, G. Panayotou, M. D. Waterfield, C. Ponzetto, P. G. Pelicci and et al. (1995). The motogenic and mitogenic responses to HGF are amplified by the Shc adaptor protein. *Oncogene* **10**(8): 1631-1638.

Peterson, T. R., M. Laplante, C. C. Thoreen, Y. Sancak, S. A. Kang, W. M. Kuehl, N. S. Gray and D. M. Sabatini (2009). DEPTOR is an mTOR inhibitor frequently overexpressed in multiple myeloma cells and required for their survival. *Cell* **137**(5): 873-886.

Peyton, J. D., J. Rodon Ahnert, H. Burris, C. Britten, L. C. Chen, J. Tabernero, V. Duval, N. Rouyrre, A. P. Silva, C. Quadt and J. Baselga (2012). A dose-escalation study with the novel formulation of the oral pan-class I PI3K inhibitor BEZ235, solid dispersion system (SDS) sachet, in patients with advanced solid tumors. *Journal of clinical oncology : official journal of the American Society of Clinical Oncology* **29 suppl**: abstr 3066.

Pham, F. H., P. H. Sugden and A. Clerk (2000). Regulation of protein kinase B and 4E-BP1 by oxidative stress in cardiac myocytes. *Circ Res* **86**(12): 1252-1258.

Pike, K. G., K. Malagu, M. G. Hummersone, K. A. Menear, H. M. Duggan, S. Gomez, N. M. Martin, L. Ruston, S. L. Pass and M. Pass (2013). Optimization of potent and selective dual mTORC1 and mTORC2 inhibitors: the discovery of AZD8055 and AZD2014. *Bioorg Med Chem Lett* **23**(5): 1212-1216.

Polite, B. N., A. A. Desai, B. Manchen and W. M. Stadler (2006). Combination therapy of imatinib mesylate and interferon-alpha demonstrates minimal activity and significant toxicity in metastatic renal cell carcinoma: results of a single- institution phase II trial. *Clinical genitourinary cancer* **4**(4): 275-280.

Pollak, M. N., E. S. Schernhammer and S. E. Hankinson (2004). Insulin-like growth factors and neoplasia. *Nat Rev Cancer* **4**(7): 505-518.

Ponzetto, C., A. Bardelli, F. Maina, P. Longati, G. Panayotou, R. Dhand, M. D. Waterfield and P. M. Comoglio (1993). A novel recognition motif for phosphatidylinositol 3-kinase binding mediates its association with the hepatocyte growth factor/scatter factor receptor. *Mol Cell Biol* **13**(8): 4600-4608.

Ponzetto, C., A. Bardelli, Z. Zhen, F. Maina, P. dalla Zonca, S. Giordano, A. Graziani, G. Panayotou and P. M. Comoglio (1994). A multifunctional docking site mediates signaling and transformation by the hepatocyte growth factor/scatter factor receptor family. *Cell* **77**(2): 261-271.

Powles, T., N. Sarwar, R. Jones, P. Wilson, E. Boleti, A. Protheroe, S. J. Crabb, J. Shamash, A. Stockdale, S. Rashid, P. Nathan and S. Chowdury (2012). An indirect comparison of the toxicity of sunitinib and pazopanib in metastatic clear cell renal cancer. *Eur J Cancer* **48**(17): 3171-3176.

Powles, T., M. Wheater, O. Din, T. Geldart, E. Boleti, A. Stockdale, S. Sundar, A. Robinson, I. Ahmed, A. Wimalasingham, W. Burke, S. J. Sarker, S. Hussain and C. Ralph (2015). A Randomised Phase 2 Study of AZD2014 Versus Everolimus in Patients with VEGF-Refractory Metastatic Clear Cell Renal Cancer. *Eur Urol*.

Procopio, G., E. Verzoni, S. Bracarda, S. Ricci, C. Sacco, L. Ridolfi, C. Porta, R. Miceli, N. Zilembo and E. Bajetta (2013). Overall survival for sorafenib plus interleukin-2 compared with sorafenib alone in metastatic renal cell carcinoma (mRCC): final results of the ROSORC trial. *Ann Oncol* **24**(12): 2967-2971.

Puzanov, I., C. R. Lindsay, L. Goff, J. Sosman, J. Gilbert, J. Berlin, S. Poondru, R. Simantov, R. Gedrich, A. Stephens, E. Chan and T. R. Evans (2015). A phase I study of continuous oral dosing of OSI-906, a dual inhibitor of insulin-like growth factor-1 and insulin receptors, in patients with advanced solid tumors. *Clin Cancer Res* **21**(4): 701-711.

Qu, Y., X. Wu, Y. Yin, Y. Yang, D. Ma and H. Li (2014). Antitumor activity of selective MEK1/2 inhibitor AZD6244 in combination with PI3K/mTOR inhibitor BEZ235 in gefitinib-resistant NSCLC xenograft models. *J Exp Clin Cancer Res* **33**: 52.

Quek, R., Q. Wang, J. A. Morgan, G. I. Shapiro, J. E. Butrynski, N. Ramaiya, T. Huftalen, N. Jederlinic, J. Manola, A. J. Wagner, G. D. Demetri and S. George (2011). Combination mTOR and IGF-1R inhibition: phase I trial of everolimus and figitumumab in patients with advanced sarcomas and other solid tumors. *Clin Cancer Res* **17**(4): 871-879.

Quilliam, L. A., S. Y. Huff, K. M. Rabun, W. Wei, W. Park, D. Broek and C. J. Der (1994). Membrane-targeting potentiates guanine nucleotide exchange factor CDC25 and SOS1 activation of Ras transforming activity. *Proc Natl Acad Sci U S A* **91**(18): 8512-8516.

Ramirez-Valle, F., M. L. Badura, S. Braunstein, M. Narasimhan and R. J. Schneider (2010). Mitotic raptor promotes mTORC1 activity, G(2)/M cell cycle progression, and internal ribosome entry site-mediated mRNA translation. *Mol Cell Biol* **30**(13): 3151-3164.

Rathkopf, D., B. Y. Wong, R. W. Ross, A. Anand, E. Tanaka, M. M. Woo, J. Hu, A. Dzik-Jurasz, W. Yang and H. I. Scher (2010). A phase I study of oral panobinostat alone and in combination with docetaxel in patients with castration-resistant prostate cancer. *Cancer Chemother Pharmacol* **66**(1): 181-189.

Raught, B., F. Peiretti, A. C. Gingras, M. Livingstone, D. Shahbazian, G. L. Mayeur, R. D. Polakiewicz, N. Sonenberg and J. W. Hershey (2004). Phosphorylation of eucaryotic translation initiation factor 4B Ser422 is modulated by S6 kinases. *Embo j* **23**(8): 1761-1769.

Ray, L. B. and T. W. Sturgill (1988). Characterization of insulin-stimulated microtubule-associated protein kinase. Rapid isolation and stabilization of a novel serine/threonine kinase from 3T3-L1 cells. *J Biol Chem* **263**(25): 12721-12727.

Reedijk, M., S. Odorcic, L. Chang, H. Zhang, N. Miller, D. R. McCready, G. Lockwood and S. E. Egan (2005). High-level coexpression of JAG1 and NOTCH1 is observed in human breast cancer and is associated with poor overall survival. *Cancer Res* **65**(18): 8530-8537.

Renshaw, J., K. R. Taylor, R. Bishop, M. Valenti, A. De Haven Brandon, S. Gowan, S. A. Eccles, R. R. Ruddle, L. D. Johnson, F. I. Raynaud, J. L. Selfe, K. Thway, T. Pietsch, A. D. Pearson and J. Shipley (2013). Dual blockade of the PI3K/AKT/mTOR (AZD8055) and

RAS/MEK/ERK (AZD6244) pathways synergistically inhibits rhabdomyosarcoma cell growth in vitro and in vivo. *Clin Cancer Res* **19**(21): 5940-5951.

Ricci, C., B. Scappini, V. Divoky, S. Gatto, F. Onida, S. Verstovsek, H. M. Kantarjian and M. Beran (2002). Mutation in the ATP-binding pocket of the ABL kinase domain in an STI571-resistant BCR/ABL-positive cell line. *Cancer research* **62**(21): 5995-5998.

Rikimaru, T., A. Taketomi, Y. Yamashita, K. Shirabe, T. Hamatsu, M. Shimada and Y. Maehara (2007). Clinical significance of histone deacetylase 1 expression in patients with hepatocellular carcinoma. *Oncology* **72**(1-2): 69-74.

Rini, B. I., B. Escudier, P. Tomczak, A. Kaprin, C. Szczylik, T. E. Hutson, M. D. Michaelson, V. A. Gorbunova, M. E. Gore, I. G. Rusakov, S. Negrier, Y. C. Ou, D. Castellano, H. Y. Lim, H. Uemura, J. Tarazi, D. Cella, C. Chen, B. Rosbrook, S. Kim and R. J. Motzer (2011). Comparative effectiveness of axitinib versus sorafenib in advanced renal cell carcinoma (AXIS): a randomised phase 3 trial. *Lancet* **378**(9807): 1931-1939.

Rochlitz, C. F., S. Peter, G. Willroth, E. de Kant, H. Lobeck, D. Huhn and R. Herrmann (1992). Mutations in the ras protooncogenes are rare events in renal cell cancer. *Eur J Cancer* **28**(2-3): 333-336.

Rokhlin, O. W., A. F. Taghiyev, K. U. Bayer, D. Bumcrot, V. E. Koteliansk, R. A. Glover and M. B. Cohen (2007). Calcium/calmodulin-dependent kinase II plays an important role in prostate cancer cell survival. *Cancer Biol Ther* **6**(5): 732-742.

Ruvinsky, I. and O. Meyuhas (2006). Ribosomal protein S6 phosphorylation: from protein synthesis to cell size. *Trends Biochem Sci* **31**(6): 342-348.

Ryan, C. W., J. Vuky, J. S. Chan, Z. Chen, T. M. Beer and D. Nauman (2011). A phase II study of everolimus in combination with imatinib for previously treated advanced renal carcinoma. *Investigational new drugs* **29**(2): 374-379.

Sabatini, D. M., H. Erdjument-Bromage, M. Lui, P. Tempst and S. H. Snyder (1994). RAFT1: a mammalian protein that binds to FKBP12 in a rapamycin-dependent fashion and is homologous to yeast TORs. *Cell* **78**(1): 35-43.

Sabine, V. S., A. H. Sims, E. J. Macaskill, L. Renshaw, J. S. Thomas, J. M. Dixon and J. M. Bartlett (2010). Gene expression profiling of response to mTOR inhibitor everolimus in pre-operatively treated post-menopausal women with oestrogen receptor-positive breast cancer. *Breast Cancer Res Treat* **122**(2): 419-428.

Samuels, Y., Z. Wang, A. Bardelli, N. Silliman, J. Ptak, S. Szabo, H. Yan, A. Gazdar, S. M. Powell, G. J. Riggins, J. K. Willson, S. Markowitz, K. W. Kinzler, B. Vogelstein and V. E. Velculescu (2004). High frequency of mutations of the PIK3CA gene in human cancers. *Science* **304**(5670): 554.

Sancak, Y., L. Bar-Peled, R. Zoncu, A. L. Markhard, S. Nada and D. M. Sabatini (2010). Ragulator-Rag complex targets mTORC1 to the lysosomal surface and is necessary for its activation by amino acids. *Cell* **141**(2): 290-303.

Sancak, Y., T. R. Peterson, Y. D. Shaul, R. A. Lindquist, C. C. Thoreen, L. Bar-Peled and D. M. Sabatini (2008). The Rag GTPases bind raptor and mediate amino acid signaling to mTORC1. *Science* **320**(5882): 1496-1501.

Sancak, Y., C. C. Thoreen, T. R. Peterson, R. A. Lindquist, S. A. Kang, E. Spooner, S. A. Carr and D. M. Sabatini (2007). PRAS40 is an insulin-regulated inhibitor of the mTORC1 protein kinase. *Mol Cell* **25**(6): 903-915.

Santoni, M., F. Pantano, C. Amantini, M. Nabissi, A. Conti, L. Burattini, A. Zoccoli, R. Berardi, G. Santoni, G. Tonini, D. Santini and S. Cascinu (2014). Emerging strategies to overcome the resistance to current mTOR inhibitors in renal cell carcinoma. *Biochim Biophys Acta* **1845**(2): 221-231.

Sarbassov, D. D., S. M. Ali, D. H. Kim, D. A. Guertin, R. R. Latek, H. Erdjument-Bromage, P. Tempst and D. M. Sabatini (2004). Rictor, a novel binding partner of mTOR, defines a rapamycin-insensitive and raptor-independent pathway that regulates the cytoskeleton. *Curr Biol* **14**(14): 1296-1302.

Sarbassov, D. D., S. M. Ali, S. Sengupta, J. H. Sheen, P. P. Hsu, A. F. Bagley, A. L. Markhard and D. M. Sabatini (2006). Prolonged rapamycin treatment inhibits mTORC2 assembly and Akt/PKB. *Molecular cell* **22**(2): 159-168.

Sarbassov, D. D., D. A. Guertin, S. M. Ali and D. M. Sabatini (2005). Phosphorylation and regulation of Akt/PKB by the rictor-mTOR complex. *Science* **307**(5712): 1098-1101.

Schachter, T. N., T. Shen, Y. Liu and M. F. Schneider (2012). Kinetics of nuclear-cytoplasmic translocation of Foxo1 and Foxo3A in adult skeletal muscle fibers. *Am J Physiol Cell Physiol* **303**(9): C977-990.

Scheid, M. P., P. A. Marignani and J. R. Woodgett (2002). Multiple phosphoinositide 3-kinase-dependent steps in activation of protein kinase B. *Mol Cell Biol* **22**(17): 6247-6260.

Scheid, M. P., K. M. Schubert and V. Duronio (1999). Regulation of bad phosphorylation and association with Bcl-x(L) by the MAPK/Erk kinase. *J Biol Chem* **274**(43): 31108-31113.

Schmidt, L., F. M. Duh, F. Chen, T. Kishida, G. Glenn, P. Choyke, S. W. Scherer, Z. Zhuang, I. Lubensky, M. Dean, R. Allikmets, A. Chidambaram, U. R. Bergerheim, J. T. Feltis, C. Casadevall, A. Zamarron, M. Bernues, S. Richard, C. J. Lips, M. M. Walther, L. C. Tsui, L. Geil, M. L. Orcutt, T. Stackhouse, J. Lipan, L. Slife, H. Brauch, J. Decker, G. Niehans, M. D. Hughson, H. Moch, S. Storkel, M. I. Lerman, W. M. Linehan and B. Zbar (1997). Germline and somatic mutations in the tyrosine kinase domain of the MET proto-oncogene in papillary renal carcinomas. *Nat Genet* **16**(1): 68-73.

Schmidt, L., K. Junker, N. Nakaigawa, T. Kinjerski, G. Weirich, M. Miller, I. Lubensky, H. P. Neumann, H. Brauch, J. Decker, C. Vocke, J. A. Brown, R. Jenkins, S. Richard, U. Bergerheim, B. Gerrard, M. Dean, W. M. Linehan and B. Zbar (1999). Novel mutations of the MET proto-oncogene in papillary renal carcinomas. *Oncogene* **18**(14): 2343-2350.

Schmidt, L., K. Junker, G. Weirich, G. Glenn, P. Choyke, I. Lubensky, Z. Zhuang, M. Jeffers, G. Vande Woude, H. Neumann, M. Walther, W. M. Linehan and B. Zbar (1998). Two North American families with hereditary papillary renal carcinoma and identical novel mutations in the MET proto-oncogene. *Cancer Res* **58**(8): 1719-1722.

Schmidt, L. S., M. L. Nickerson, D. Angeloni, G. M. Glenn, M. M. Walther, P. S. Albert, M. B. Warren, P. L. Choyke, C. A. Torres-Cabala, M. J. Merino, J. Brunet, V. Berez, J. Borras, G. Sesia, L. Middelton, J. L. Phillips, C. Stolle, B. Zbar, S. E. Pautler and W. M. Linehan (2004). Early onset hereditary papillary renal carcinoma: germline missense mutations in the tyrosine kinase domain of the met proto-oncogene. *J Urol* **172**(4 Pt 1): 1256-1261.

Schonthal, A. H. (2001). Role of serine/threonine protein phosphatase 2A in cancer. *Cancer Lett* **170**(1): 1-13.

Schroeter, E. H., J. A. Kisslinger and R. Kopan (1998). Notch-1 signalling requires ligand-induced proteolytic release of intracellular domain. *Nature* **393**(6683): 382-386.

Schwartz, G. K., W. D. Tap, L. X. Qin, M. B. Livingston, S. D. Undevia, B. Chmielowski, M. Agulnik, S. M. Schuetze, D. R. Reed, S. H. Okuno, J. A. Ludwig, V. Keedy, P. Rietschel, A. S. Kraft, D. Adkins, B. A. Van Tine, B. Brockstein, V. Yim, C. Bitas, A. Abdullah, C. R. Antonescu, M. Condy, M. A. Dickson, S. D. Vasudeva, A. L. Ho, L. A. Doyle, H. X. Chen and R. G. Maki (2013). Cixutumumab and temsirolimus for patients with bone and soft-tissue sarcoma: a multicentre, open-label, phase 2 trial. *The lancet oncology* **14**(4): 371-382.

Seger, R., N. G. Ahn, J. Posada, E. S. Munar, A. M. Jensen, J. A. Cooper, M. H. Cobb and E. G. Krebs (1992). Purification and characterization of mitogen-activated protein kinase activator(s) from epidermal growth factor-stimulated A431 cells. *J Biol Chem* **267**(20): 14373-14381.

Seki, N., T. Takasu, K. Mandai, M. Nakata, H. Saeki, Y. Heike, I. Takata, Y. Segawa, T. Hanafusa and K. Eguchi (2002). Expression of eukaryotic initiation factor 4E in atypical adenomatous hyperplasia and adenocarcinoma of the human peripheral lung. *Clin Cancer Res* **8**(10): 3046-3053.

Sell, C., G. Dumenil, C. Deveaud, M. Miura, D. Coppola, T. DeAngelis, R. Rubin, A. Efstratiadis and R. Baserga (1994). Effect of a null mutation of the insulin-like growth factor I receptor gene on growth and transformation of mouse embryo fibroblasts. *Mol Cell Biol* **14**(6): 3604-3612.

Sell, C., A. Ptasznik, C. D. Chang, J. Swantek, V. J. Cristofalo and R. Baserga (1993). IGF-1 receptor levels and the proliferation of young and senescent human fibroblasts. *Biochem Biophys Res Commun* **194**(1): 259-265.

Serra, V., B. Markman, M. Scaltriti, P. J. Eichhorn, V. Valero, M. Guzman, M. L. Botero, E. Llonch, F. Atzori, S. Di Cosimo, M. Maira, C. Garcia-Echeverria, J. L. Parra, J. Arribas and J. Baselga (2008). NVP-BEZ235, a dual PI3K/mTOR inhibitor, prevents PI3K signaling and inhibits the growth of cancer cells with activating PI3K mutations. *Cancer research* **68**(19): 8022-8030.

Seshacharyulu, P., P. Pandey, K. Datta and S. K. Batra (2013). Phosphatase: PP2A structural importance, regulation and its aberrant expression in cancer. *Cancer Lett* **335**(1): 9-18.

Shao, W., J. Growney, Y. X. Feng, P. Wang, Y. Yan-Neale, G. O'Connor, P. Kwon, Y. Yao, S. Fawell and P. Atadja (2008). Potent anticancer activity of a pan-deacetylase inhibitor panobinostat (LBH589) as a single agent in *in vitro* and *in vivo* tumour models. *99th AACR Annual Meeting*: Abstract Number 735.

Shapiro, G. I., R. Frank, U. B. Dandamudi, T. Hengelage, L. Zhao, L. Gazi, M. G. Porro, M. M. Woo and L. D. Lewis (2012). The effect of food on the bioavailability of panobinostat, an orally active pan-histone deacetylase inhibitor, in patients with advanced cancer. *Cancer Chemother Pharmacol* **69**(2): 555-562.

Shapiro, J. A., M. A. Williams and N. S. Weiss (1999a). Body mass index and risk of renal cell carcinoma. *Epidemiology* **10**(2): 188-191.

Shapiro, J. A., M. A. Williams, N. S. Weiss, A. Stergachis, A. Z. LaCroix and W. E. Barlow (1999b). Hypertension, antihypertensive medication use, and risk of renal cell carcinoma. *Am J Epidemiol* **149**(6): 521-530.

Sharma, S. V., D. Y. Lee, B. Li, M. P. Quinlan, F. Takahashi, S. Maheswaran, U. McDermott, N. Azizian, L. Zou, M. A. Fischbach, K. K. Wong, K. Brandstetter, B. Wittner, S. Ramaswamy, M. Classon and J. Settleman (2010). A chromatin-mediated reversible drug-tolerant state in cancer cell subpopulations. *Cell* **141**(1): 69-80.

Shi, Y., H. Yan, P. Frost, J. Gera and A. Lichtenstein (2005). Mammalian target of rapamycin inhibitors activate the AKT kinase in multiple myeloma cells by up-regulating the insulin-like growth factor receptor/insulin receptor substrate-1/phosphatidylinositol 3-kinase cascade. *Mol Cancer Ther* **4**(10): 1533-1540.

Sipeki, S., E. Bander, L. Buday, G. Farkas, E. Bacsy, D. K. Ways and A. Farago (1999). Phosphatidylinositol 3-kinase contributes to Erk1/Erk2 MAP kinase activation associated with hepatocyte growth factor-induced cell scattering. *Cell Signal* **11**(12): 885-890.

Sjolund, J., M. Johansson, S. Manna, C. Norin, A. Pietras, S. Beckman, E. Nilsson, B. Ljungberg and H. Axelson (2008). Suppression of renal cell carcinoma growth by inhibition of Notch signaling in vitro and in vivo. *J Clin Invest* **118**(1): 217-228.

Smolen, G. A., R. Sordella, B. Muir, G. Mohapatra, A. Barmettler, H. Archibald, W. J. Kim, R. A. Okimoto, D. W. Bell, D. C. Sgroi, J. G. Christensen, J. Settleman and D. A. Haber (2006). Amplification of MET may identify a subset of cancers with extreme sensitivity to the selective tyrosine kinase inhibitor PHA-665752. *Proc Natl Acad Sci U S A* **103**(7): 2316-2321.

Soga, N., K. Yamakado, H. Gohara, H. Takaki, T. Hiraki, T. Yamada, K. Arima, K. Takeda, S. Kanazawa and Y. Sugimura (2009). Percutaneous radiofrequency ablation for unresectable pulmonary metastases from renal cell carcinoma. *BJU Int* **104**(6): 790-794.

Sorich, M. J., M. D. Wiese, A. Rowland, G. Kichenadasse, R. A. McKinnon and C. S. Karapetis (2014). Extended RAS mutations and anti-EGFR monoclonal antibody survival benefit in metastatic colorectal cancer: a meta-analysis of randomized controlled trials. *Ann Oncol*.

Sos, M. L., K. Michel, T. Zander, J. Weiss, P. Frommolt, M. Peifer, D. Li, R. Ullrich, M. Koker, F. Fischer, T. Shimamura, D. Rauh, C. Mermel, S. Fischer, I. Stuckrath, S. Heynck, R. Beroukhim, W. Lin, W. Winckler, K. Shah, T. LaFramboise, W. F. Moriarty, M. Hanna, L. Tolosi, J. Rahnenfuhrer, R. Verhaak, D. Chiang, G. Getz, M. Hellmich, J. Wolf, L. Girard, M. Peyton, B. A. Weir, T. H. Chen, H. Greulich, J. Barretina, G. I. Shapiro, L. A. Garraway, A. F. Gazdar, J. D. Minna, M. Meyerson, K. K. Wong and R. K. Thomas (2009). Predicting drug susceptibility of non-small cell lung cancers based on genetic lesions. *J Clin Invest* **119**(6): 1727-1740.

Srigley, J. R. and B. Delahunt (2009). Uncommon and recently described renal carcinomas. *Mod Pathol* **22 Suppl 2**: S2-s23.

Srinivasan, D. and R. Plattner (2006). Activation of Abl tyrosine kinases promotes invasion of aggressive breast cancer cells. *Cancer Res* **66**(11): 5648-5655.

Steck, P. A., M. A. Pershouse, S. A. Jasser, W. K. Yung, H. Lin, A. H. Ligon, L. A. Langford, M. L. Baumgard, T. Hattier, T. Davis, C. Frye, R. Hu, B. Swedlund, D. H. Teng and S. V. Tavtigian (1997). Identification of a candidate tumour suppressor gene, MMAC1, at chromosome 10q23.3 that is mutated in multiple advanced cancers. *Nat Genet* **15**(4): 356-362.

Sternberg, C. N., I. D. Davis, J. Mardiak, C. Szczylik, E. Lee, J. Wagstaff, C. H. Barrios, P. Salman, O. A. Gladkov, A. Kavina, J. J. Zarba, M. Chen, L. McCann, L. Pandite, D. F. Roychowdhury and R. E. Hawkins (2010). Pazopanib in locally advanced or metastatic renal cell carcinoma: results of a randomized phase III trial. *J Clin Oncol* **28**(6): 1061-1068.

Sternberg, C. N., R. E. Hawkins, J. Wagstaff, P. Salman, J. Mardiak, C. H. Barrios, J. J. Zarba, O. A. Gladkov, E. Lee, C. Szczylik, L. McCann, S. D. Rubin, M. Chen and I. D. Davis (2013). A randomised, double-blind phase III study of pazopanib in patients with advanced and/or metastatic renal cell carcinoma: final overall survival results and safety update. *Eur J Cancer* **49**(6): 1287-1296.

Steuerman, R., O. Shevah and Z. Laron (2011). Congenital IGF1 deficiency tends to confer protection against post-natal development of malignancies. *Eur J Endocrinol* **164**(4): 485-489.

Sung, F. L., E. P. Hui, Q. Tao, H. Li, N. B. Tsui, Y. M. Lo, B. B. Ma, K. F. To, A. L. Harris and A. T. Chan (2007). Genome-wide expression analysis using microarray identified complex signaling pathways modulated by hypoxia in nasopharyngeal carcinoma. *Cancer Lett* **253**(1): 74-88.

Tabernero, J., F. Rojo, E. Calvo, H. Burris, I. Judson, K. Hazell, E. Martinelli, S. Ramon y Cajal, S. Jones, L. Vidal, N. Shand, T. Macarulla, F. J. Ramos, S. Dimitrijevic, U. Zoellner, P. Tang, M. Stumm, H. A. Lane, D. Lebwohl and J. Baselga (2008). Dose- and schedule-dependent inhibition of the mammalian target of rapamycin pathway with everolimus: a phase I tumor pharmacodynamic study in patients with advanced solid tumors. *J Clin Oncol* **26**(10): 1603-1610.

Tait, S., K. Dutta, D. Cowburn, J. Warwicker, A. J. Doig and J. E. McCarthy (2010). Local control of a disorder-order transition in 4E-BP1 underpins regulation of translation via eIF4E. *Proc Natl Acad Sci U S A* **107**(41): 17627-17632.

Tamburini, J., N. Chapuis, V. Bardet, S. Park, P. Sujobert, L. Willems, N. Ifrah, F. Dreyfus, P. Mayeux, C. Lacombe and D. Bouscary (2008). Mammalian target of rapamycin (mTOR) inhibition activates phosphatidylinositol 3-kinase/Akt by up-regulating insulin-like growth factor-1 receptor signaling in acute myeloid leukemia: rationale for therapeutic inhibition of both pathways. *Blood* **111**(1): 379-382.

Tannir, N. M., E. Plimack, C. Ng, P. Tamboli, N. B. Bekele, L. Xiao, L. Smith, Z. Lim, L. Pagliaro, J. Araujo, A. Aparicio, S. Matin, C. G. Wood and E. Jonasch (2012). A phase 2 trial of sunitinib in patients with advanced non-clear cell renal cell carcinoma. *Eur Urol* **62**(6): 1013-1019.

Tao, J. J., P. Castel, N. Radosevic-Robin, M. Elkabets, N. Auricchio, N. Aceto, G. Weitsman, P. Barber, B. Vojnovic, H. Ellis, N. Morse, N. T. Viola-Villegas, A. Bosch, D. Juric, S. Hazra, S. Singh, P. Kim, A. Bergamaschi, S. Maheswaran, T. Ng, F. Penault-Llorca, J. S. Lewis, L. A. Carey, C. M. Perou, J. Baselga and M. Scaltriti (2014). Antagonism of EGFR and HER3 enhances the response to inhibitors of the PI3K-Akt pathway in triple-negative breast cancer. *Sci Signal* **7**(318): ra29.

Tapia, O., I. Riquelme, P. Leal, A. Sandoval, S. Aedo, H. Weber, P. Letelier, E. Bellolio, M. Villaseca, P. Garcia and J. C. Roa (2014). The PI3K/AKT/mTOR pathway is activated in gastric cancer with potential prognostic and predictive significance. *Virchows Arch* **465**(1): 25-33.

Thomas, G. V., C. Tran, I. K. Mellinghoff, D. S. Welsbie, E. Chan, B. Fueger, J. Czernin and C. L. Sawyers (2006). Hypoxia-inducible factor determines sensitivity to inhibitors of mTOR in kidney cancer. *Nat Med* **12**(1): 122-127.

Thoreen, C. C., S. A. Kang, J. W. Chang, Q. Liu, J. Zhang, Y. Gao, L. J. Reichling, T. Sim, D. M. Sabatini and N. S. Gray (2009). An ATP-competitive mammalian target of rapamycin inhibitor reveals rapamycin-resistant functions of mTORC1. *The Journal of biological chemistry* **284**(12): 8023-8032.

Tomlinson, I. P., N. A. Alam, A. J. Rowan, E. Barclay, E. E. Jaeger, D. Kelsell, I. Leigh, P. Gorman, H. Lamlum, S. Rahman, R. R. Roylance, S. Olpin, S. Bevan, K. Barker, N. Hearle, R. S. Houlston, M. Kiuru, R. Lehtonen, A. Karhu, S. Vilkki, P. Laiho, C. Eklund, O. Vierimaa, K. Aittomaki, M. Hietala, P. Sistonen, A. Paetau, R. Salovaara, R. Herva, V. Launonen and L. A. Aaltonen (2002). Germline mutations in FH predispose to dominantly inherited uterine fibroids, skin leiomyomata and papillary renal cell cancer. *Nat Genet* **30**(4): 406-410.

Ulanet, D. B., D. L. Ludwig, C. R. Kahn and D. Hanahan (2010). Insulin receptor functionally enhances multistage tumor progression and conveys intrinsic resistance to IGF-1R targeted therapy. *Proc Natl Acad Sci U S A* **107**(24): 10791-10798.

Ullrich, A., A. Gray, A. W. Tam, T. Yang-Feng, M. Tsubokawa, C. Collins, W. Henzel, T. Le Bon, S. Kathuria, E. Chen and et al. (1986). Insulin-like growth factor I receptor primary structure: comparison with insulin receptor suggests structural determinants that define functional specificity. *Embo j* **5**(10): 2503-2512.

Venkannagari, S., W. Fiskus, K. Peth, P. Atadja, M. Hidalgo, A. Maitra and K. N. Bhalla (2012). Superior efficacy of co-treatment with dual PI3K/mTOR inhibitor NVP-BEZ235 and pan-histone deacetylase inhibitor against human pancreatic cancer. *Oncotarget* **3**(11): 1416-1427.

Verheul, H. M., B. Salumbides, K. Van Erp, H. Hammers, D. Z. Qian, T. Sanni, P. Atadja and R. Pili (2008). Combination strategy targeting the hypoxia inducible factor-1 alpha with mammalian target of rapamycin and histone deacetylase inhibitors. *Clin Cancer Res* **14**(11): 3589-3597.

Vezina, C., A. Kudelski and S. N. Sehgal (1975). Rapamycin (AY-22,989), a new antifungal antibiotic. I. Taxonomy of the producing streptomycete and isolation of the active principle. *J Antibiot (Tokyo)* **28**(10): 721-726.

Vuky, J., C. Isacson, M. Fotoohi, J. dela Cruz, H. Otero, V. Picozzi, T. Malpass, D. Aboulafia and A. Jacobs (2006). Phase II trial of imatinib (Gleevec) in patients with metastatic renal cell carcinoma. *Investigational new drugs* **24**(1): 85-88.

Wagle, N., B. C. Grabiner, E. M. Van Allen, A. Amin-Mansour, A. Taylor-Weiner, M. Rosenberg, N. Gray, J. A. Barletta, Y. Guo, S. J. Swanson, D. T. Ruan, G. J. Hanna, R. I. Haddad, G. Getz, D. J. Kwiatkowski, S. L. Carter, D. M. Sabatini, P. A. Janne, L. A. Garraway and J. H. Lorch (2014a). Response and acquired resistance to everolimus in anaplastic thyroid cancer. *N Engl J Med* **371**(15): 1426-1433.

Wagle, N., B. C. Grabiner, E. M. Van Allen, E. Hodis, S. Jacobus, J. G. Supko, M. Stewart, T. K. Choueiri, L. Gandhi, J. M. Cleary, A. A. Elfiky, M. E. Taplin, E. C. Stack, S. Signoretti, M. Loda, G. I. Shapiro, D. M. Sabatini, E. S. Lander, S. B. Gabriel, P. W. Kantoff, L. A. Garraway and J. E. Rosenberg (2014b). Activating mTOR mutations in a patient with an extraordinary response on a phase I trial of everolimus and pazopanib. *Cancer Discov* **4**(5): 546-553.

Wagner, A. J., H. A. Burris, J. S. de Bono, G. C. Jayson, J. C. Bendell, C. Gomez-Roca, S. Dolly, Y.-K. Zee, J. A. Ware, K. Yan, M. Derynck, S. Holden and J.-C. Soria (2009). Pharmacokinetics and pharmacodynamic biomarkers for the dual PI3K/mTOR inhibitor GDC-0980: Initial phase I evaluation. *Molecular Cancer Therapeutics* **8**(12 Suppl.): B137.

Wan, X., B. Harkavy, N. Shen, P. Grohar and L. J. Helman (2007). Rapamycin induces feedback activation of Akt signaling through an IGF-1R-dependent mechanism. *Oncogene* **26**(13): 1932-1940.

Wang, G. L., B. H. Jiang, E. A. Rue and G. L. Semenza (1995). Hypoxia-inducible factor 1 is a basic-helix-loop-helix-PAS heterodimer regulated by cellular O2 tension. *Proc Natl Acad Sci U S A* **92**(12): 5510-5514.

Wang, H., Q. Cao and A. Z. Dudek (2012). Phase II study of panobinostat and bortezomib in patients with pancreatic cancer progressing on gemcitabine-based therapy. *Anticancer Res* **32**(3): 1027-1031.

Wang, H., Y. Ji, G. Wu, K. Sun, Y. Sun, W. Li, B. Wang, B. He, Q. Zhang, Z. Dai and Z. Wu (2015). l-Tryptophan Activates Mammalian Target of Rapamycin and Enhances Expression of Tight Junction Proteins in Intestinal Porcine Epithelial Cells. *J Nutr* **145**(6): 1156-1162.

Wang, Z., Y. Li, D. Kong, S. Banerjee, A. Ahmad, A. S. Azmi, S. Ali, J. L. Abbruzzese, G. E. Gallick and F. H. Sarkar (2009). Acquisition of epithelial-mesenchymal transition phenotype of gemcitabine-resistant pancreatic cancer cells is linked with activation of the notch signaling pathway. *Cancer Res* **69**(6): 2400-2407.

Wazir, U., R. F. Newbold, W. G. Jiang, A. K. Sharma and K. Mokbel (2013). Prognostic and therapeutic implications of mTORC1 and Rictor expression in human breast cancer. *Oncol Rep* **29**(5): 1969-1974.

Weichert, W., A. Roske, V. Gekeler, T. Beckers, M. P. Ebert, M. Pross, M. Dietel, C. Denkert and C. Rocken (2008a). Association of patterns of class I histone deacetylase expression with patient prognosis in gastric cancer: a retrospective analysis. *Lancet Oncol* **9**(2): 139-148.

Weichert, W., A. Roske, V. Gekeler, T. Beckers, C. Stephan, K. Jung, F. R. Fritzsche, S. Niesporek, C. Denkert, M. Dietel and G. Kristiansen (2008b). Histone deacetylases 1, 2 and 3 are highly expressed in prostate cancer and HDAC2 expression is associated with shorter PSA relapse time after radical prostatectomy. *Br J Cancer* **98**(3): 604-610.

Weichert, W., A. Roske, S. Niesporek, A. Noske, A. C. Buckendahl, M. Dietel, V. Gekeler, M. Boehm, T. Beckers and C. Denkert (2008c). Class I histone deacetylase expression has independent prognostic impact in human colorectal cancer: specific role of class I histone deacetylases in vitro and in vivo. *Clin Cancer Res* **14**(6): 1669-1677.

Weigel, M. T., S. Banerjee, M. Arnedos, J. Salter, R. A'Hern, M. Dowsett and L. A. Martin (2013). Enhanced expression of the PDGFR/Abl signaling pathway in aromatase inhibitor-resistant breast cancer. *Ann Oncol* **24**(1): 126-133.

Wersall, P. J., H. Blomgren, P. Pisa, I. Lax, K. M. Kalkner and C. Svedman (2006). Regression of non-irradiated metastases after extracranial stereotactic radiotherapy in metastatic renal cell carcinoma. *Acta Oncol* **45**(4): 493-497.

West, A. C. and R. W. Johnstone (2014). New and emerging HDAC inhibitors for cancer treatment. *The Journal of clinical investigation* **124**(1): 30-39.

Wilhelm, S. M., C. Carter, L. Tang, D. Wilkie, A. McNabola, H. Rong, C. Chen, X. Zhang, P. Vincent, M. McHugh, Y. Cao, J. Shujath, S. Gawlak, D. Eveleigh, B. Rowley, L. Liu, L. Adnane, M. Lynch, D. Auclair, I. Taylor, R. Gedrich, A. Voznesensky, B. Riedl, L. E. Post, G. Bollag and P. A. Trail (2004). BAY 43-9006 exhibits broad spectrum oral antitumor activity and targets the RAF/MEK/ERK pathway and receptor tyrosine kinases involved in tumor progression and angiogenesis. *Cancer Res* **64**(19): 7099-7109.

Wilson, T. R., J. Fridlyand, Y. Yan, E. Penuel, L. Burton, E. Chan, J. Peng, E. Lin, Y. Wang, J. Sosman, A. Ribas, J. Li, J. Moffat, D. P. Sutherlin, H. Koeppen, M. Merchant, R. Neve and J. Settleman (2012). Widespread potential for growth-factor-driven resistance to anticancer kinase inhibitors. *Nature* **487**(7408): 505-509.

Wilson-Edell, K. A., M. A. Yevtushenko, D. E. Rothschild, A. N. Rogers and C. C. Benz (2014). mTORC1/C2 and pan-HDAC inhibitors synergistically impair breast cancer growth by convergent AKT and polysome inhibiting mechanisms. *Breast Cancer Res Treat* **144**(2): 287-298.

Wright, J. D., C. W. Reuter and M. J. Weber (1995). An incomplete program of cellular tyrosine phosphorylations induced by kinase-defective epidermal growth factor receptors. *J Biol Chem* **270**(20): 12085-12093.

Xie, M., L. Zhang, C. S. He, F. Xu, J. L. Liu, Z. H. Hu, L. P. Zhao and Y. Tian (2012). Activation of Notch-1 enhances epithelial-mesenchymal transition in gefitinib-acquired resistant lung cancer cells. *J Cell Biochem* **113**(5): 1501-1513.

Xu, C. X., Y. Li, P. Yue, T. K. Owonikoko, S. S. Ramalingam, F. R. Khuri and S. Y. Sun (2011). The combination of RAD001 and NVP-BEZ235 exerts synergistic anticancer activity against non-small cell lung cancer in vitro and in vivo. *PLoS One* **6**(6): e20899.

Yagoda, A., B. Abi-Rached and D. Petrylak (1995). Chemotherapy for advanced renal-cell carcinoma: 1983-1993. *Seminars in oncology* **22**(1): 42-60.

Yamazaki, K., M. Sakamoto, T. Ohta, Y. Kanai, M. Ohki and S. Hirohashi (2003). Overexpression of KIT in chromophobe renal cell carcinoma. *Oncogene* **22**(6): 847-852.

Yang, D. Q. and M. B. Kastan (2000). Participation of ATM in insulin signalling through phosphorylation of eIF-4E-binding protein 1. *Nat Cell Biol* **2**(12): 893-898.

Yang, J., S. A. Mani, J. L. Donaher, S. Ramaswamy, R. A. Itzykson, C. Come, P. Savagner, I. Gitelman, A. Richardson and R. A. Weinberg (2004). Twist, a master regulator of morphogenesis, plays an essential role in tumor metastasis. *Cell* **117**(7): 927-939.

Yang, J. C., L. Haworth, R. M. Sherry, P. Hwu, D. J. Schwartzentruber, S. L. Topalian, S. M. Steinberg, H. X. Chen and S. A. Rosenberg (2003). A randomized trial of bevacizumab, an anti-vascular endothelial growth factor antibody, for metastatic renal cancer. *N Engl J Med* **349**(5): 427-434.

Yang, S., X. Xiao, X. Meng and K. K. Leslie (2011). A mechanism for synergy with combined mTOR and PI3 kinase inhibitors. *PLoS One* **6**(10): e26343.

Yang, W., J. Soares, P. Greninger, E. J. Edelman, H. Lightfoot, S. Forbes, N. Bindal, D. Beare, J. A. Smith, I. R. Thompson, S. Ramaswamy, P. A. Futreal, D. A. Haber, M. R. Stratton, C. Benes, U. McDermott and M. J. Garnett (2013). Genomics of Drug Sensitivity in Cancer (GDSC): a resource for therapeutic biomarker discovery in cancer cells. *Nucleic Acids Res* **41**(Database issue): D955-961.

Yano, S., T. Yamada, S. Takeuchi, K. Tachibana, Y. Minami, Y. Yatabe, T. Mitsudomi, H. Tanaka, T. Kimura, S. Kudoh, H. Nokihara, Y. Ohe, J. Yokota, H. Uramoto, K. Yasumoto, K. Kiura, M. Higashiyama, M. Oda, H. Saito, J. Yoshida, K. Kondoh and M. Noguchi (2011). Hepatocyte growth factor expression in EGFR mutant lung cancer with intrinsic and acquired resistance to tyrosine kinase inhibitors in a Japanese cohort. *J Thorac Oncol* **6**(12): 2011-2017.

Yao, J. C., M. H. Shah, T. Ito, C. L. Bohas, E. M. Wolin, E. Van Cutsem, T. J. Hobday, T. Okusaka, J. Capdevila, E. G. de Vries, P. Tomassetti, M. E. Pavel, S. Hoosen, T. Haas, J. Lincy, D. Lebwohl and K. Oberg (2011). Everolimus for advanced pancreatic neuroendocrine tumors. *N Engl J Med* **364**(6): 514-523.

Yap, S. A., A. Finelli, D. R. Urbach, G. A. Tomlinson and S. M. Alibhai (2014). Partial Nephrectomy for the Treatment of Renal Cell Carcinoma and the Risk of End Stage Renal Disease. *BJU Int*.

Yeh, T. C., V. Marsh, B. A. Bernat, J. Ballard, H. Colwell, R. J. Evans, J. Parry, D. Smith, B. J. Brandhuber, S. Gross, A. Marlow, B. Hurley, J. Lyssikatos, P. A. Lee, J. D. Winkler, K. Koch and E. Wallace (2007). Biological characterization of ARRY-142886 (AZD6244), a potent, highly selective mitogen-activated protein kinase kinase 1/2 inhibitor. *Clinical cancer research : an official journal of the American Association for Cancer Research* **13**(5): 1576-1583.

Yip, C. K., K. Murata, T. Walz, D. M. Sabatini and S. A. Kang (2010). Structure of the human mTOR complex I and its implications for rapamycin inhibition. *Mol Cell* **38**(5): 768-774.

Yuen, J. S., E. Akkaya, Y. Wang, M. Takiguchi, S. Peak, M. Sullivan, A. S. Protheroe and V. M. Macaulay (2009). Validation of the type 1 insulin-like growth factor receptor as a therapeutic target in renal cancer. *Molecular cancer therapeutics* **8**(6): 1448-1459.

Yuen, J. S., M. E. Cockman, M. Sullivan, A. Protheroe, G. D. Turner, I. S. Roberts, C. W. Pugh, H. Werner and V. M. Macaulay (2007). The VHL tumor suppressor inhibits expression of the IGF1R and its loss induces IGF1R upregulation in human clear cell renal carcinoma. *Oncogene* **26**(45): 6499-6508.

Zacharek, S. J., Y. Xiong and S. D. Shumway (2005). Negative regulation of TSC1-TSC2 by mammalian D-type cyclins. *Cancer Res* **65**(24): 11354-11360.

Zatyka, M., N. F. da Silva, S. C. Clifford, M. R. Morris, M. S. Wiesener, K. U. Eckardt, R. S. Houlston, F. M. Richards, F. Latif and E. R. Maher (2002). Identification of cyclin D1 and other novel targets for the von Hippel-Lindau tumor suppressor gene by expression array analysis and investigation of cyclin D1 genotype as a modifier in von Hippel-Lindau disease. *Cancer Res* **62**(13): 3803-3811.

Zeng, J. Y., S. Sharma, Y. Q. Zhou, H. P. Yao, X. Hu, R. Zhang and M. H. Wang (2014). Synergistic activities of MET/RON inhibitor BMS-777607 and mTOR inhibitor AZD8055 to polyploid cells derived from pancreatic cancer and cancer stem cells. *Mol Cancer Ther* **13**(1): 37-48.

Zhang, D., A. A. Samani and P. Brodt (2003). The role of the IGF-I receptor in the regulation of matrix metalloproteinases, tumor invasion and metastasis. *Horm Metab Res* **35**(11-12): 802-808.

Zhang, H., N. Bajraszewski, E. Wu, H. Wang, A. P. Moseman, S. L. Dabora, J. D. Griffin and D. J. Kwiatkowski (2007). PDGFRs are critical for PI3K/Akt activation and negatively regulated by mTOR. *J Clin Invest* **117**(3): 730-738.

Zhang, H., D. Berel, Y. Wang, P. Li, N. A. Bhowmick, R. A. Figlin and H. L. Kim (2013). A comparison of Ku0063794, a dual mTORC1 and mTORC2 inhibitor, and temsirolimus in preclinical renal cell carcinoma models. *PLoS One* **8**(1): e54918.

Zhang, Y. and X. F. Zheng (2012). mTOR-independent 4E-BP1 phosphorylation is associated with cancer resistance to mTOR kinase inhibitors. *Cell Cycle* **11**(3): 594-603.

Zhu, H., X. Zhou, S. Redfield, J. Lewin and L. Miele (2013). Elevated Jagged-1 and Notch-1 expression in high grade and metastatic prostate cancers. *Am J Transl Res* **5**(3): 368-378.

Zhu, T. N., H. J. He, S. Kole, T. D'Souza, R. Agarwal, P. J. Morin and M. Bernier (2007). Filamin A-mediated down-regulation of the exchange factor Ras-GRF1 correlates with decreased matrix metalloproteinase-9 expression in human melanoma cells. *J Biol Chem* **282**(20): 14816-14826.

Zoncu, R., L. Bar-Peled, A. Efeyan, S. Wang, Y. Sancak and D. M. Sabatini (2011). mTORC1 senses lysosomal amino acids through an inside-out mechanism that requires the vacuolar H(+)-ATPase. *Science* **334**(6056): 678-683.

# Appendix 1: Microarray screen data RCC4B20 cells vs solvent treated RCC4S cells

| AffyID | SYMBOL | M | P.Value |
|---|---|---|---|
| 8058708 | ABCA12 | 1.087 | 0.021 |
| 7929779 | ABCC2 | -1.484 | 0.003 |
| 8123137 | ACAT2 | -0.935 | 0.041 |
| 8049471 | ACKR3 | 0.873 | 0.041 |
| 8121277 | AIM1 | -0.983 | 0.024 |
| 7903440 | AMY1A | 1.161 | 0.014 |
| 7918134 | AMY1A | 1.161 | 0.014 |
| 7903425 | AMY1A | 1.161 | 0.014 |
| 7903414 | AMY2A | 1.413 | 0.006 |
| 7929653 | ANKRD2 | -0.990 | 0.045 |
| 8121095 | ANKRD6 | 0.945 | 0.037 |
| 7932744 | ARMC4 | -1.289 | 0.020 |
| 8106722 | ATP6AP1L | 1.026 | 0.047 |
| 7930714 | ATRNL1 | 0.936 | 0.034 |
| 7918694 | BCL2L15 | -1.456 | 0.005 |
| 8106494 | BHMT2 | 1.072 | 0.019 |
| 8021963 | C18orf56 | -0.899 | 0.030 |
| 7989501 | CA12 | 1.100 | 0.027 |
| 7996198 | CCDC113 | 1.012 | 0.032 |
| 8045857 | CCDC148 | 1.401 | 0.018 |
| 8089544 | CCDC80 | 1.079 | 0.018 |
| 8006433 | CCL2 | -1.949 | 0.003 |
| 8104663 | CDH6 | 1.004 | 0.024 |
| 8020267 | CEP192 | -0.876 | 0.037 |
| 7908459 | CFH | 2.217 | 0.001 |
| 8047401 | CFLAR | 1.072 | 0.028 |
| 7969815 | CLYBL | 1.036 | 0.037 |
| 8161460 | CNTNAP3 | 1.751 | 0.003 |
| 8155540 | CNTNAP3 | 1.751 | 0.003 |
| 8155359 | CNTNAP3 | 1.480 | 0.005 |
| 7997642 | CRISPLD2 | -0.918 | 0.037 |
| 7951662 | CRYAB | 1.651 | 0.003 |
| 8141328 | CYP3A5 | 1.550 | 0.005 |
| 8112260 | DEPDC1B | -0.843 | 0.037 |
| 7950067 | DHCR7 | -0.934 | 0.037 |
| 8093191 | DLG1 | 0.909 | 0.035 |
| 8036079 | DMKN | 0.971 | 0.044 |
| 7934026 | DNA2 | -1.119 | 0.014 |
| 7933933 | DNAJC12 | -0.915 | 0.043 |
| 8064976 | DNAJC9 | -0.876 | 0.037 |
| 8021297 | DYNAP | 1.279 | 0.008 |
| 8024792 | EBI3 | 1.110 | 0.029 |
| 8007949 | EFCAB13 | 1.752 | 0.005 |
| 7949503 | EFEMP2 | 0.913 | 0.027 |

| AffyID | SYMBOL | M | P.Value |
|---|---|---|---|
| 8123920 | ELOVL2 | -1.402 | 0.005 |
| 8022118 | EPB41L3 | -0.978 | 0.050 |
| 8068593 | ETS2 | -0.920 | 0.037 |
| 8121547 | FAM229B | 1.009 | 0.026 |
| 7954631 | FAR2 | 1.944 | 0.003 |
| 8152703 | FBXO32 | 1.480 | 0.004 |
| 8092750 | FGF12 | 1.146 | 0.037 |
| 8125919 | FKBP5 | -1.121 | 0.018 |
| 7970737 | FLT3 | 1.811 | 0.003 |
| 8058765 | FN1 | -0.883 | 0.042 |
| 7942332 | FOLR1 | 0.977 | 0.037 |
| 8161964 | FRMD3 | 0.978 | 0.043 |
| 7913694 | FUCA1 | 1.116 | 0.014 |
| 8175666 | GABRE | 1.126 | 0.030 |
| 8024485 | GADD45B | 1.141 | 0.014 |
| 7945321 | GLB1L2 | 1.719 | 0.003 |
| 8020164 | GNAL | 0.858 | 0.044 |
| 8081214 | GPR15 | -1.249 | 0.027 |
| 7996081 | GPR56 | -1.094 | 0.037 |
| 8084880 | HES1 | 1.059 | 0.016 |
| 8151457 | HEY1 | 0.829 | 0.046 |
| 8124492 | HIST1H2BK | 0.995 | 0.037 |
| 7943787 | HSPB2 | 0.987 | 0.034 |
| 7931754 | IDI1 | -1.027 | 0.048 |
| 7945663 | IFITM10 | 1.055 | 0.037 |
| 8166593 | IL1RAPL1 | -1.209 | 0.018 |
| 8104901 | IL7R | -1.293 | 0.024 |
| 8095680 | IL8 | -1.898 | 0.020 |
| 8070826 | ITGB2 | 1.510 | 0.004 |
| 8064978 | JAG1 | 1.204 | 0.014 |
| 8168412 | JPX | 1.038 | 0.049 |
| 7902977 | KIAA1107 | 1.368 | 0.013 |
| 8084219 | KLHL24 | 0.894 | 0.048 |
| 8015337 | KRT15 | 0.955 | 0.044 |
| 8071049 | LINC00328 | 1.916 | 0.005 |
| 7904478 | LINC00328 | 1.715 | 0.009 |
| 7974198 | LRR1 | -0.831 | 0.046 |
| 7957433 | LRRIQ1 | 0.978 | 0.050 |
| 8148040 | MAL2 | 0.809 | 0.047 |
| 7926259 | MCM10 | -1.047 | 0.030 |
| 8062766 | MYBL2 | -0.929 | 0.035 |
| 8174119 | NA | 2.874 | 0.000 |
| 8124160 | NA | -1.534 | 0.005 |
| 7894196 | NA | -1.332 | 0.008 |

| AffyID | SYMBOL | M | P.Value |
|---|---|---|---|
| 8117565 | NA | -1.375 | 0.009 |
| 7895254 | NA | -1.532 | 0.014 |
| 8064098 | NA | -1.907 | 0.021 |
| 7894096 | NA | -1.155 | 0.023 |
| 7892744 | NA | 1.862 | 0.024 |
| 7896023 | NA | -1.237 | 0.024 |
| 8155453 | NA | 1.371 | 0.024 |
| 8161375 | NA | 1.371 | 0.024 |
| 8050236 | NA | -0.935 | 0.027 |
| 7961960 | NA | -1.099 | 0.027 |
| 7893637 | NA | -1.418 | 0.028 |
| 7893878 | NA | -1.281 | 0.028 |
| 7895566 | NA | -1.093 | 0.030 |
| 8180400 | NA | -1.648 | 0.034 |
| 7893525 | NA | -1.101 | 0.034 |
| 8076461 | NA | 1.104 | 0.037 |
| 7895698 | NA | 1.499 | 0.041 |
| 7894206 | NA | -1.301 | 0.043 |
| 7892938 | NA | -1.203 | 0.044 |
| 7893398 | NA | -1.430 | 0.044 |
| 7894191 | NA | -1.676 | 0.045 |
| 7894848 | NA | -0.905 | 0.048 |
| 8149148 | NA | 0.847 | 0.050 |
| 8019857 | NDC80 | -0.953 | 0.044 |
| 7916986 | NEGR1 | 1.304 | 0.018 |
| 8148049 | NOV | 0.980 | 0.043 |
| 8014956 | NR1D1 | 1.251 | 0.028 |
| 8123739 | NRN1 | -1.531 | 0.005 |
| 8000574 | NUPR1 | 1.227 | 0.010 |
| 7916167 | ORC1 | -1.068 | 0.024 |
| 8169389 | PAK3 | 1.157 | 0.014 |
| 7928944 | PAPSS2 | -1.533 | 0.005 |
| 8035694 | PBX4 | -0.944 | 0.043 |
| 8150714 | PCMTD1 | 0.842 | 0.050 |
| 8144802 | PDGFRL | 1.085 | 0.014 |
| 8008263 | PDK2 | 1.114 | 0.014 |
| 7998820 | PDPK1 | 1.115 | 0.016 |
| 7992682 | PDPK1 | 1.093 | 0.018 |
| 7915787 | PIK3R3 | -1.000 | 0.043 |
| 8101429 | PLAC8 | -3.900 | 0.000 |
| 7929388 | PLCE1 | -1.381 | 0.007 |
| 8097356 | PLK4 | -0.871 | 0.048 |
| 8001547 | PLLP | 0.970 | 0.029 |
| 8091306 | PLSCR4 | 1.070 | 0.015 |
| 7926545 | PLXDC2 | 1.513 | 0.003 |
| 8067233 | PMEPA1 | 0.891 | 0.042 |
| 8173869 | POF1B | 1.112 | 0.014 |
| 7928589 | PPIF | -0.875 | 0.043 |
| 8022251 | PPP4R1 | -0.910 | 0.028 |
| 8037267 | PSG2 | -1.594 | 0.011 |
| 8179727 | PSORS1C3 | -1.430 | 0.018 |
| 8124897 | PSORS1C3 | -1.430 | 0.018 |
| 8126853 | PTCHD4 | 2.564 | 0.000 |

| AffyID | SYMBOL | M | P.Value |
|---|---|---|---|
| 8021301 | RAB27B | 1.271 | 0.014 |
| 7927186 | RASSF4 | -1.090 | 0.017 |
| 8022914 | RPRD1A | 0.779 | 0.047 |
| 8128123 | RRAGD | 1.524 | 0.005 |
| 7920278 | S100A3 | -1.201 | 0.021 |
| 7903393 | S1PR1 | -0.832 | 0.041 |
| 8085716 | SATB1 | 0.917 | 0.044 |
| 7929816 | SCD | -1.398 | 0.006 |
| 7935776 | SCD | -1.089 | 0.014 |
| 8059345 | SCG2 | 1.550 | 0.003 |
| 8046020 | SCN2A | 1.016 | 0.041 |
| 8057797 | SDPR | -1.121 | 0.028 |
| 8140668 | SEMA3A | 1.054 | 0.027 |
| 8140534 | SEMA3C | 0.838 | 0.050 |
| 8120833 | SH3BGRL2 | 1.184 | 0.028 |
| 8021091 | SIGLEC15 | 1.420 | 0.005 |
| 8128459 | SIM1 | -1.948 | 0.003 |
| 8150537 | SLC20A2 | -0.949 | 0.044 |
| 7929383 | SLC35G1 | -1.152 | 0.017 |
| 7917052 | SLC44A5 | 1.204 | 0.046 |
| 8095585 | SLC4A4 | -0.859 | 0.032 |
| 8172280 | SLC9A7 | 1.301 | 0.021 |
| 8030366 | SNORD35A | -0.945 | 0.041 |
| 7918973 | SPAG17 | 0.886 | 0.041 |
| 7915955 | SPATA6 | 1.024 | 0.027 |
| 8028311 | SPINT2 | 0.892 | 0.037 |
| 8168749 | SRPX2 | 1.206 | 0.012 |
| 8136115 | STRIP2 | -1.152 | 0.024 |
| 8066822 | SULF2 | 1.325 | 0.037 |
| 8123080 | SYTL3 | -1.013 | 0.026 |
| 7983828 | TEX9 | 1.454 | 0.014 |
| 8057599 | TFPI | 0.984 | 0.030 |
| 8066214 | TGM2 | 1.008 | 0.037 |
| 8099841 | TLR6 | -1.299 | 0.024 |
| 7953936 | TMEM52B | -2.148 | 0.003 |
| 7983734 | TMOD2 | 1.619 | 0.006 |
| 8126839 | TNFRSF21 | 0.878 | 0.037 |
| 7912145 | TNFRSF9 | -1.704 | 0.009 |
| 8151890 | TP53INP1 | 0.914 | 0.037 |
| 8121838 | TPD52L1 | -1.523 | 0.004 |
| 8143643 | TPK1 | -1.103 | 0.029 |
| 8019842 | TYMS | -0.785 | 0.049 |
| 8089596 | WDR52 | 1.075 | 0.034 |
| 8173261 | ZC4H2 | 1.297 | 0.008 |
| 8065517 | ZNF337 | 0.833 | 0.049 |

AffyID: Affymetrix gene ID number

M: log2 fold change in expression

# Appendix 2: Microarray screen data RCC4B20 cells vs BEZ235 treated RCC4S cells

| AffyID | SYMBOL | M | P.Value |
|---|---|---|---|
| 8058708 | ABCA12 | 1.087 | 0.021 |
| 7929779 | ABCC2 | -1.484 | 0.003 |
| 8123137 | ACAT2 | -0.935 | 0.041 |
| 8049471 | ACKR3 | 0.873 | 0.041 |
| 8121277 | AIM1 | -0.983 | 0.024 |
| 7903440 | AMY1A | 1.161 | 0.014 |
| 7918134 | AMY1A | 1.161 | 0.014 |
| 7903425 | AMY1A | 1.161 | 0.014 |
| 7903414 | AMY2A | 1.413 | 0.006 |
| 7929653 | ANKRD2 | -0.990 | 0.045 |
| 8121095 | ANKRD6 | 0.945 | 0.037 |
| 7932744 | ARMC4 | -1.289 | 0.020 |
| 8106722 | ATP6AP1L | 1.026 | 0.047 |
| 7930714 | ATRNL1 | 0.936 | 0.034 |
| 7918694 | BCL2L15 | -1.456 | 0.005 |
| 8106494 | BHMT2 | 1.072 | 0.019 |
| 8021963 | C18orf56 | -0.899 | 0.030 |
| 7989501 | CA12 | 1.100 | 0.027 |
| 7996198 | CCDC113 | 1.012 | 0.032 |
| 8045857 | CCDC148 | 1.401 | 0.018 |
| 8089544 | CCDC80 | 1.079 | 0.018 |
| 8006433 | CCL2 | -1.949 | 0.003 |
| 8104663 | CDH6 | 1.004 | 0.024 |
| 8020267 | CEP192 | -0.876 | 0.037 |
| 7908459 | CFH | 2.217 | 0.001 |
| 8047401 | CFLAR | 1.072 | 0.028 |
| 7969815 | CLYBL | 1.036 | 0.037 |
| 8161460 | CNTNAP3 | 1.751 | 0.003 |
| 8155540 | CNTNAP3 | 1.751 | 0.003 |
| 8155359 | CNTNAP3 | 1.480 | 0.005 |
| 7997642 | CRISPLD2 | -0.918 | 0.037 |
| 7951662 | CRYAB | 1.651 | 0.003 |
| 8141328 | CYP3A5 | 1.550 | 0.005 |
| 8112260 | DEPDC1B | -0.843 | 0.037 |
| 7950067 | DHCR7 | -0.934 | 0.037 |
| 8093191 | DLG1 | 0.909 | 0.035 |
| 8036079 | DMKN | 0.971 | 0.044 |
| 7934026 | DNA2 | -1.119 | 0.014 |
| 7933933 | DNAJC12 | -0.915 | 0.043 |
| 8064976 | DNAJC9 | -0.876 | 0.037 |
| 8021297 | DYNAP | 1.279 | 0.008 |
| 8024792 | EBI3 | 1.110 | 0.029 |
| 8007949 | EFCAB13 | 1.752 | 0.005 |
| 7949503 | EFEMP2 | 0.913 | 0.027 |
| 8123920 | ELOVL2 | -1.402 | 0.005 |

| AffyID | SYMBOL | M | P.Value |
|---|---|---|---|
| 8022118 | EPB41L3 | -0.978 | 0.050 |
| 8068593 | ETS2 | -0.920 | 0.037 |
| 8121547 | FAM229B | 1.009 | 0.026 |
| 7954631 | FAR2 | 1.944 | 0.003 |
| 8152703 | FBXO32 | 1.480 | 0.004 |
| 8092750 | FGF12 | 1.146 | 0.037 |
| 8125919 | FKBP5 | -1.121 | 0.018 |
| 7970737 | FLT3 | 1.811 | 0.003 |
| 8058765 | FN1 | -0.883 | 0.042 |
| 7942332 | FOLR1 | 0.977 | 0.037 |
| 8161964 | FRMD3 | 0.978 | 0.043 |
| 7913694 | FUCA1 | 1.116 | 0.014 |
| 8175666 | GABRE | 1.126 | 0.030 |
| 8024485 | GADD45B | 1.141 | 0.014 |
| 7945321 | GLB1L2 | 1.719 | 0.003 |
| 8020164 | GNAL | 0.858 | 0.044 |
| 8081214 | GPR15 | -1.249 | 0.027 |
| 7996081 | GPR56 | -1.094 | 0.037 |
| 8084880 | HES1 | 1.059 | 0.016 |
| 8151457 | HEY1 | 0.829 | 0.046 |
| 8124492 | HIST1H2B K | 0.995 | 0.037 |
| 7943787 | HSPB2 | 0.987 | 0.034 |
| 7931754 | IDI1 | -1.027 | 0.048 |
| 7945663 | IFITM10 | 1.055 | 0.037 |
| 8166593 | IL1RAPL1 | -1.209 | 0.018 |
| 8104901 | IL7R | -1.293 | 0.024 |
| 8095680 | IL8 | -1.898 | 0.020 |
| 8070826 | ITGB2 | 1.510 | 0.004 |
| 8064978 | JAG1 | 1.204 | 0.014 |
| 8168412 | JPX | 1.038 | 0.049 |
| 7902977 | KIAA1107 | 1.368 | 0.013 |
| 8084219 | KLHL24 | 0.894 | 0.048 |
| 8015337 | KRT15 | 0.955 | 0.044 |
| 8071049 | LINC00328 | 1.916 | 0.005 |
| 7904478 | LINC00328 | 1.715 | 0.009 |
| 7974198 | LRR1 | -0.831 | 0.046 |
| 7957433 | LRRIQ1 | 0.978 | 0.050 |
| 8148040 | MAL2 | 0.809 | 0.047 |
| 7926259 | MCM10 | -1.047 | 0.030 |
| 8062766 | MYBL2 | -0.929 | 0.035 |
| 8174119 | NA | 2.874 | 0.000 |
| 8124160 | NA | -1.534 | 0.005 |
| 7894196 | NA | -1.332 | 0.008 |
| 8117565 | NA | -1.375 | 0.009 |

| AffyID | SYMBOL | M | P.Value |
|---|---|---|---|
| 7895254 | NA | -1.532 | 0.014 |
| 8064098 | NA | -1.907 | 0.021 |
| 7894096 | NA | -1.155 | 0.023 |
| 7892744 | NA | 1.862 | 0.024 |
| 7896023 | NA | -1.237 | 0.024 |
| 8155453 | NA | 1.371 | 0.024 |
| 8161375 | NA | 1.371 | 0.024 |
| 8050236 | NA | -0.935 | 0.027 |
| 7961960 | NA | -1.099 | 0.027 |
| 7893637 | NA | -1.418 | 0.028 |
| 7893878 | NA | -1.281 | 0.028 |
| 7895566 | NA | -1.093 | 0.030 |
| 8180400 | NA | -1.648 | 0.034 |
| 7893525 | NA | -1.101 | 0.034 |
| 8076461 | NA | 1.104 | 0.037 |
| 7895698 | NA | 1.499 | 0.041 |
| 7894206 | NA | -1.301 | 0.043 |
| 7892938 | NA | -1.203 | 0.044 |
| 7893398 | NA | -1.430 | 0.044 |
| 7894191 | NA | -1.676 | 0.045 |
| 7894848 | NA | -0.905 | 0.048 |
| 8149148 | NA | 0.847 | 0.050 |
| 8019857 | NDC80 | -0.953 | 0.044 |
| 7916986 | NEGR1 | 1.304 | 0.018 |
| 8148049 | NOV | 0.980 | 0.043 |
| 8014956 | NR1D1 | 1.251 | 0.028 |
| 8123739 | NRN1 | -1.531 | 0.005 |
| 8000574 | NUPR1 | 1.227 | 0.010 |
| 7916167 | ORC1 | -1.068 | 0.024 |
| 8169389 | PAK3 | 1.157 | 0.014 |
| 7928944 | PAPSS2 | -1.533 | 0.005 |
| 8035694 | PBX4 | -0.944 | 0.043 |
| 8150714 | PCMTD1 | 0.842 | 0.050 |
| 8144802 | PDGFRL | 1.085 | 0.014 |
| 8008263 | PDK2 | 1.114 | 0.014 |
| 7998820 | PDPK1 | 1.115 | 0.016 |
| 7992682 | PDPK1 | 1.093 | 0.018 |
| 7915787 | PIK3R3 | -1.000 | 0.043 |
| 8101429 | PLAC8 | -3.900 | 0.000 |
| 7929388 | PLCE1 | -1.381 | 0.007 |
| 8097356 | PLK4 | -0.871 | 0.048 |
| 8001547 | PLLP | 0.970 | 0.029 |
| 8091306 | PLSCR4 | 1.070 | 0.015 |
| 7926545 | PLXDC2 | 1.513 | 0.003 |
| 8067233 | PMEPA1 | 0.891 | 0.042 |
| 8173869 | POF1B | 1.112 | 0.014 |
| 7928589 | PPIF | -0.875 | 0.043 |
| 8022251 | PPP4R1 | -0.910 | 0.028 |
| 8037267 | PSG2 | -1.594 | 0.011 |
| 8179727 | PSORS1C3 | -1.430 | 0.018 |
| 8124897 | PSORS1C3 | -1.430 | 0.018 |
| 8126853 | PTCHD4 | 2.564 | 0.000 |

| AffyID | SYMBOL | M | P.Value |
|---|---|---|---|
| 8021301 | RAB27B | 1.271 | 0.014 |
| 7927186 | RASSF4 | -1.090 | 0.017 |
| 8022914 | RPRD1A | 0.779 | 0.047 |
| 8128123 | RRAGD | 1.524 | 0.005 |
| 7920278 | S100A3 | -1.201 | 0.021 |
| 7903393 | S1PR1 | -0.832 | 0.041 |
| 8085716 | SATB1 | 0.917 | 0.044 |
| 7929816 | SCD | -1.398 | 0.006 |
| 7935776 | SCD | -1.089 | 0.014 |
| 8059345 | SCG2 | 1.550 | 0.003 |
| 8046020 | SCN2A | 1.016 | 0.041 |
| 8057797 | SDPR | -1.121 | 0.028 |
| 8140668 | SEMA3A | 1.054 | 0.027 |
| 8140534 | SEMA3C | 0.838 | 0.050 |
| 8120833 | SH3BGRL2 | 1.184 | 0.028 |
| 8021091 | SIGLEC15 | 1.420 | 0.005 |
| 8128459 | SIM1 | -1.948 | 0.003 |
| 8150537 | SLC20A2 | -0.949 | 0.044 |
| 7929383 | SLC35G1 | -1.152 | 0.017 |
| 7917052 | SLC44A5 | 1.204 | 0.046 |
| 8095585 | SLC4A4 | -0.859 | 0.032 |
| 8172280 | SLC9A7 | 1.301 | 0.021 |
| 8030366 | SNORD35A | -0.945 | 0.041 |
| 7918973 | SPAG17 | 0.886 | 0.041 |
| 7915955 | SPATA6 | 1.024 | 0.027 |
| 8028311 | SPINT2 | 0.892 | 0.037 |
| 8168749 | SRPX2 | 1.206 | 0.012 |
| 8136115 | STRIP2 | -1.152 | 0.024 |
| 8066822 | SULF2 | 1.325 | 0.037 |
| 8123080 | SYTL3 | -1.013 | 0.026 |
| 7983828 | TEX9 | 1.454 | 0.014 |
| 8057599 | TFPI | 0.984 | 0.030 |
| 8066214 | TGM2 | 1.008 | 0.037 |
| 8099841 | TLR6 | -1.299 | 0.024 |
| 7953936 | TMEM52B | -2.148 | 0.003 |
| 7983734 | TMOD2 | 1.619 | 0.006 |
| 8126839 | TNFRSF21 | 0.878 | 0.037 |
| 7912145 | TNFRSF9 | -1.704 | 0.009 |
| 8151890 | TP53INP1 | 0.914 | 0.037 |
| 8121838 | TPD52L1 | -1.523 | 0.004 |
| 8143643 | TPK1 | -1.103 | 0.029 |
| 8019842 | TYMS | -0.785 | 0.049 |
| 8089596 | WDR52 | 1.075 | 0.034 |
| 8173261 | ZC4H2 | 1.297 | 0.008 |
| 8065517 | ZNF337 | 0.833 | 0.049 |

AffyID: Affymetrix gene ID number

M: log2 fold change in expression